Cosmic Rays – Overview and Open Questions

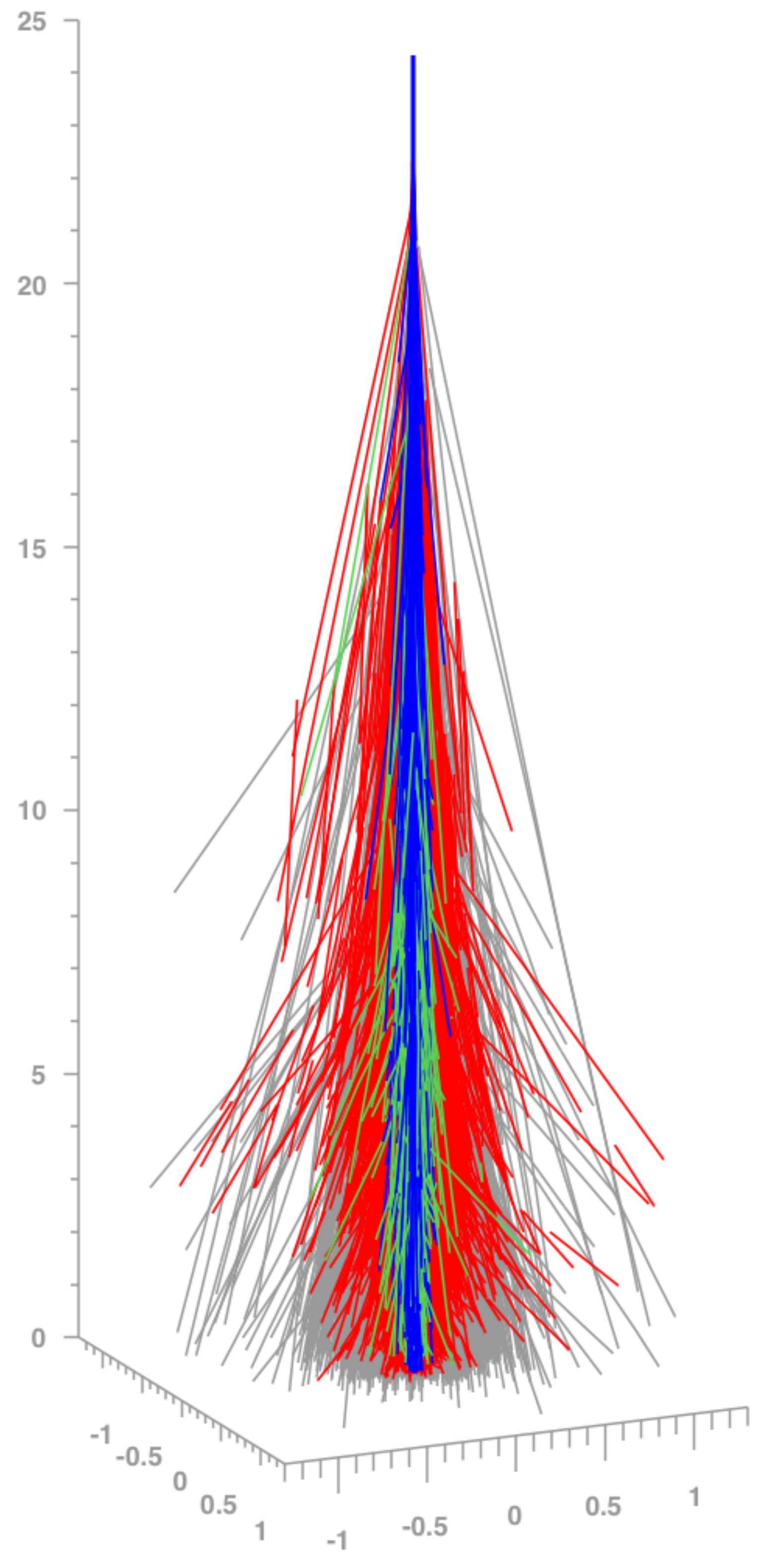

Ralph Engel, *Karlsruhe Institute of Technology*

KIT
Karlsruhe Institute of Technology

The cosmic ray spectrum and power laws in nature

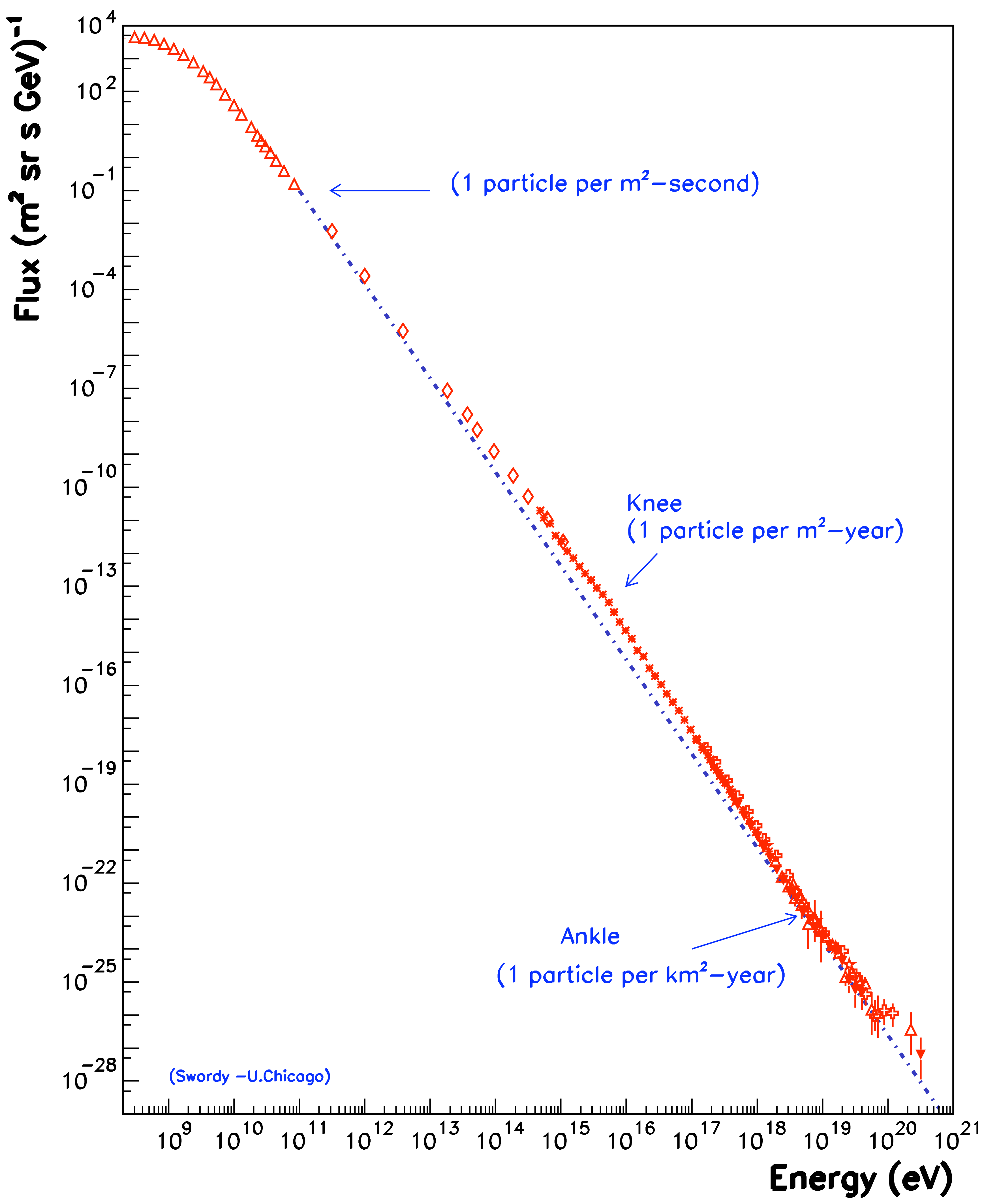

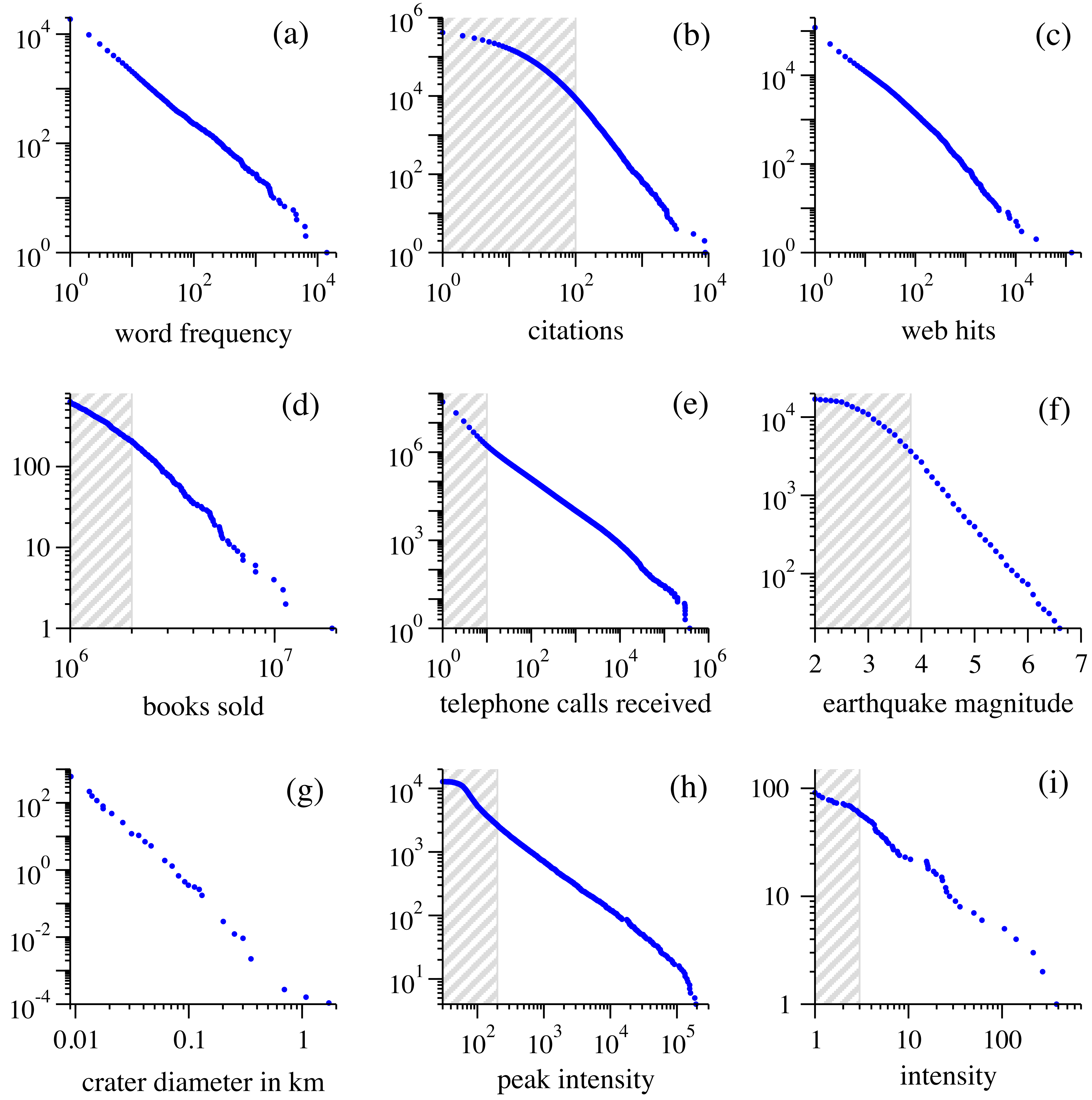

(M. Newman cond-mat/0412004)

The cosmic ray spectrum and power laws in nature

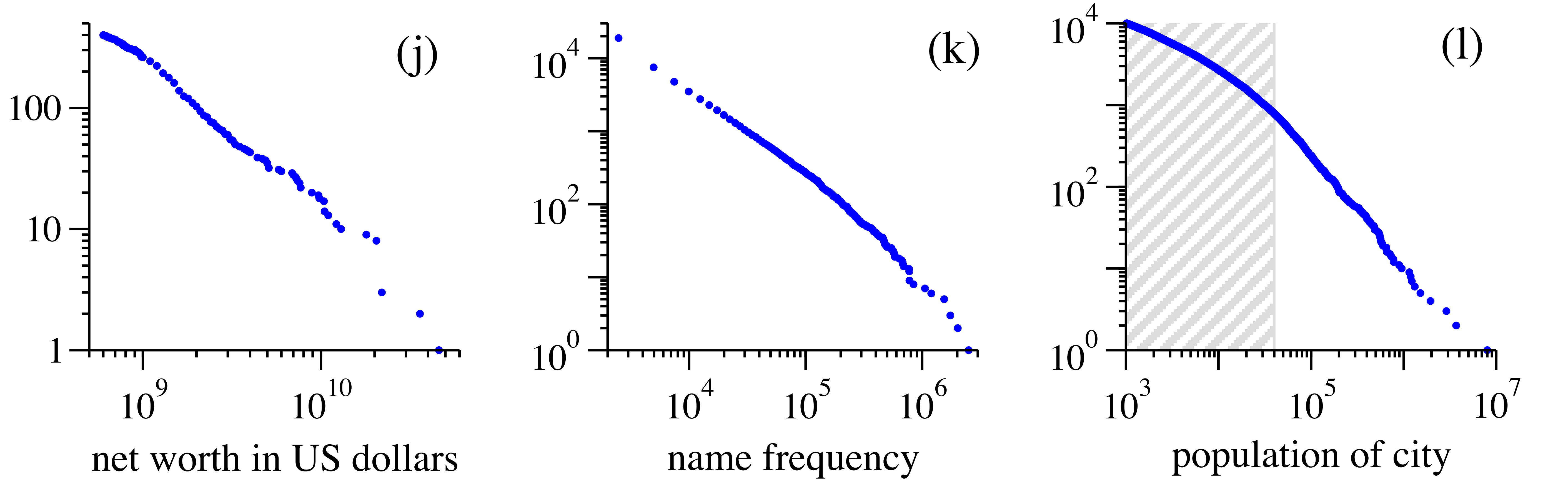

FIG. 4 Cumulative distributions or "rank/frequency plots" of twelve quantities reputed to follow power laws. The distributions were computed as described in Appendix A. Data in the shaded regions were excluded from the calculations of the exponents in Table I. Source references for the data are given in the text. (a) Numbers of occurrences of words in the novel *Moby Dick* by Hermann Melville. (b) Numbers of citations to scientific papers published in 1981, from time of publication until June 1997. (c) Numbers of hits on web sites by 60 000 users of the America Online Internet service for the day of 1 December 1997. (d) Numbers of copies of bestselling books sold in the US between 1895 and 1965. (e) Number of calls received by AT&T telephone customers in the US for a single day. (f) Magnitude of earthquakes in California between January 1910 and May 1992. Magnitude is proportional to the logarithm of the maximum amplitude of the earthquake, and hence the distribution obeys a power law even though the horizontal axis is linear. (g) Diameter of craters on the moon. Vertical axis is measured per square kilometre. (h) Peak gamma-ray intensity of solar flares in counts per second, measured from Earth orbit between February 1980 and November 1989. (i) Intensity of wars from 1816 to 1980, measured as battle deaths per 10 000 of the population of the participating countries. (j) Aggregate net worth in dollars of the richest individuals in the US in October 2003. (k) Frequency of occurrence of family names in the US in the year 1990. (l) Populations of US cities in the year 2000.

(M. Newman cond-mat/0412004)

The cosmic ray spectrum and power laws in nature

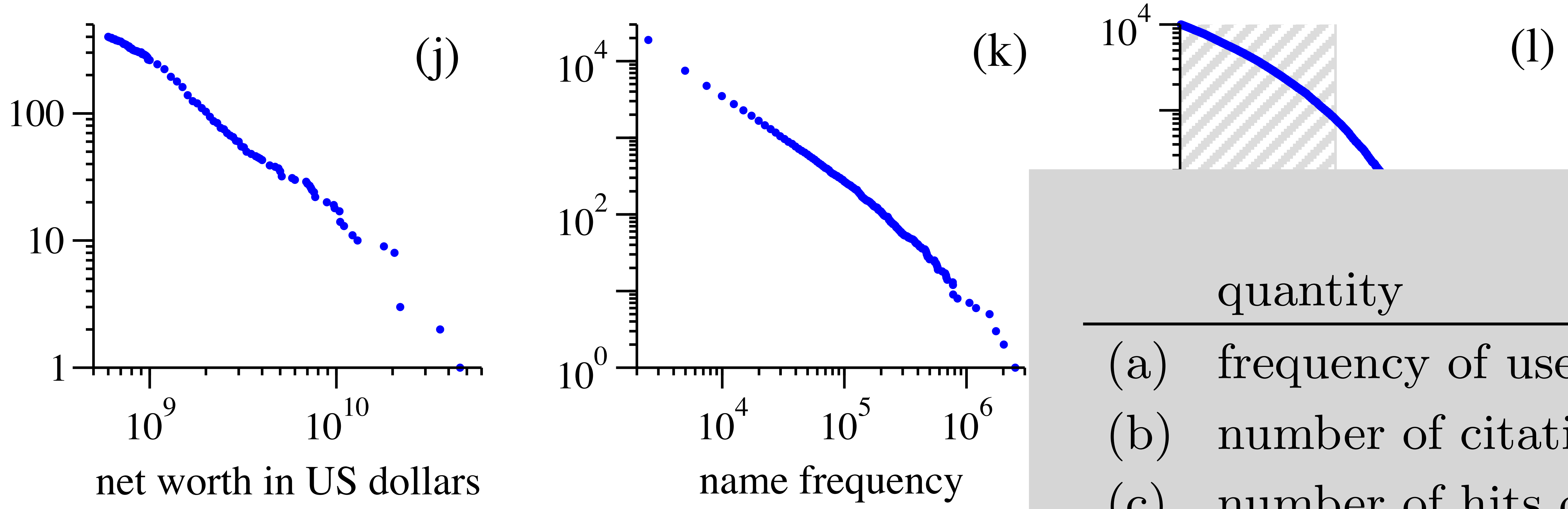

FIG. 4 Cumulative distributions or "rank/frequency plots" of twelve quantiti
were computed as described in Appendix A. Data in the shaded regions were
in Table I. Source references for the data are given in the text. (a) Number
by Hermann Melville. (b) Numbers of citations to scientific papers publish
1997. (c) Numbers of hits on web sites by 60 000 users of the America Online
(d) Numbers of copies of bestselling books sold in the US between 1895 ar
telephone customers in the US for a single day. (f) Magnitude of earthquakes i
Magnitude is proportional to the logarithm of the maximum amplitude of th
power law even though the horizontal axis is linear. (g) Diameter of craters c
kilometre. (h) Peak gamma-ray intensity of solar flares in counts per secon
1980 and November 1989. (i) Intensity of wars from 1816 to 1980, measured a
participating countries. (j) Aggregate net worth in dollars of the richest indiv
of occurrence of family names in the US in the year 1990. (l) Populations of

	quantity	minimum $x_{\min}$	exponent α
(a)	frequency of use of words	1	2.20(1)
(b)	number of citations to papers	100	3.04(2)
(c)	number of hits on web sites	1	2.40(1)
(d)	copies of books sold in the US	2 000 000	3.51(16)
(e)	telephone calls received	10	2.22(1)
(f)	magnitude of earthquakes	3.8	3.04(4)
(g)	diameter of moon craters	0.01	3.14(5)
(h)	intensity of solar flares	200	1.83(2)
(i)	intensity of wars	3	1.80(9)
(j)	net worth of Americans	\$600m	2.09(4)
(k)	frequency of family names	10 000	1.94(1)
(l)	population of US cities	40 000	2.30(5)

(M. Newman cond-mat/0412004)

The cosmic ray spectrum and power laws in nature

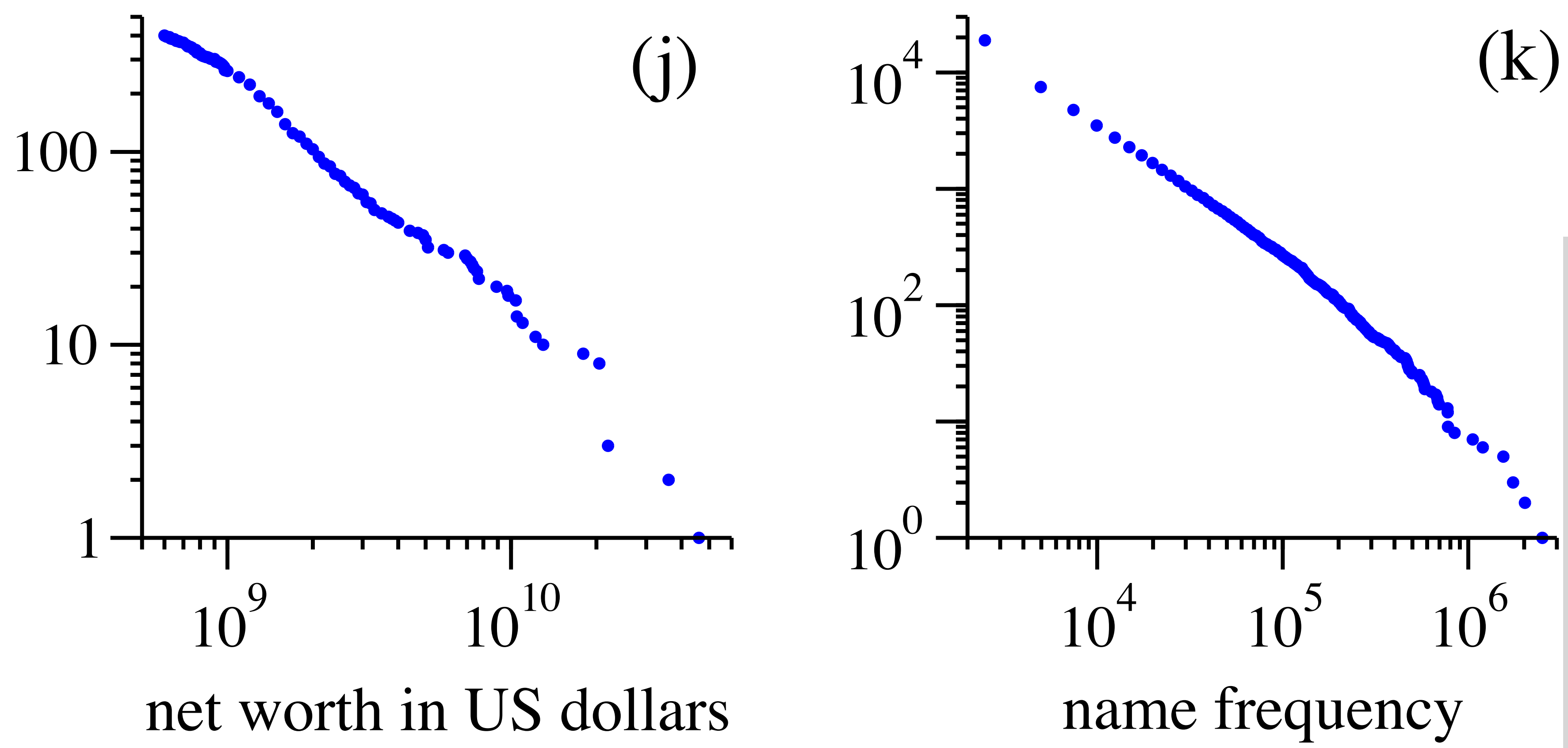

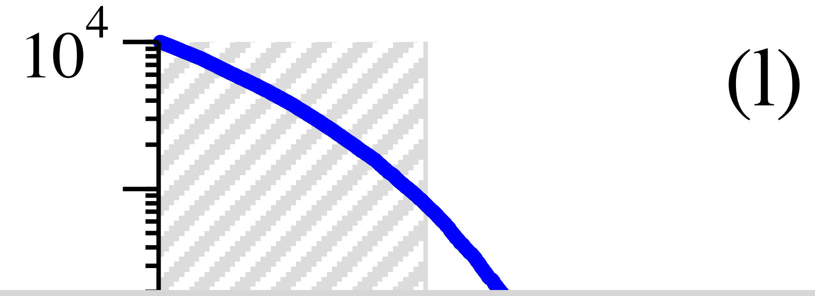

FIG. 4 Cumulative distributions or "rank/frequency plots" of twelve quantiti
were computed as described in Appendix A. Data in the shaded regions were
in Table I. Source references for the data are given in the text. (a) Number
by Hermann Melville. (b) Numbers of citations to scientific papers publish
1997. (c) Numbers of hits on web sites by 60 000 users of the America Online
(d) Numbers of copies of bestselling books sold in the US between 1895 ar
telephone customers in the US for a single day. (f) Magnitude of earthquakes i
M
p
k
1980 and November 1989. (i) Intensity of wars from 1816 to 1980, measured a
participating countries. (j) Aggregate net worth in dollars of the richest indiv
of occurrence of family names in the US in the year 1990. (l) Populations of

	quantity	minimum $x_{\min}$	exponent α
(a)	frequency of use of words	1	2.20(1)
(b)	number of citations to papers	100	3.04(2)
(c)	number of hits on web sites	1	2.40(1)
(d)	copies of books sold in the US	2 000 000	3.51(16)
(e)	telephone calls received	10	2.22(1)
(f)	magnitude of earthquakes	3.8	3.04(4)
(g)	diameter of moon craters	0.01	3.14(5)
(h)	intensity of solar flares	200	1.83(2)
			.80(9)
			.09(4)
(k)	frequency of family names	10 000	1.94(1)
(l)	population of US cities	40 000	2.30(5)

We would not be able to learn much from a feature-less power-law flux

(M. Newman cond-mat/0412004)

The cosmic ray spectrum some 10 – 15 years ago

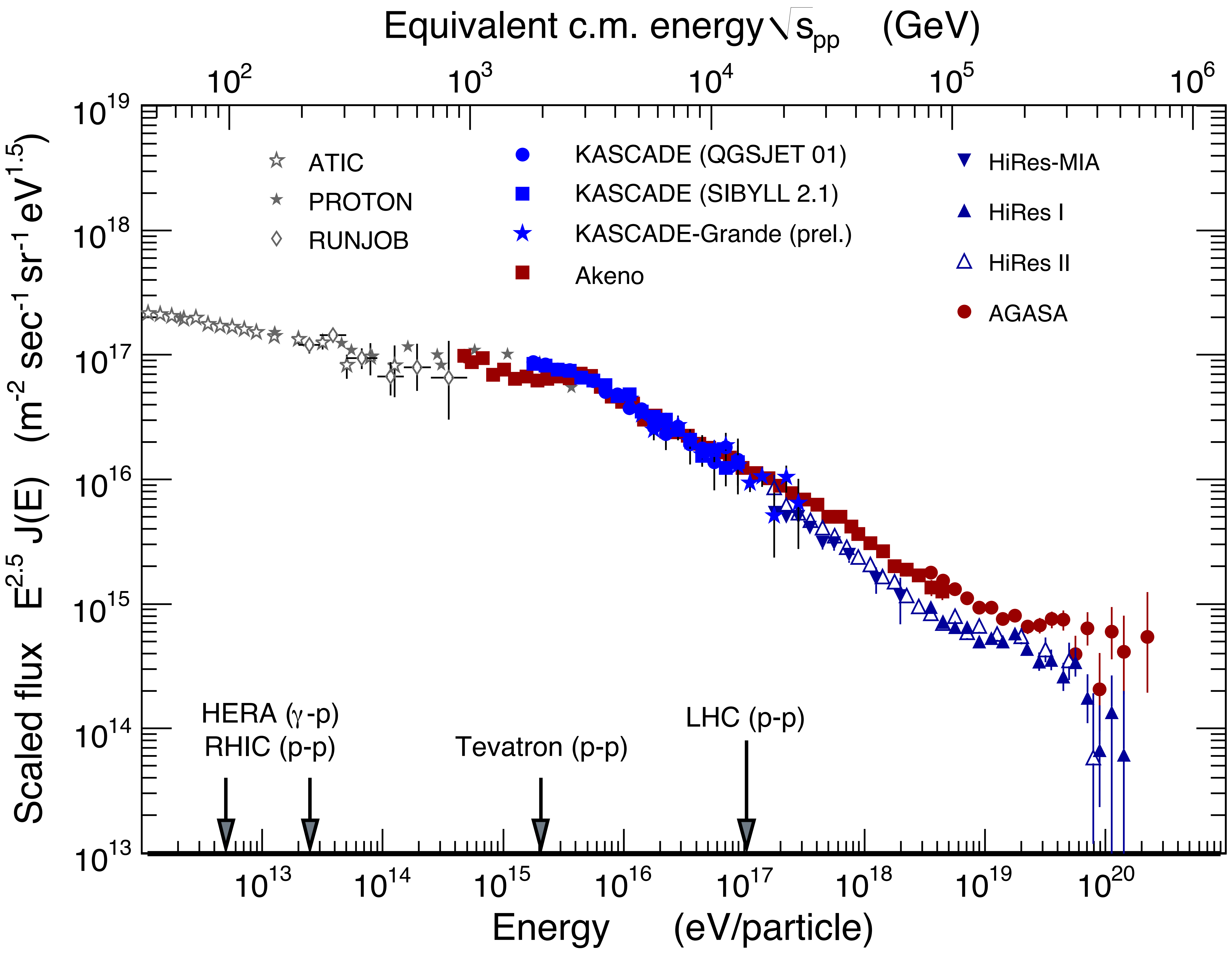

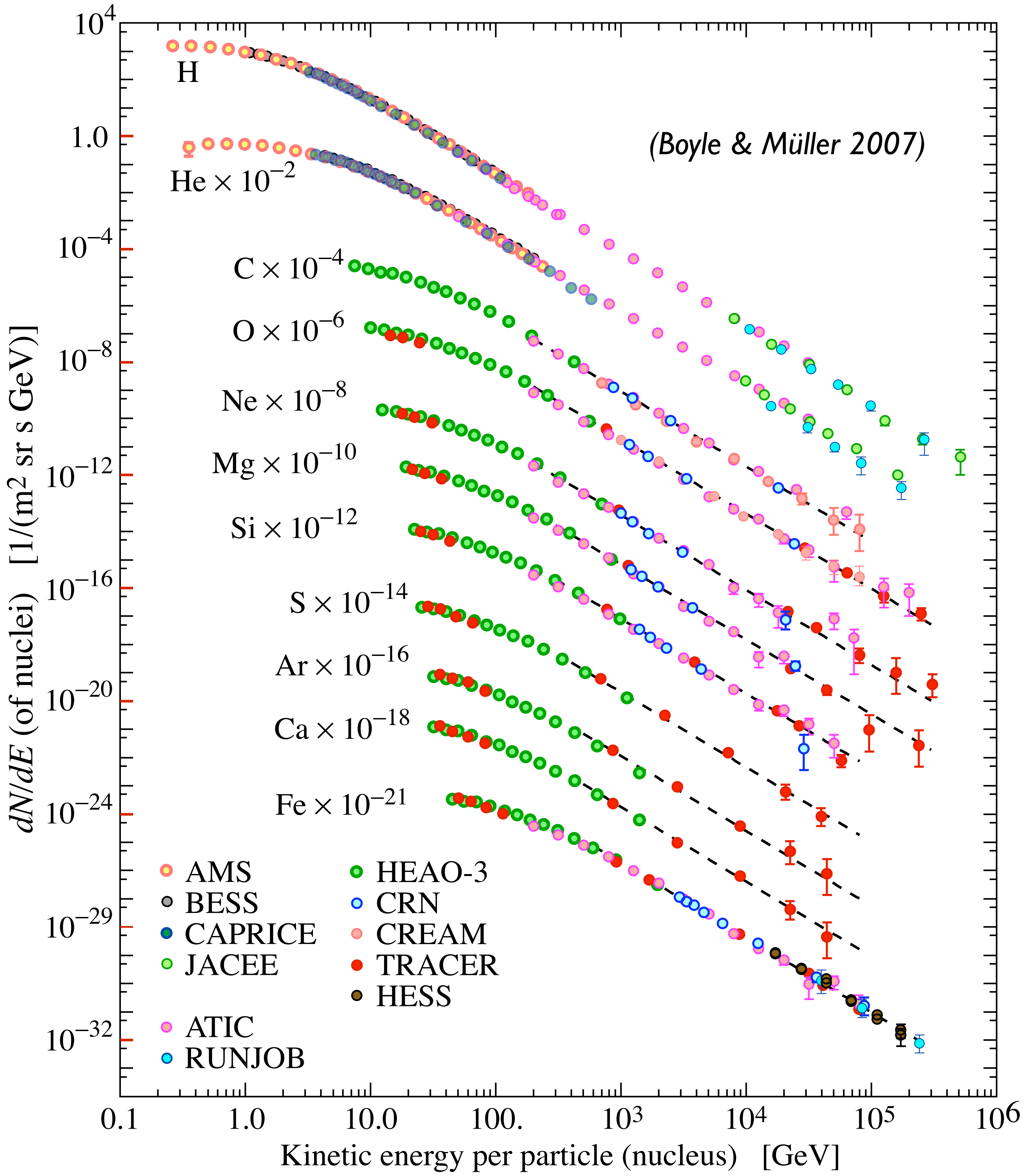

- Knee and ankle clearly established
- Indications for second knee
- Featureless power laws

Extrapolation to ultra-high energy unclear

Fluxes of individual elements approx. power law with same index

Standard model of galactic cosmic rays

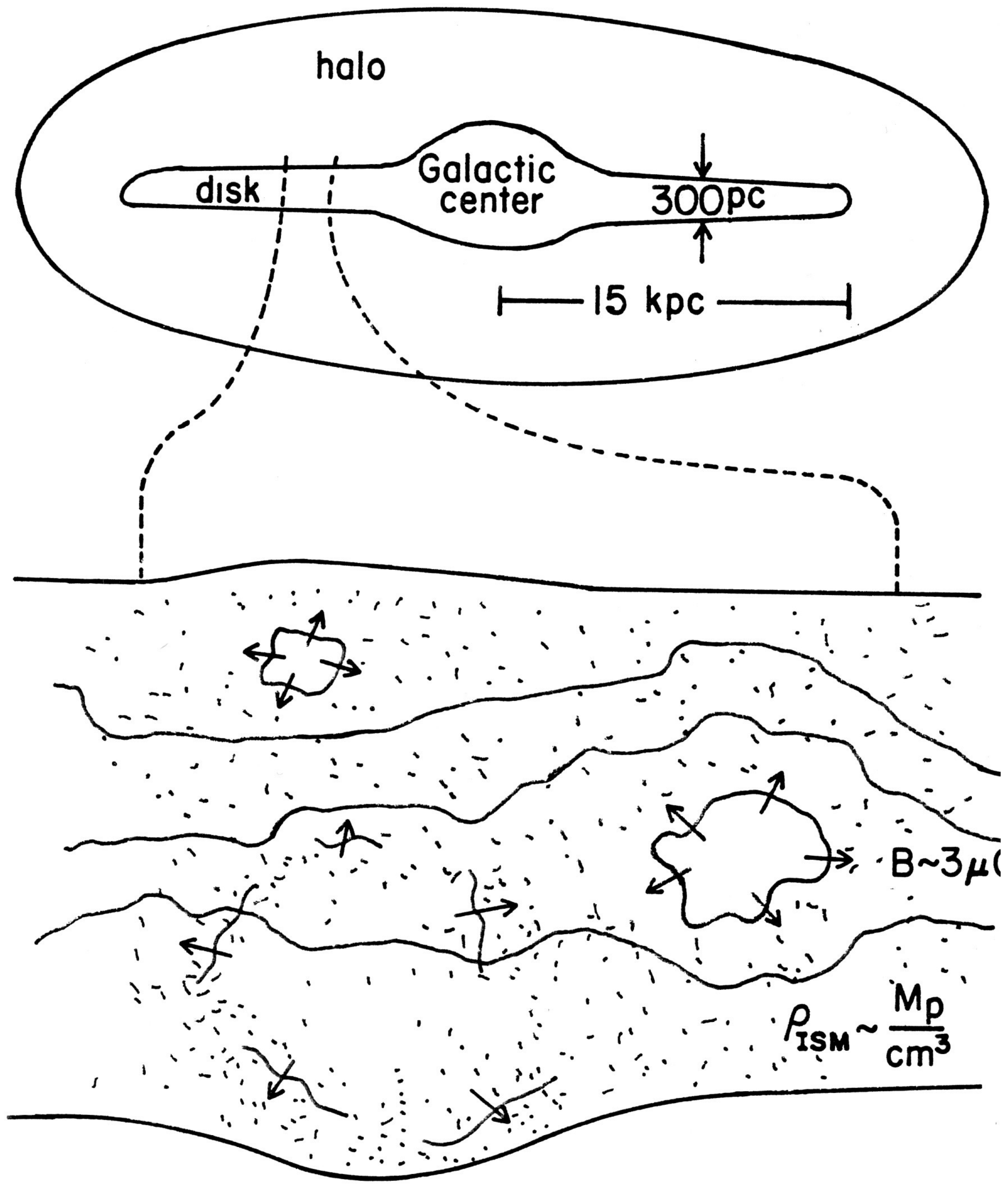

Argument of energy balance: SNR

Fermi shock acceleration on shocks ~ E^{-2}

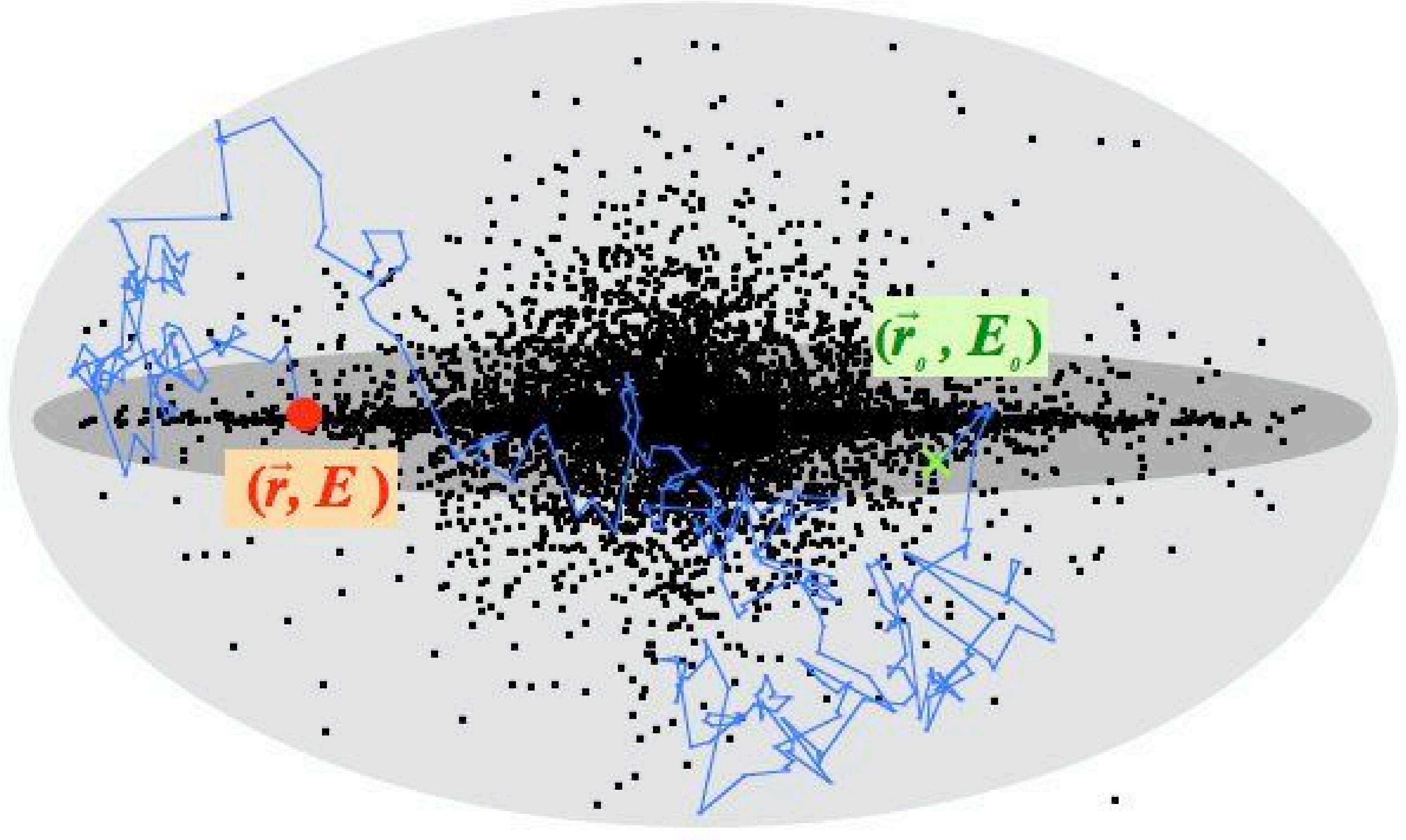

Magnetic diffusion in disk and halo

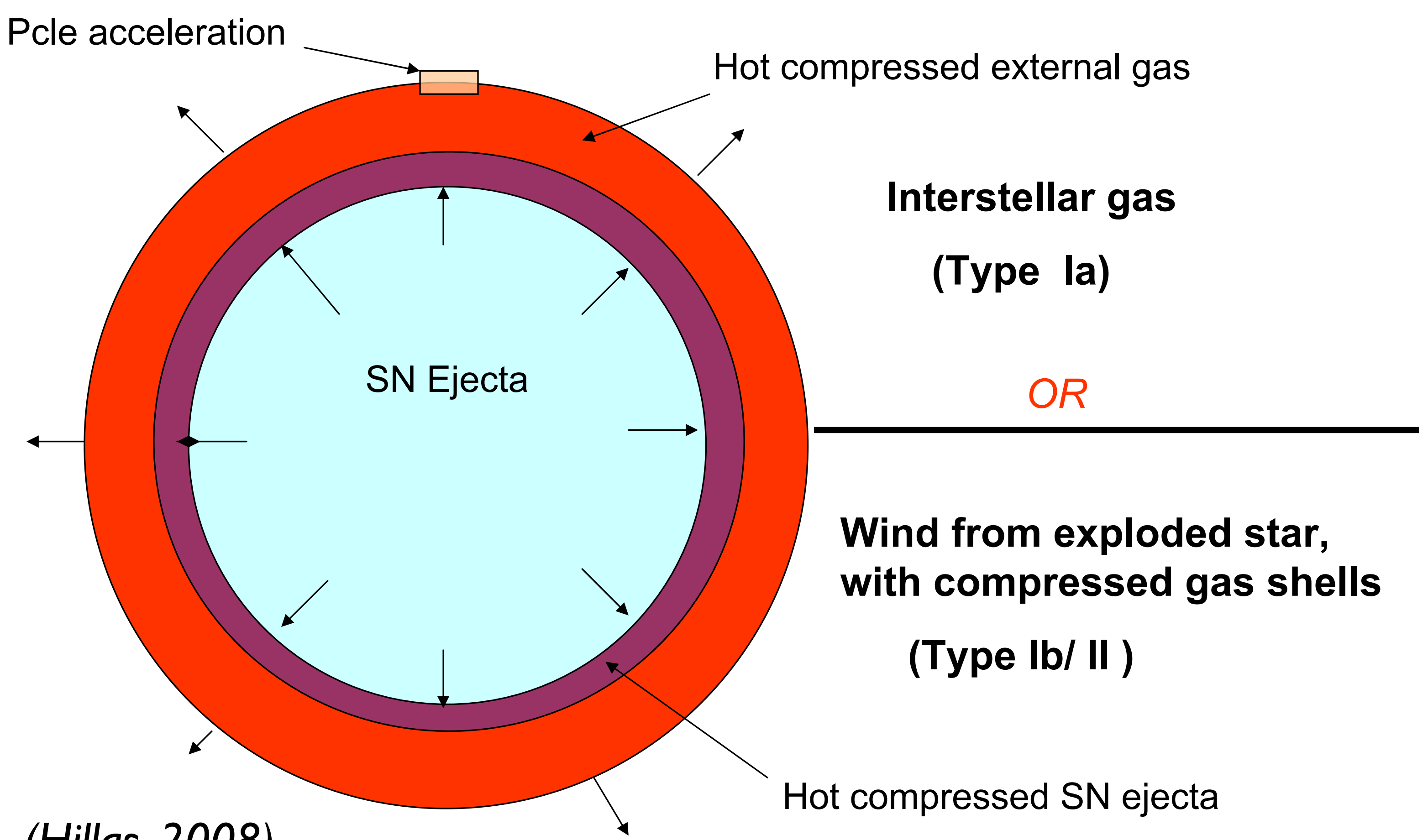

(Hillas, 2008)

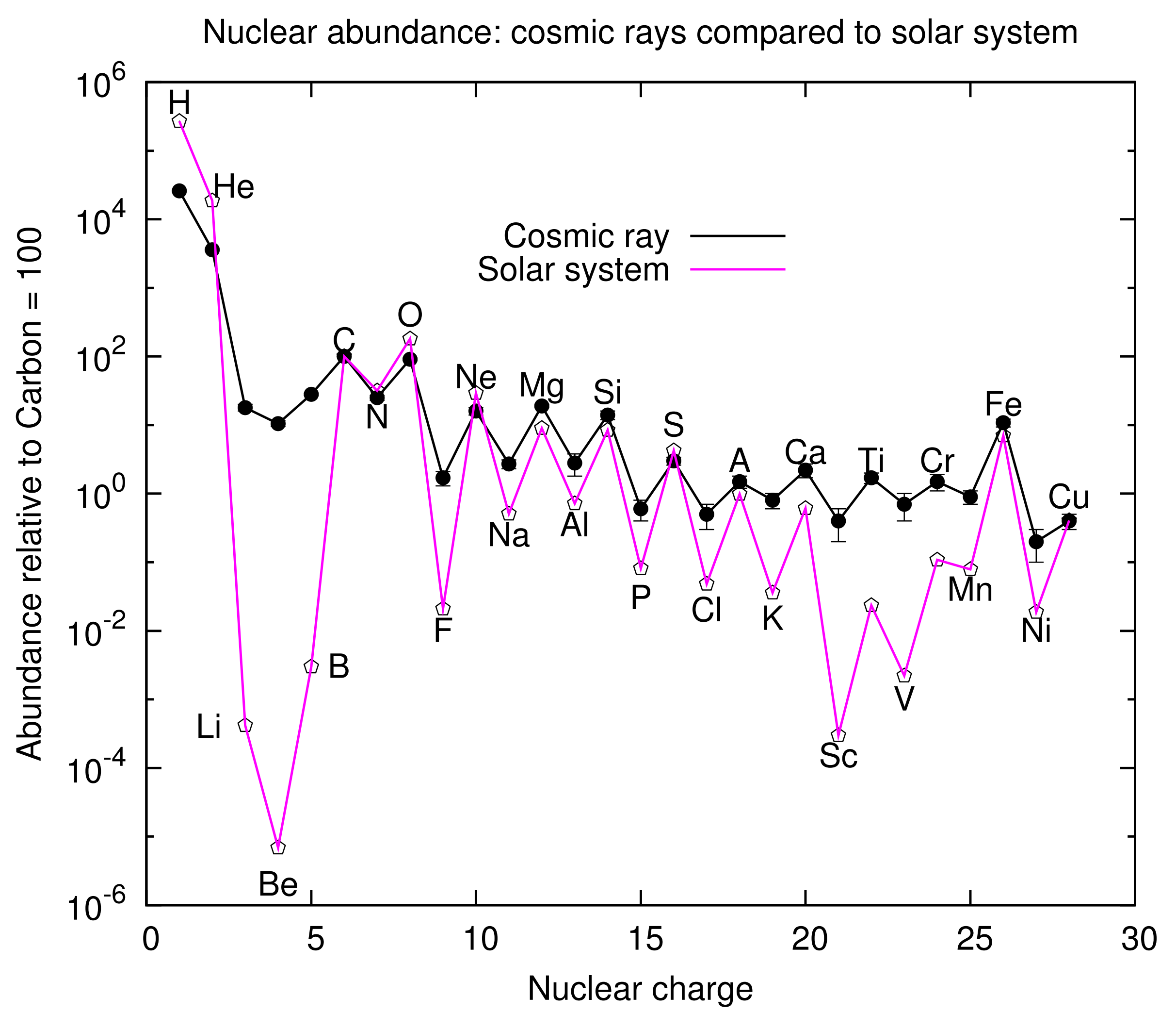

Production of secondary particles

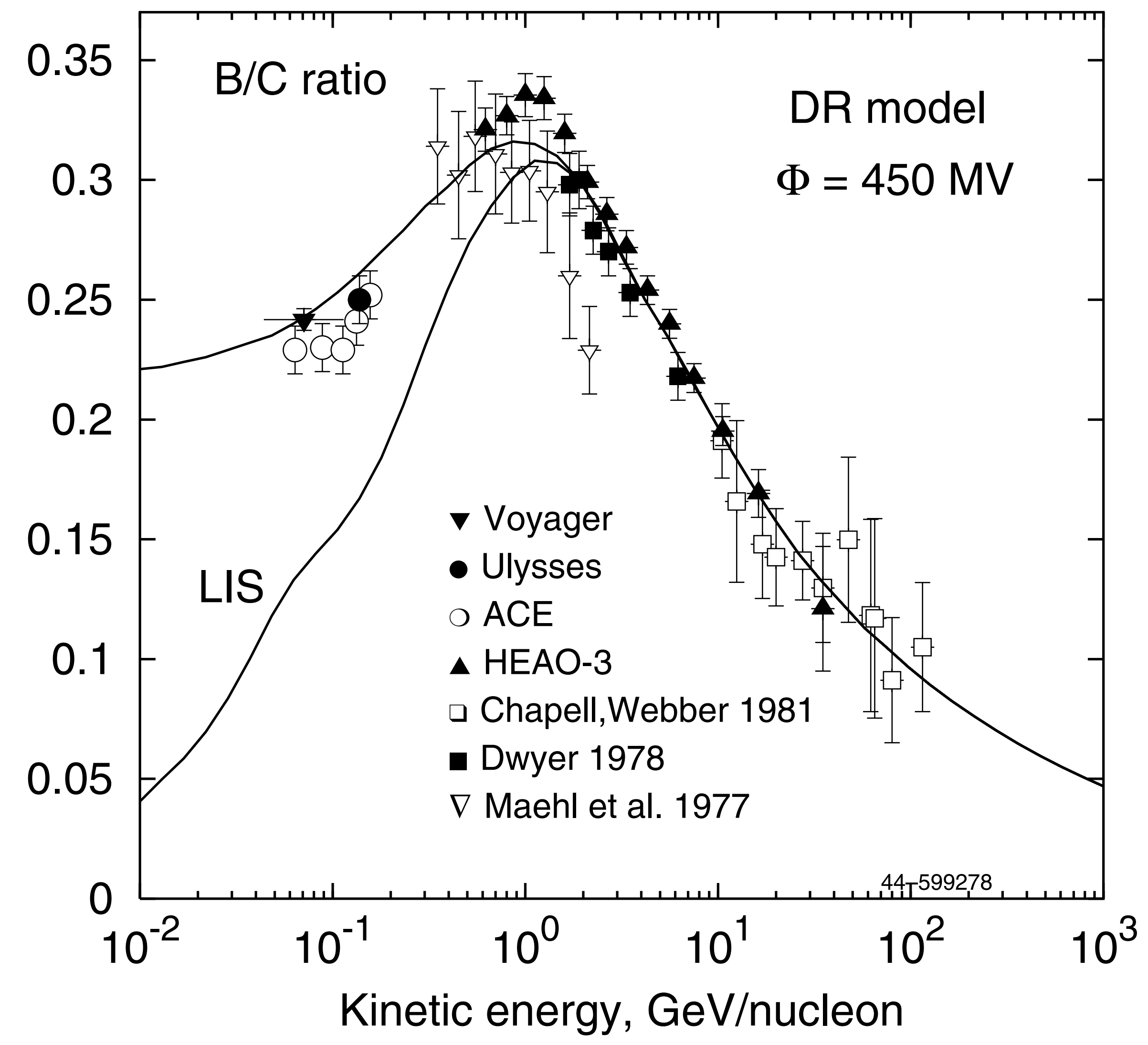

Interpretation of knee in standard model ?

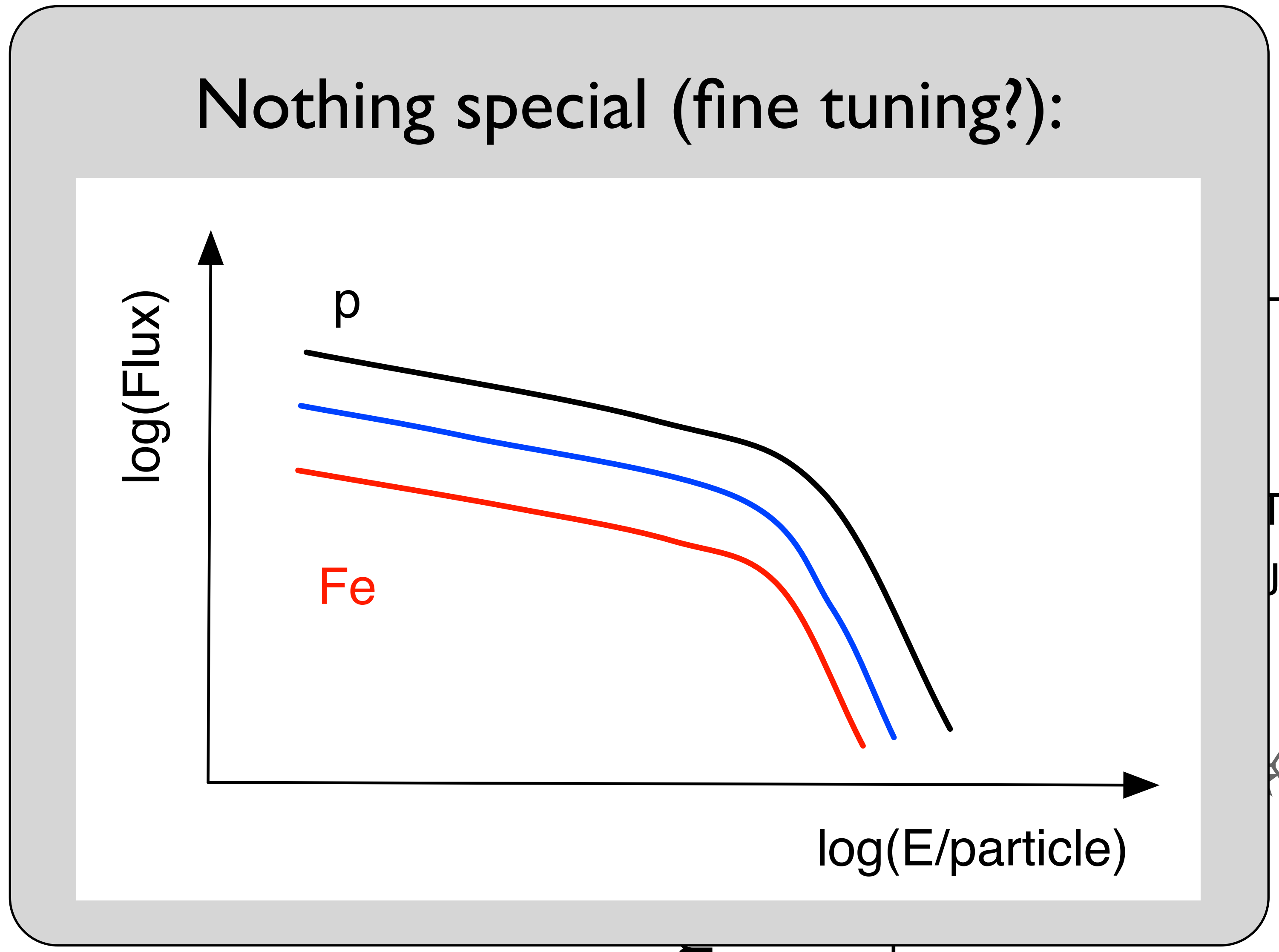

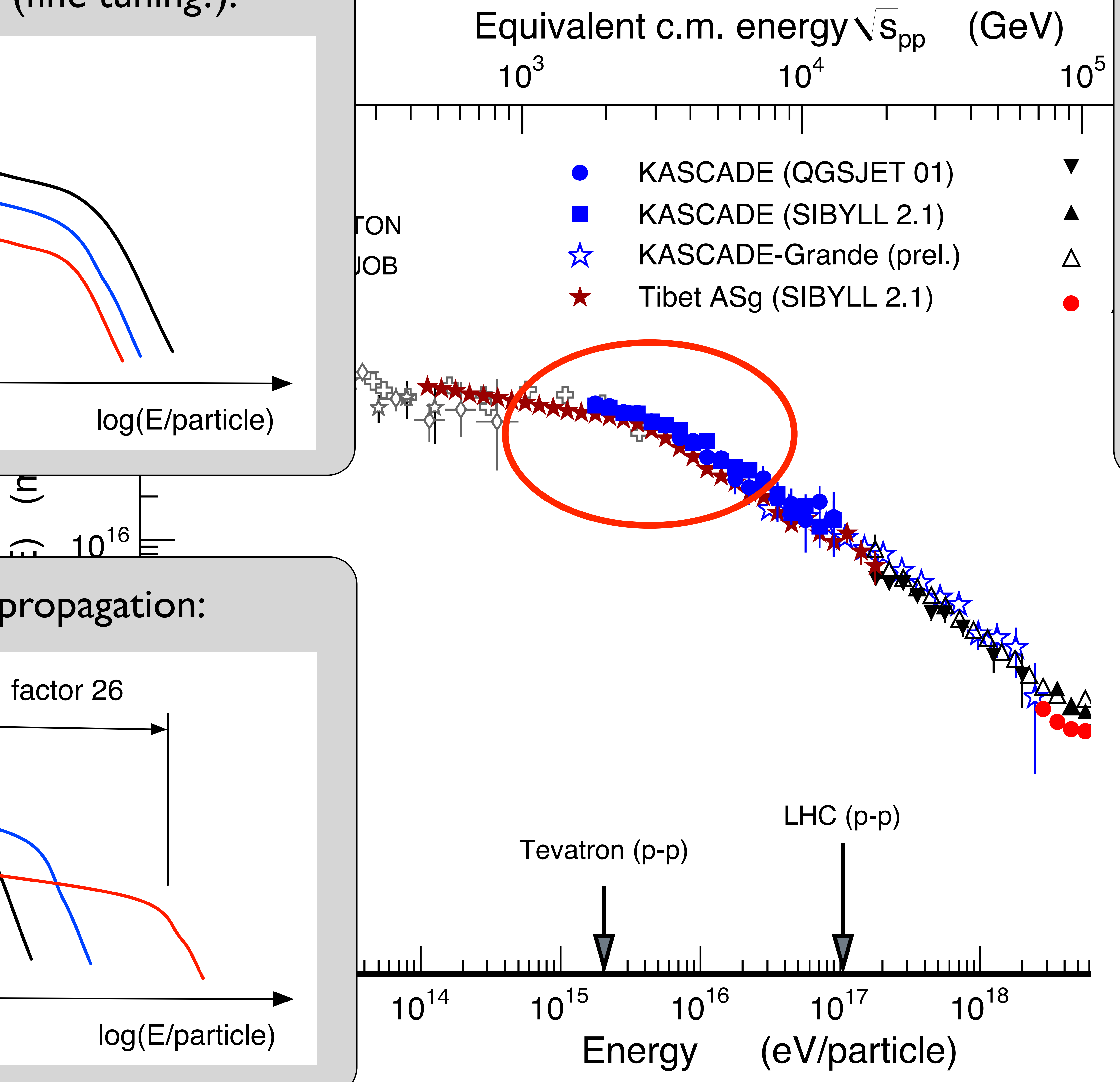

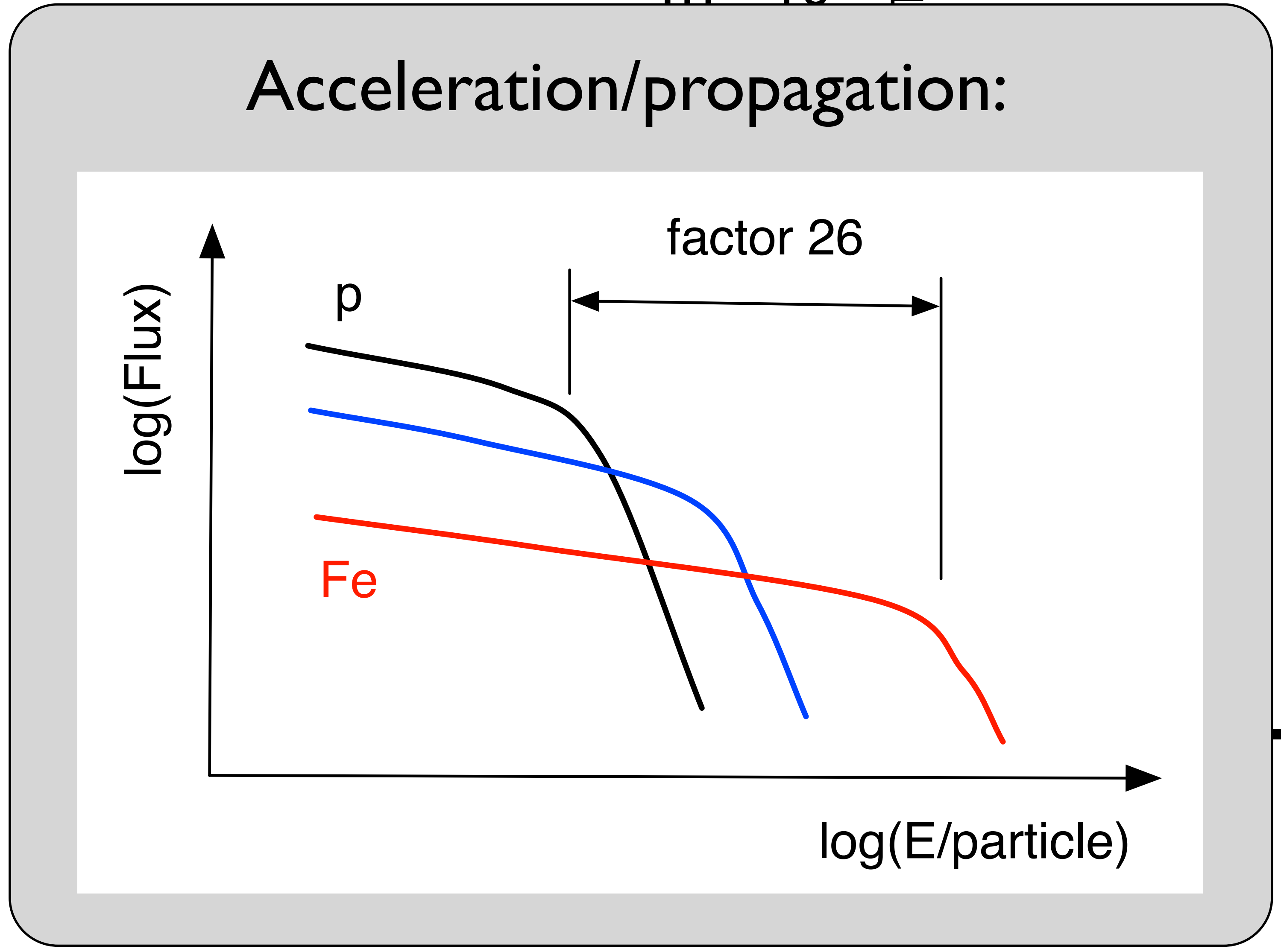

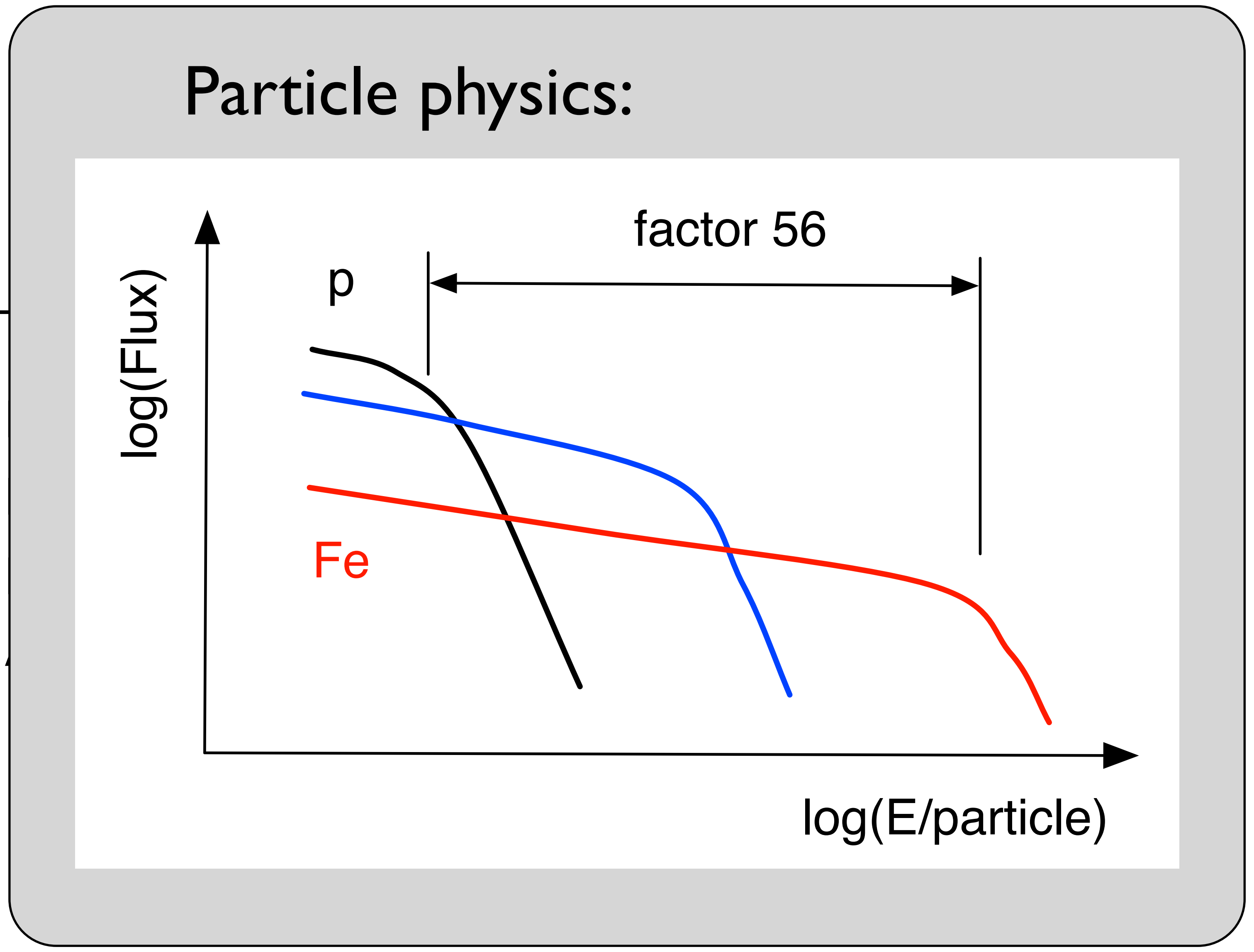

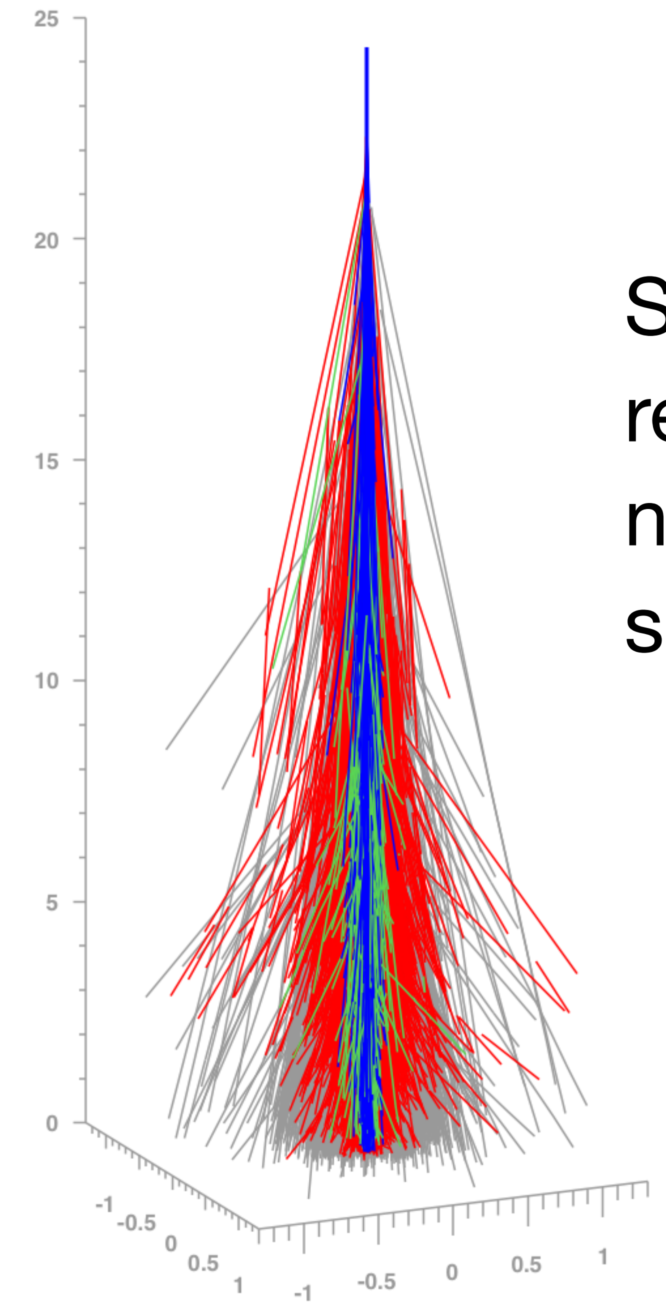

Shower energy wrongly reconstructed due to new particle physics setting at knee energy

The cosmic ray spectrum and power laws in nature

Example:
KASCADE-Grande

CORSIKA simulation

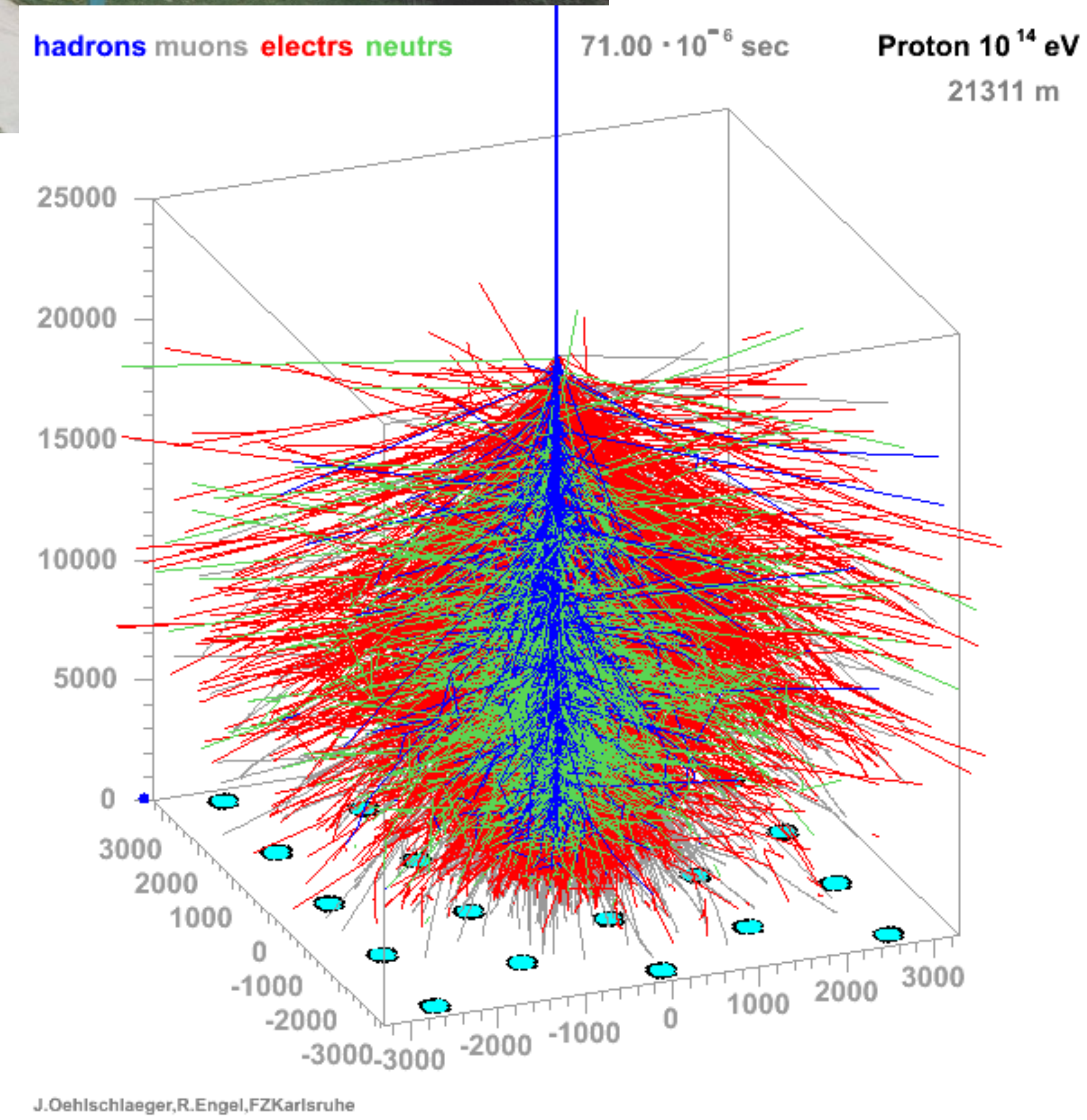

Combined energy-composition analysis

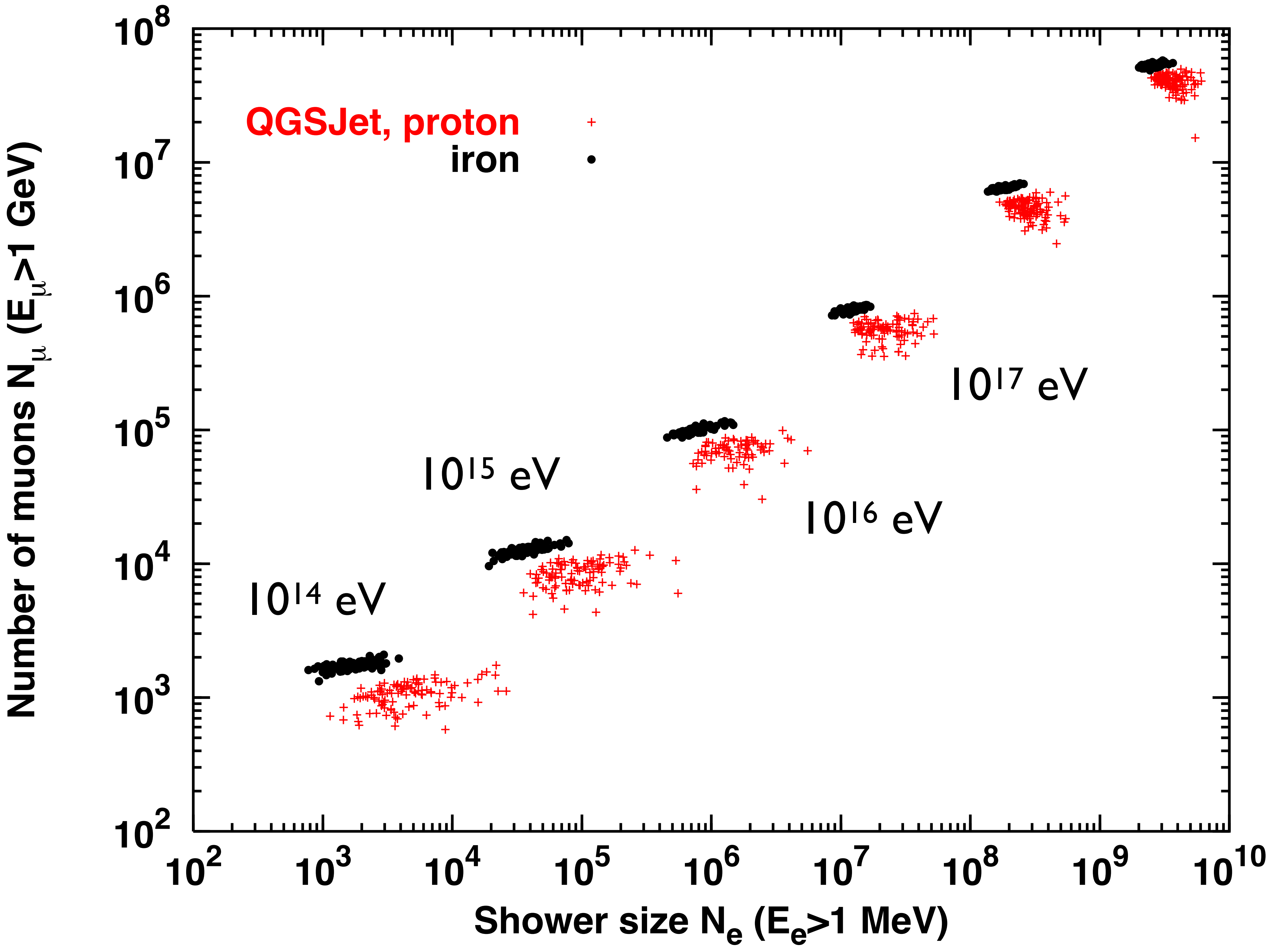

Mass composition at the knee: KASCADE data

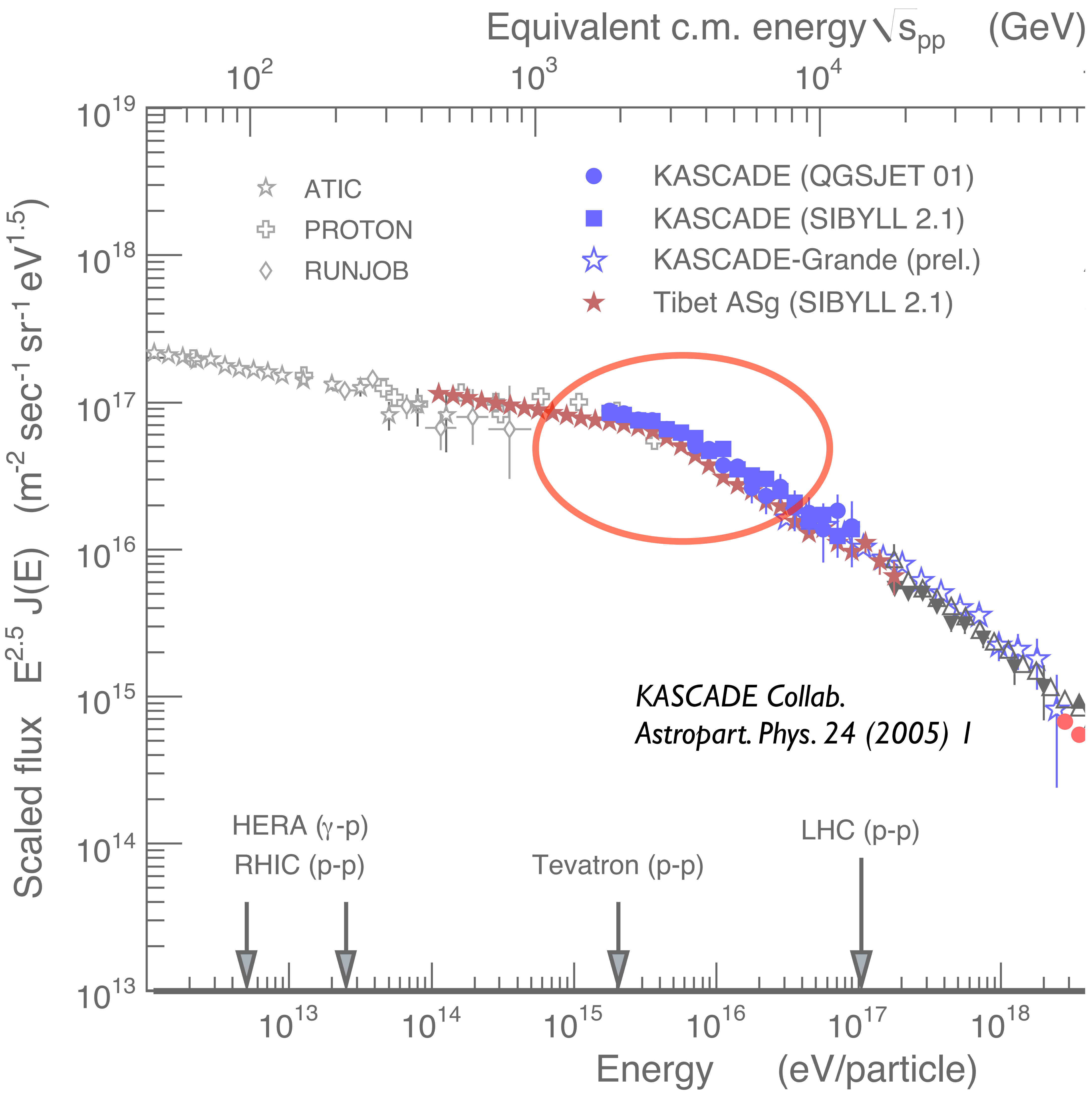

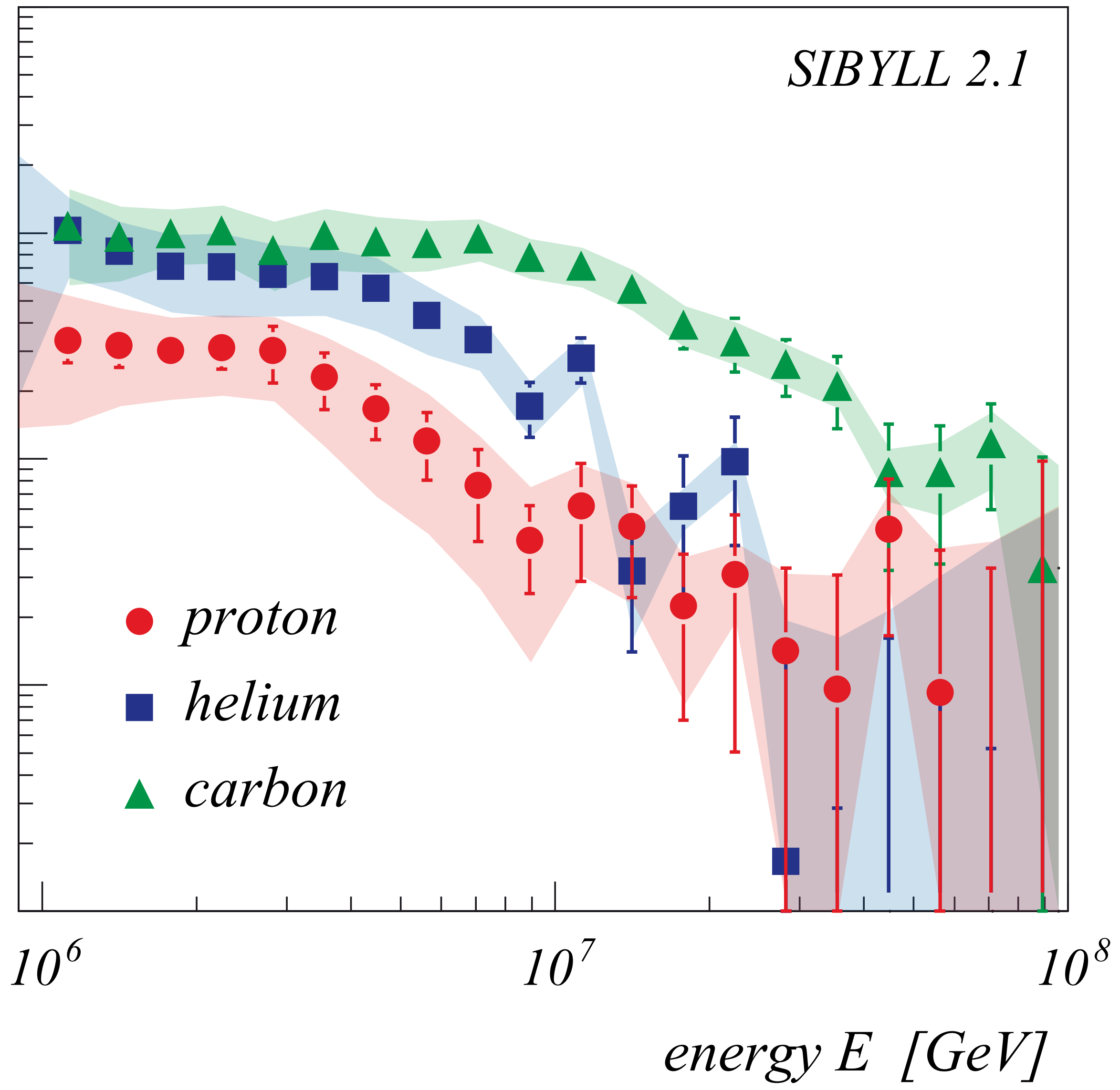

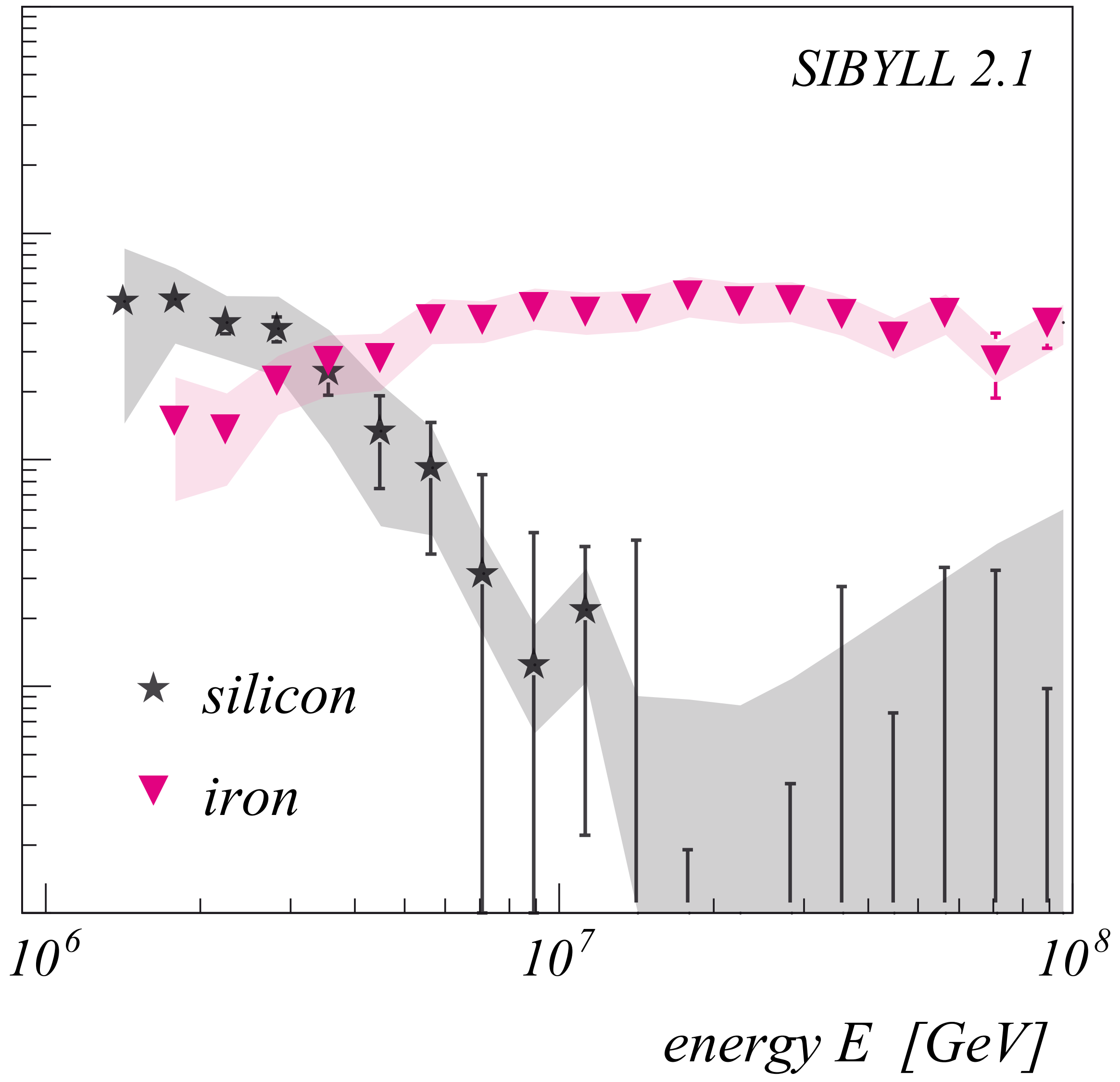

Mass composition at the knee: KASCADE data

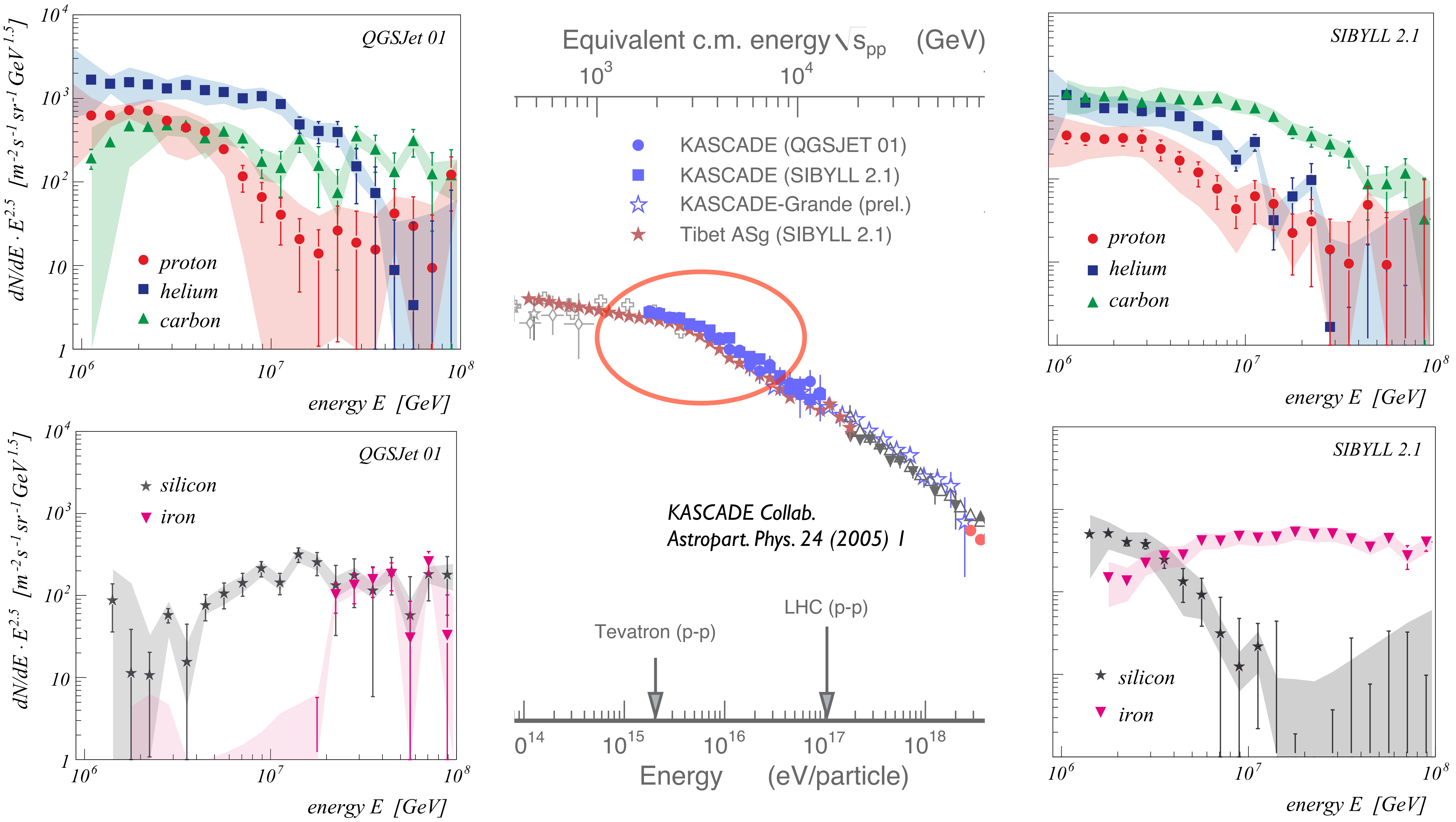

LHC data and interpretation of knee

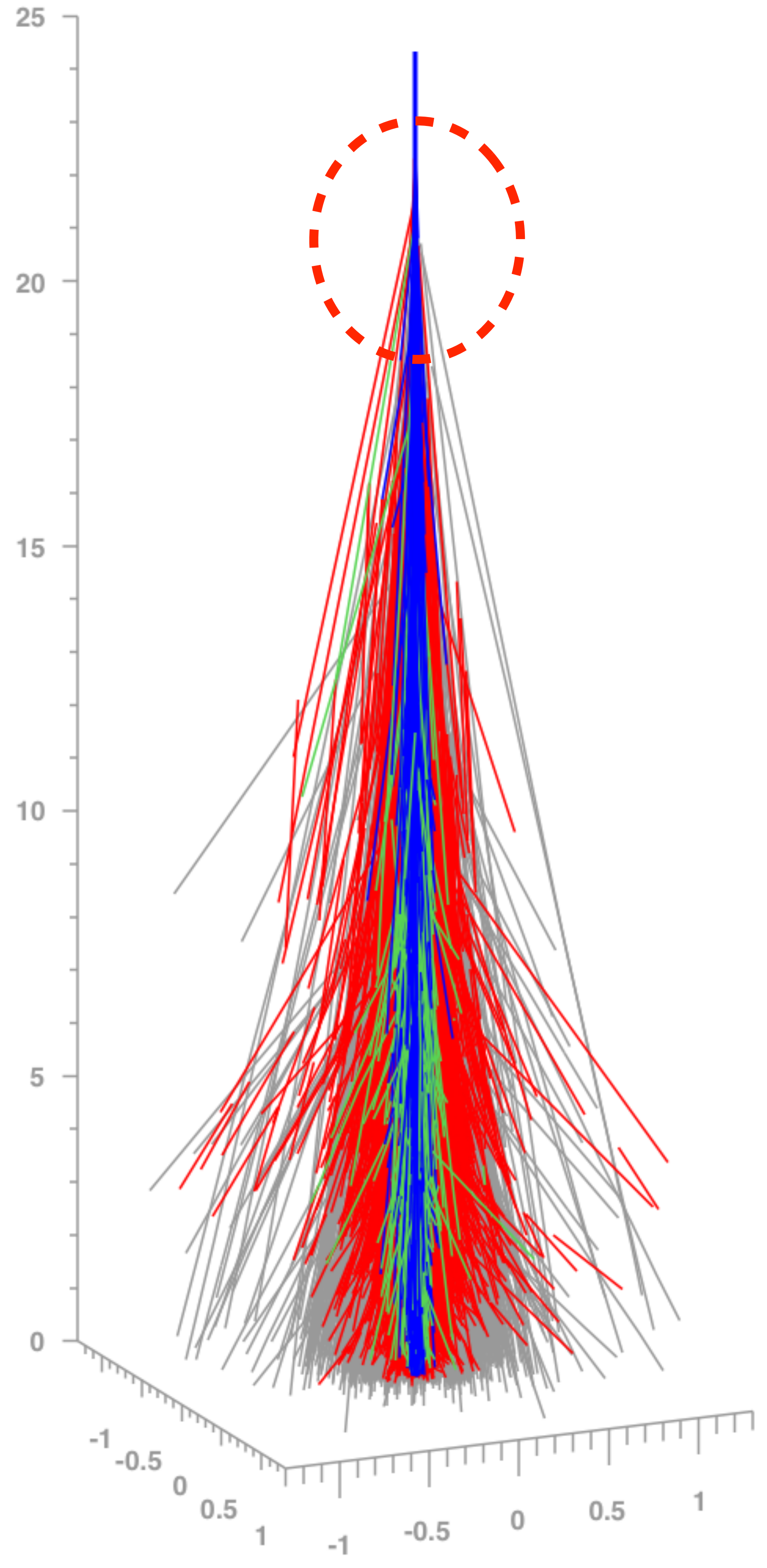

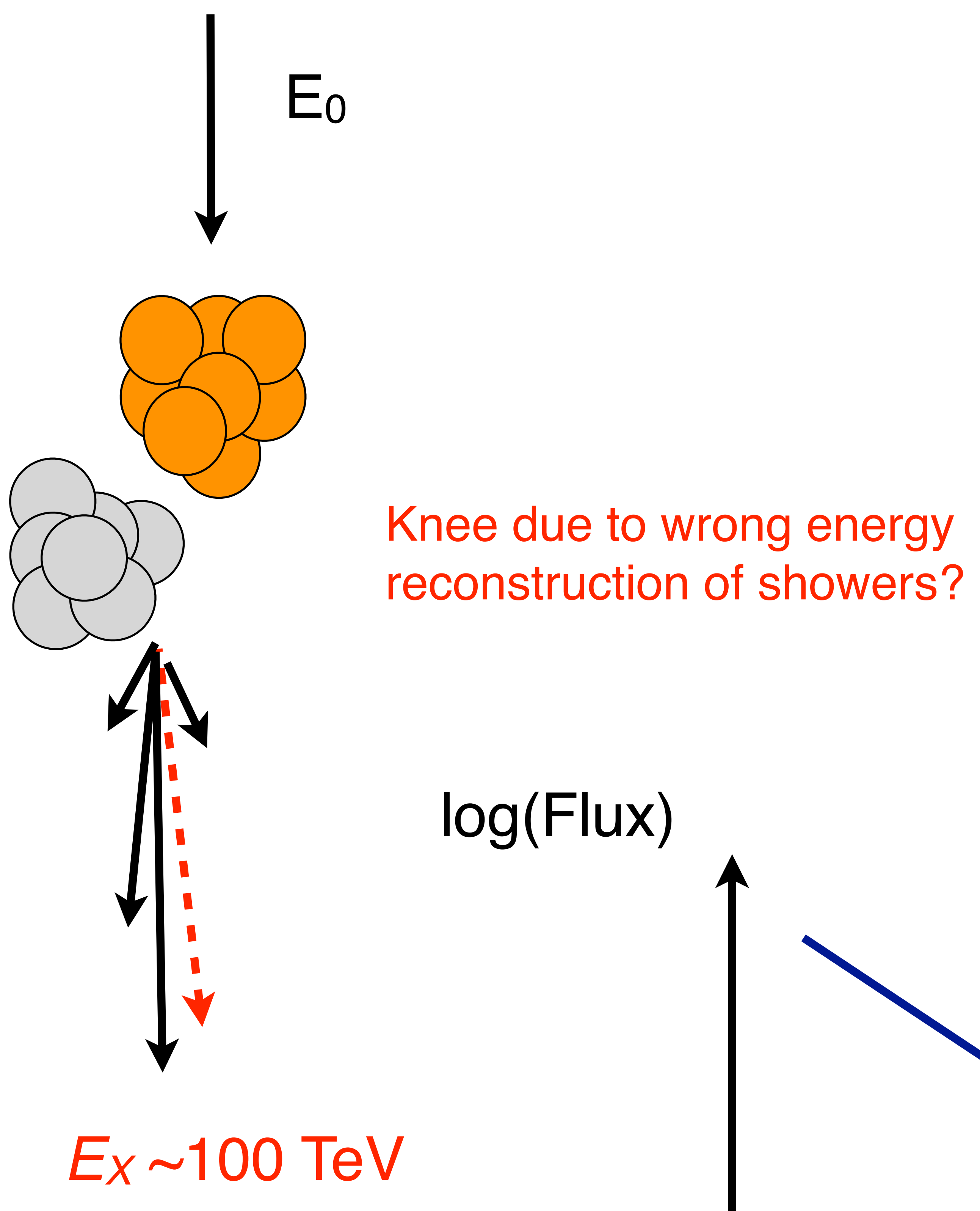

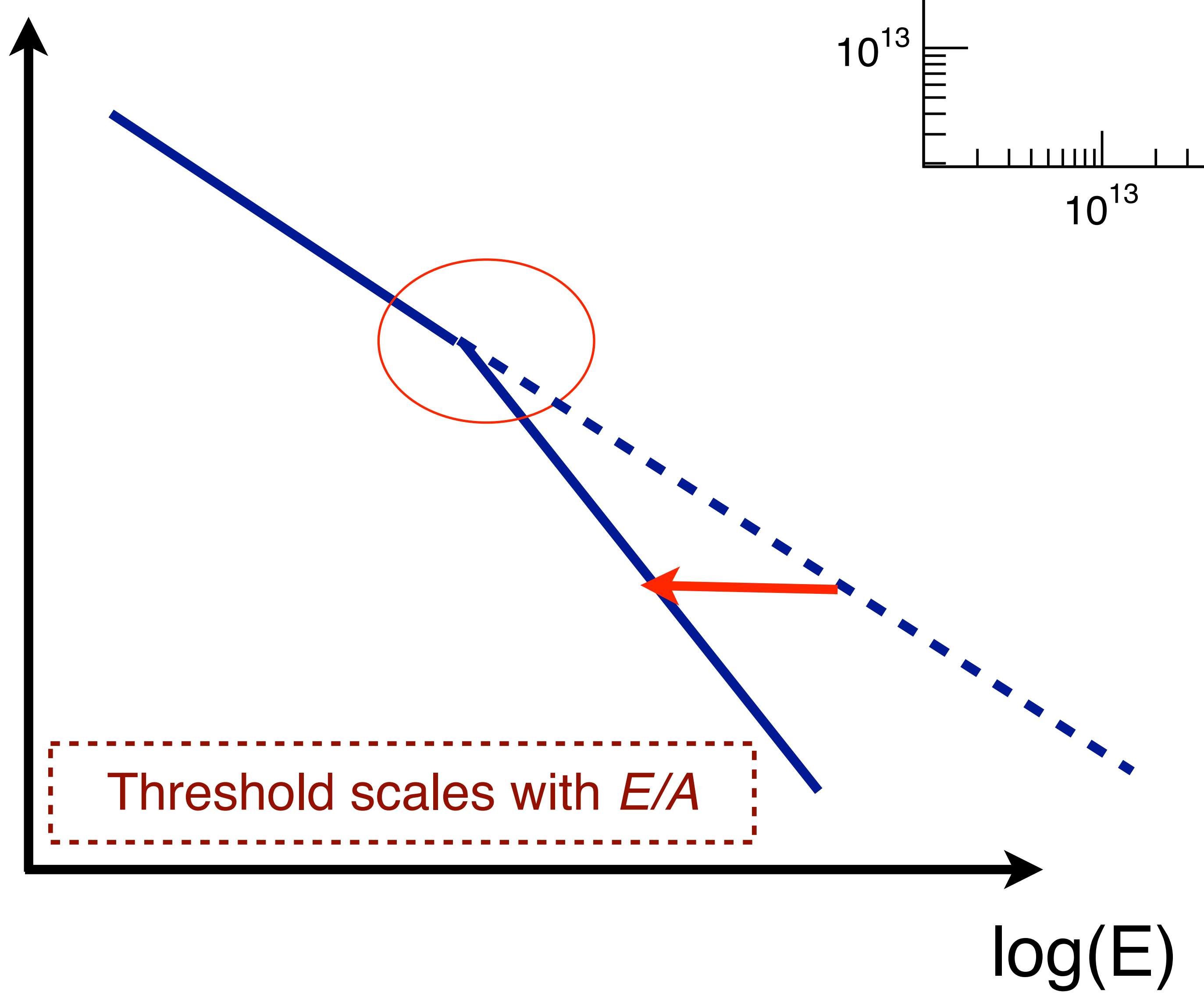

Petrukhin, NPB 151 (2006) 57
Barcelo at al. JACP 06 (2009) 027
Dixit et al. EPJC 68 (2010) 573
Petrukhin NPB 212 (2011) 235

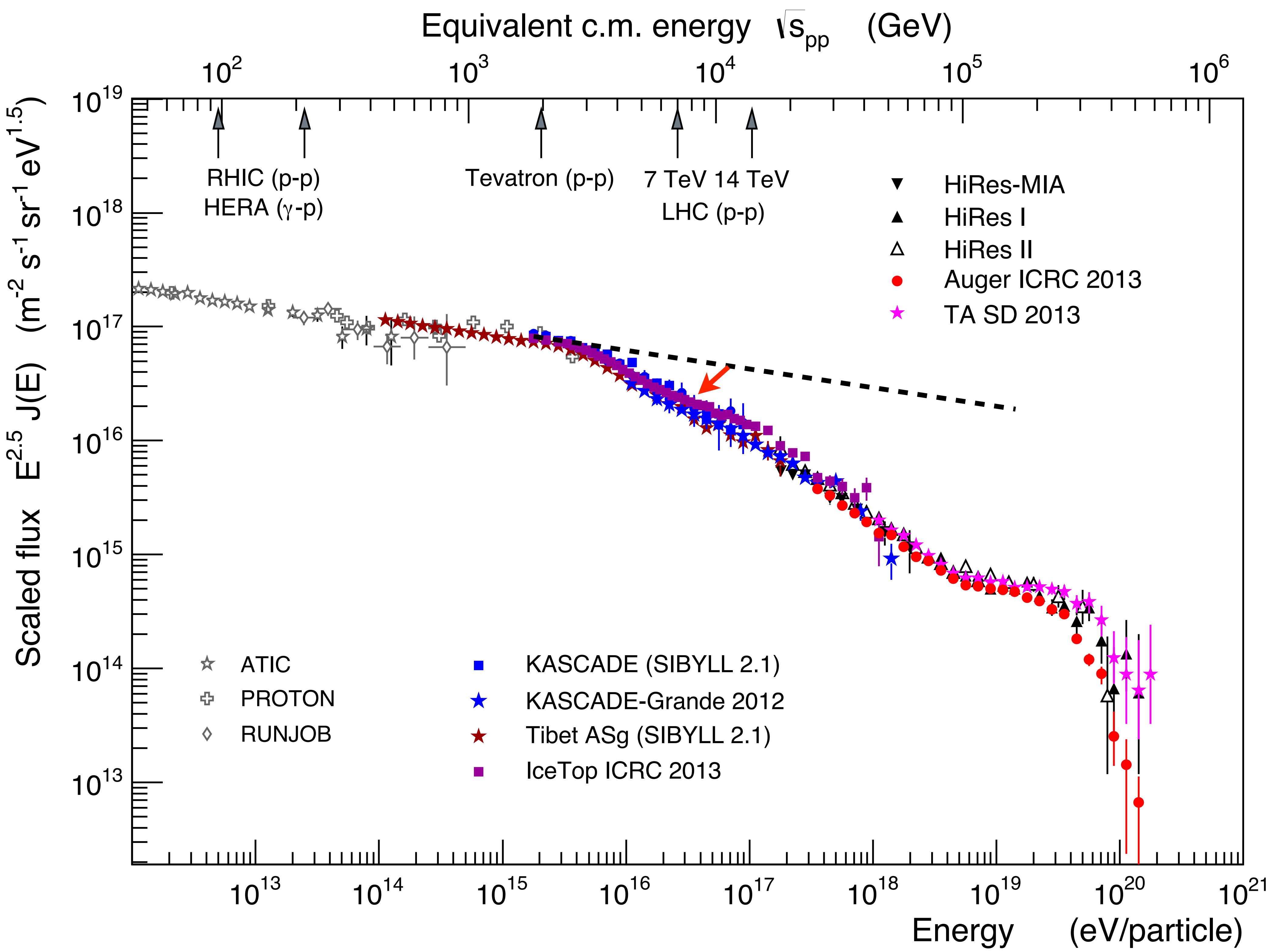

~20% of energy needs to be transferred to invisible channel

No indications for missing energy processes at LHC

(d'Enterria et al., Astropart. Phys. 35, 2011)

Results from other experiments: IceCube

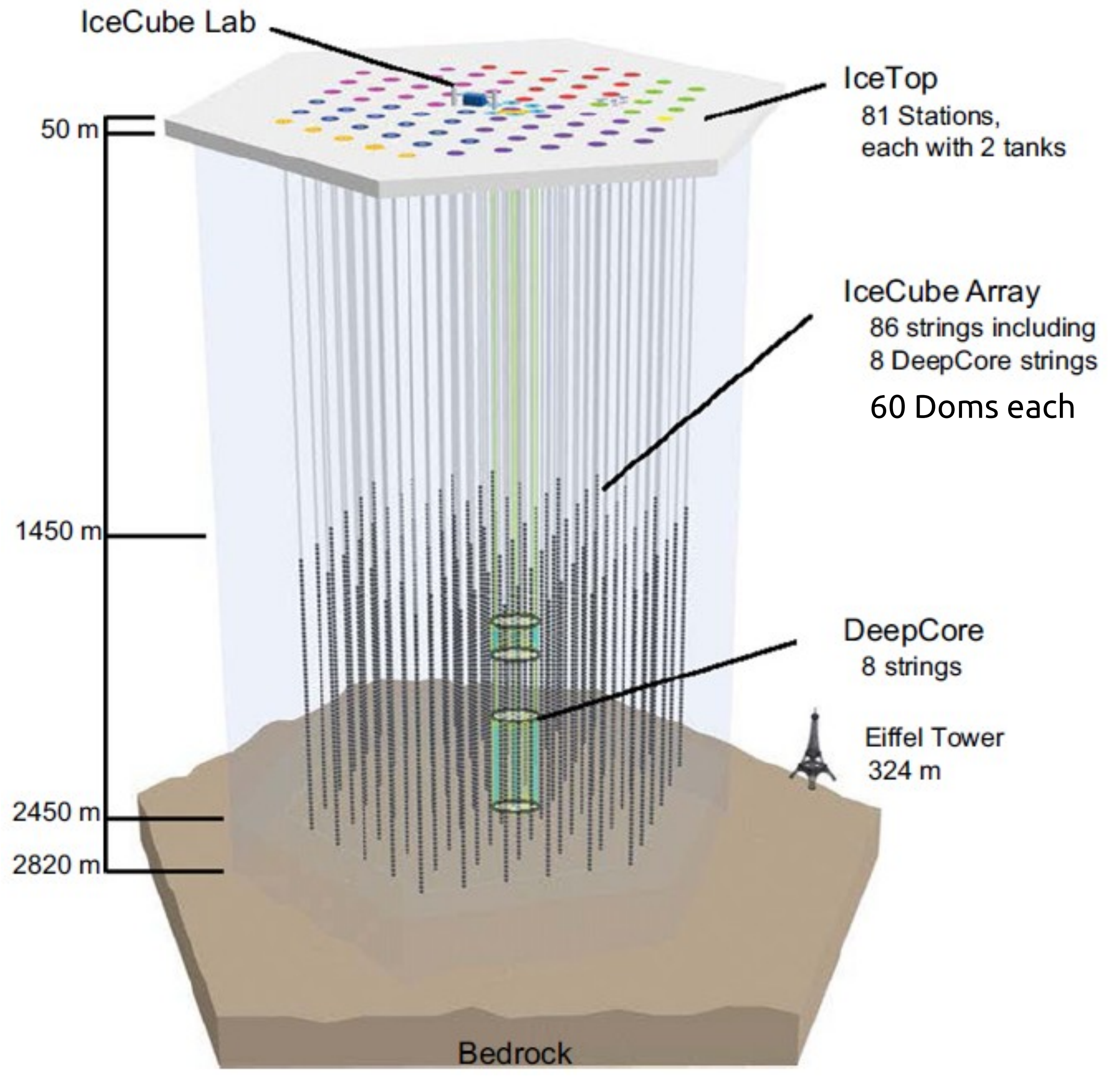

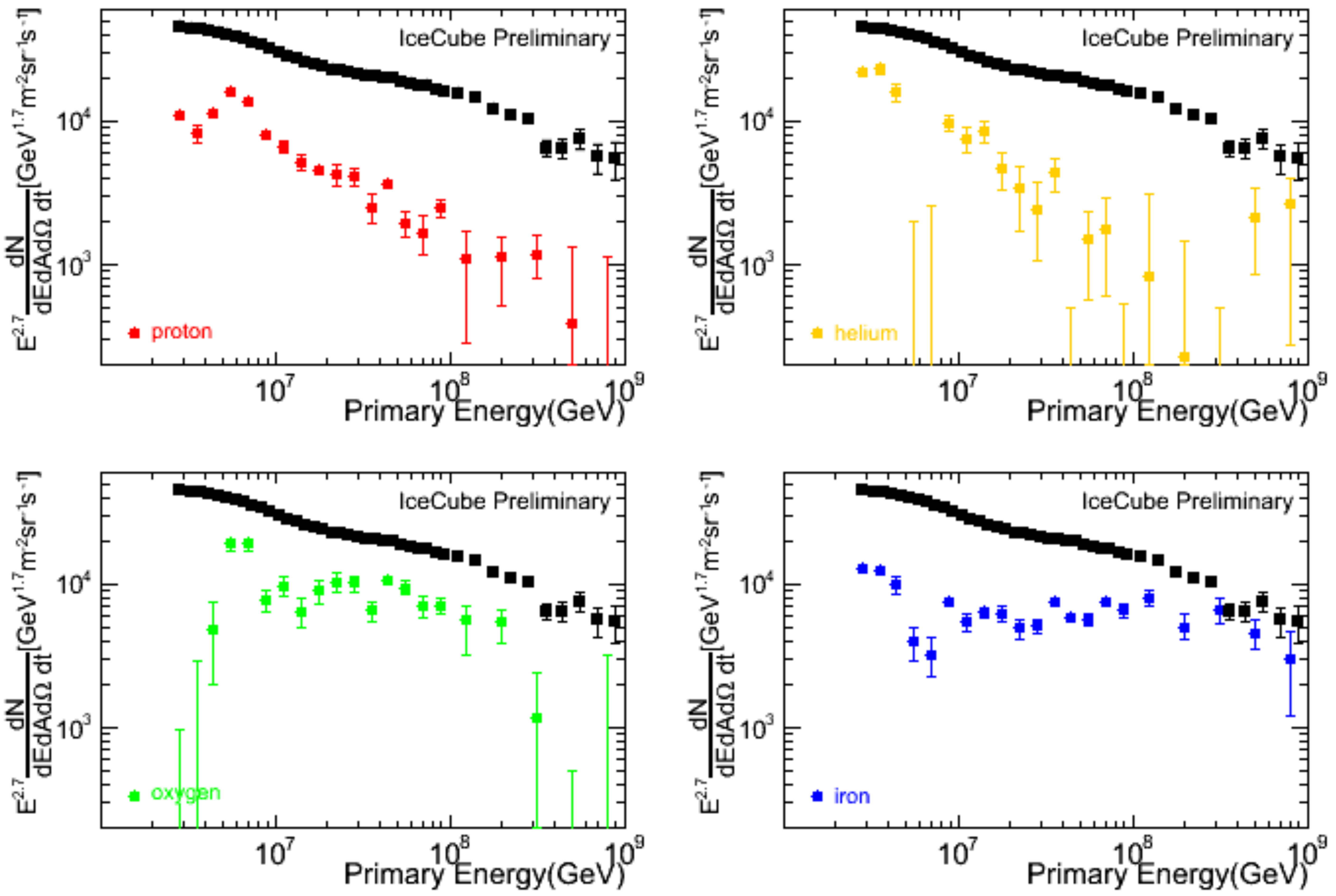

IceTop	KASCADE-Grande
‣ 1 km² covered area	0.5 km²
‣ 125 m spacing	137 m
‣ 2835 m a.s.l. 680 gcm^{-2}	1000 gcm^{-2}

Dembinski et al. EPJ Web Conf. 145 (2017) 01003

Example: diffusion / escape model for knee

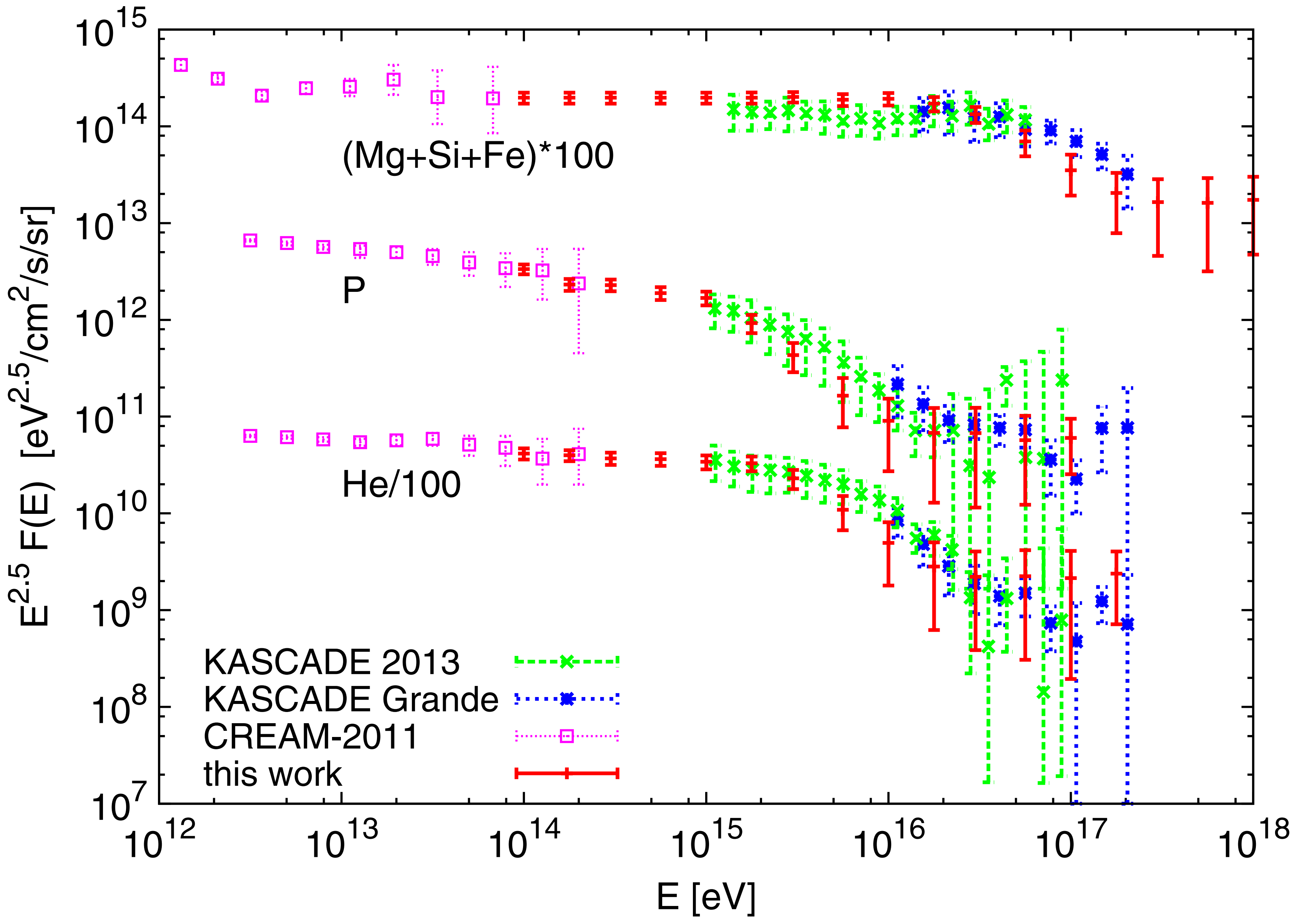

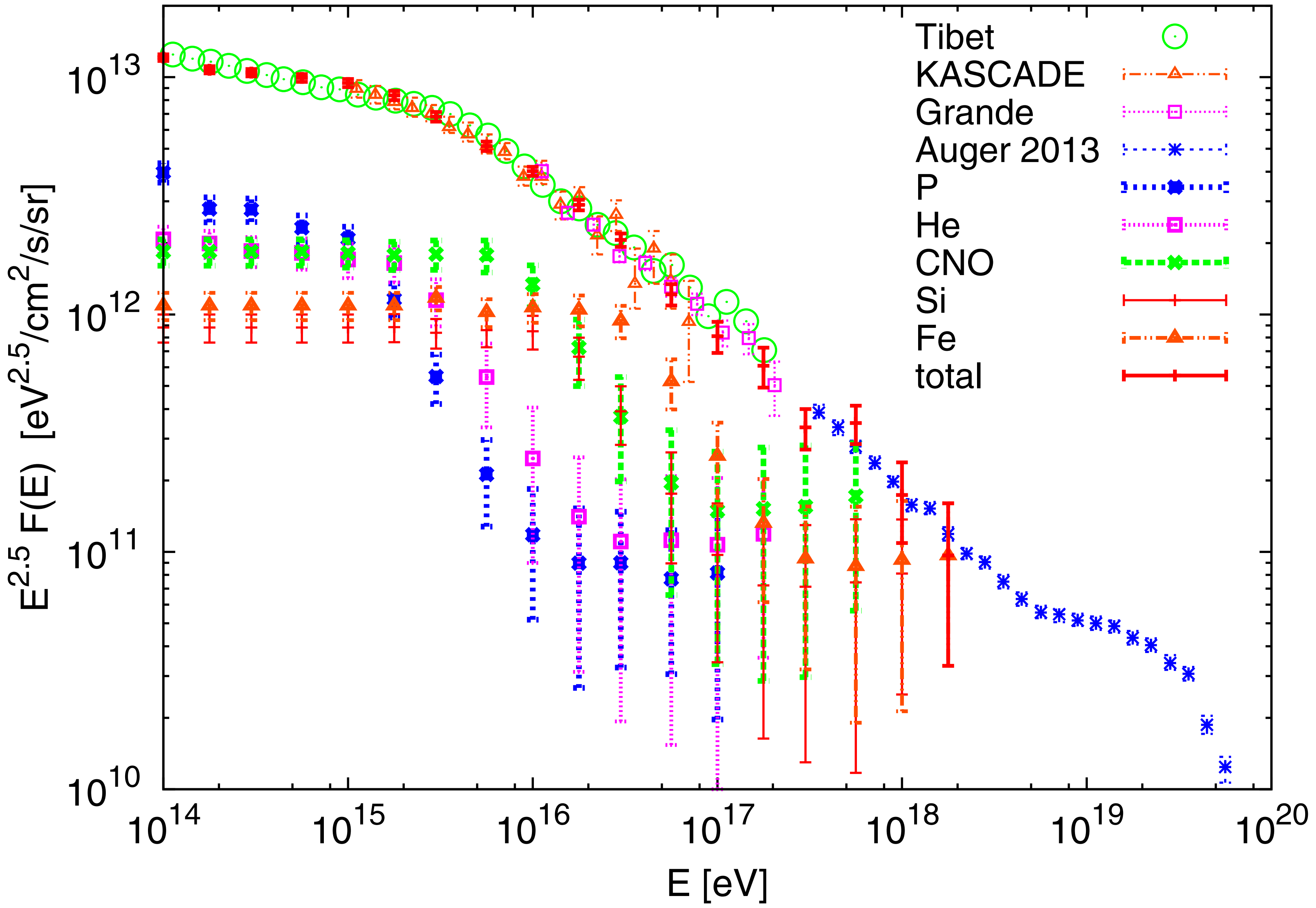

Injection of plain power laws

Kolmogorov spectrum
of turbulence

$$D(E) \propto E^{1/3}$$

Expected dipole anisotropy

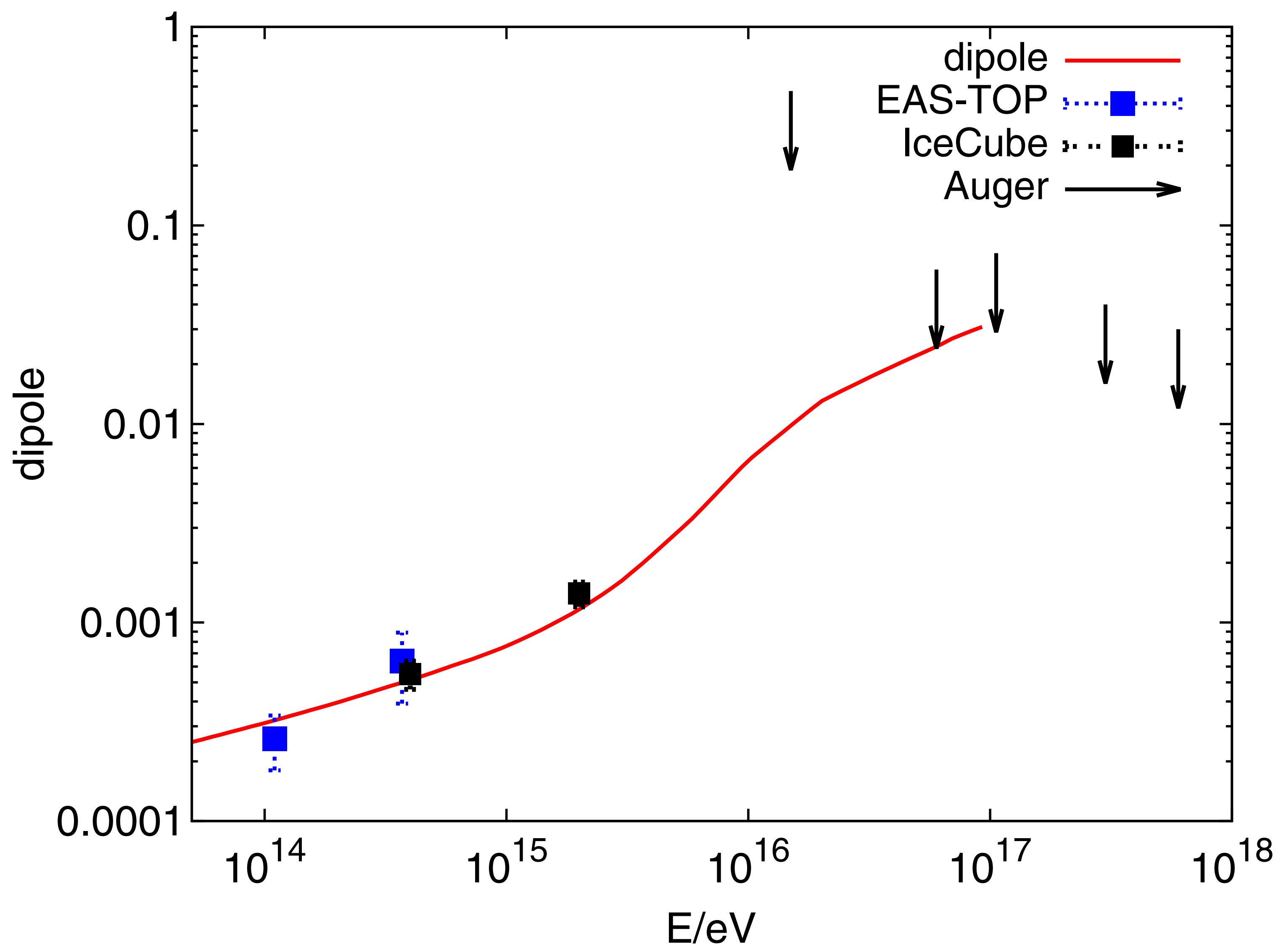

Detailed simulation of trajectories
(transition from diffusion to rectilinear propagation)

Sharpness of knee can be reproduced
High-energy particles have high charge

Giacinti et al. PRD 90 (2014) 041302

Deviations from simple standard model (i)

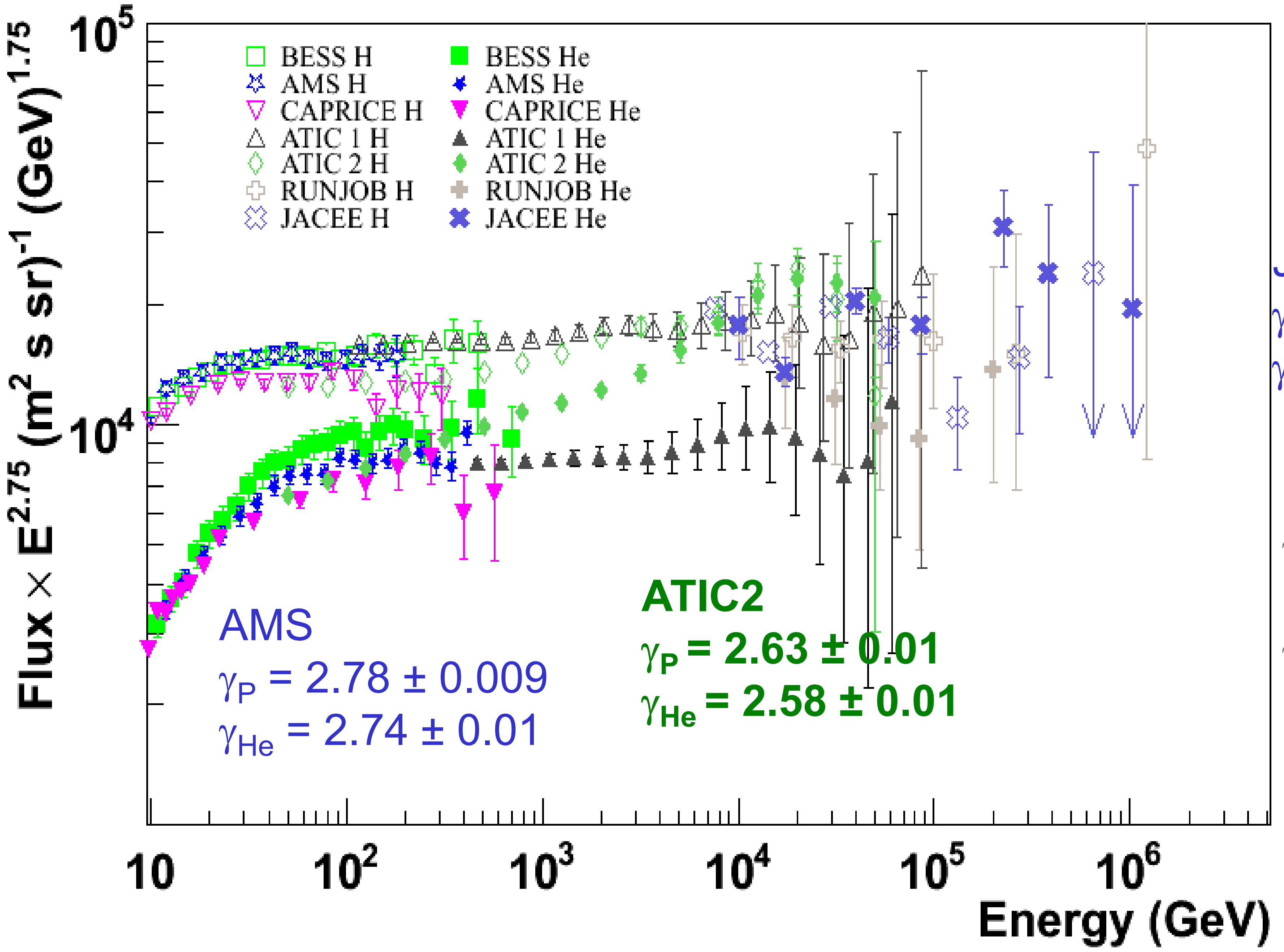

$I_j \propto E^{-\gamma}$

JACEE
γ_P = 2.80 ± 0.04
γ_{He} = 2.68+0.04-0.06

RUNJOB
γ_P = 2.78 ± 0.05
(2.74 ± 0.08)
γ_{He} = 2.81 ± 0.06
(2.78 ± 0.2)

(Seo, ICRC 2009)

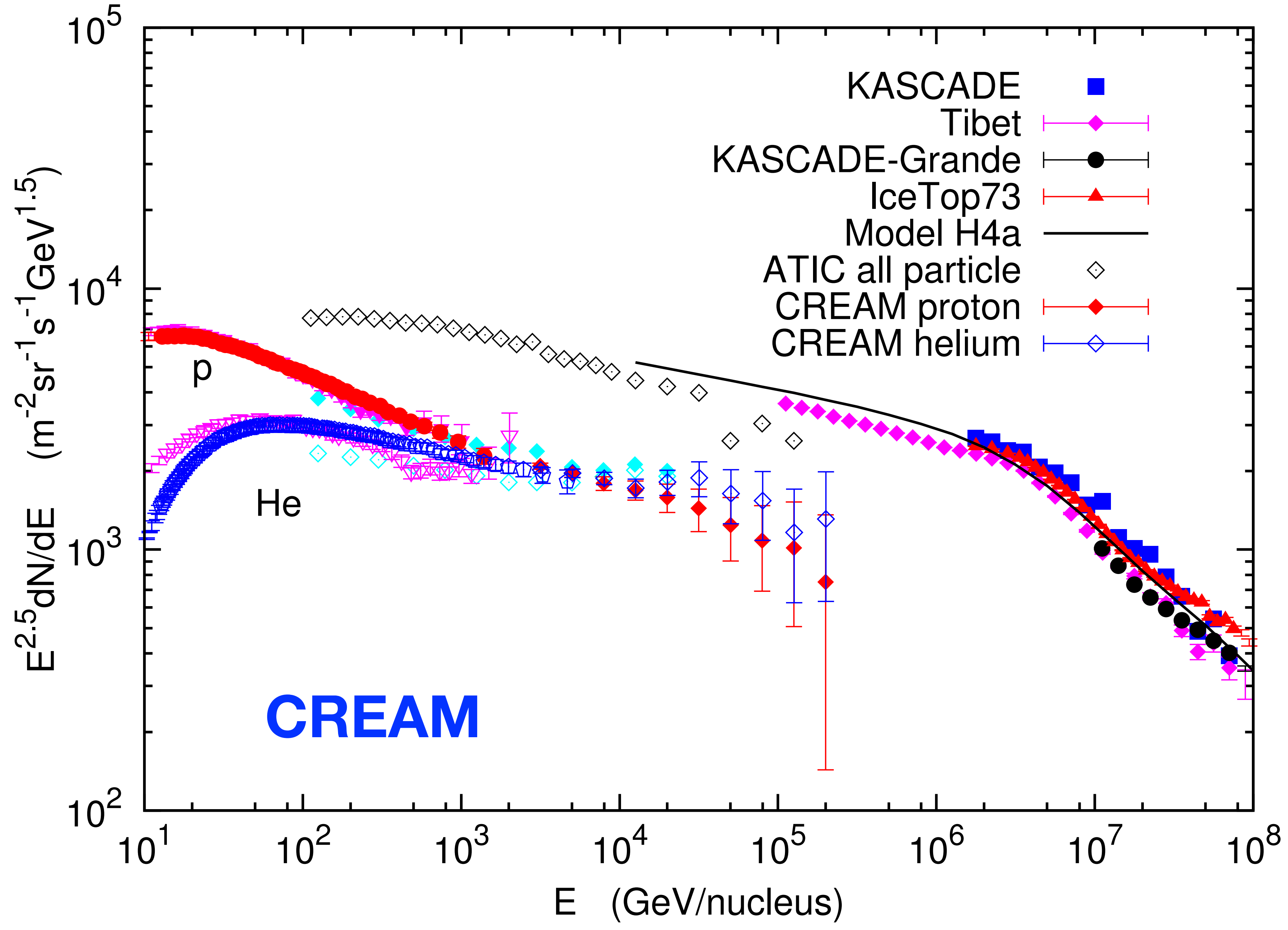

(Gaisser 2015)

Different power-law indices, crossing of proton and helium fluxes now well established

Should not have been a surprise: KASCADE had helium or carbon as most abundant element at knee

Cannot be explained in rigidity-dependent single source models: multiple source classes needed

Deviations from simple standard model (ii)

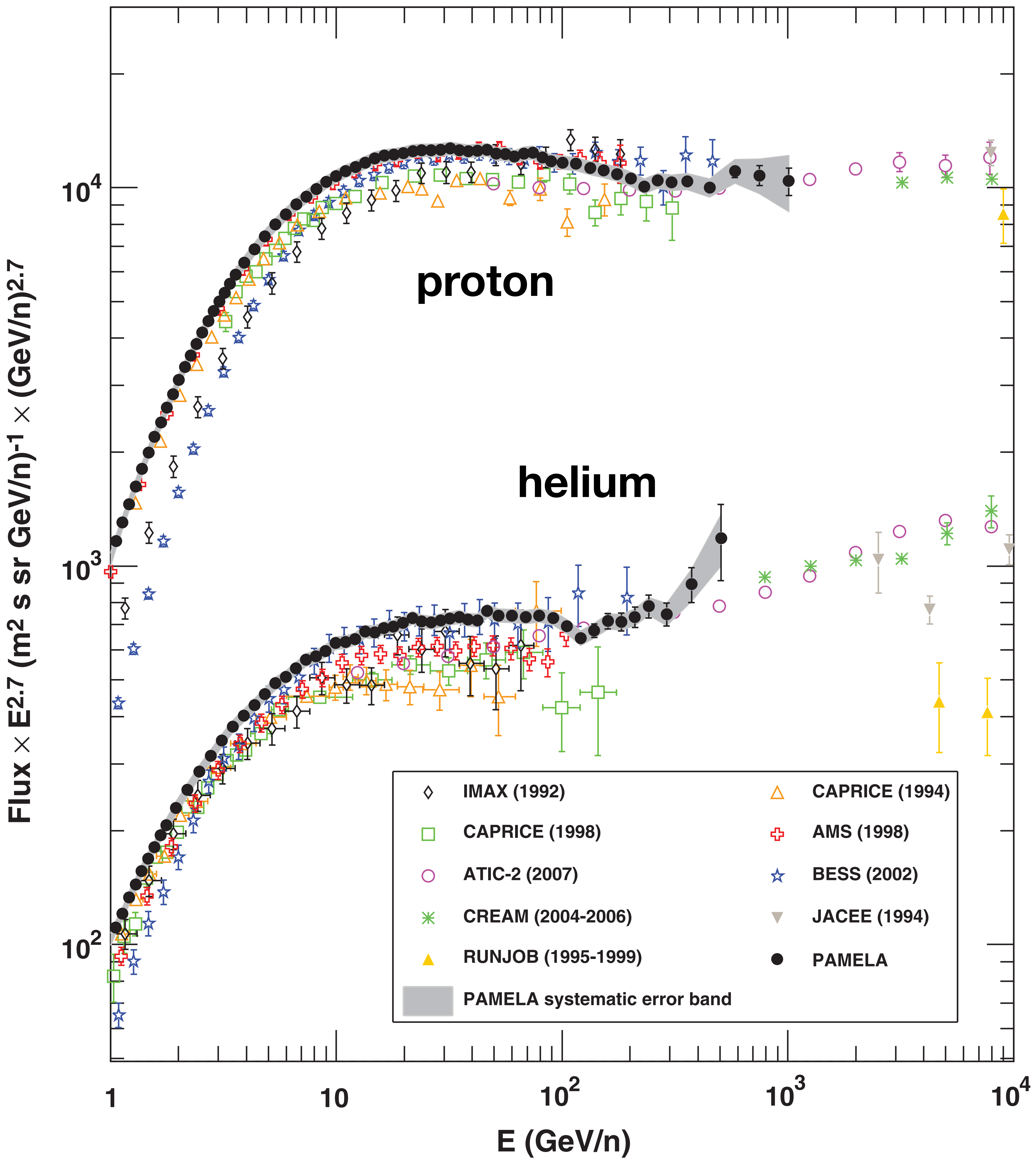

PAMELA Science 332 (2011)

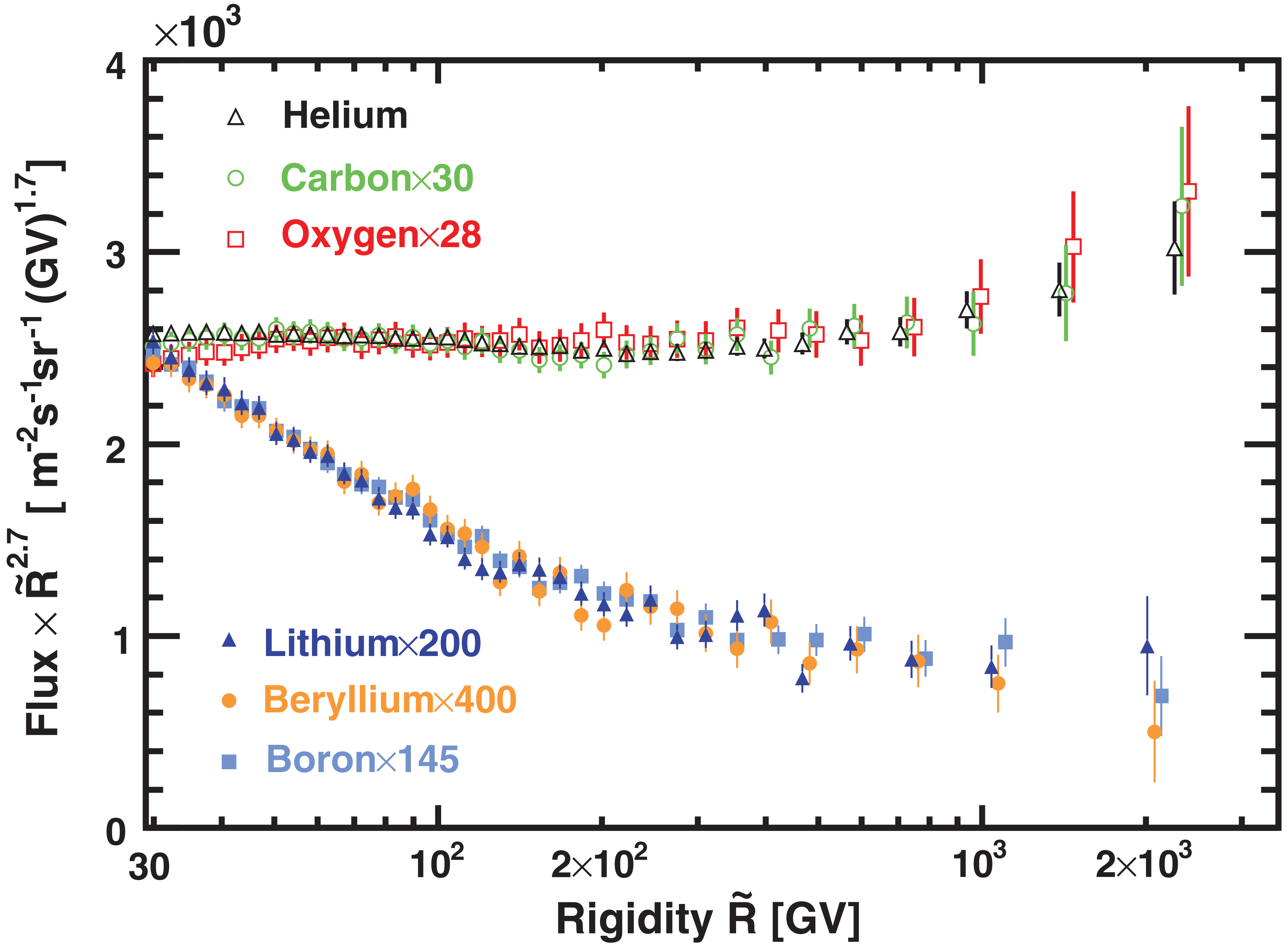

AMS, Phys.Rev.Lett. 220 (2018)

- Second population of particles released after SNR fades away
- Spectral dispersion in non-linear shock acceleration
- Different source classes or different acceleration times

Deviations from simple standard model (iii)

Tibet-III
Amenomori et al., ICRC 2011

5 TeV

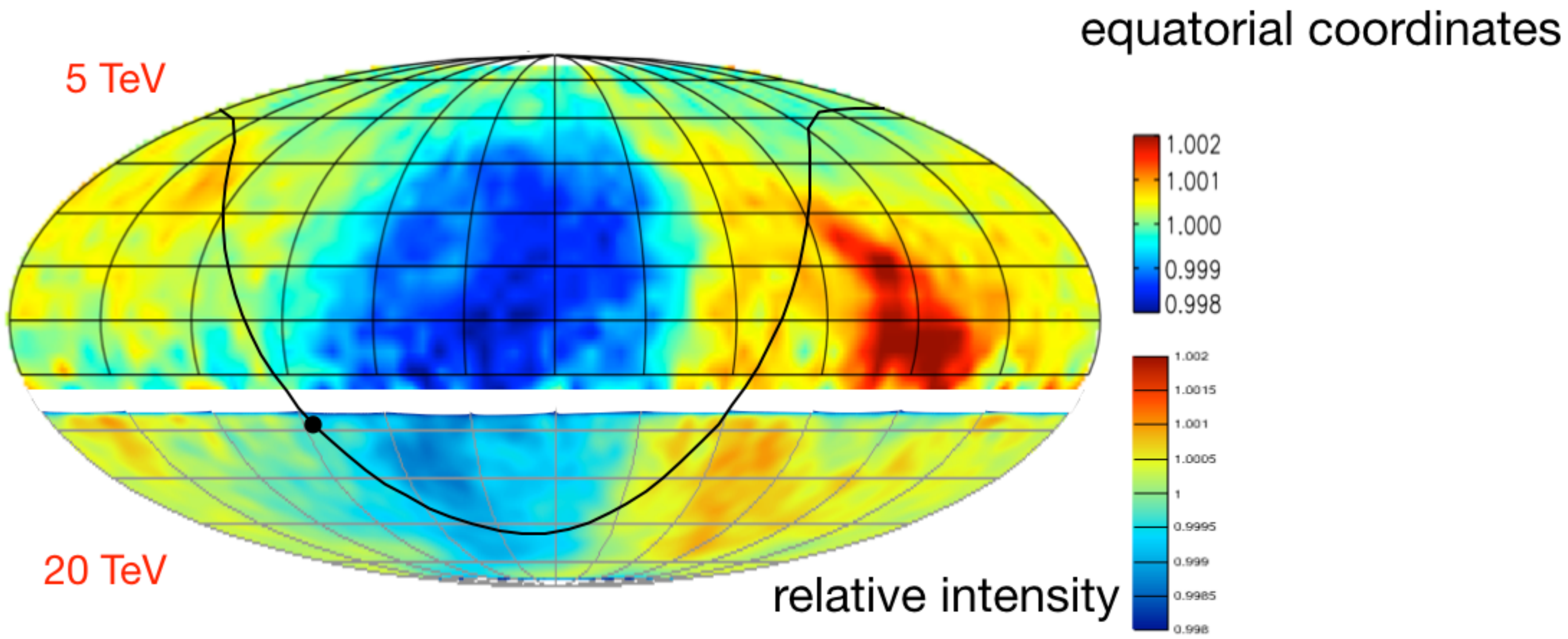

IceCube-59
Abbasi et al., ApJ, **746**, 33, 2012

20 TeV

HAWC
Abeysekara et al. 2014

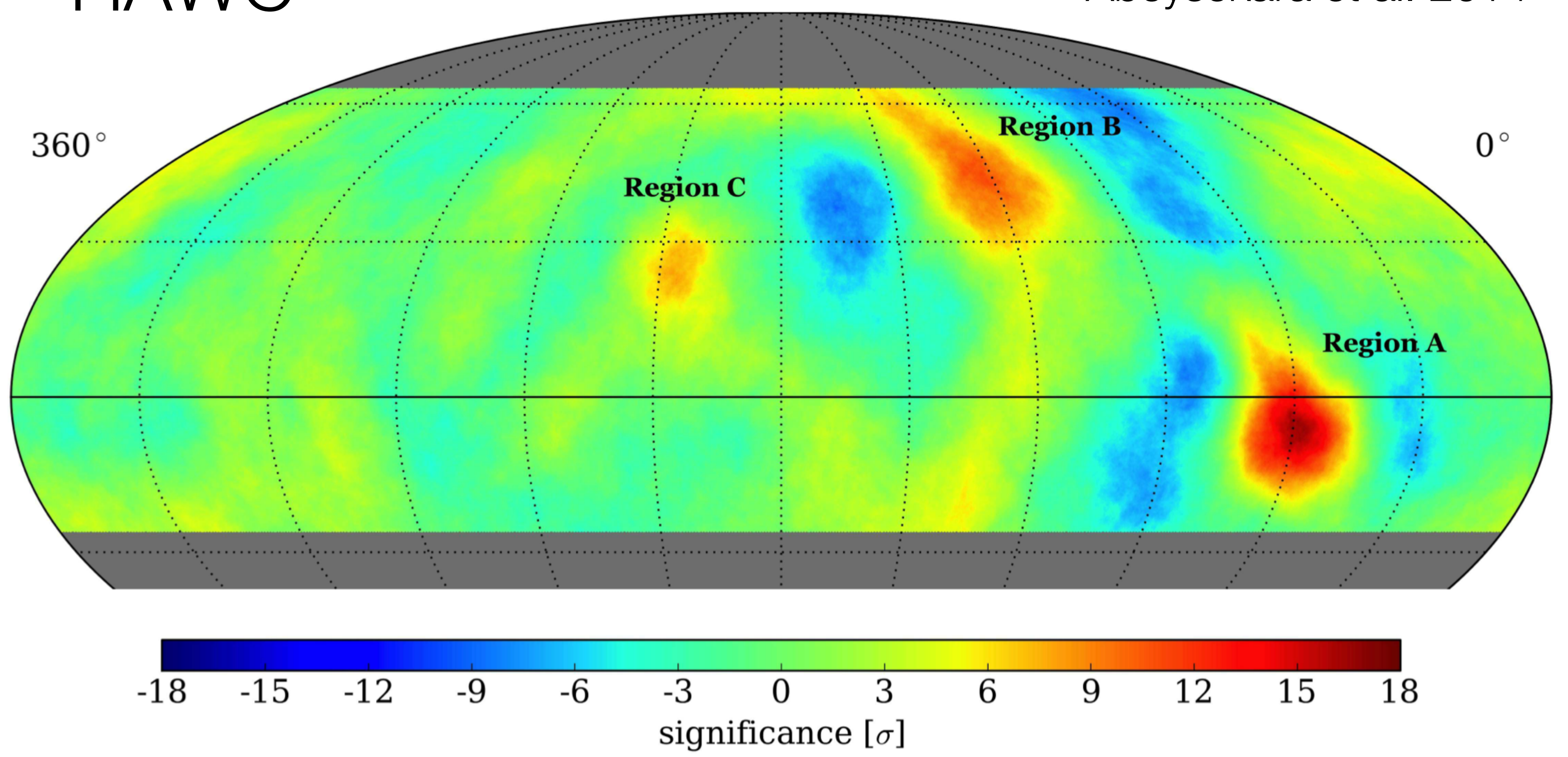

Milagro
Abdo et al., PRL, **101**, 221101, 2008

1 TeV

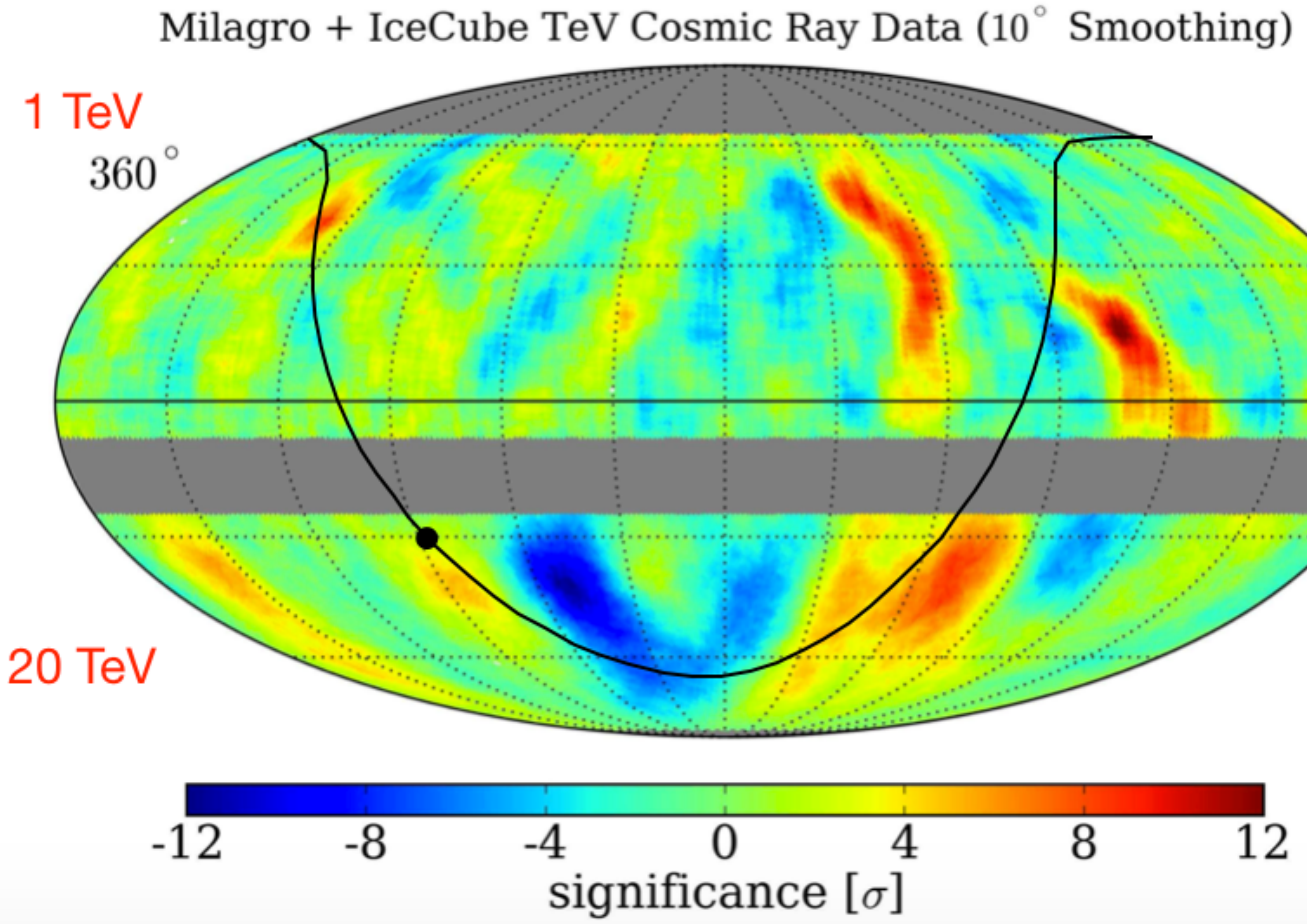

IceCube-59
Abbasi et al., ApJ, **740**, 16, 2011

20 TeV

ARGO-YBJ
Bartoli et al. (2013)

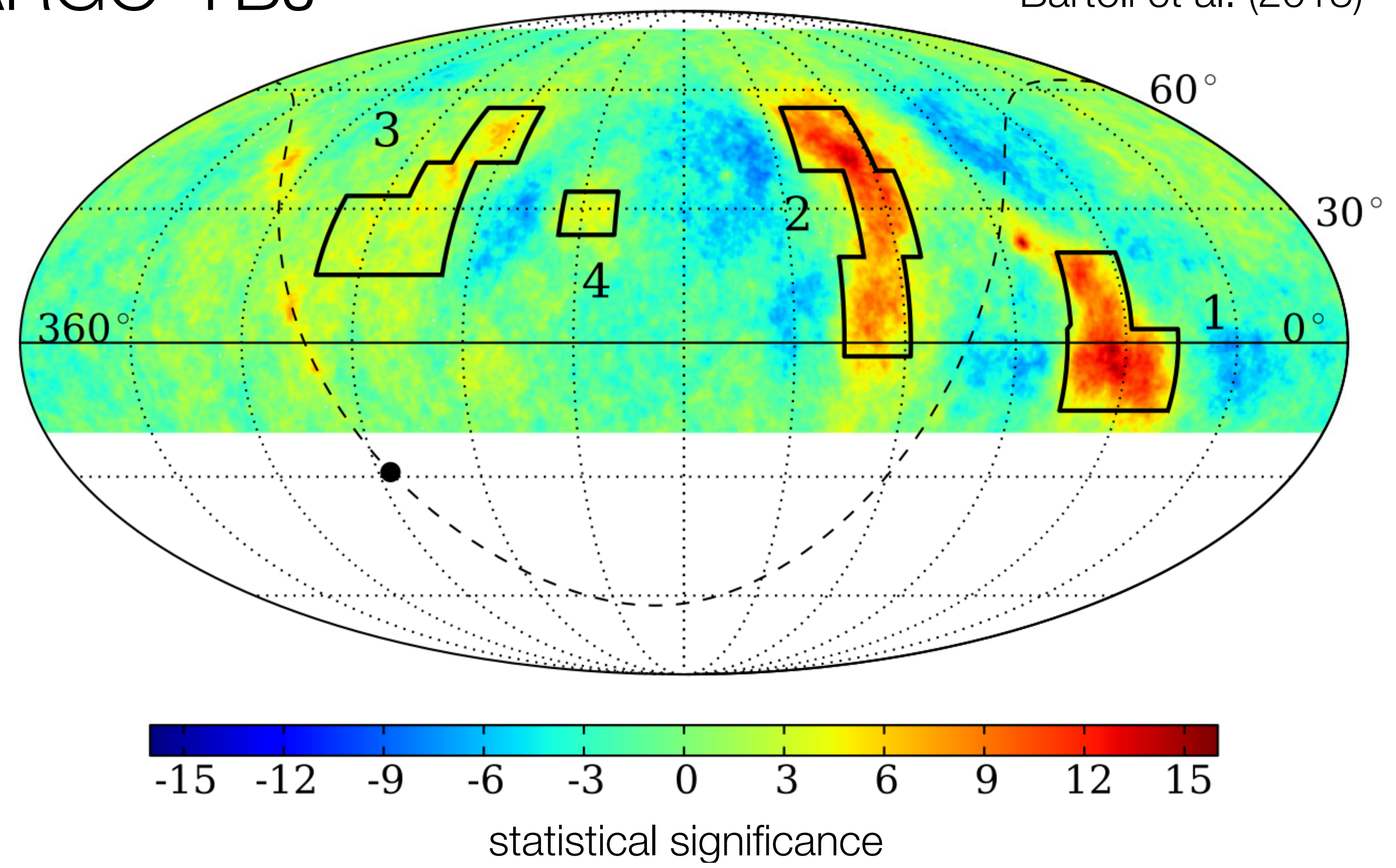

(Desiati, RAPP 2016)

Cosmic ray anisotropies in TeV energy range

Energy spectrum above the knee

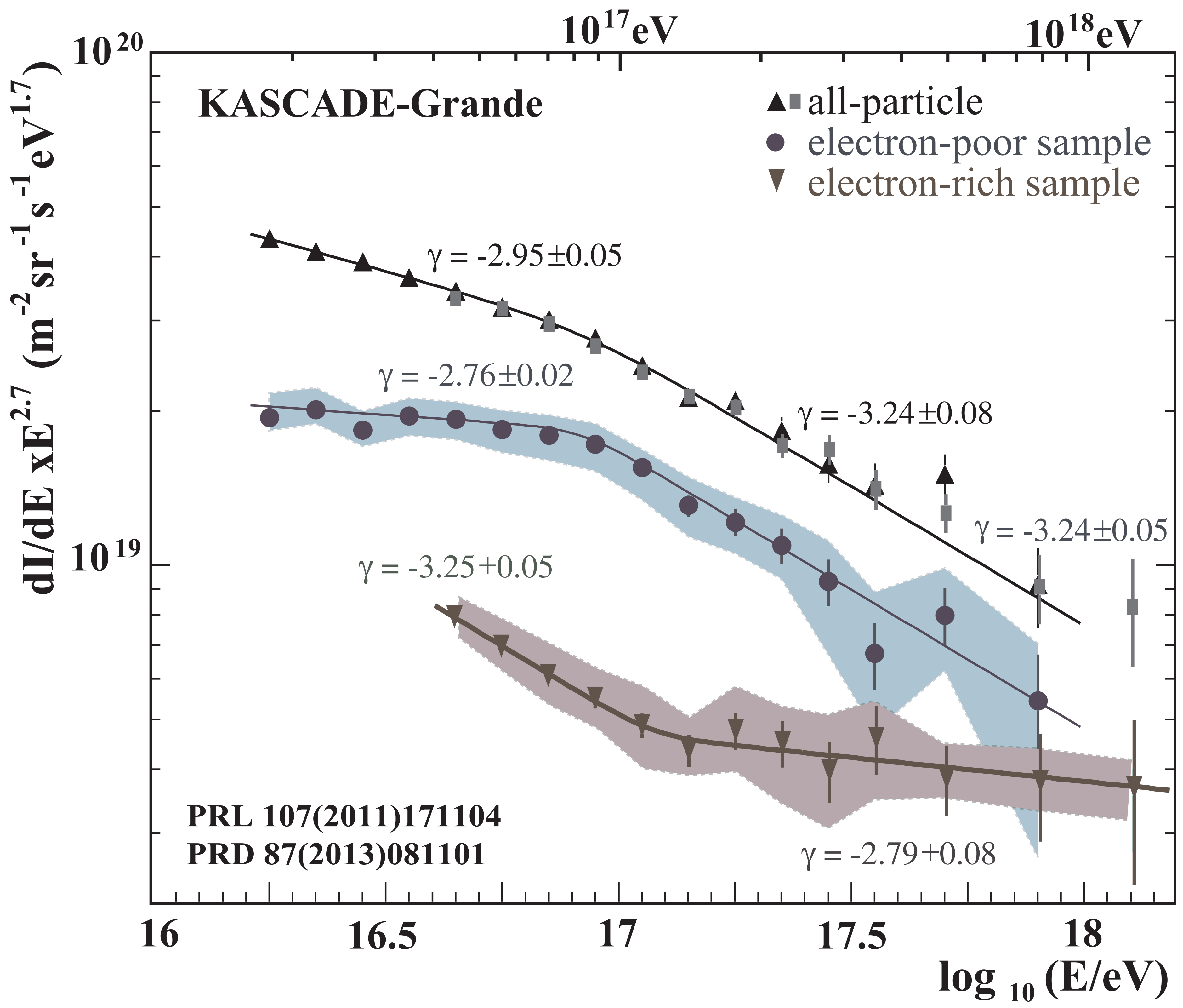

PoS(ICRC2015)334

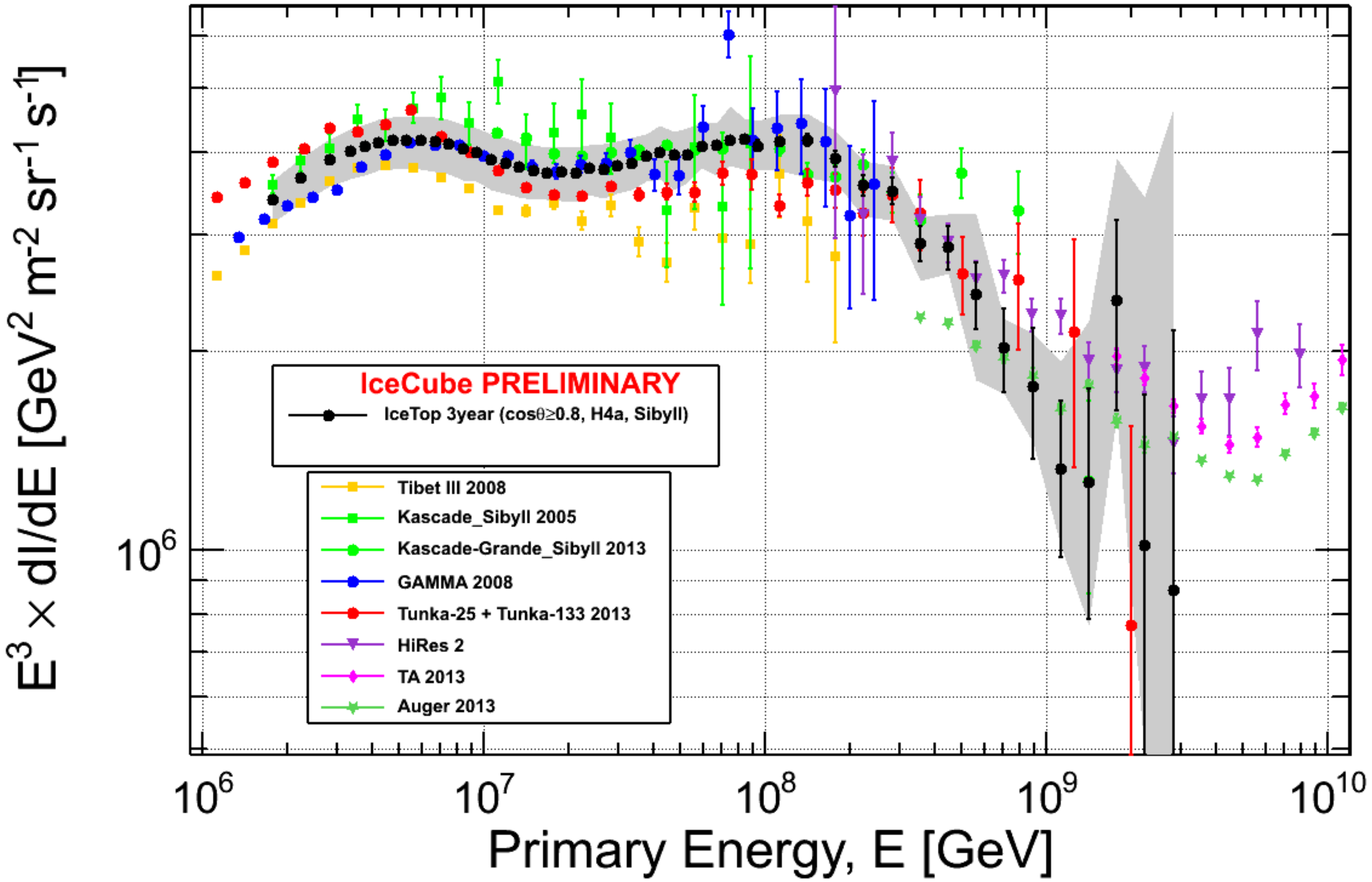

Knee of heavy particles found

Recovery of light (proton?) component

Deviation from power law established

Second knee well confirmed in data of many experiments

Generic phenomenological interpretation of flux (i)

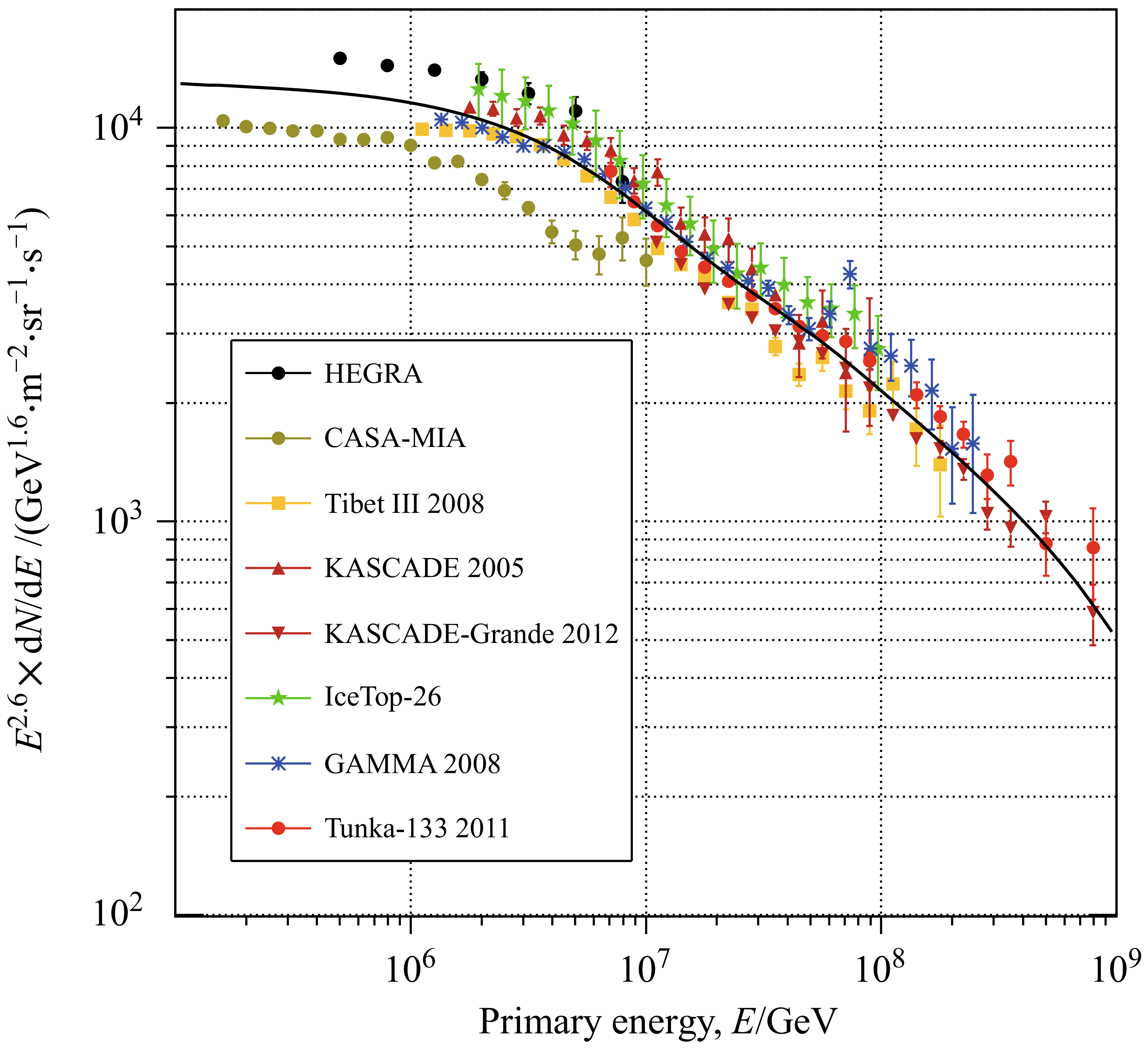

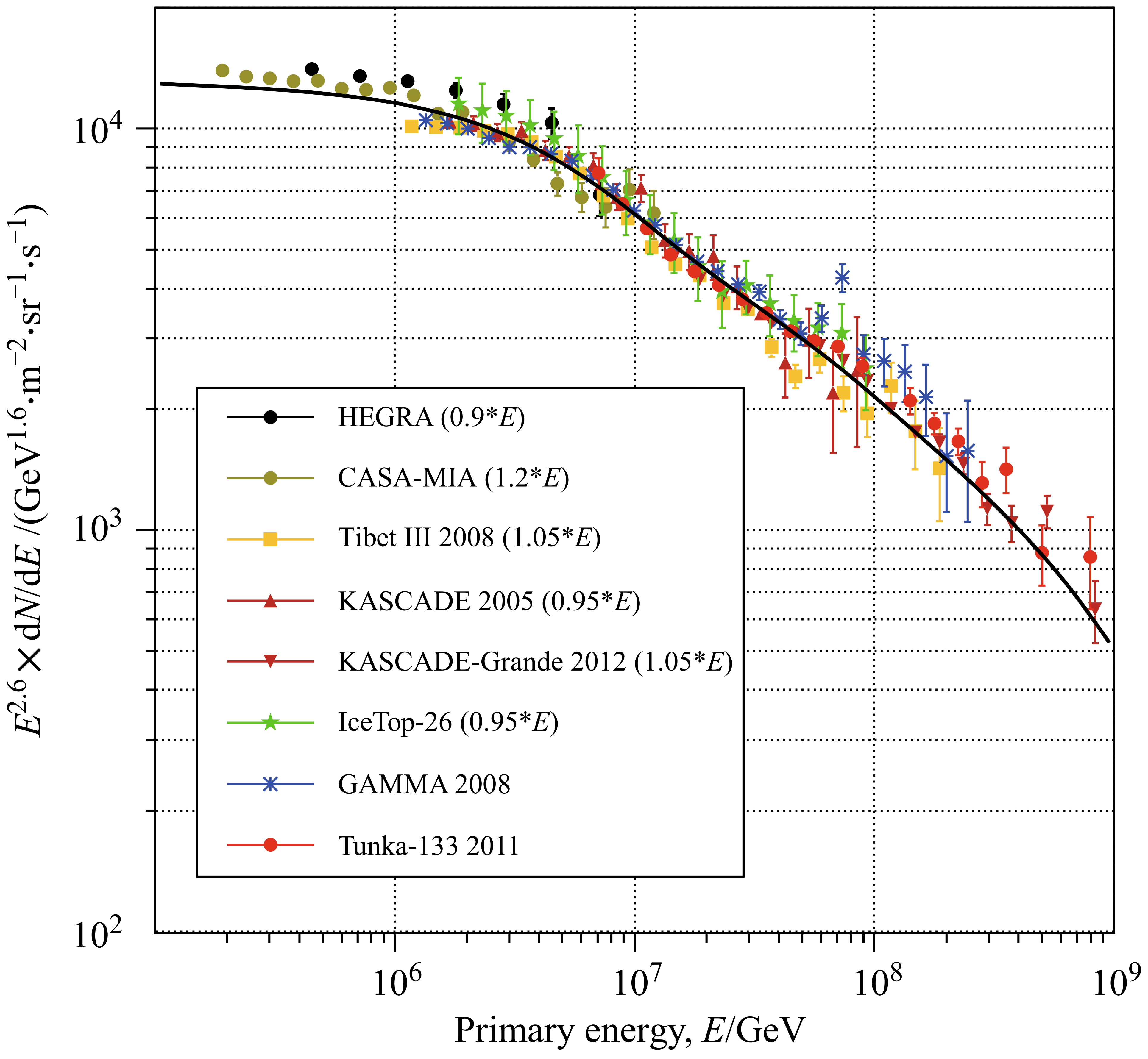

Re-scaling of fluxes by adjusting energy scales of experiments

Gaisser, Stanev, Tilav Front. Phys. 8 (2013) 748

Generic phenomenological interpretation of flux (ii)

$$\phi_i(E) = \sum_{j=1}^{3} a_{i,j}\, E^{-\gamma_{i,j}} \times \exp\left(-\frac{E}{Z_i R_{c,j}}\right)$$

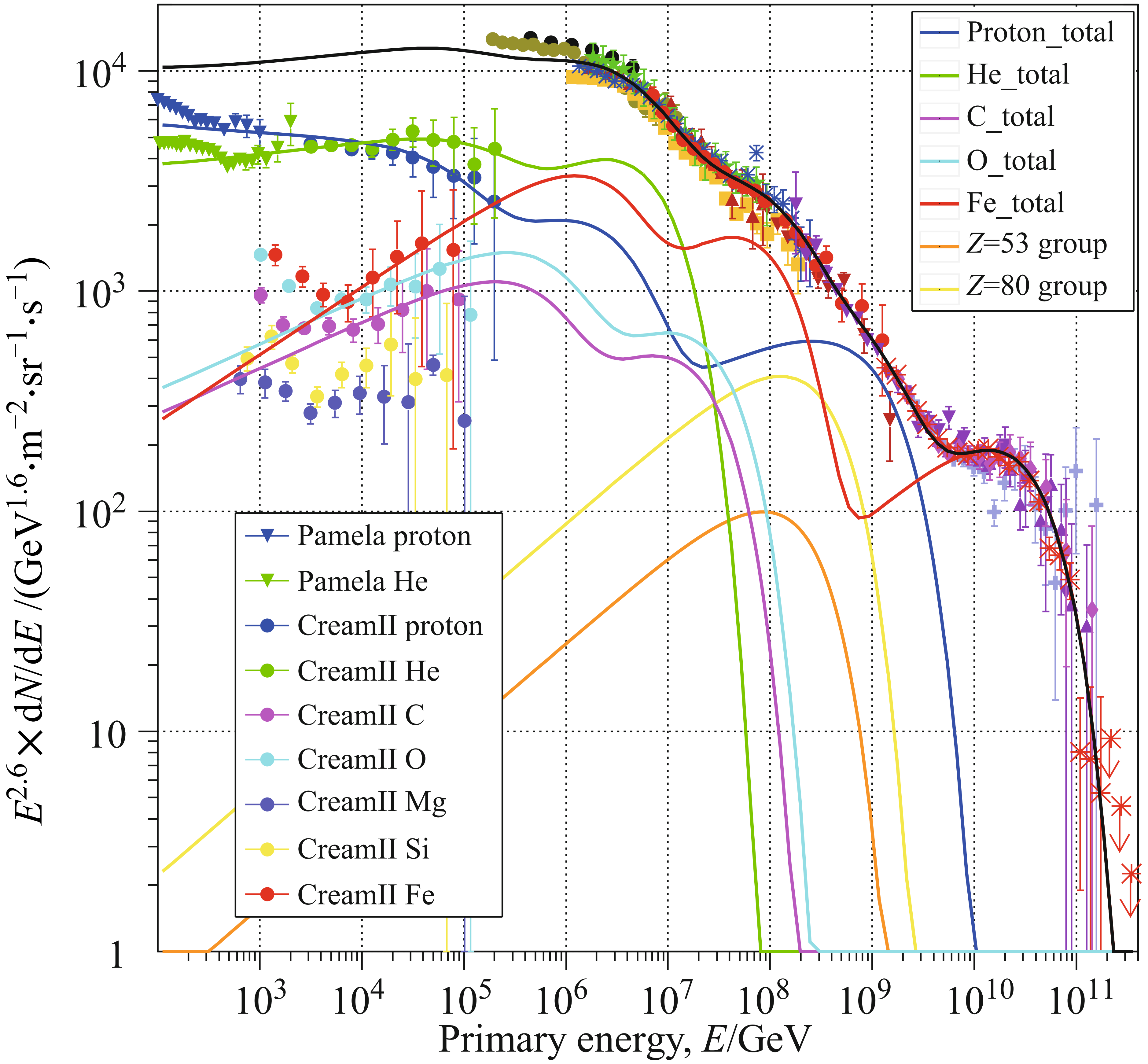

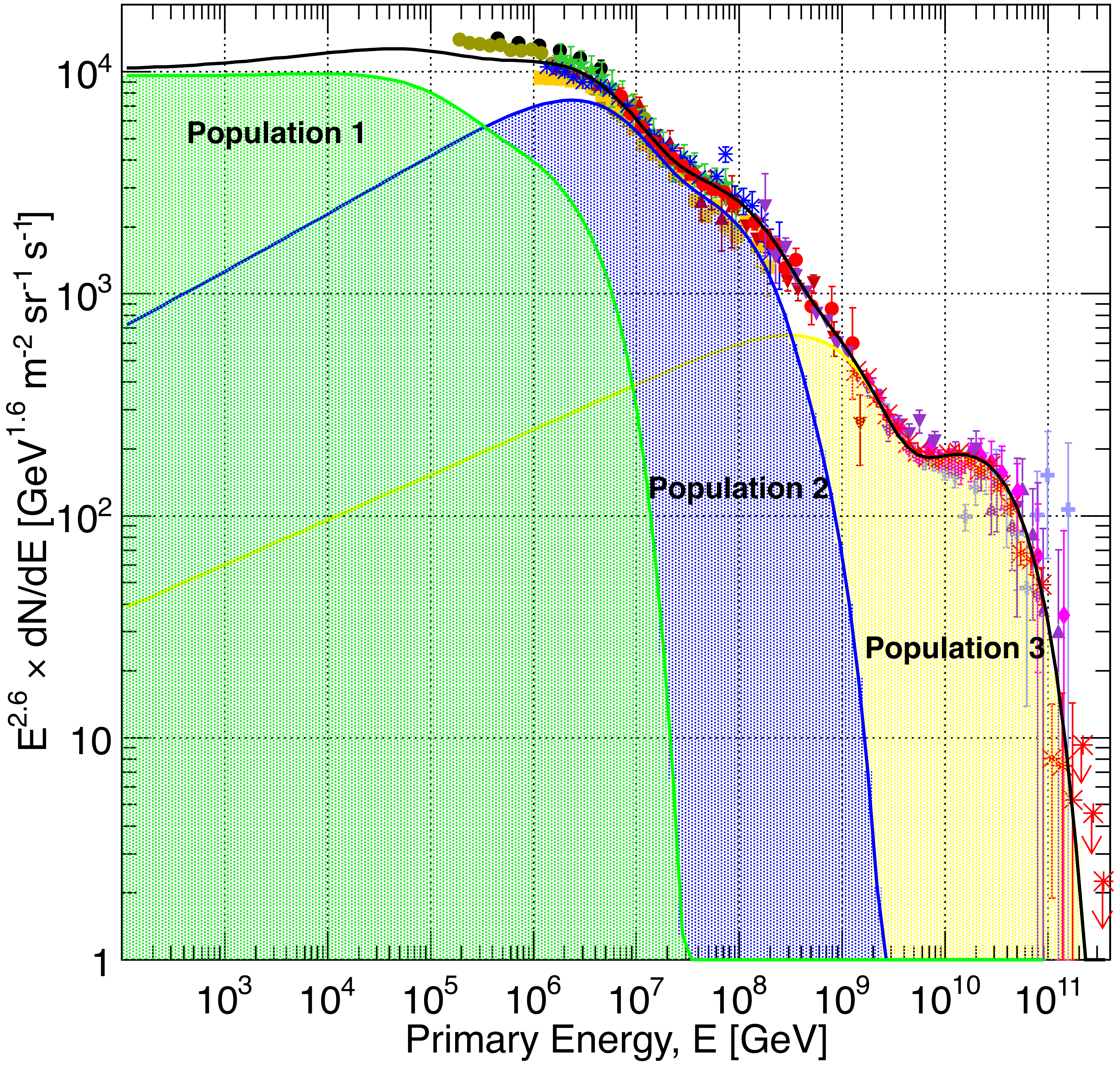

Below the knee: superposition of power laws of different index

Above the knee: superposition of exponential flux suppressions

Gaisser, Stanev, Tilav Front. Phys. 8 (2013) 748

Global spline fit – no assumptions on shape / relations in data

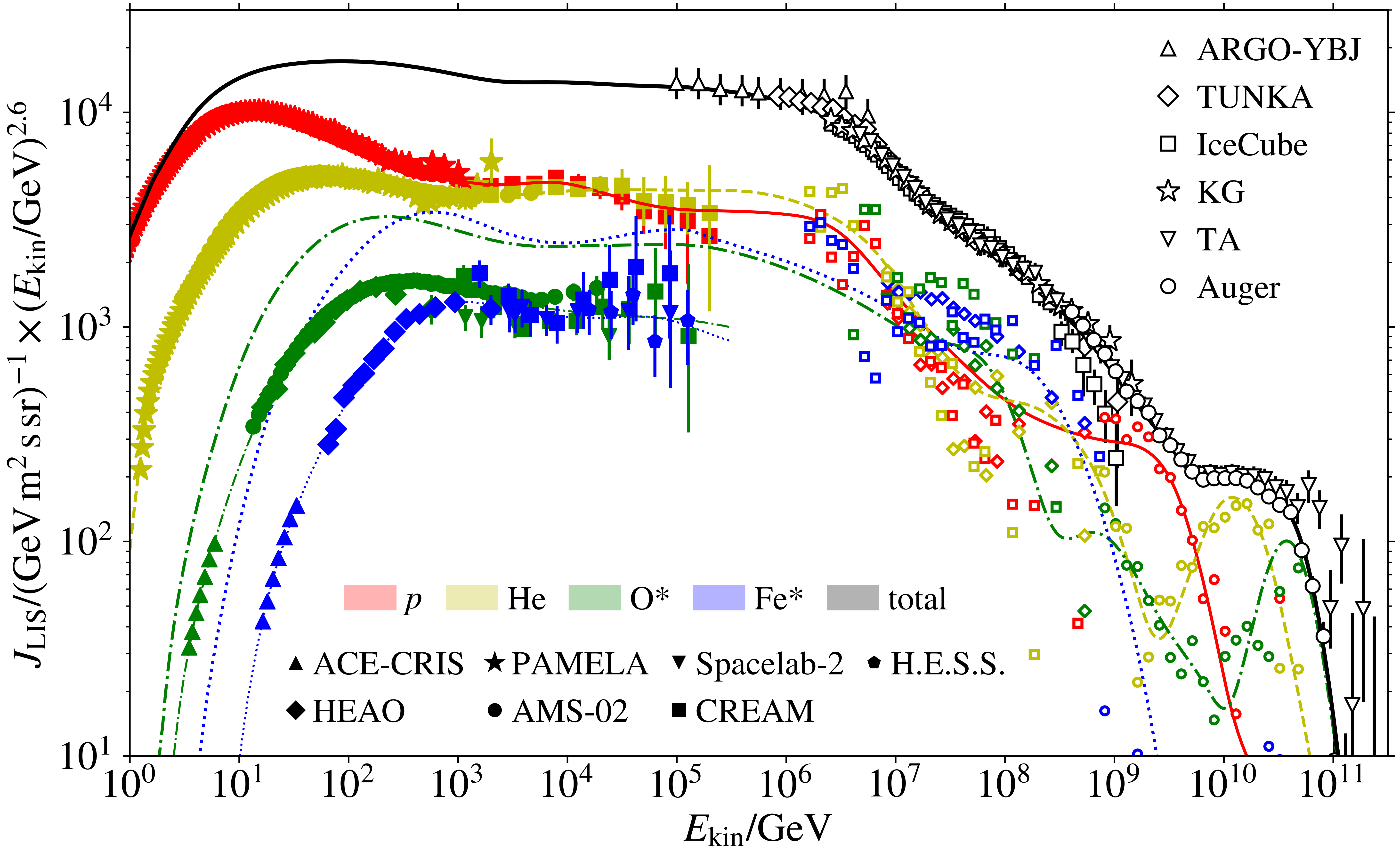

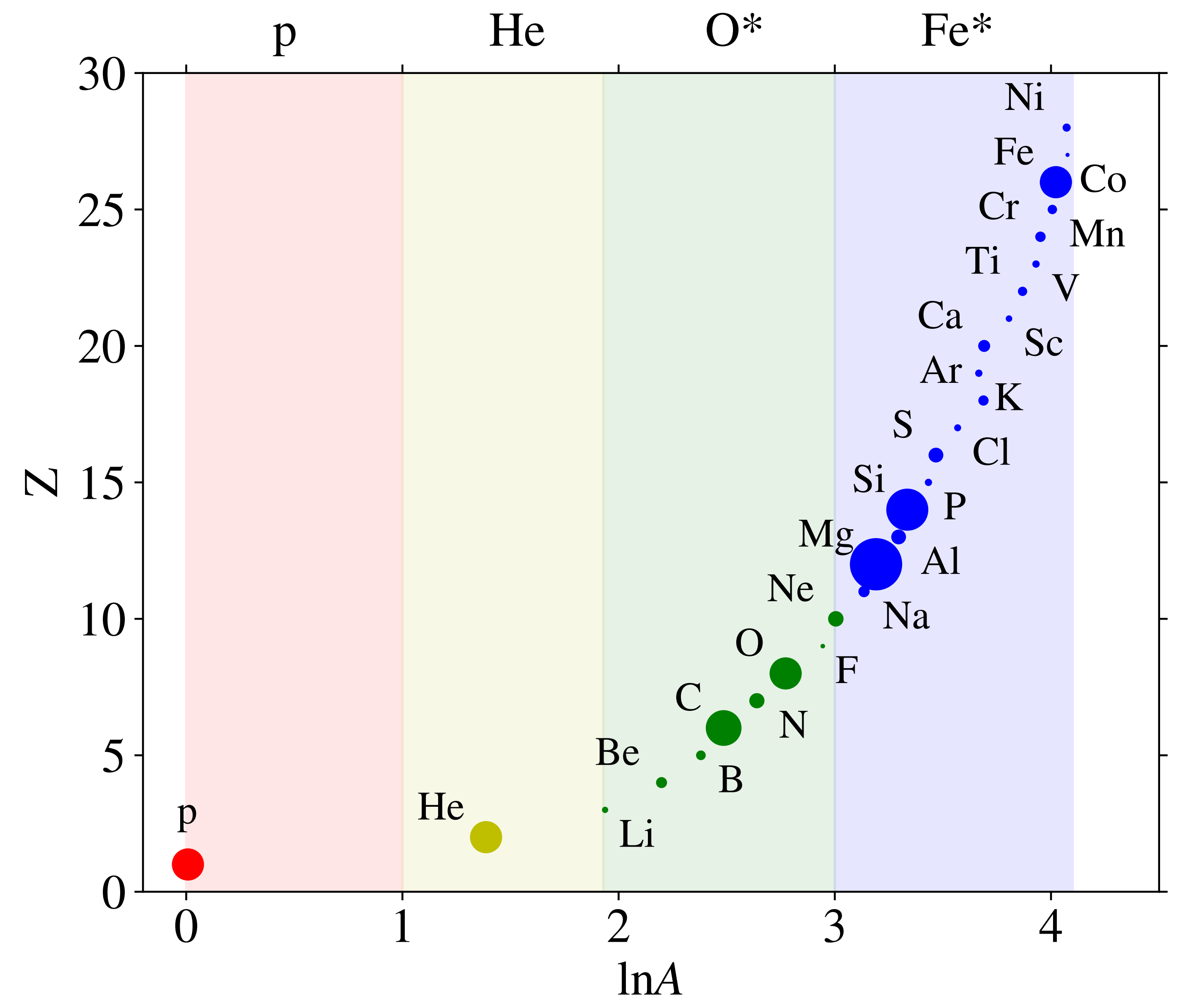

Definition of element groups important

Dembinski et al. PoS ICRC2017 (2017) 533

Spline fit segments adjusted to economically reproduce data

Proper error propagation from experimental uncertainties

From galactic to extragalactic cosmic rays

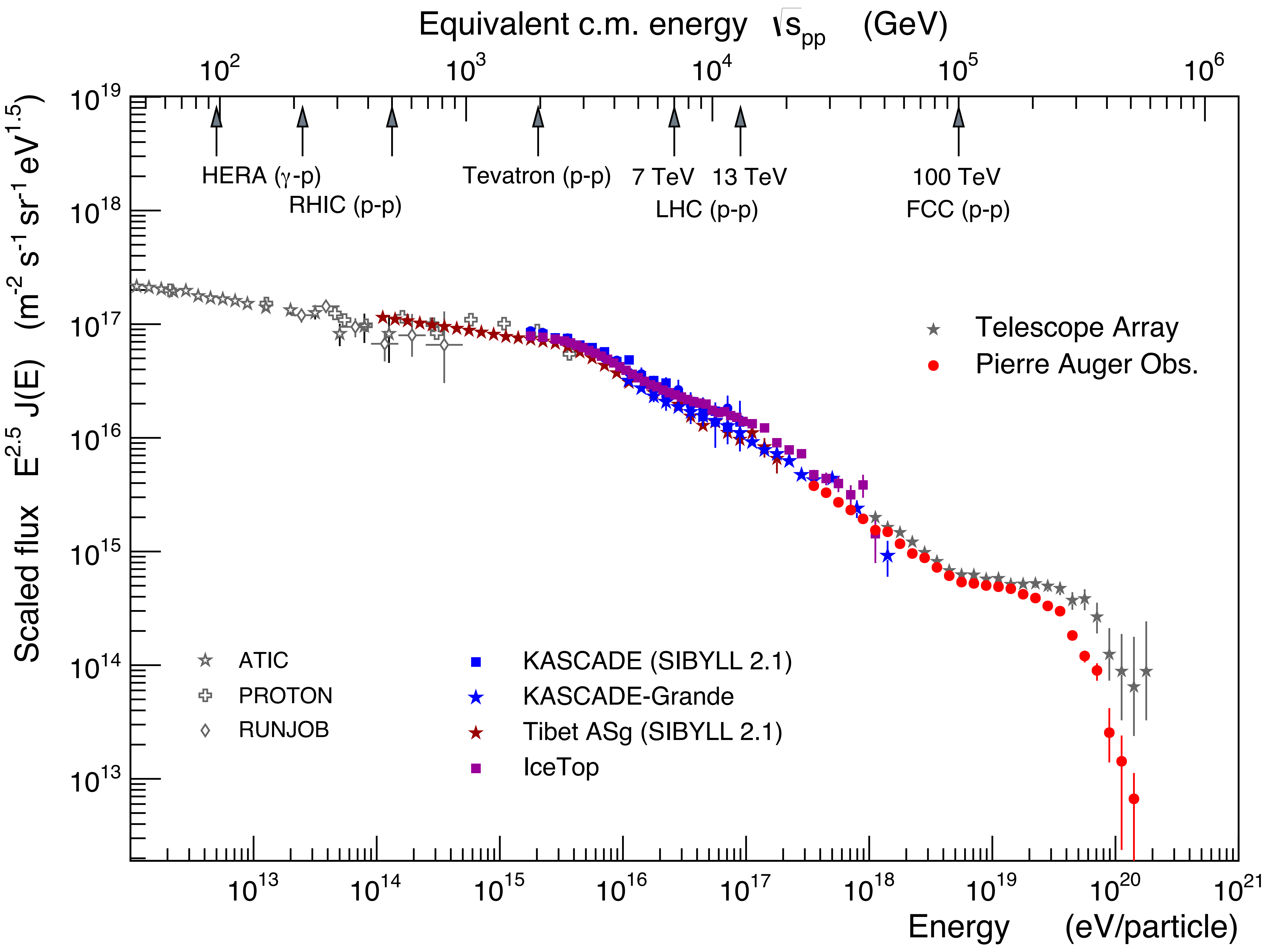

Current status of all-particle spectrum

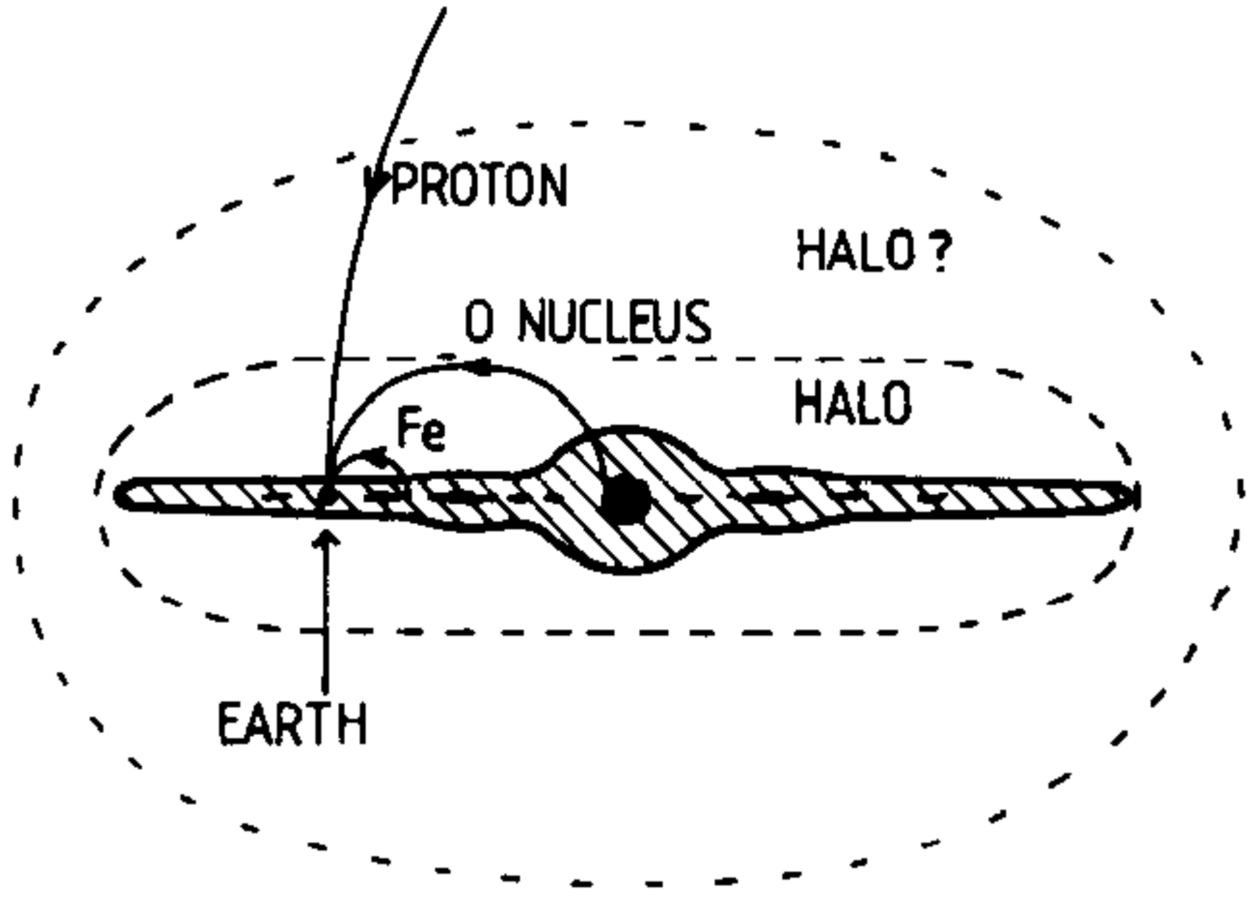

(Hillas ARAA 1984)

Simulation: sources in galactic plane

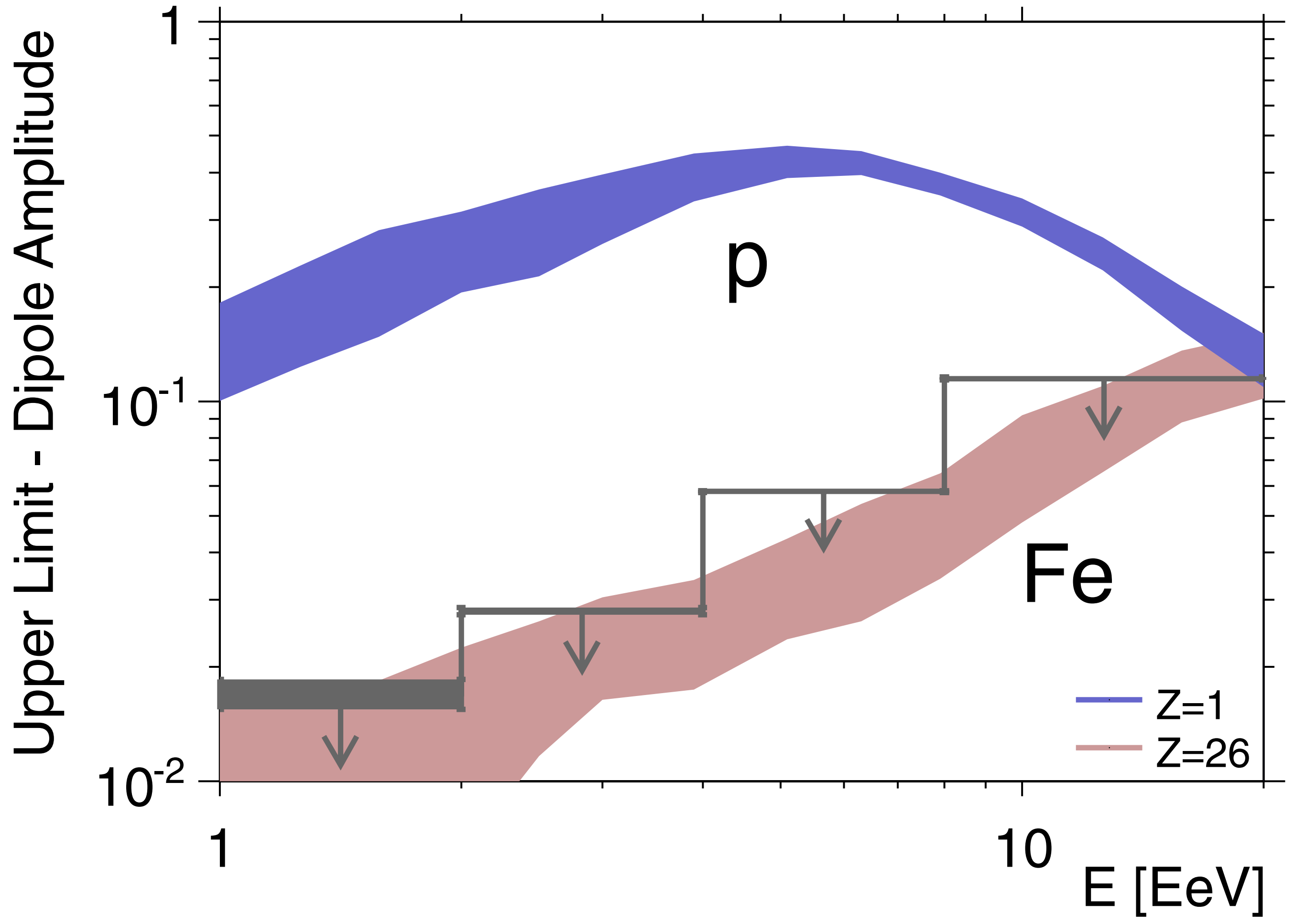

(Auger, ApJ 203, 2012,
Giacinti et al. JCAP 2012, 2015)

Ultra-high-energy cosmic rays: sources

Hillas plot (1984)

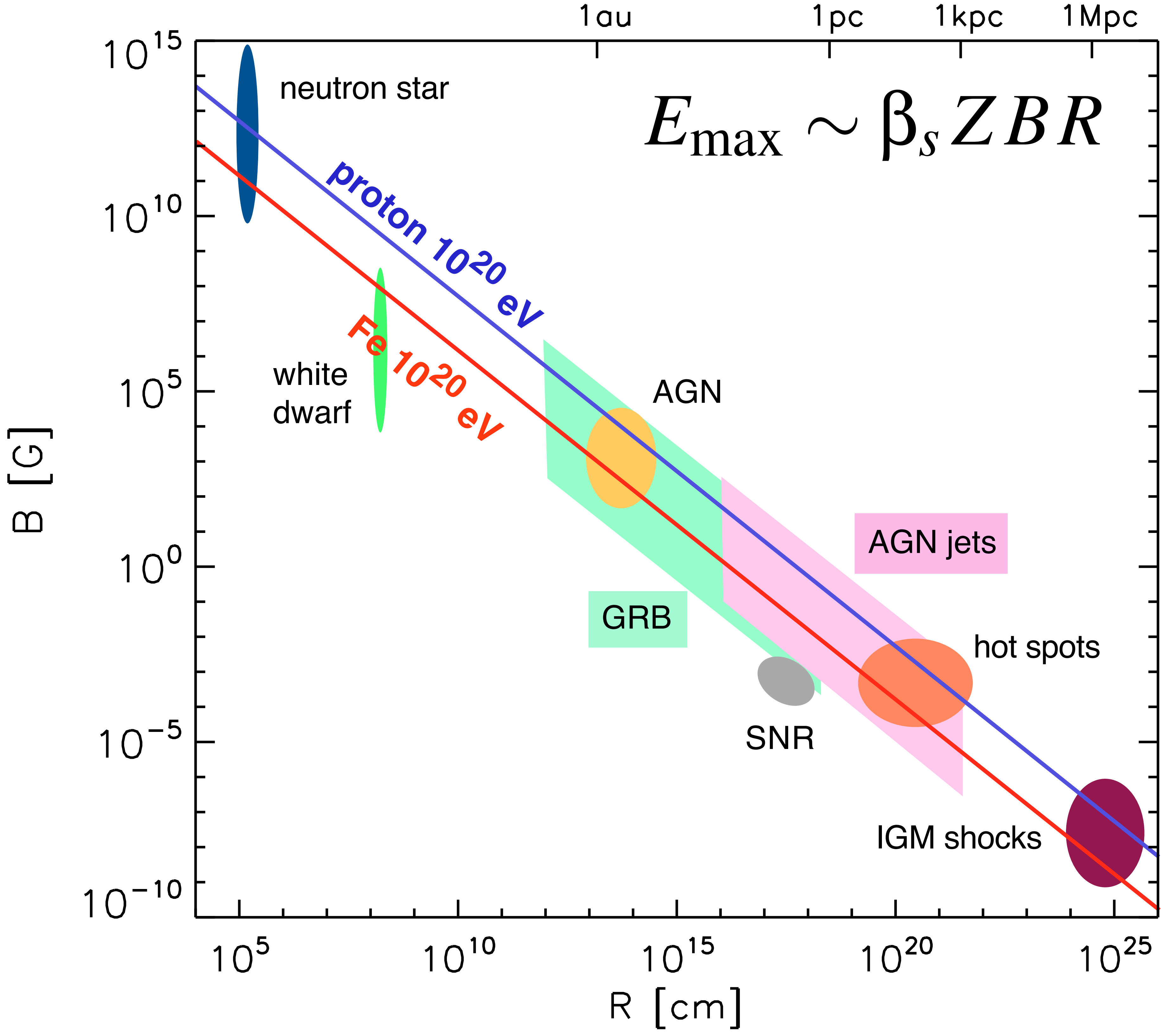

(Kotera & Olinto, ARAA 2011)

(Unger, 2006)

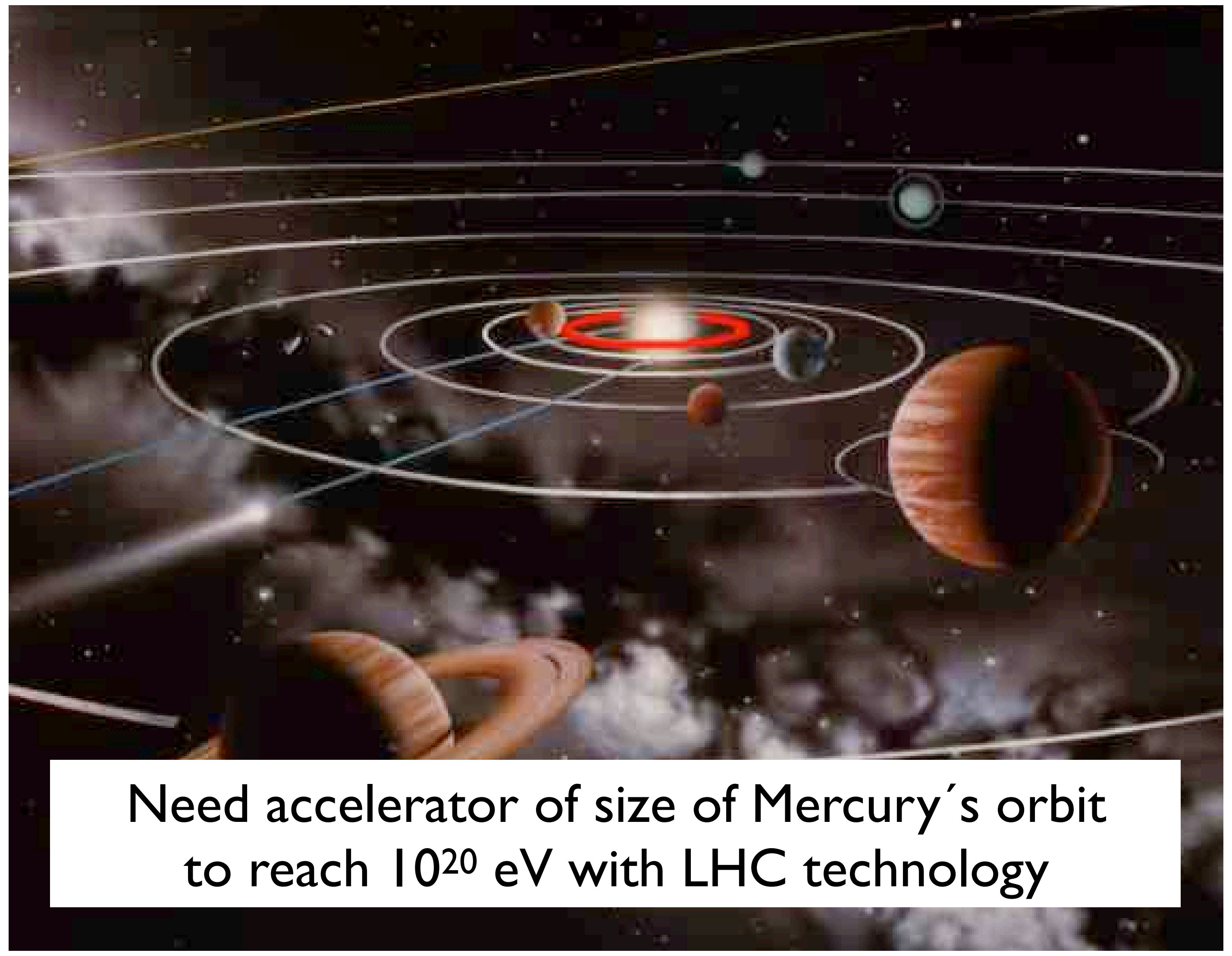

Realistic constraints more severe

- small acceleration efficiency
- synchrotron & adiabatic losses
- interactions in source region

X particles from:

- topological defects
- monopoles
- cosmic strings
- cosmic necklaces
- .....

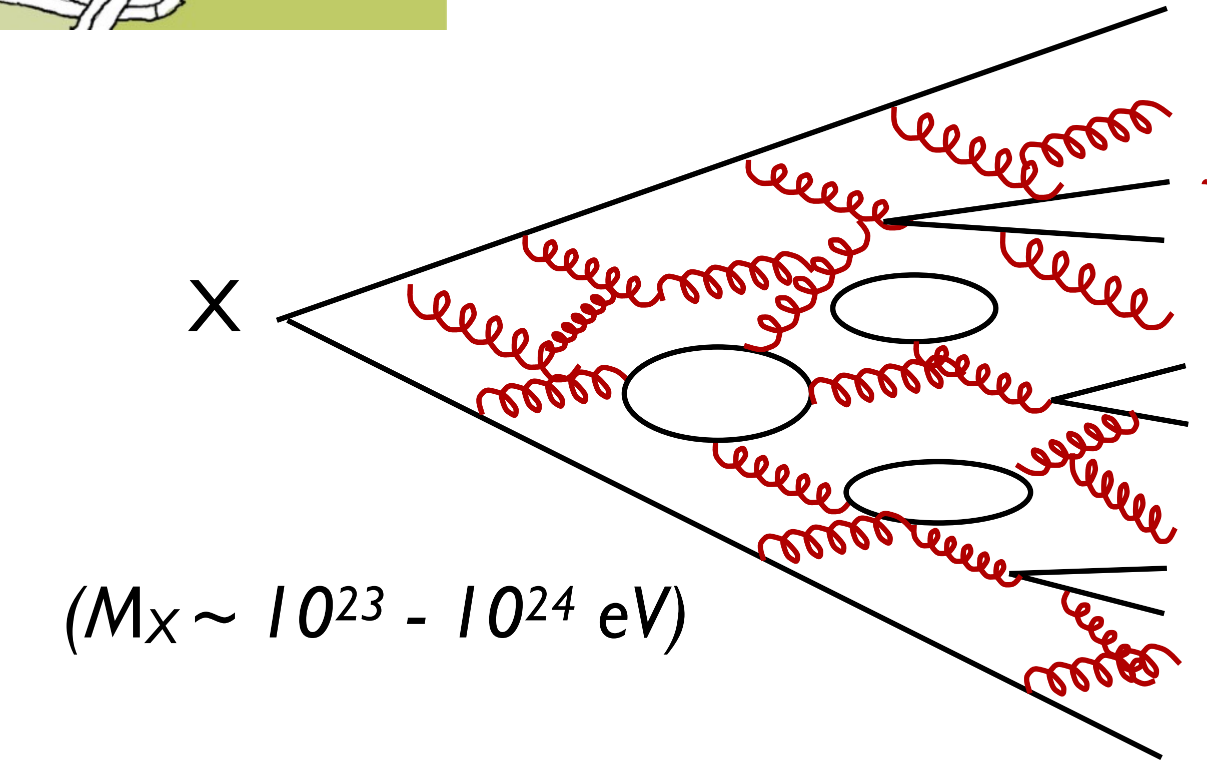

Fragmentation function

QCD: ~ $E^{-1.5}$ energy spectrum

QCD+SUSY: ~ $E^{-1.9}$ spectrum

Propagation of ultra-high-energy cosmic rays

Proton

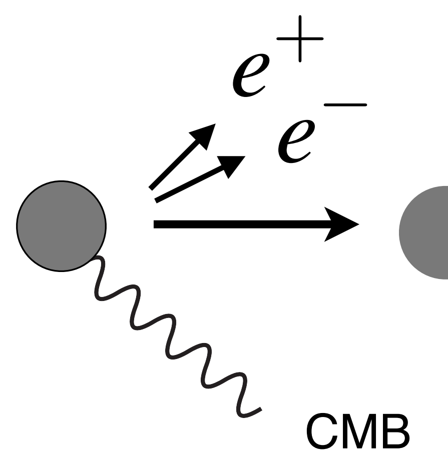

Photo-pion production
(mainly Δ resonance)

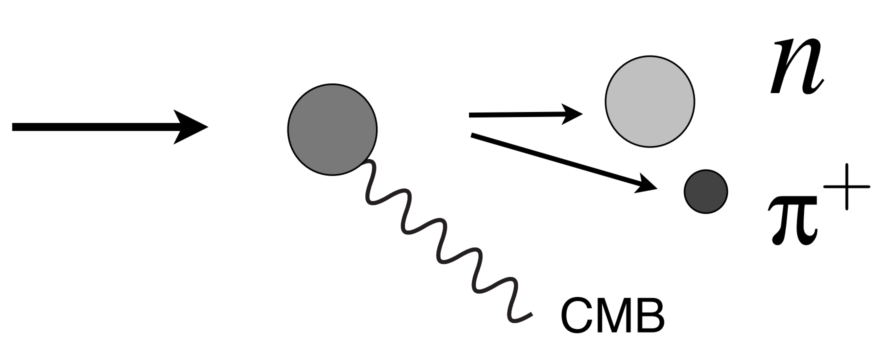

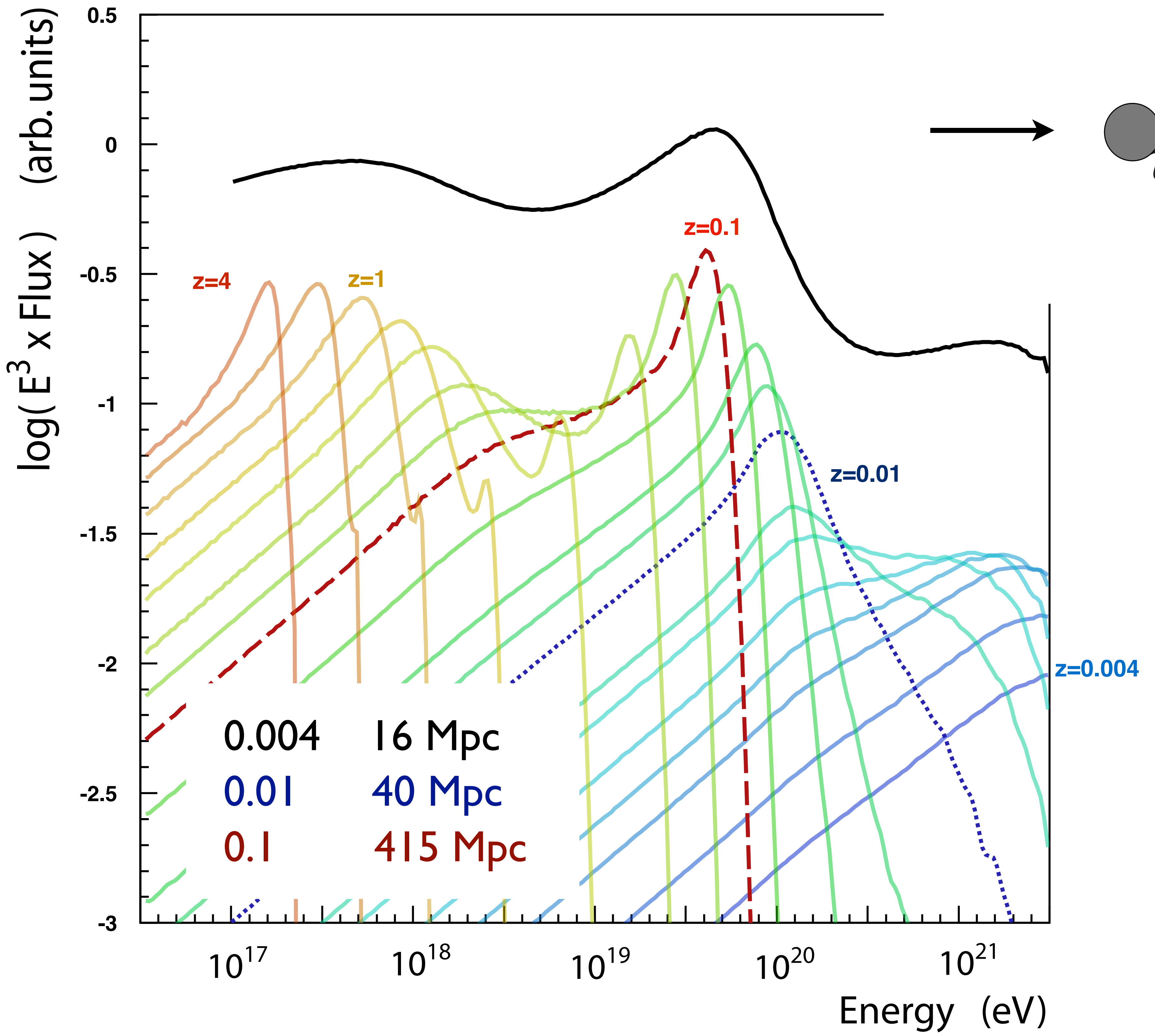

(Bergmann et al., PLB 2006)

Iron

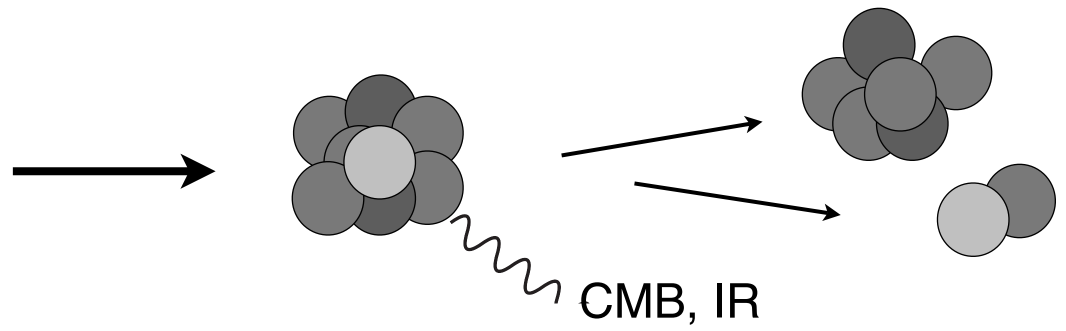

Photo-dissociation
(giant dipole resonance)

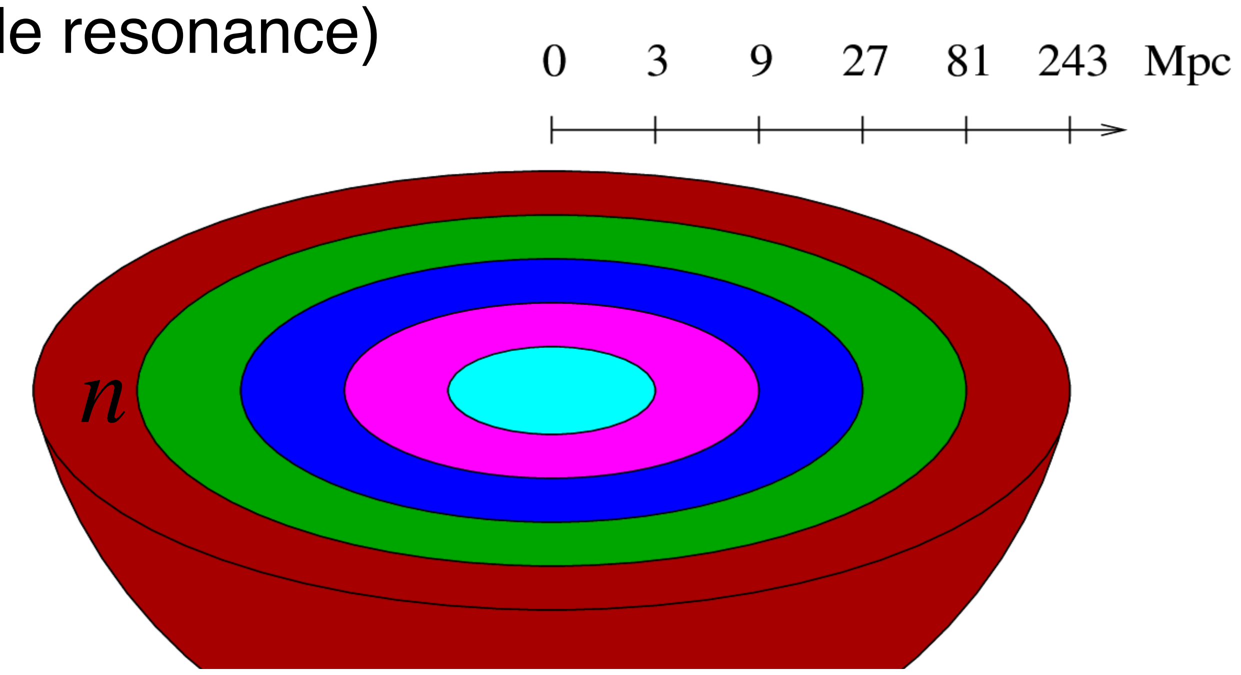

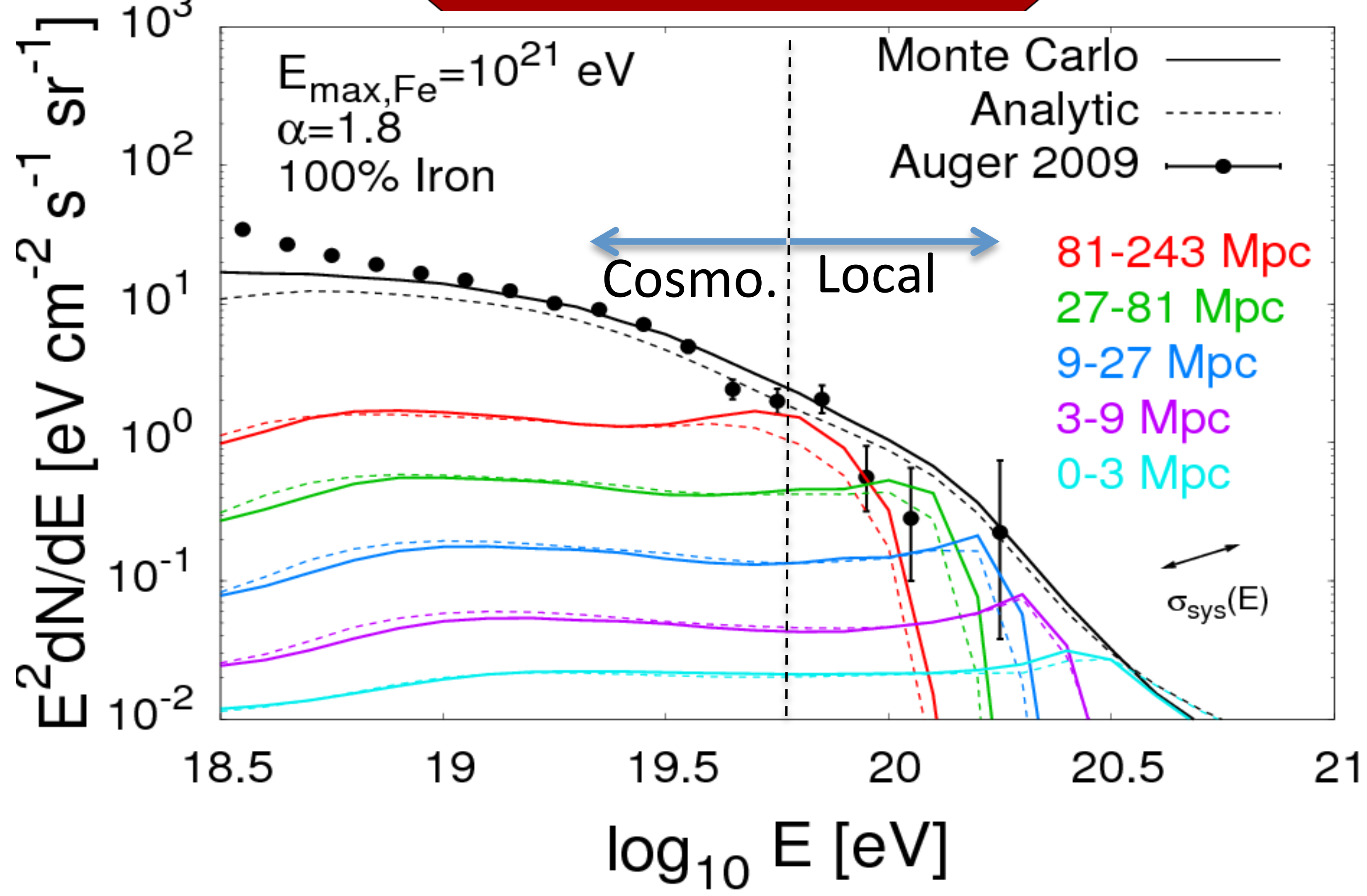

Greisen-Zatsepin-Kuzmin (GZK) effect, 1966

(Hooper, Taylor et al., PRD 2008)

Energy loss lengths of ultra-high-energy cosmic rays

(Allard et al. 2007)

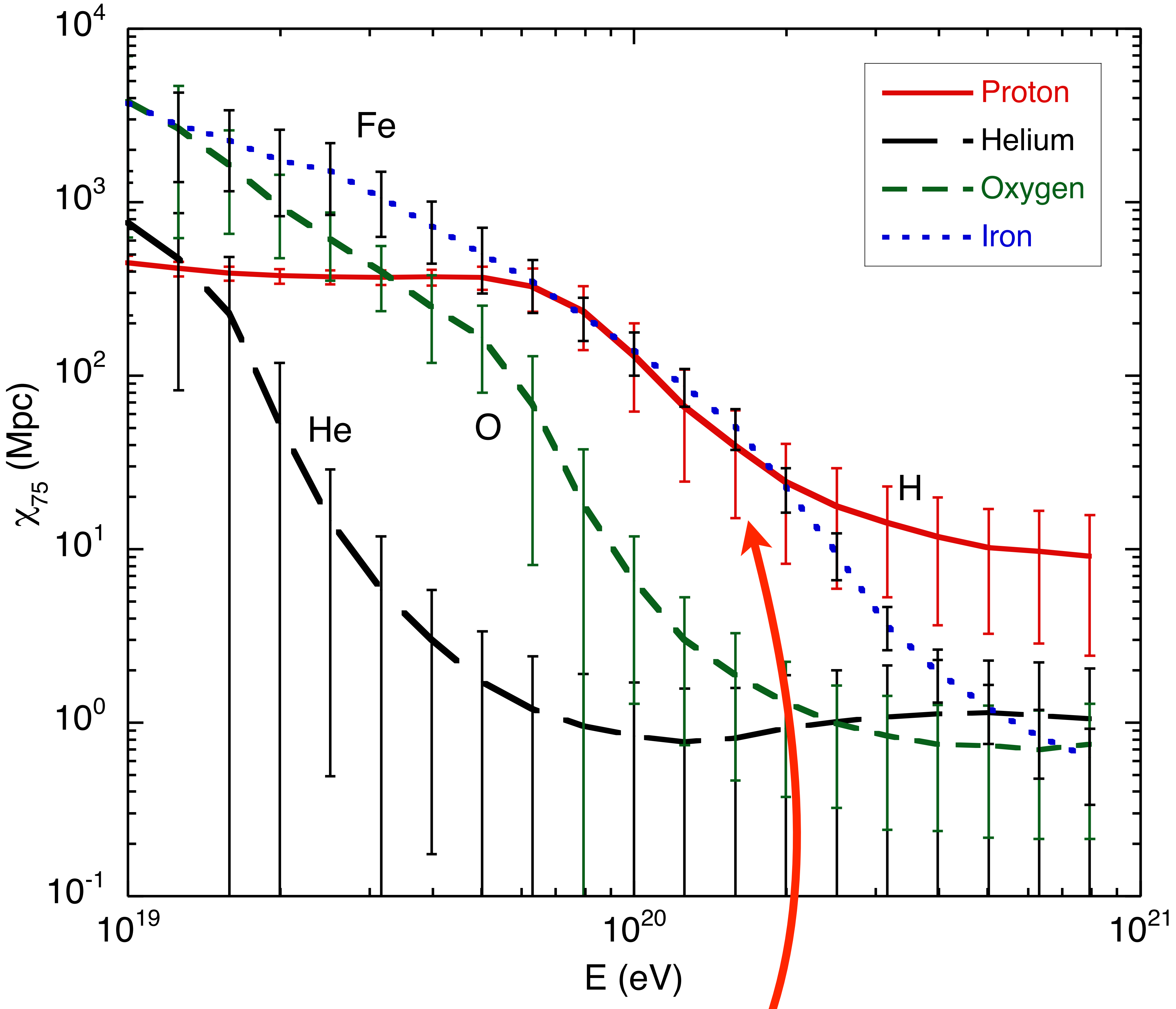

Coincidence of very similar suppression energy of p and Fe

(Aloisio, PTEP 2017)

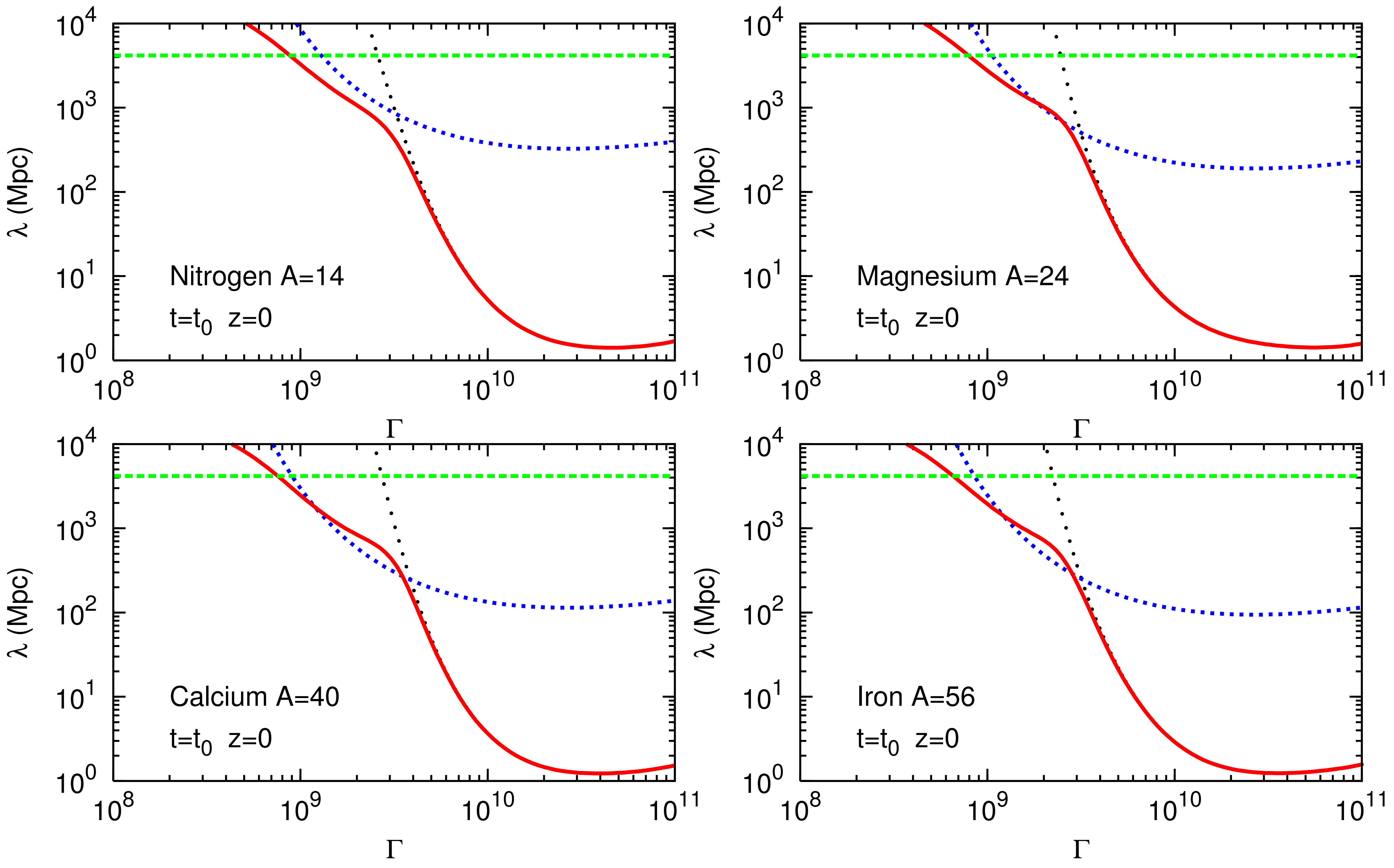

$$E = A\,\Gamma m_p$$

Energy threshold of suppression of nuclei scales with mass number (Giant dipole resonance at ~12 MeV lab.)

Ultra-high-energy cosmic rays: astronomy ?

Deflection in Galactic and extragalactic mag. fields

$$\delta \simeq 3^o \frac{B}{3\,\mu G} \frac{L}{kpc} \frac{6\times10^{19} eV}{E/Z}$$

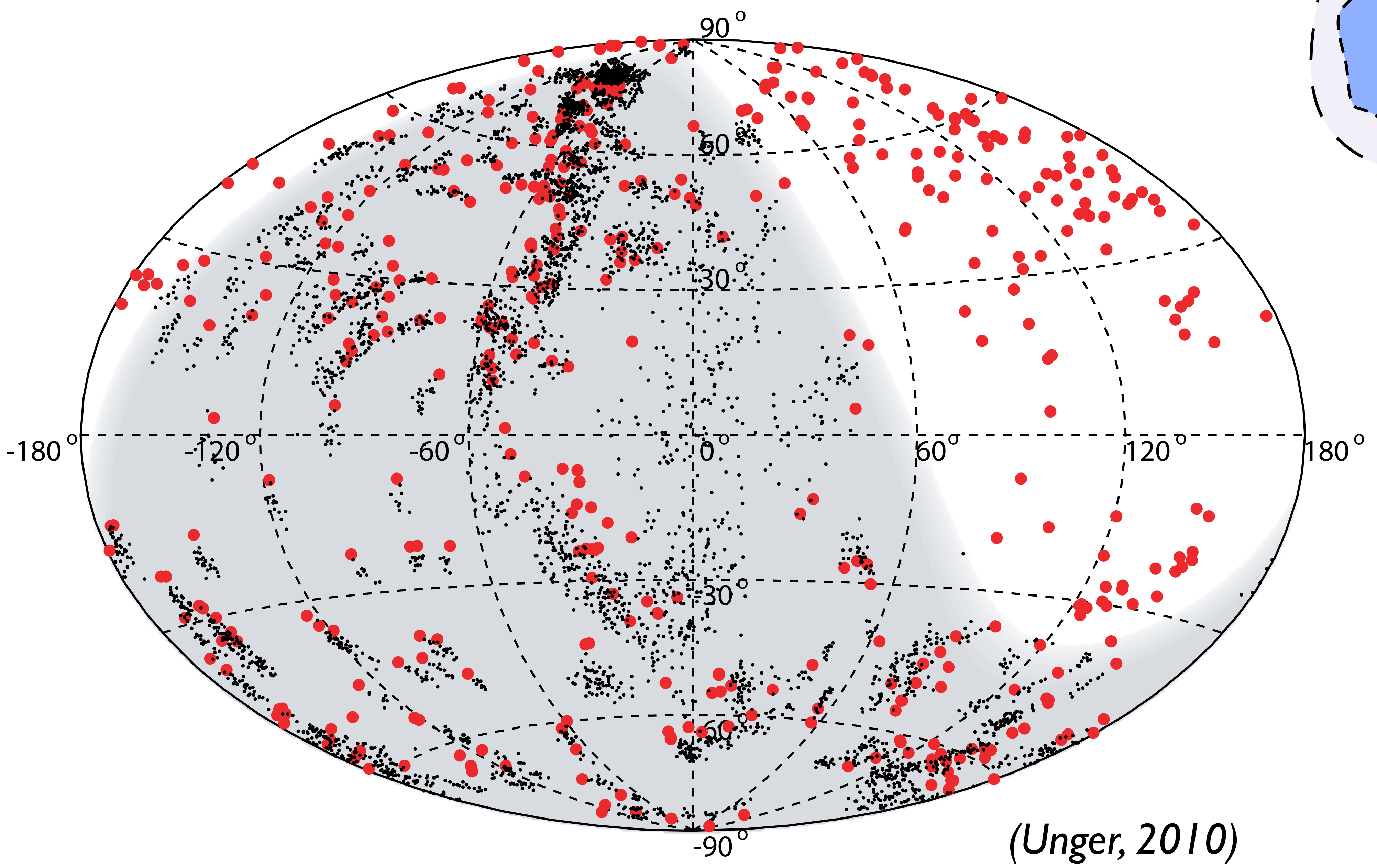

(Unger, 2010)

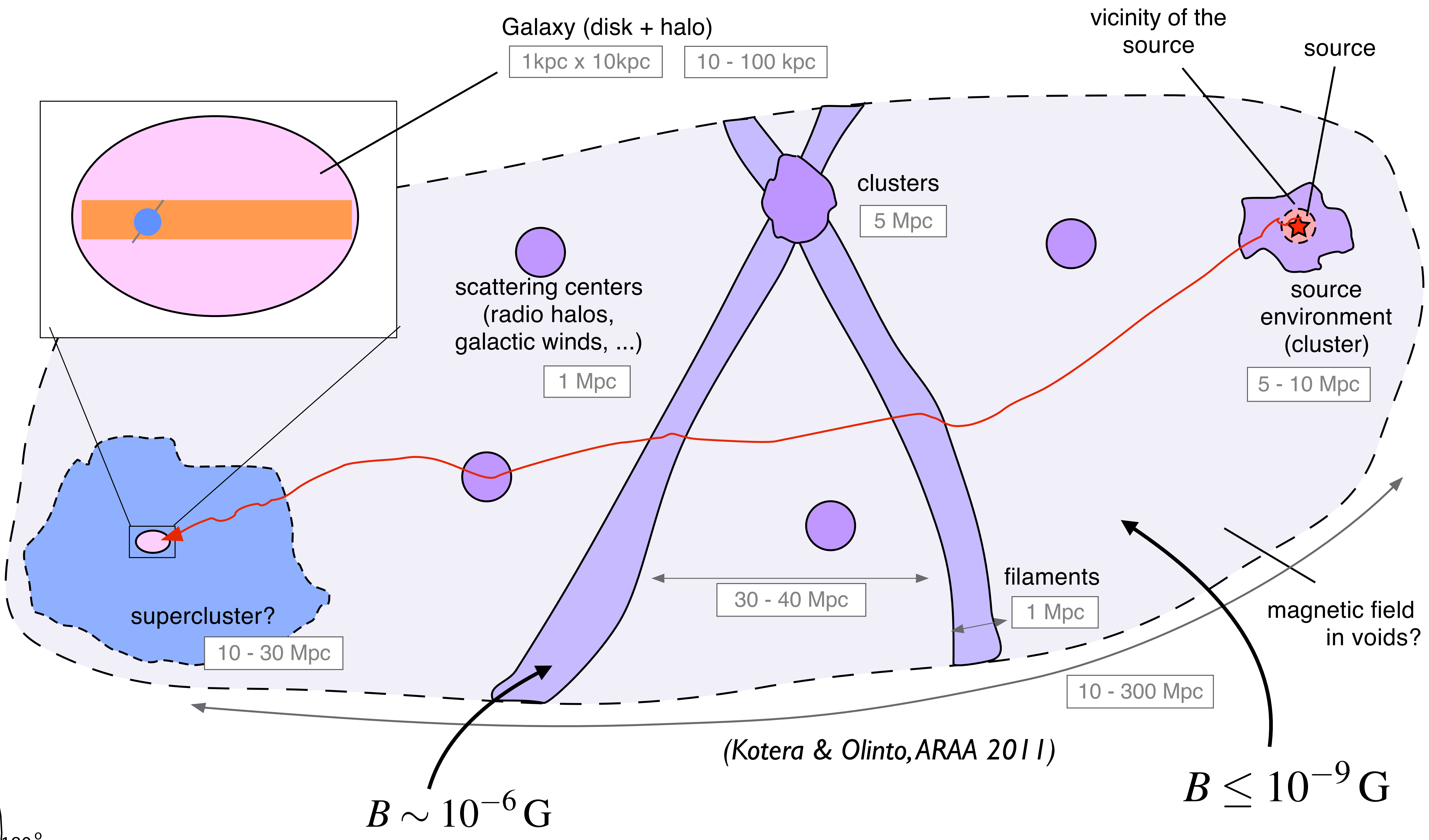

(Kotera & Olinto, ARAA 2011)

Anisotropy in arrival direction distribution on small, intermediate and large scales

Multi-messenger signals (gamma-rays and neutrinos)

Pierre Auger Observatory and Telescope Array

Telescope Array (TA)
Delta, UT, USA
507 detector stations, 680 km²
36 fluorescence telescopes

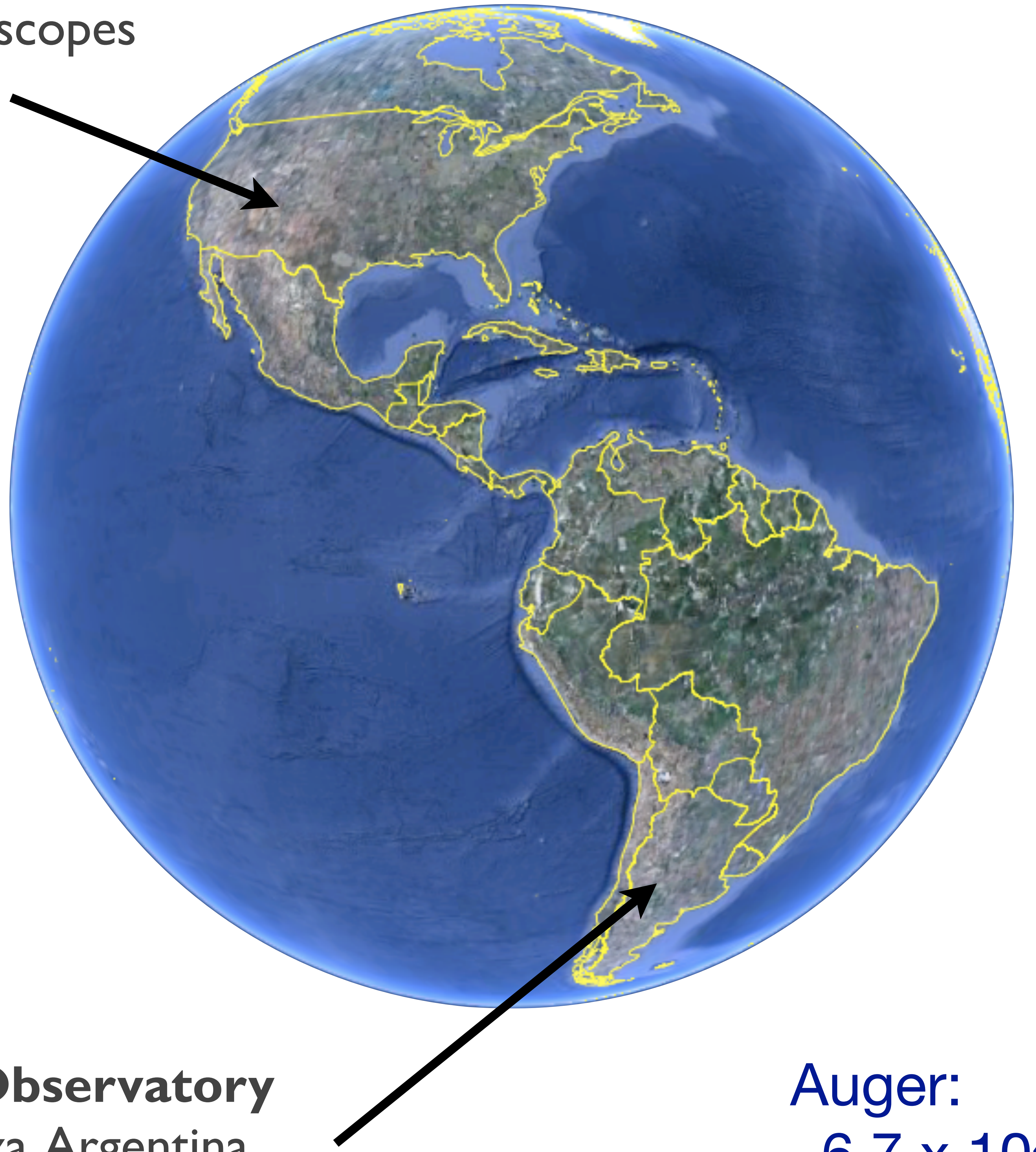

Pierre Auger Observatory
Province Mendoza, Argentina
1660 detector stations, 3000 km²
27 fluorescence telescopes

Together full sky coverage

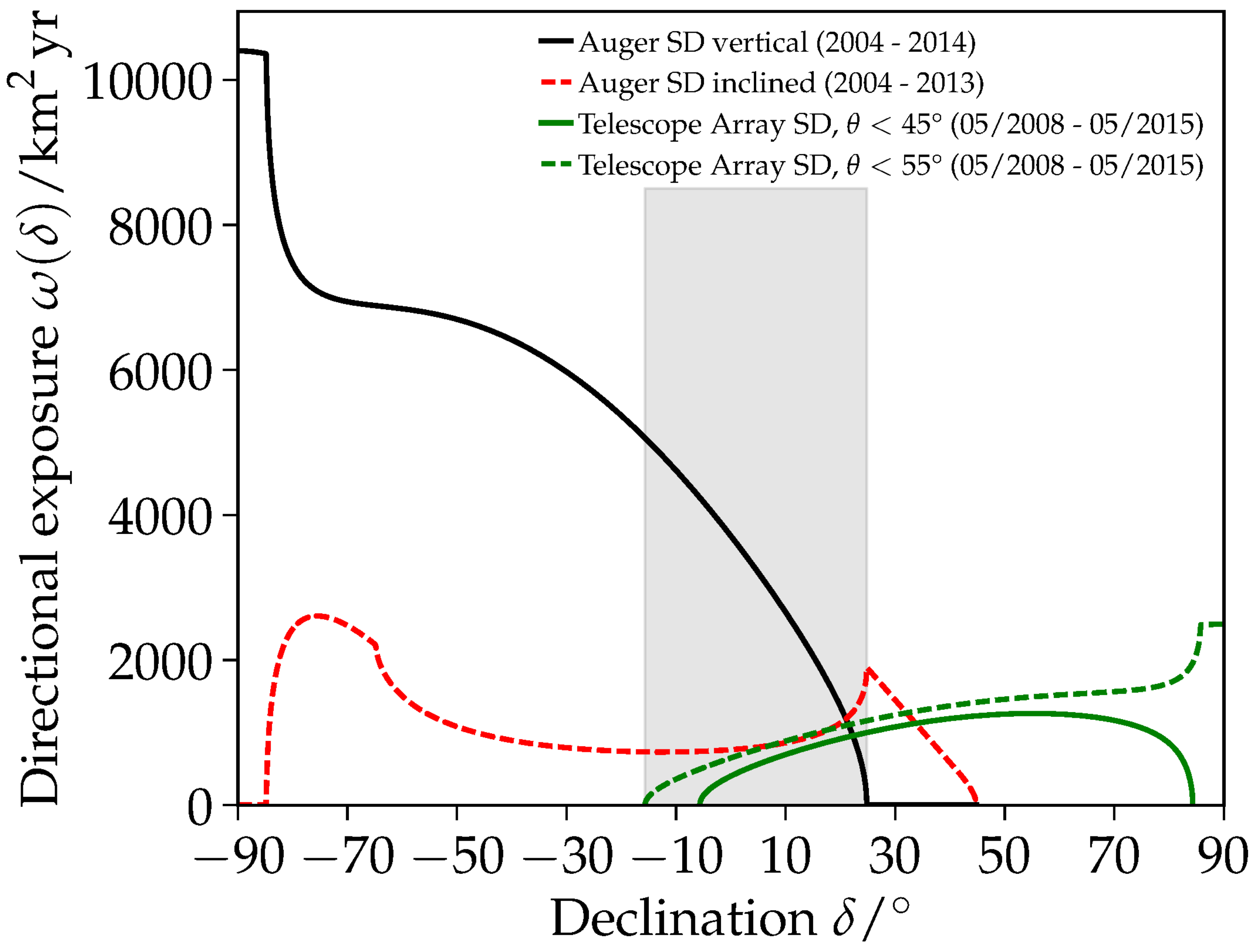

Auger:
- 6.7×10^4 km² sr yr (spectrum)
- 9×10^4 km² sr yr (anisotropy)

TA:
- 8.1×10^3 km² sr yr (spectrum)
- 8.6×10^3 km² sr yr (anisotropy)

Energy spectrum (all-particle flux)

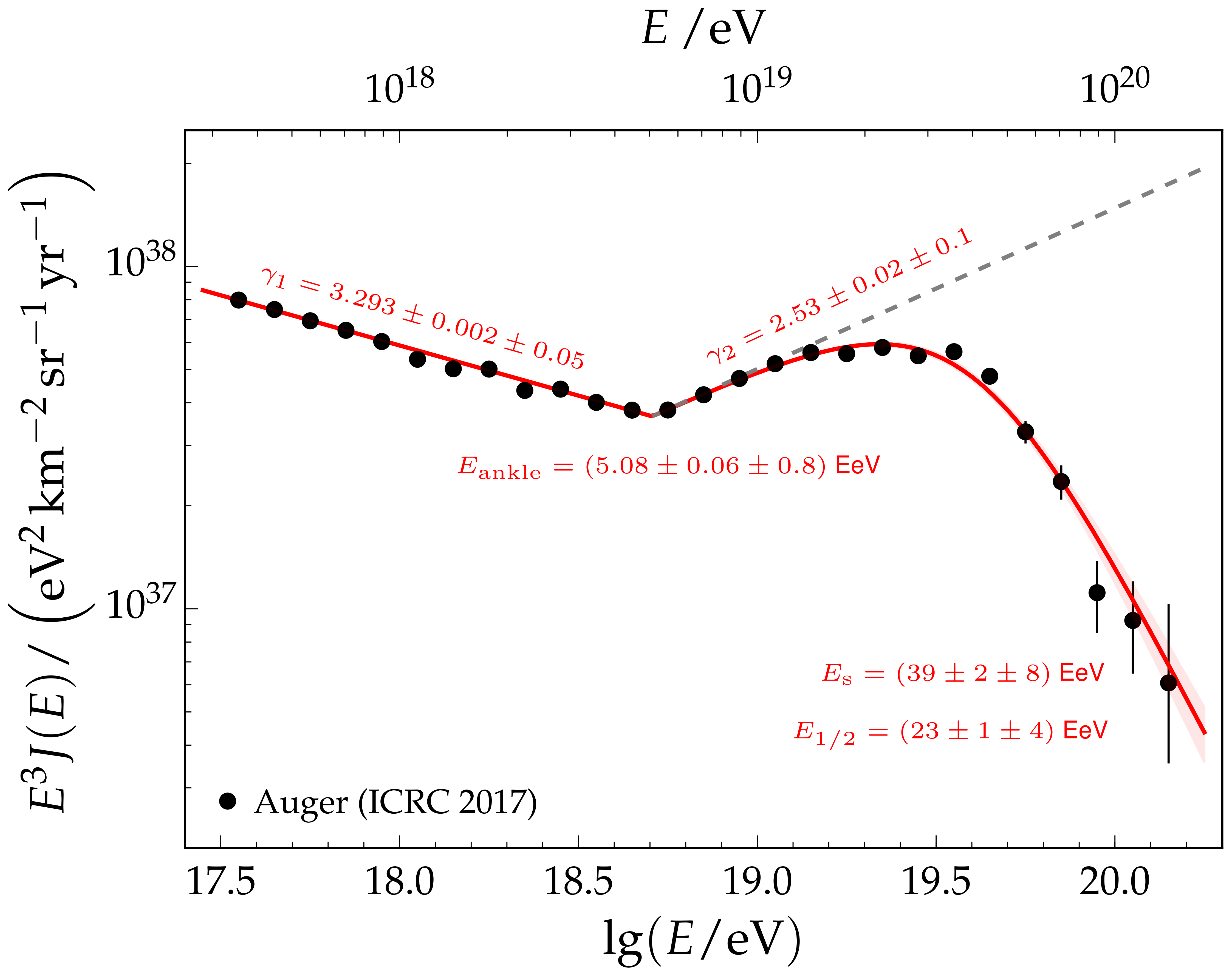

(Auger-TA Spectrum Working Group)

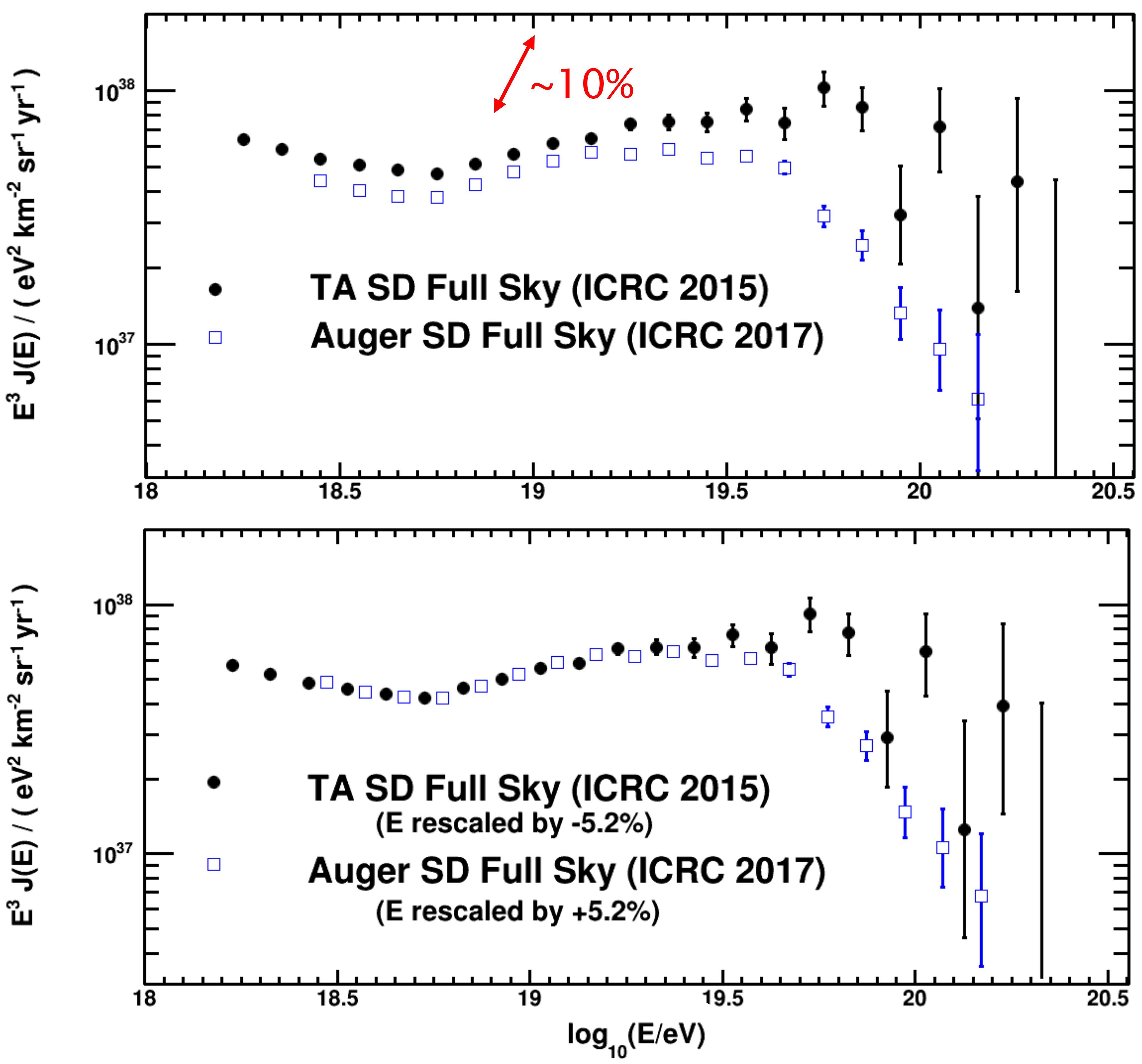

Sys. uncertainty of energy scale

Auger	$\Delta E/E = 14\%$
TA	$\Delta E/E = 21\%$

Are the energy spectra consistent with each other?

All sky

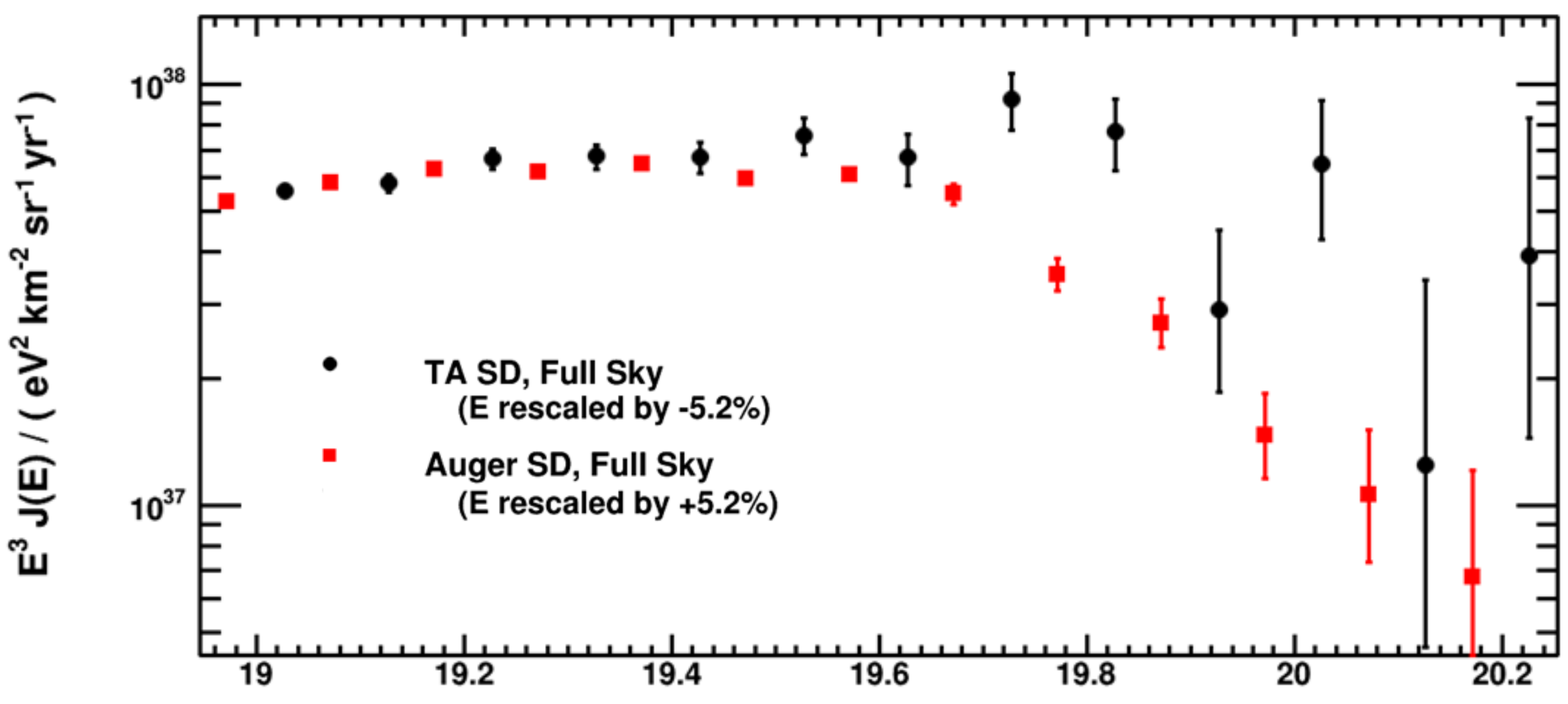

Common declination band

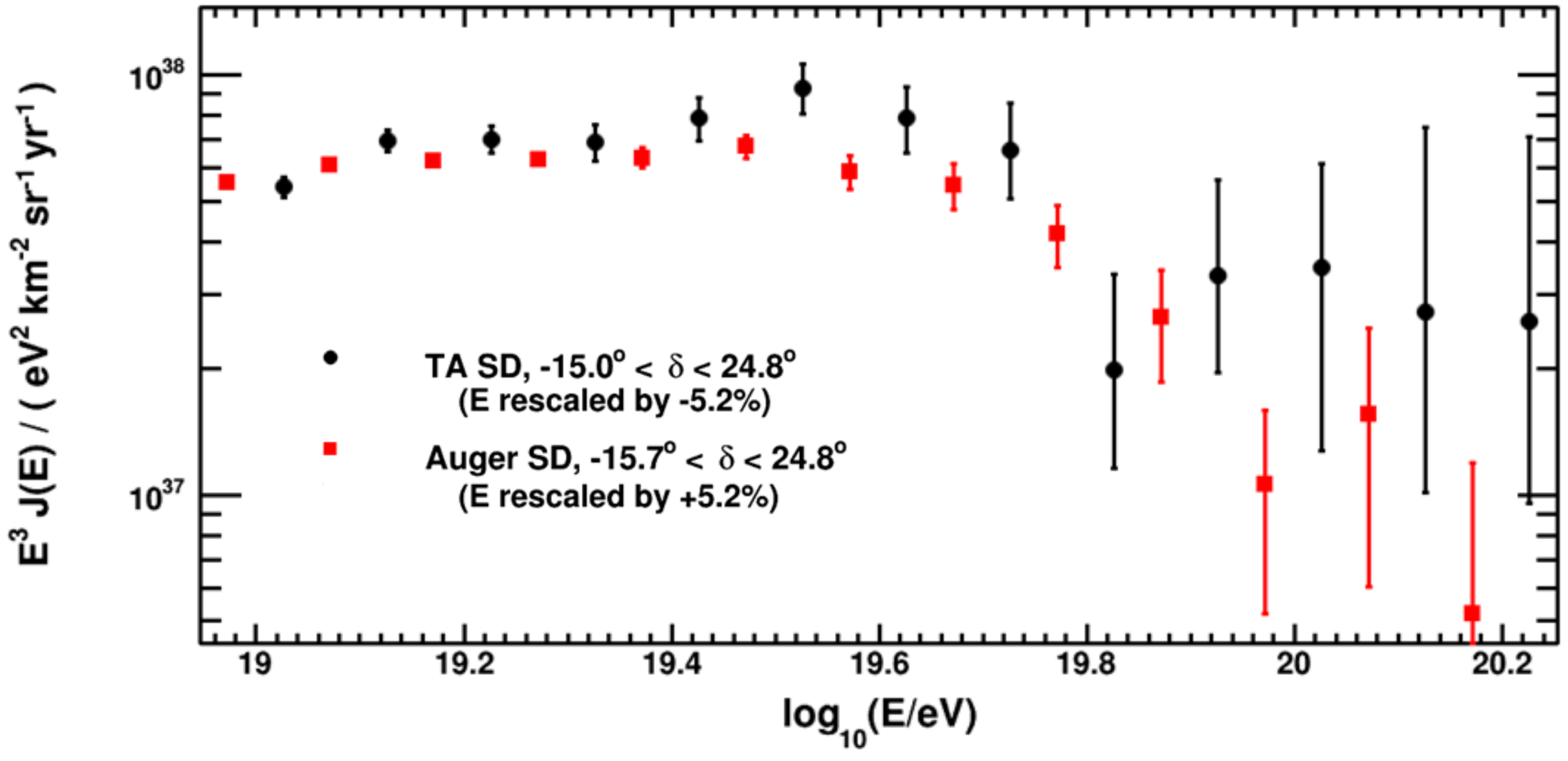

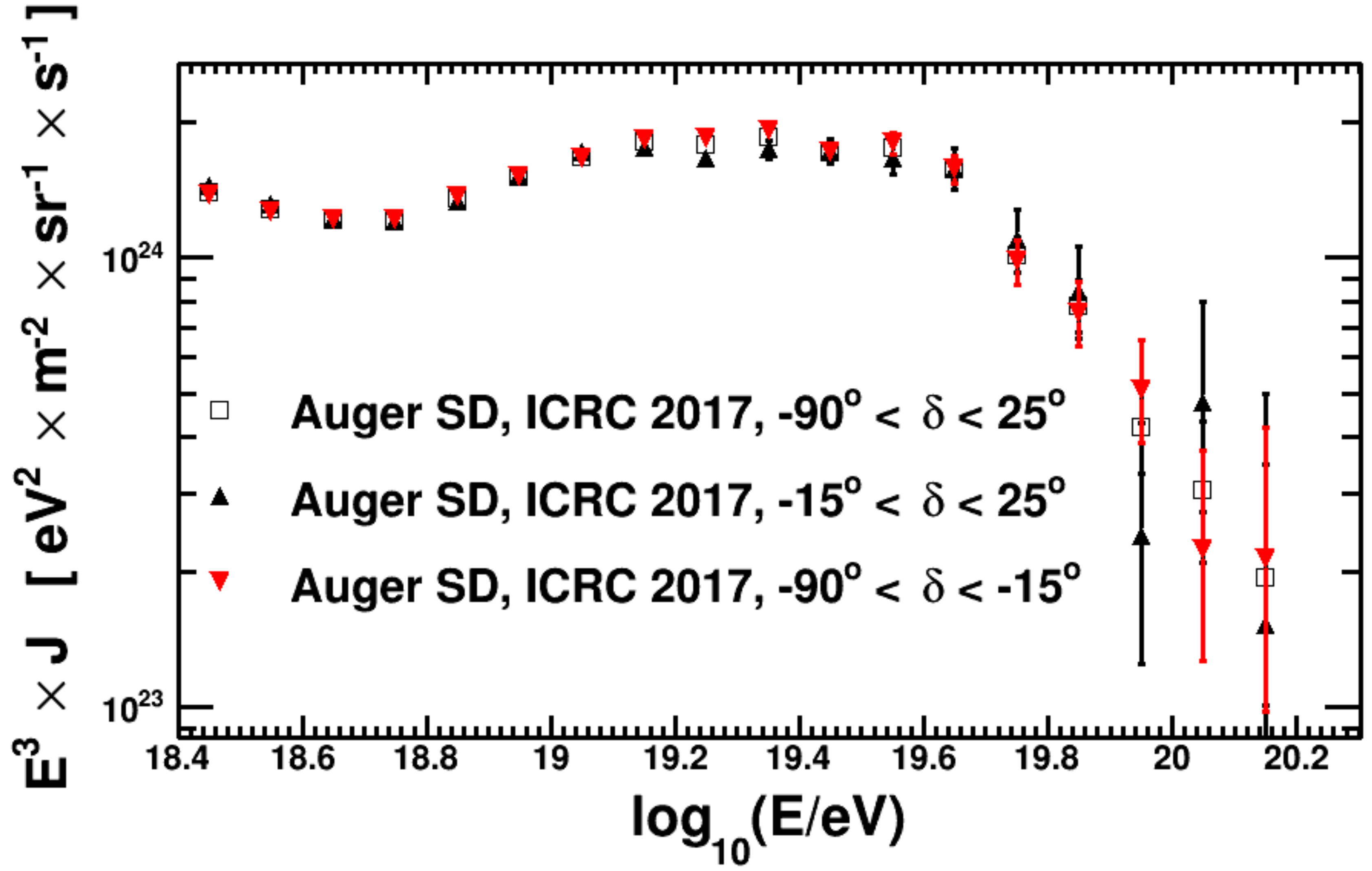

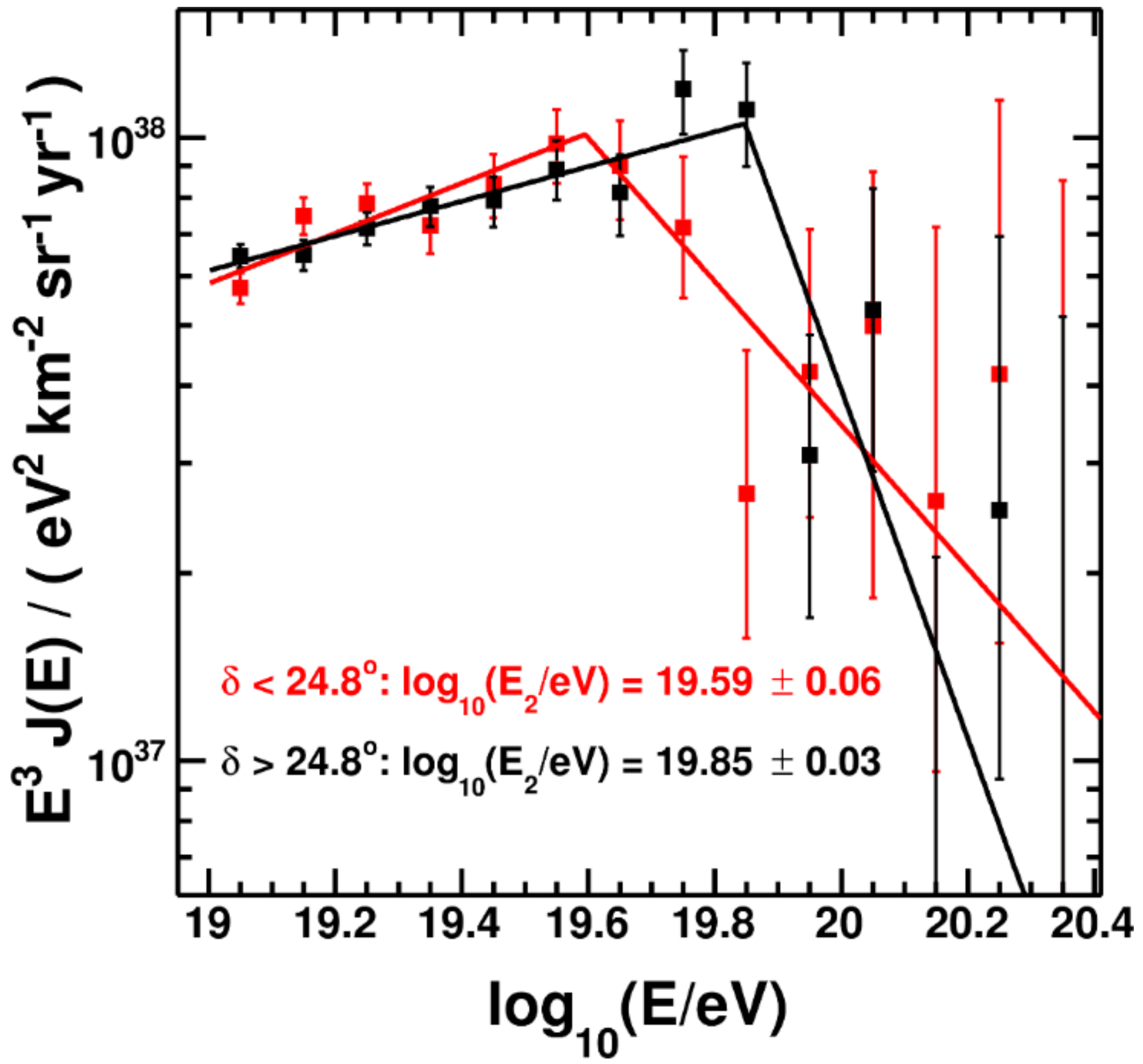

Better agreement if only common declination band considered – anisotropy ?!

Telescope Array: spectrum with TALE

(Abuzayyad, ICRC 2017)

Low energy showers develop high in atmosphere

Less light produced due to smaller number of secondary particles

Viewed at small angle to shower axis

Composition-dependent correction to go from calorimetric energy to total energy

(RE et al. Ann. Rev. Nucl. Part. Phys. 2011, 61)

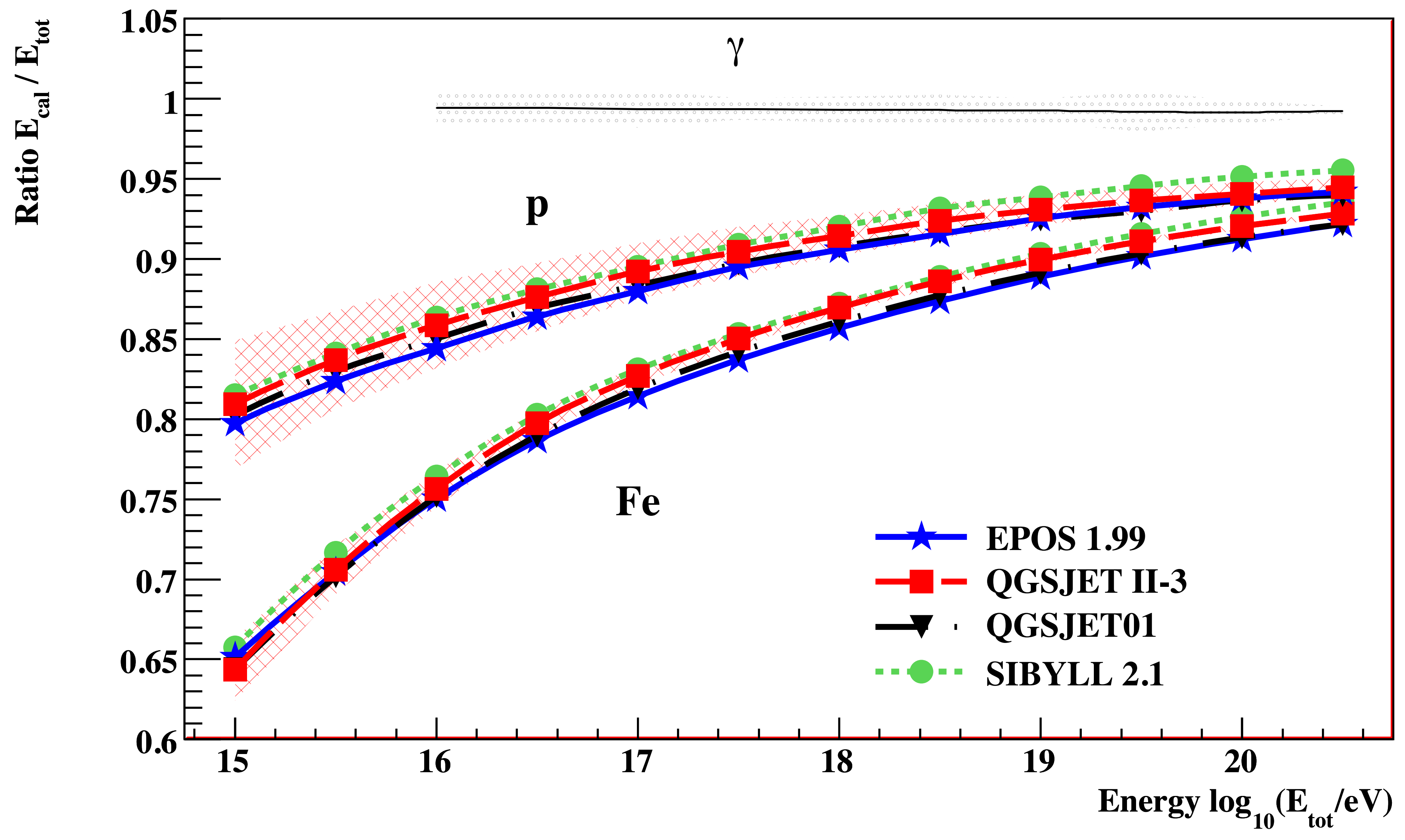

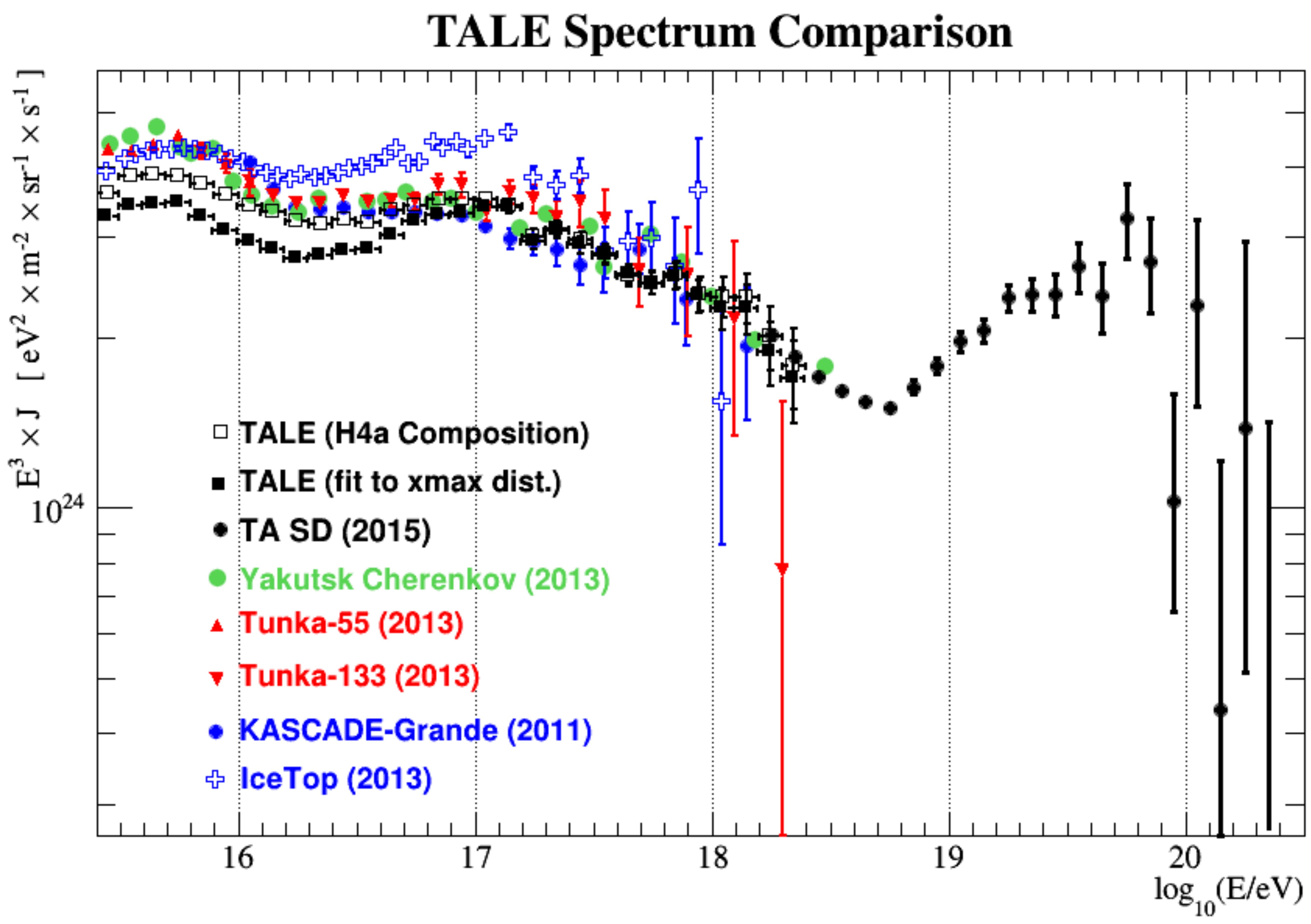

Best detection of second knee so far

Depth of shower maximum (Auger results)

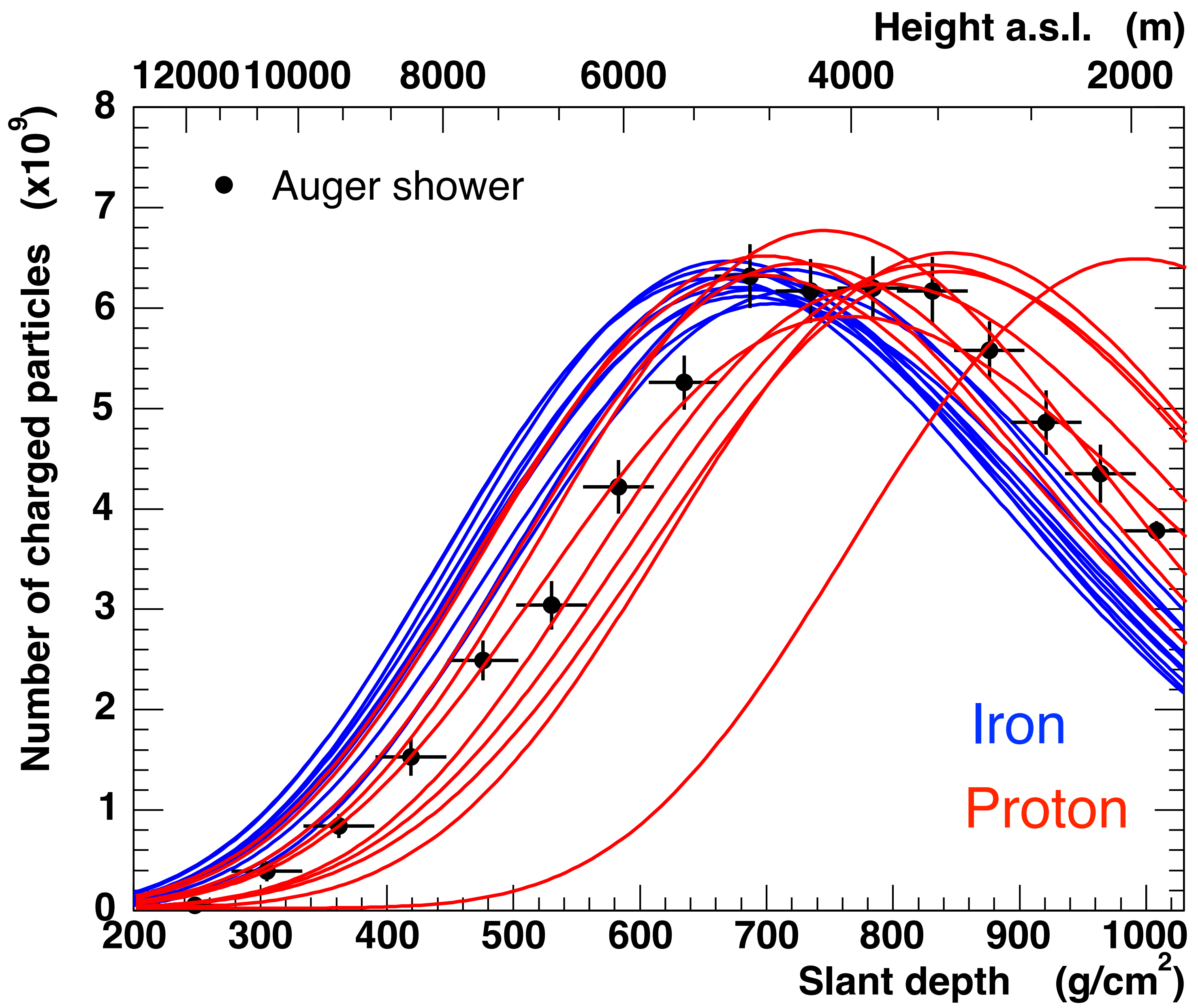

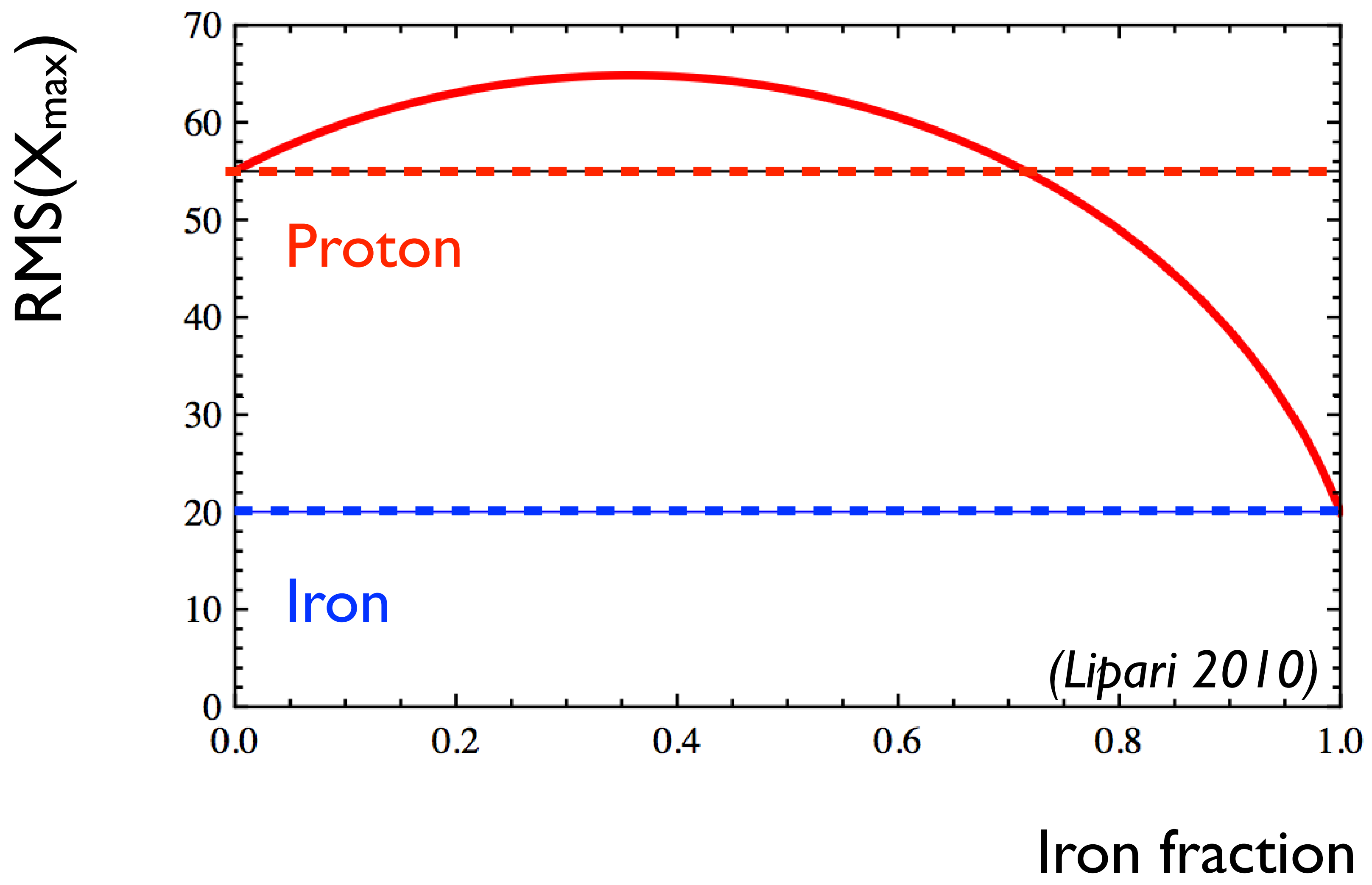

Break in elongation rate just below energy of ankle

Shower-by-shower fluctuations very small

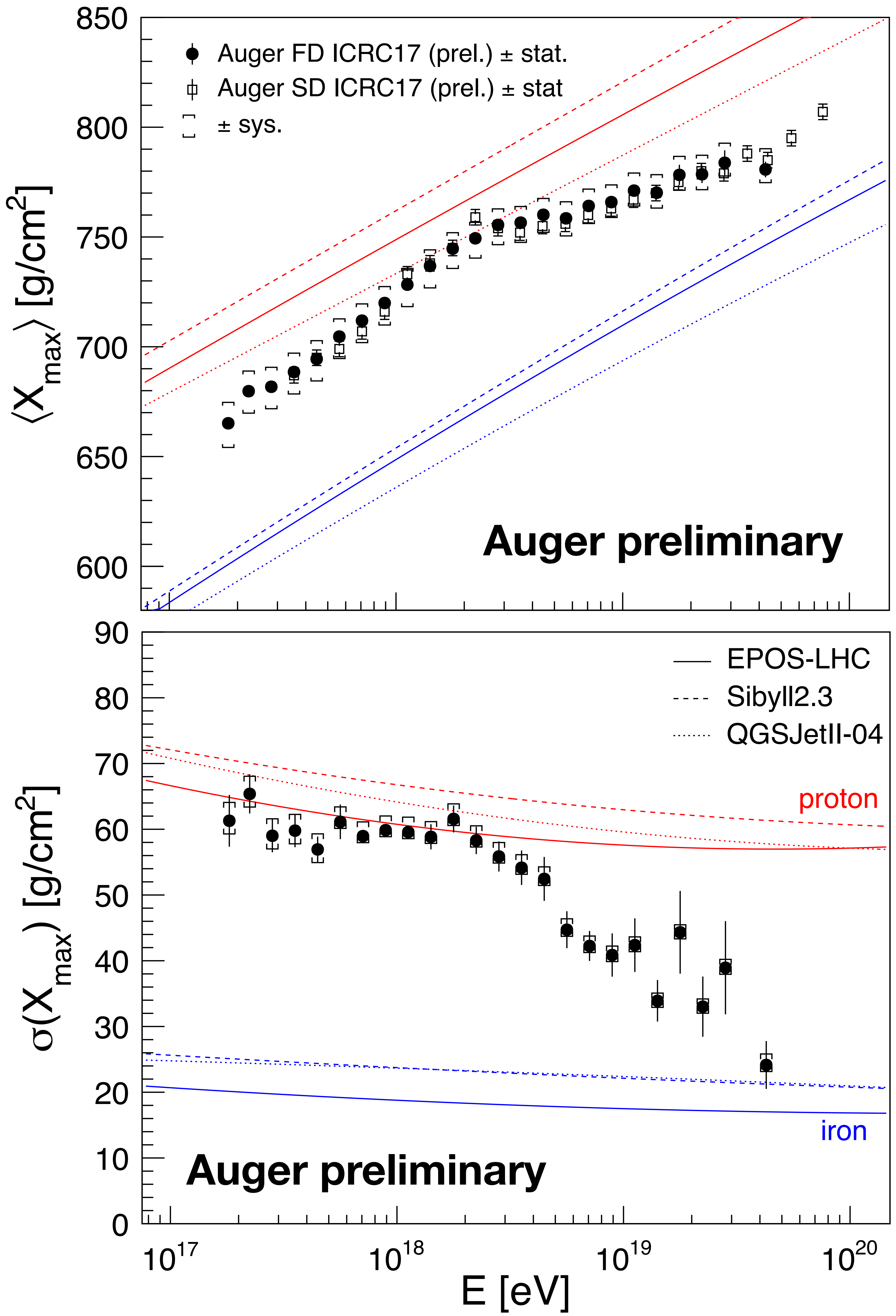

Mass composition at top of the atmosphere

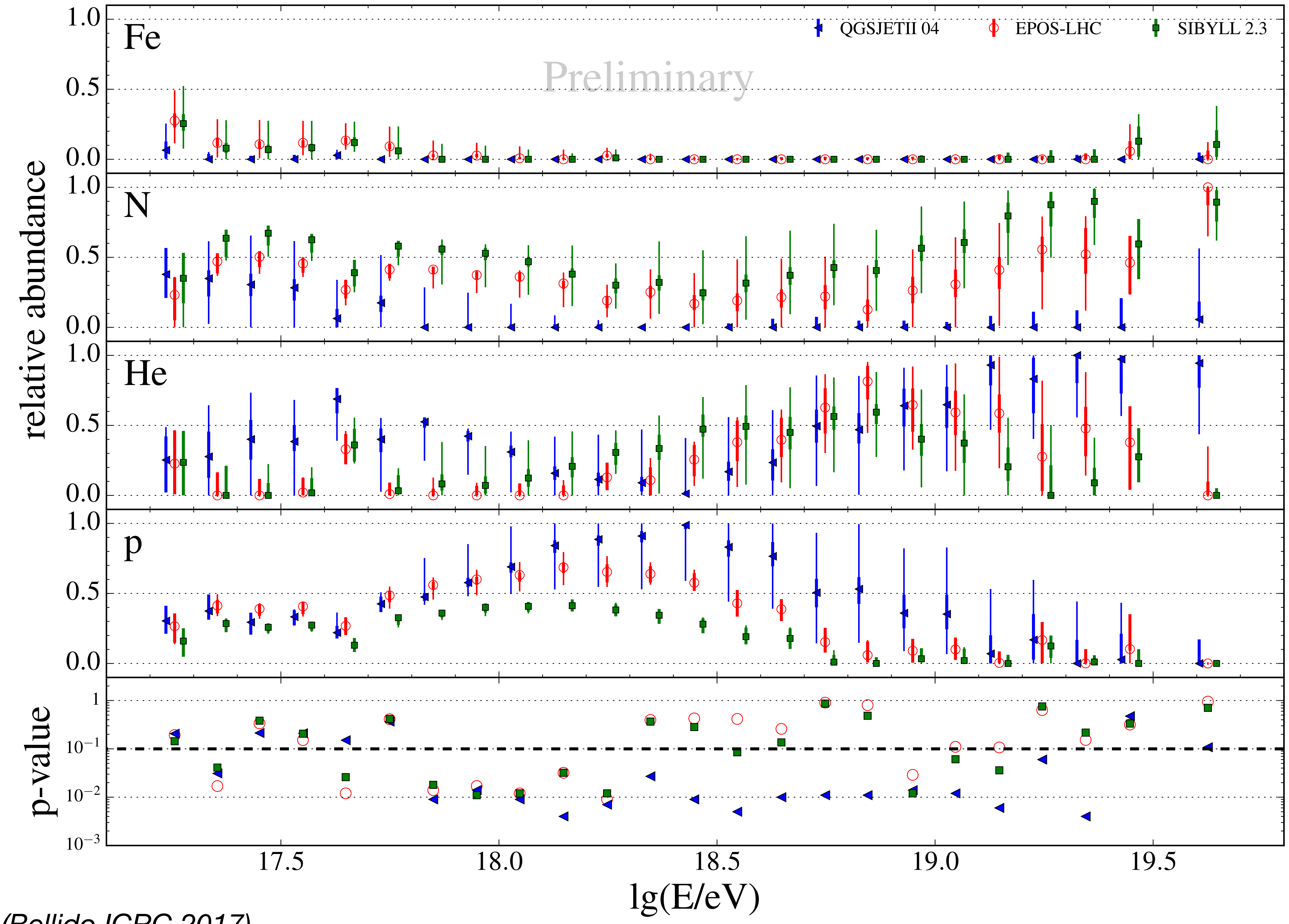

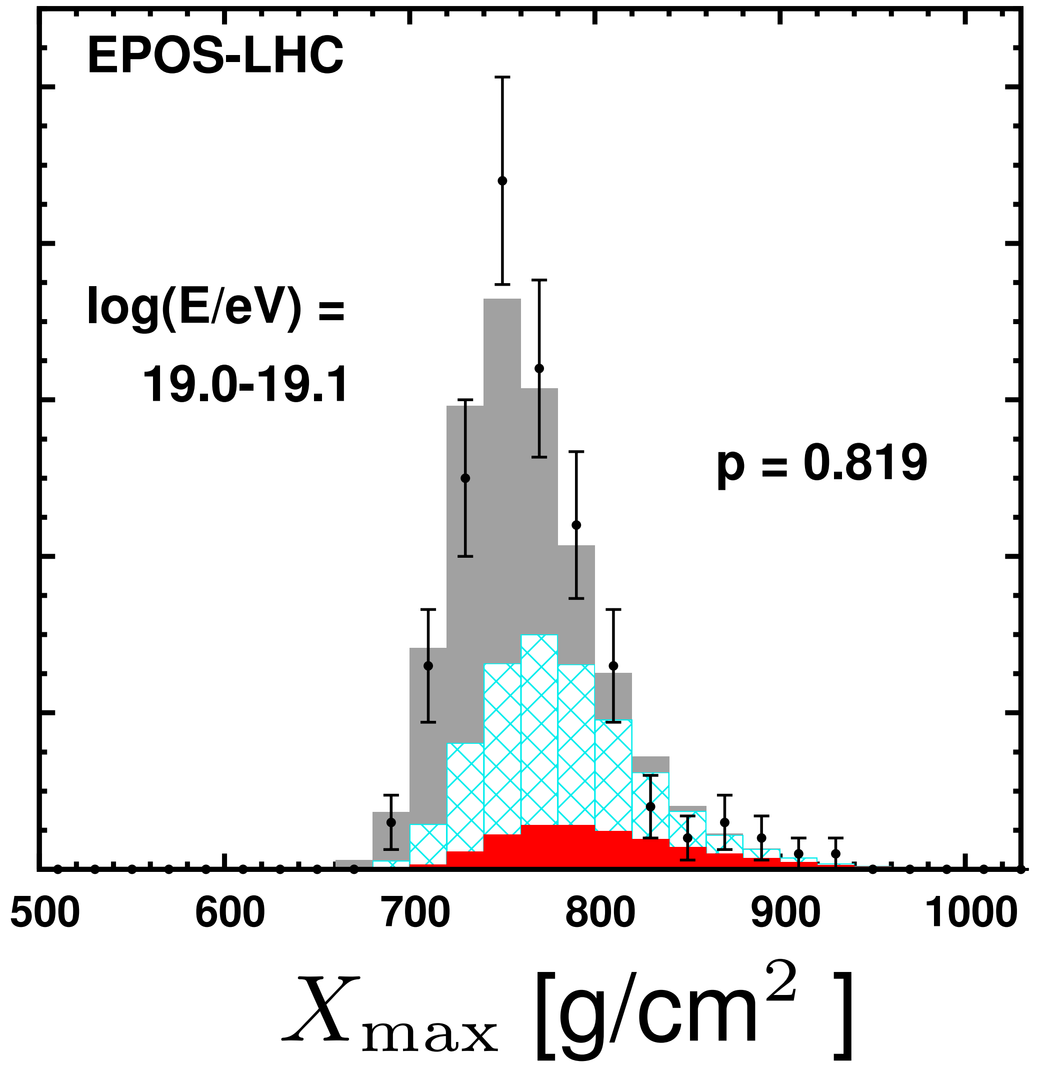

p He N Fe

LHC-tuned interaction models

Fit quality not always good

No iron needed for interpretation

Large proton fraction below ankle

No obvious scaling with rigidity

Data cover only range up to $10^{19.5}$ eV

(Bellido ICRC 2017)

Comparison with TA results

(TA composition summary, Hanlon, ICRC 2017)

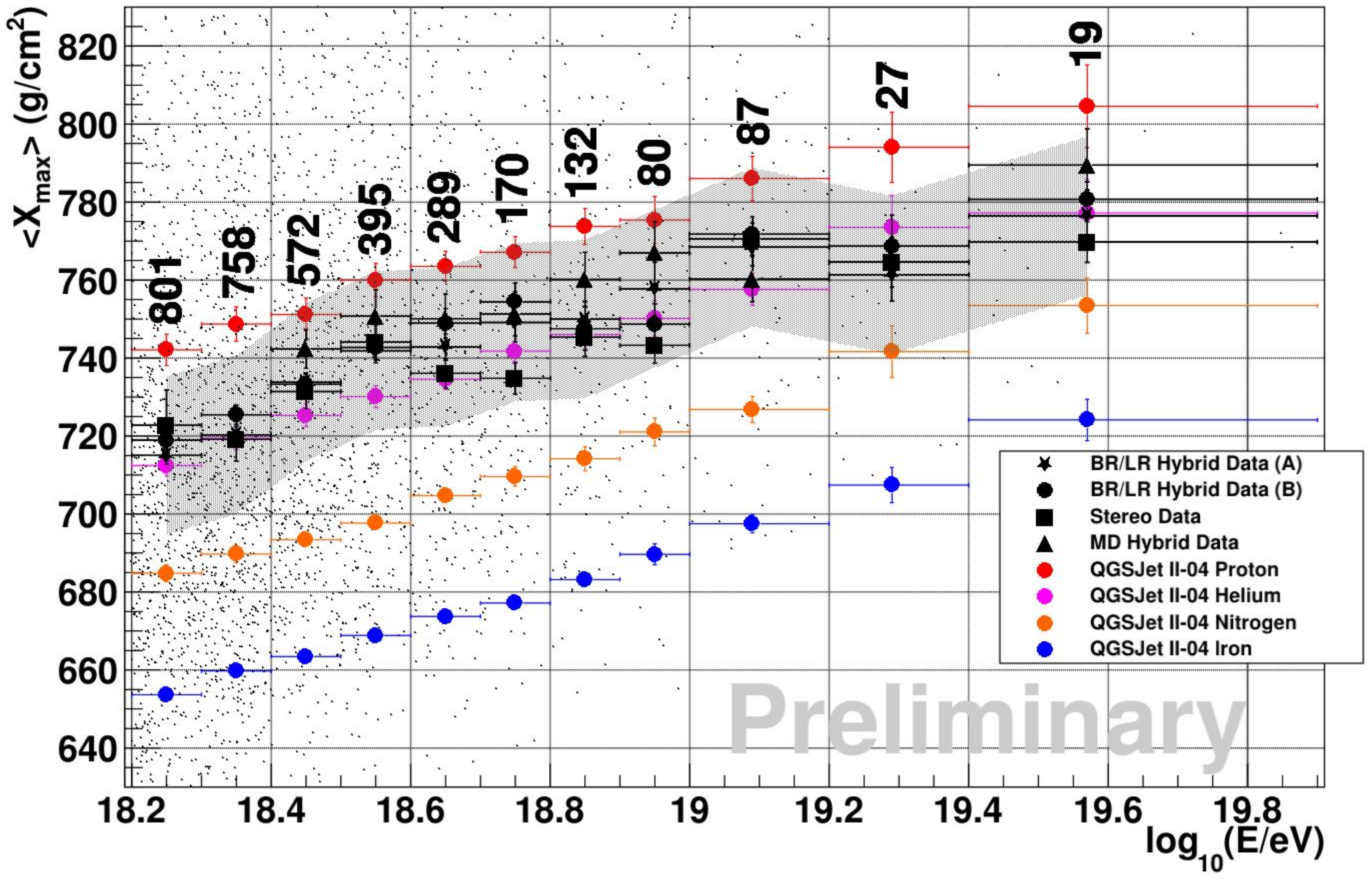

Data cannot be compared directly due to different FoV treatment

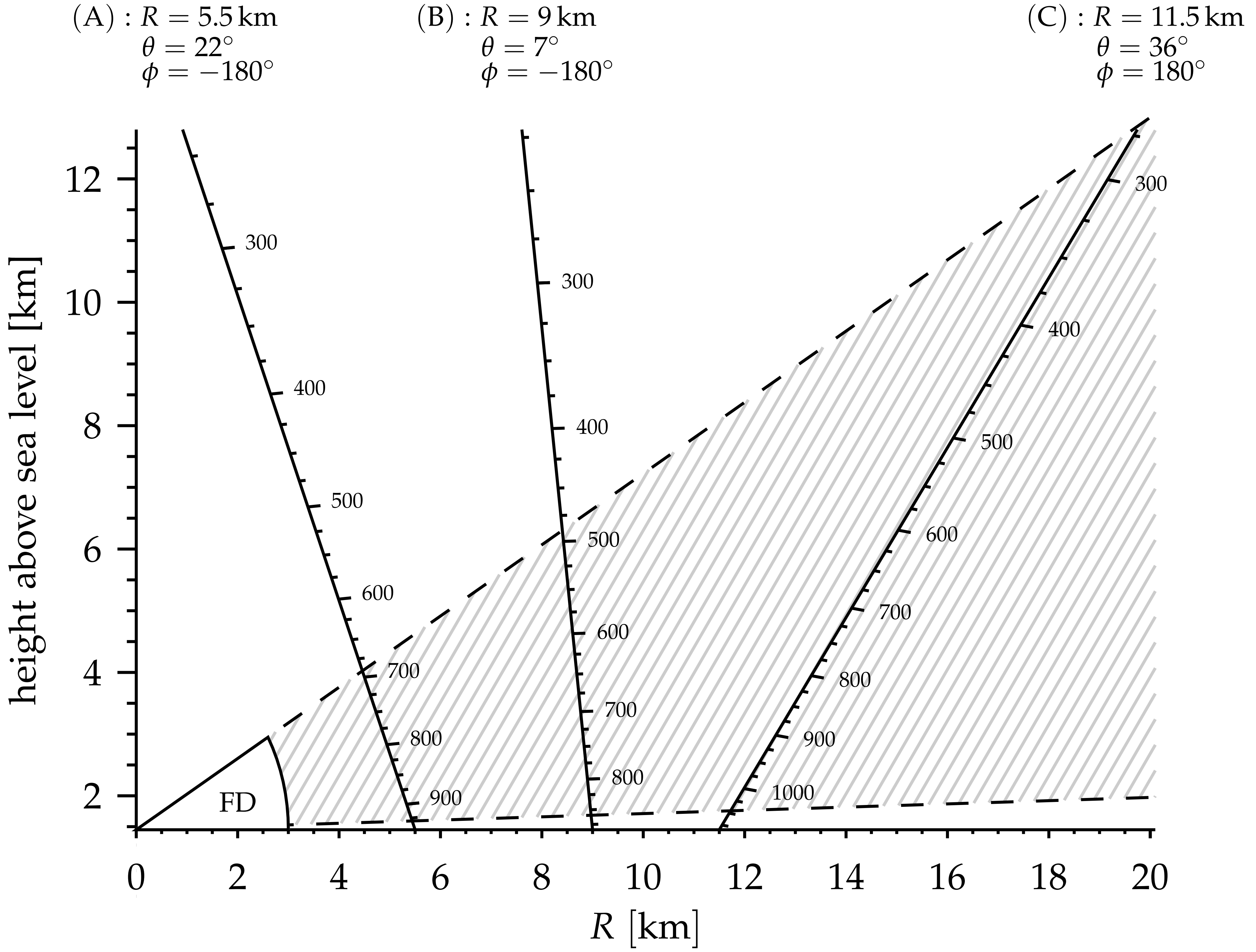

Auger: only shower geometries for which all X_{max} values visible

TA: all showers with X_{max} in field of view (bias due to detector acceptance)

Auger-TA Working Group: data of the two experiments in agreement within the exp. uncertainties (E < 10^{19} eV)

Change of model predictions thanks to LHC data

pre-LHC models

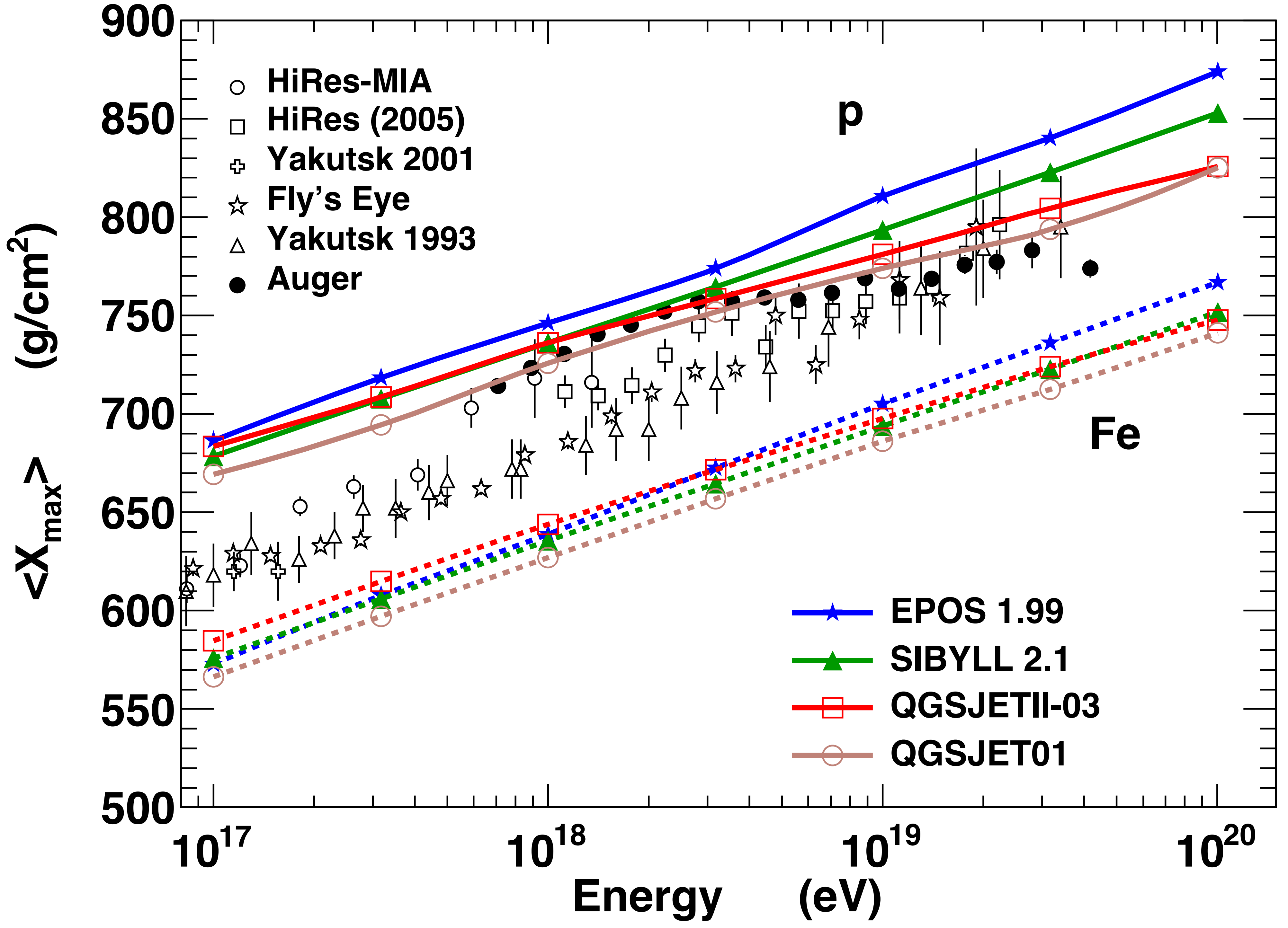

post-LHC models

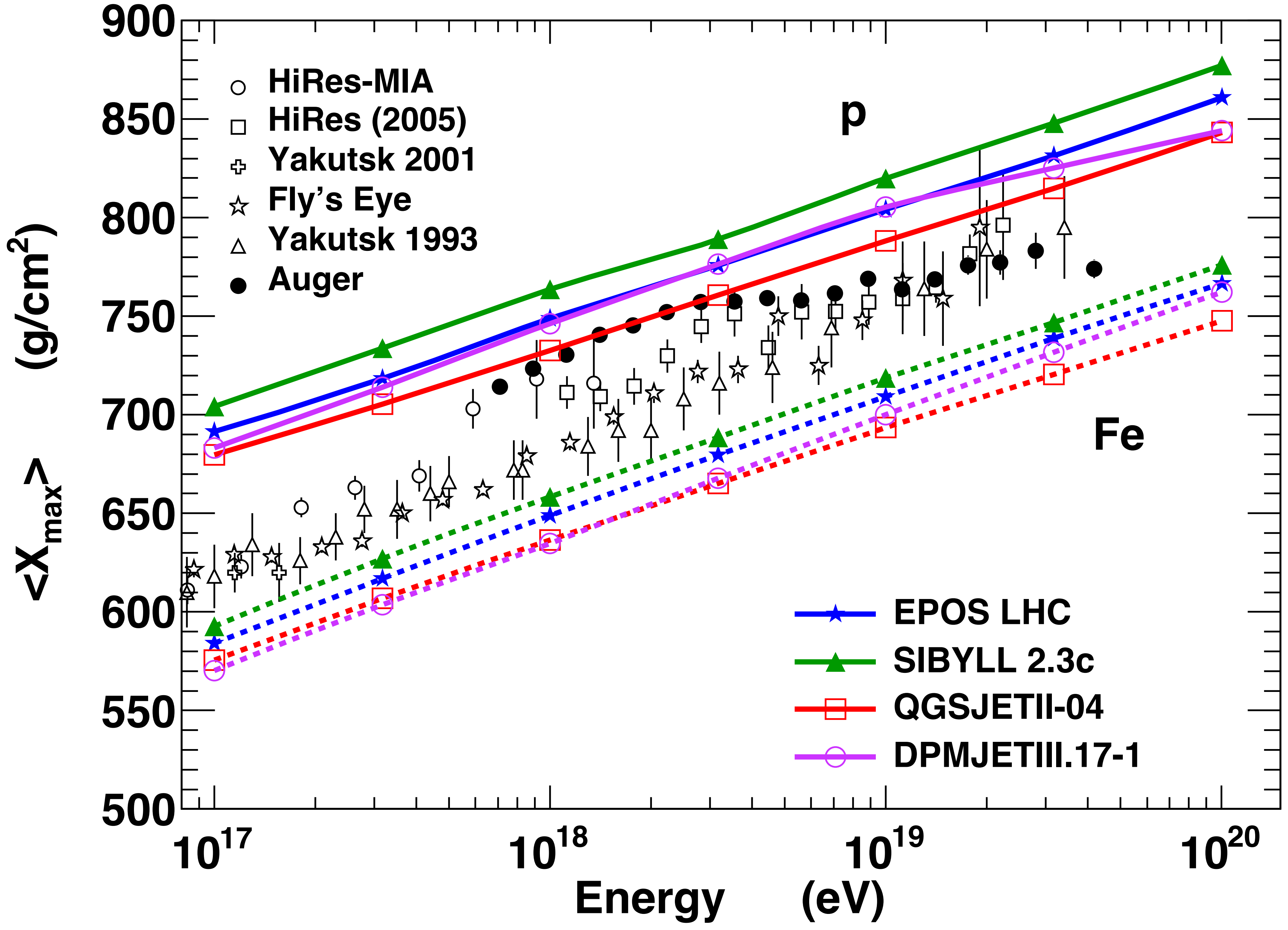

(Pierog, ICRC 2017)

Sys. X_{max} uncertainty Auger: $\Delta X_{max} = -10\,\mathrm{g/cm^2}\ +8\,\mathrm{g/cm^2}$

TA: $\Delta X_{max} = \pm 20\,\mathrm{g/cm^2}$

LHC-tuned models should be used for data interpretation

What is the origin of the flux suppression at 6×10^{19} eV?

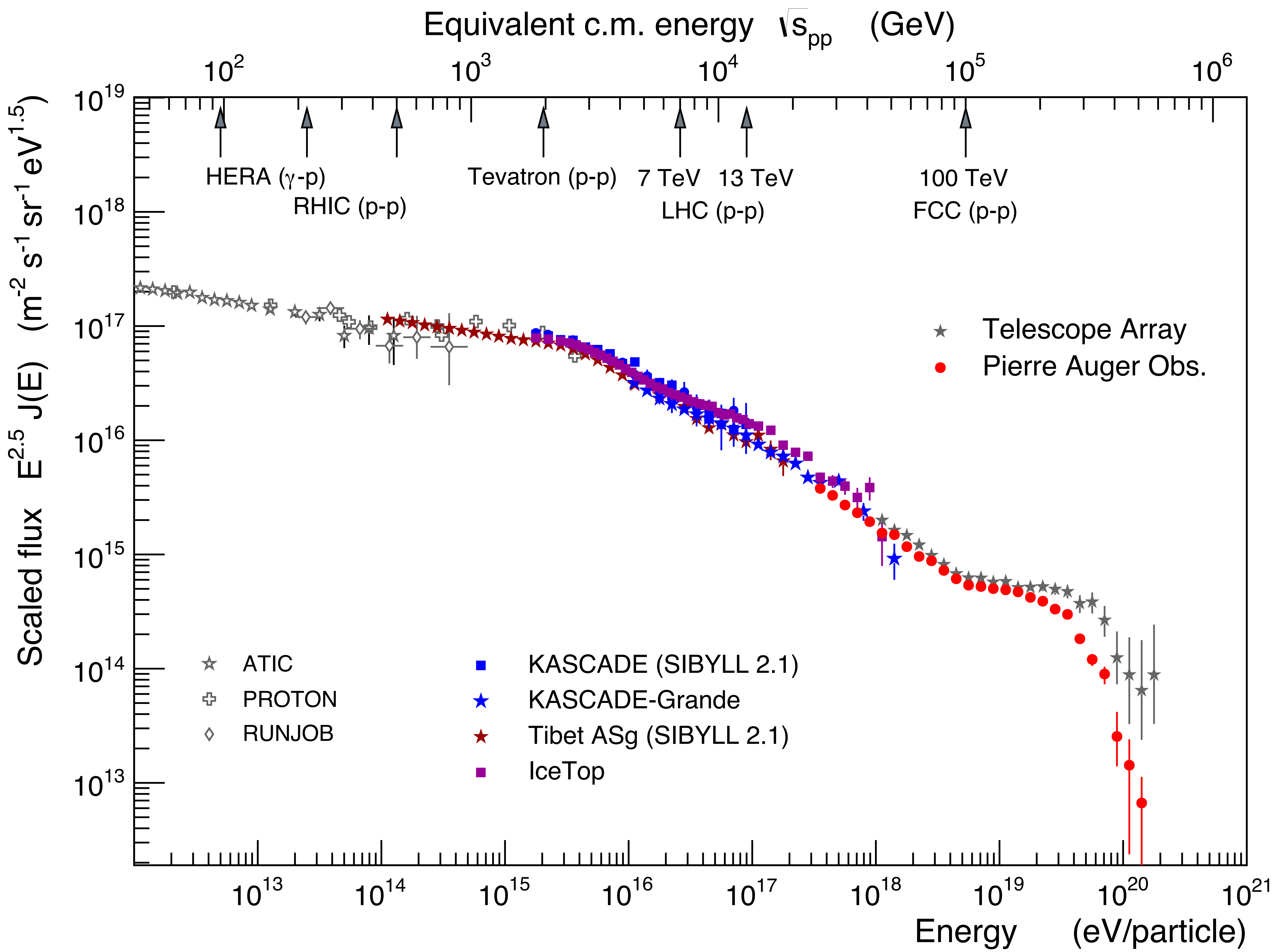

Greisen-Zatsepin-Kuzmin (GZK) effect

Photo-pion production
(mainly Δ resonance)

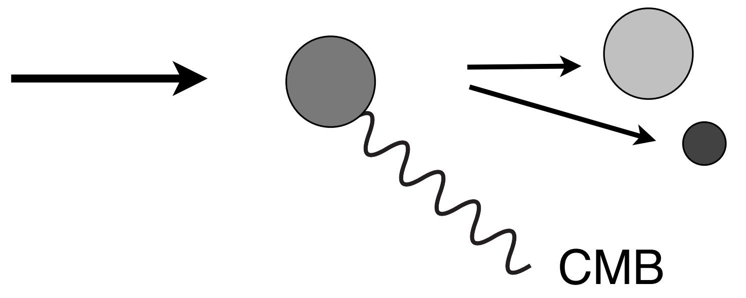

Photo-dissociation
(giant dipole resonance)

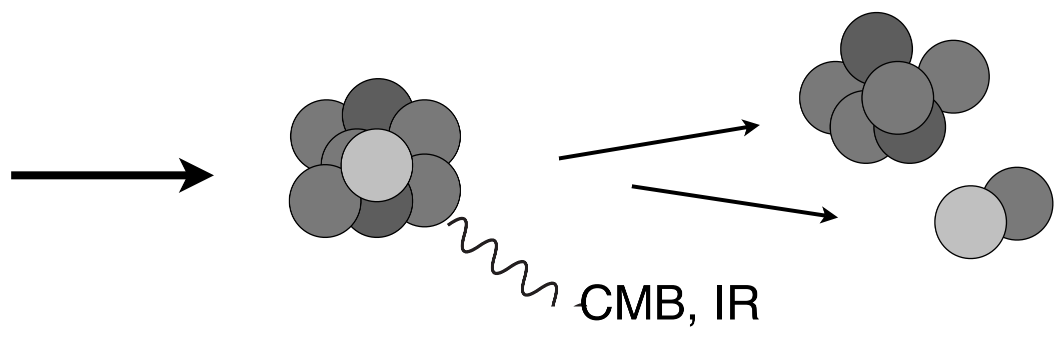

Mass composition at sources (model dependent)

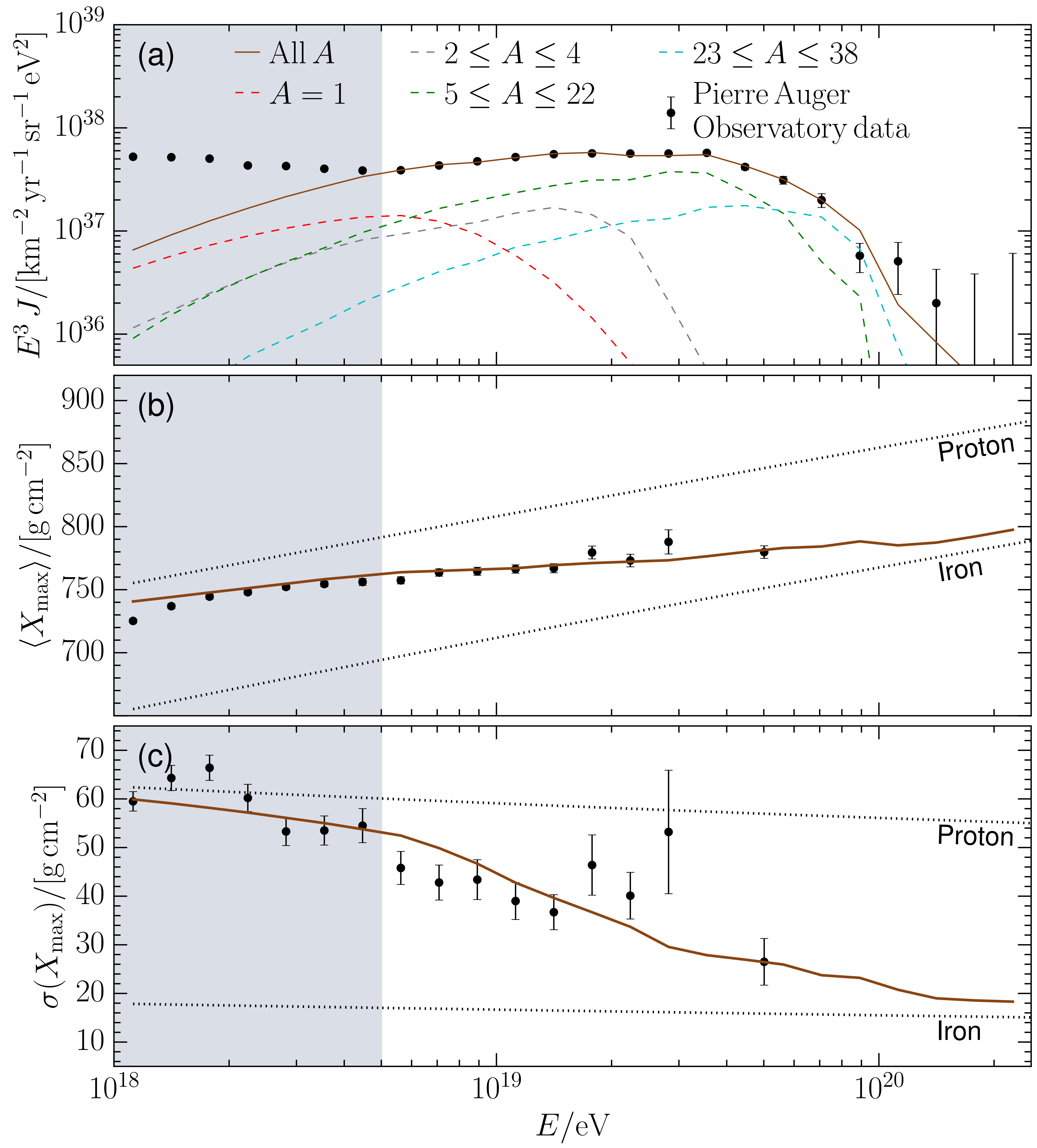

(Wittkowski ICRC 2017)

Rigidity-dependent injection spectra with exp. suppression

$$\frac{dN}{dE} = J_0 \sum_\alpha f_\alpha E_0^{-\gamma} \begin{cases} 1 & \text{for} \quad E_0/Z_\alpha < R_{\text{cut}}\,, \\ \exp\left(1 - \frac{E_0}{Z_\alpha R_{\text{cut}}}\right) & \text{for} \quad E_0/Z_\alpha \geq R_{\text{cut}} \end{cases}$$

Results for different model scenarios (CRpropa), m=0

Source properties	4D with EGMF	4D no EGMF	1D no EGMF[1]
γ	1.61	0.61	0.87
$\log_{10}(R_{\text{cut}}/\text{eV})$	18.88	18.48	18.62
f_{H}	3 %	11 %	0 %
f_{He}	2 %	14 %	0 %
f_{N}	74 %	68 %	88 %
f_{Si}	21 %	7 %	12 %
f_{Fe}	0 %	0 %	0 %

[1] Homogeneous source distribution, see [A. Aab et al., JCAP 2017, 038 (2017)]

Mass composition at sources (model dependent)

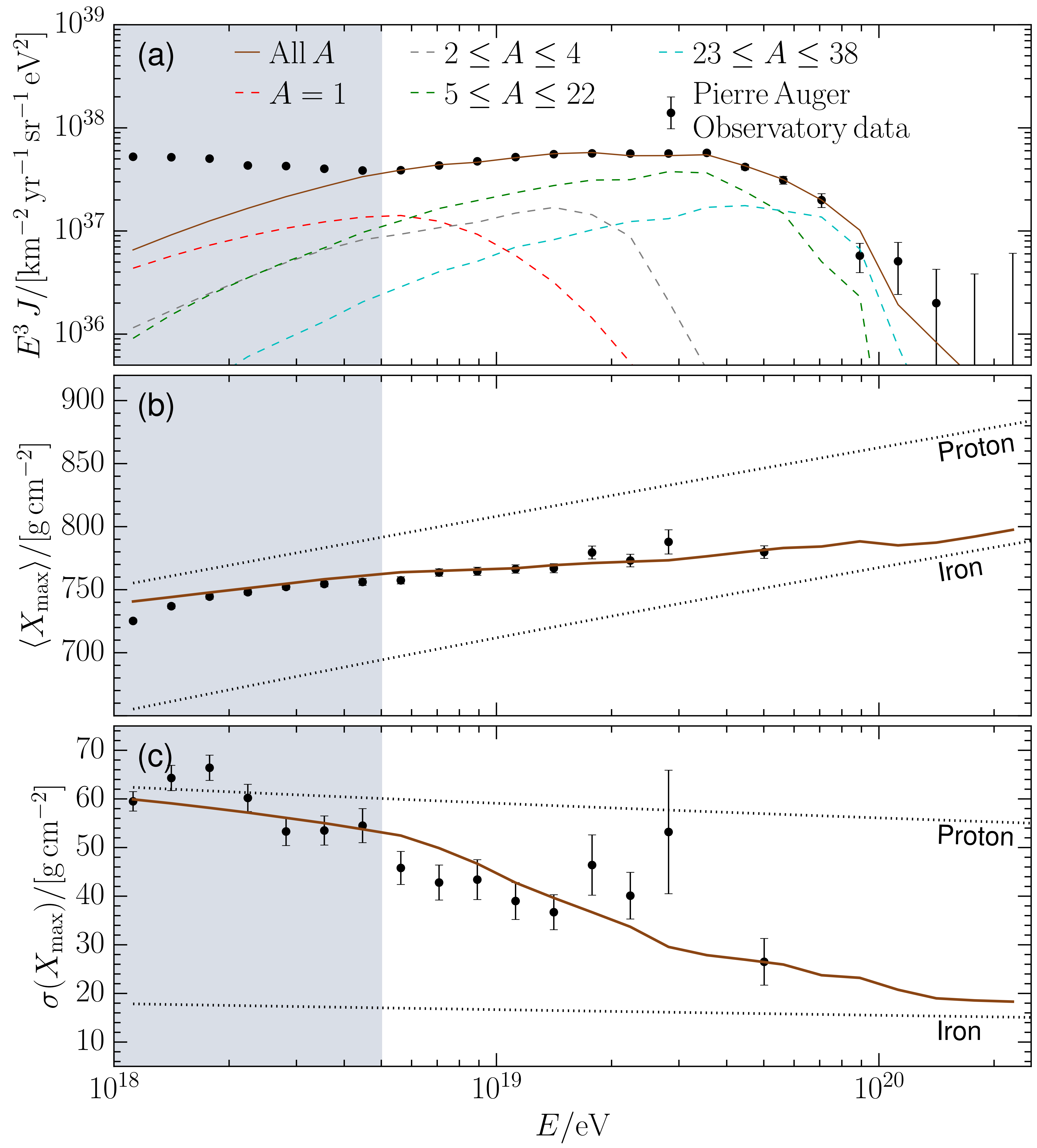

(Wittkowski ICRC 2017)

Results for different model scenarios (CRpropa), m=0

Source properties	4D with EGMF	4D no EGMF	1D no EGMF[1]
γ	1.61	0.61	0.87
$\log_{10}(R_{\mathrm{cut}}/\mathrm{eV})$	18.88	18.48	18.62
f_{H}	3 %	11 %	0 %
f_{He}	2 %	14 %	0 %
f_{N}	74 %	68 %	88 %
f_{Si}	21 %	7 %	12 %
f_{Fe}	0 %	0 %	0 %

Suppression of flux dominated by maximum injection energy

$$E_{\mathrm{cut}} = Z\, R_{\mathrm{cut}} \approx 7 \times 10^{18.6}\,\mathrm{eV} = 3 \times 10^{19}\,\mathrm{eV}$$

(Si about two times higher)

Mass composition at sources (model dependent)

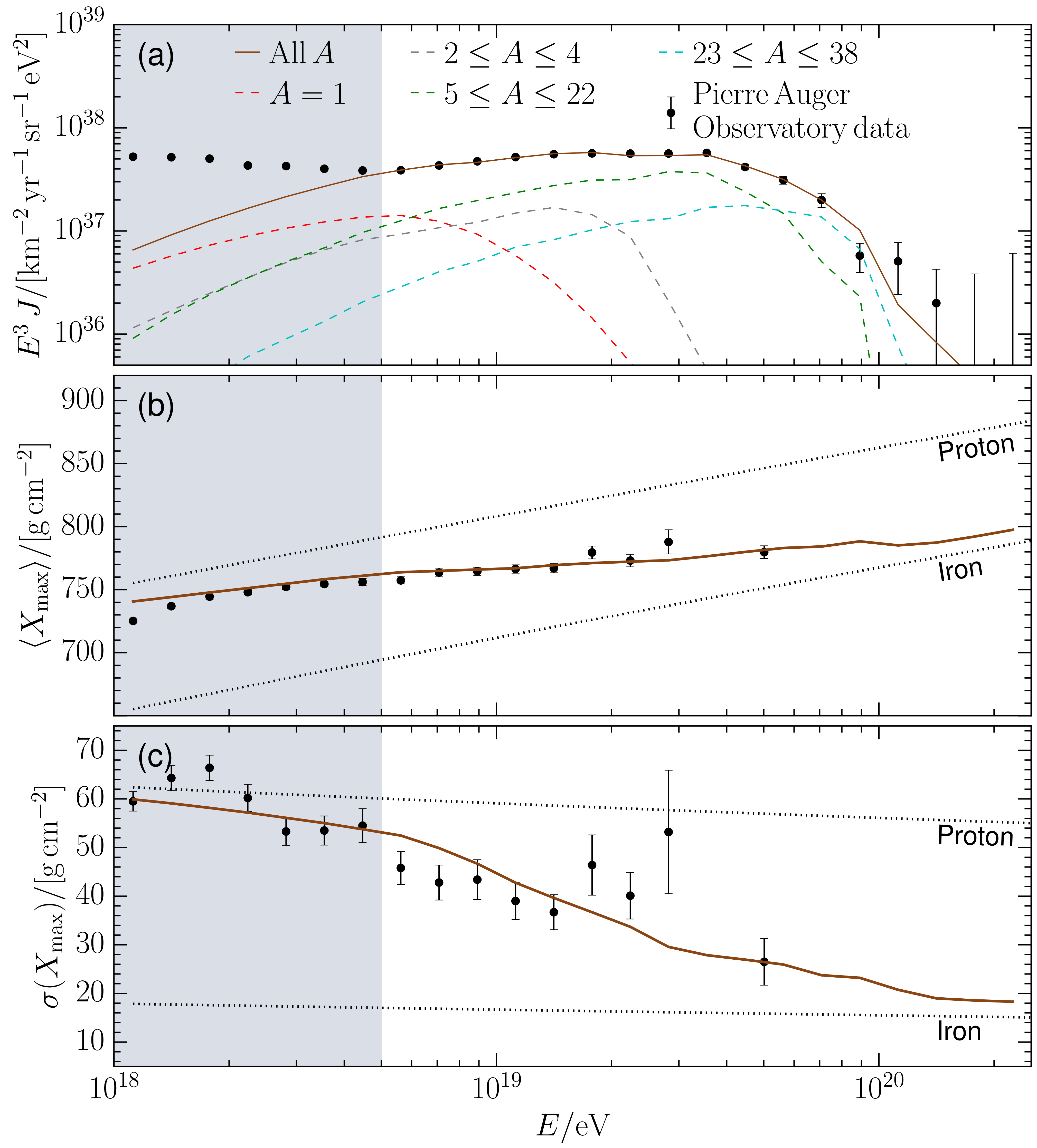

Results for different model scenarios (CRpropa), m=0

Source properties	4D with EGMF	4D no EGMF	1D no EGMF[1]
γ	1.61	0.61	0.87
$\log_{10}(R_{\mathrm{cut}}/\mathrm{eV})$	18.88	18.48	18.62
f_{H}	3 %	11 %	0 %
f_{He}	2 %	14 %	0 %
f_{N}	74 %	68 %	88 %
f_{Si}	21 %	7 %	12 %
f_{Fe}	0 %	0 %	0 %

Suppression of flux dominated by maximum injection energy

Very hard index of power law at injection

(Wittkowski ICRC 2017)

Mass composition at sources (model dependent)

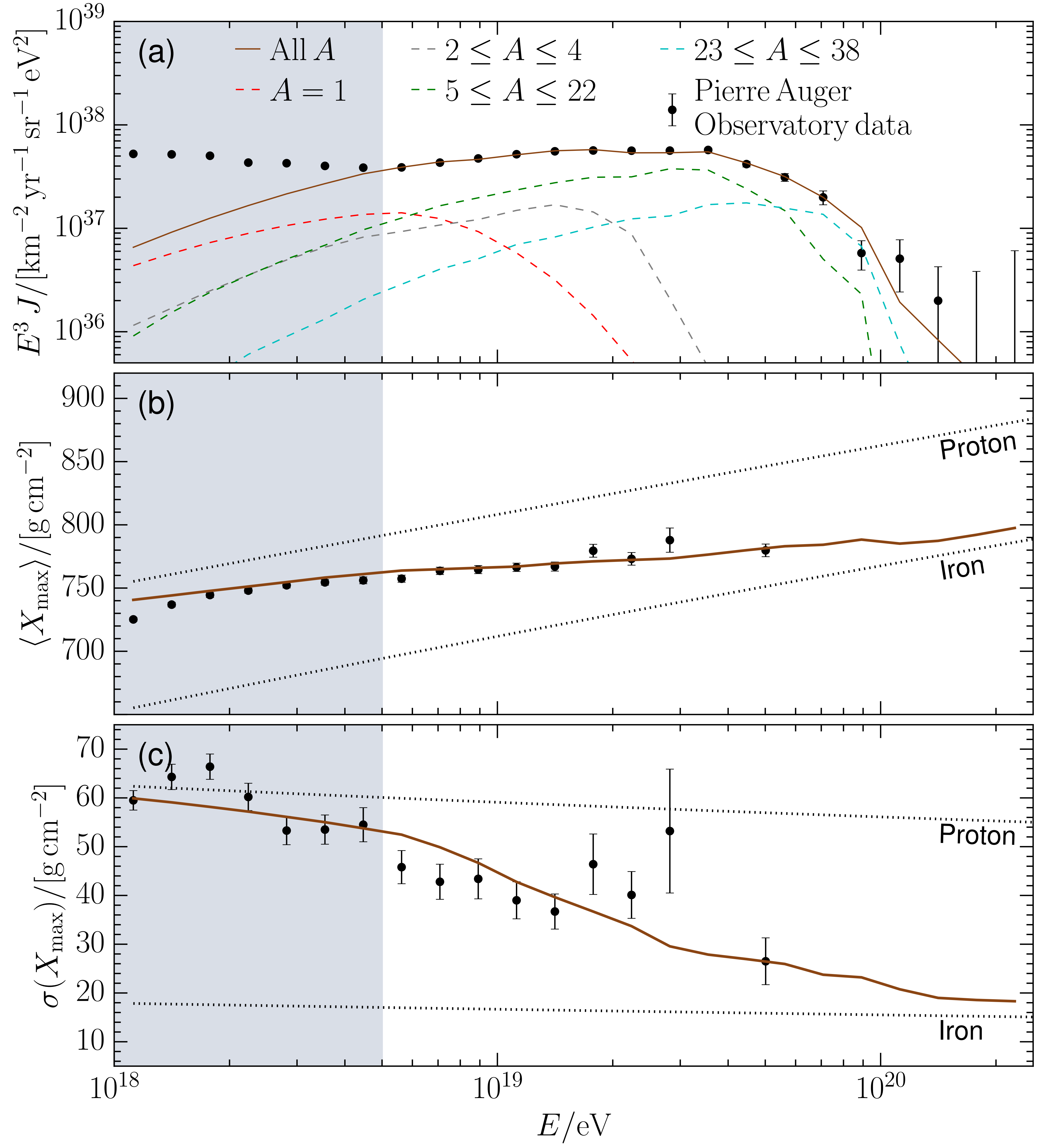

Results for different model scenarios (CRpropa), m=0

Source properties	4D with EGMF	4D no EGMF	1D no EGMF[1]
γ	1.61	0.61	0.87
$\log_{10}(R_{cut}/eV)$	18.88	18.48	18.62
f_H	3 %	11 %	0 %
f_{He}	2 %	14 %	0 %
f_N	74 %	68 %	88 %
f_{Si}	21 %	7 %	12 %
f_{Fe}	0 %	0 %	0 %

Suppression of flux dominated by maximum injection energy

Very hard index of power law at injection

Mainly primaries of the CNO and Si group injected, no Fe, very little p, p produced by spallation

(Wittkowski ICRC 2017)

Mass composition at sources (model dependent)

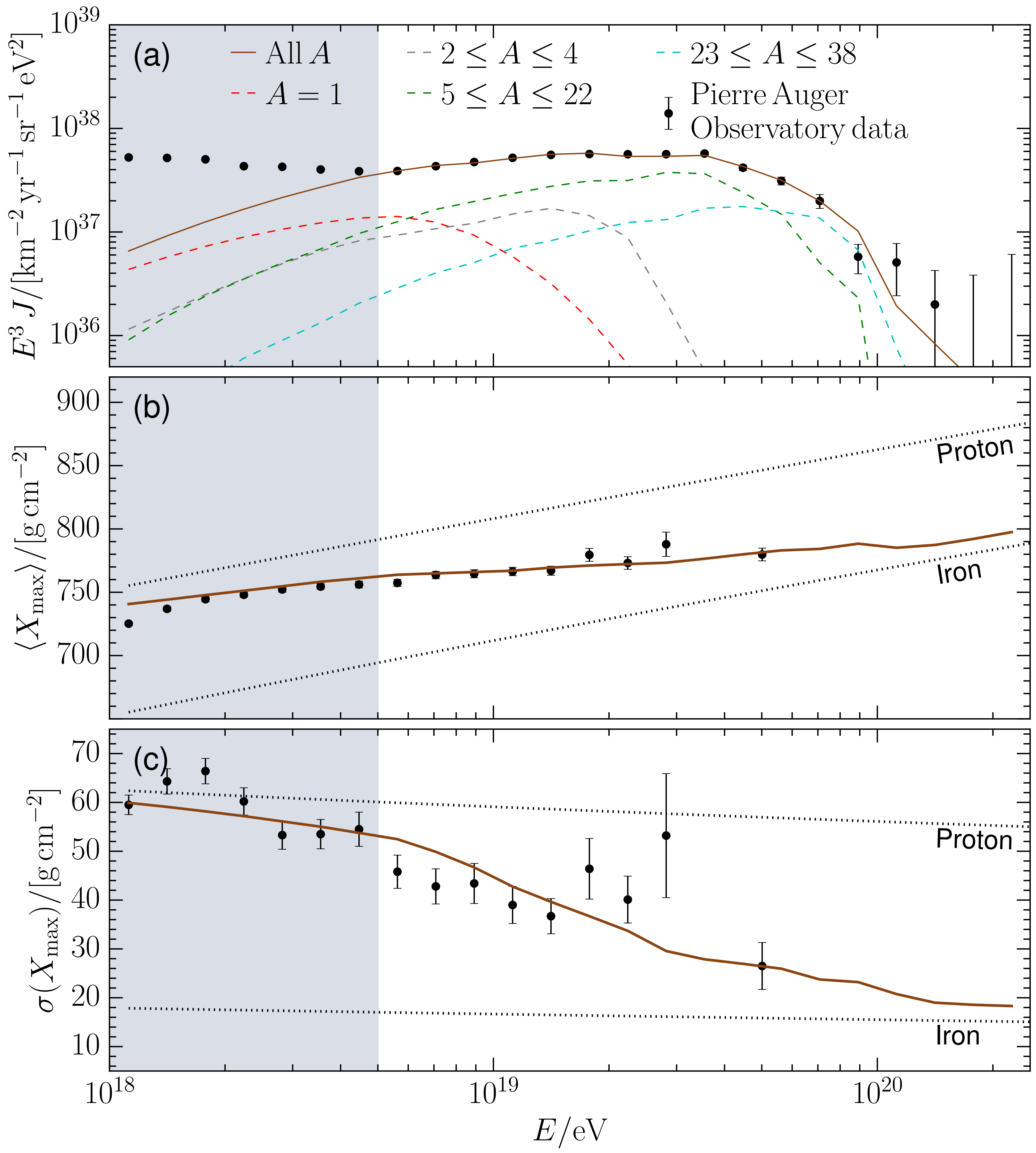

(Wittkowski ICRC 2017)

Source evolution parameter	γ	$\log_{10}(R_{\mathrm{cut}}/\mathrm{eV})$	$D_{\mathrm{min}}{}^2$
$m = 3$	1.20	18.70	184
$m = 0$	1.61	18.88	192
$m = -3$	1.78	18.77	199
$m = -6$	1.95	18.77	202
$m = -9$	2.05	18.78	203

Fermi: low-luminosity, high-synchrotron peaked (HSP) BL Lacs

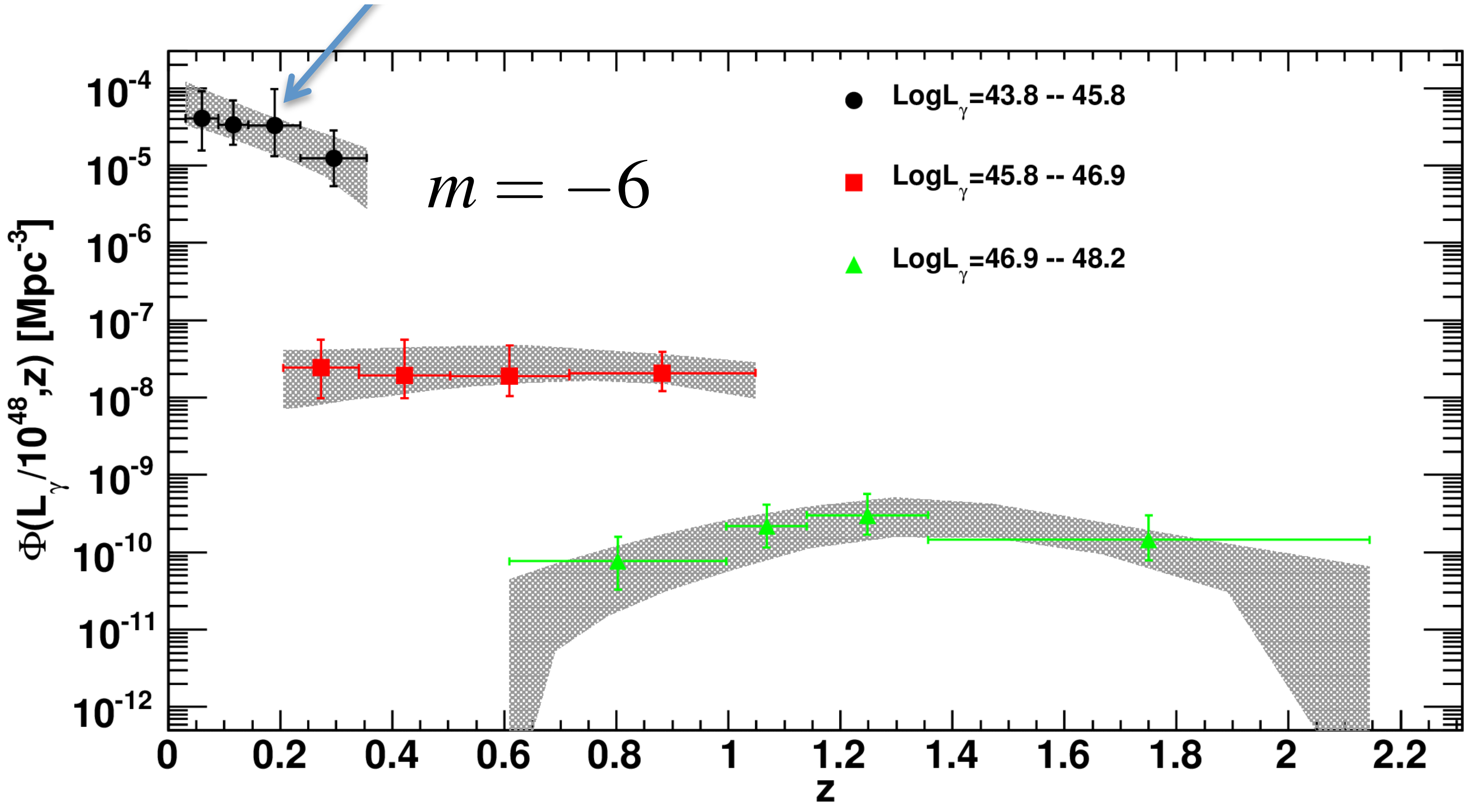

(Taylor, ICRC 2017)

Ajello et al. (2014), 1310.0006

Large-scale anisotropy (Auger data)

Combination of vertical and inclined showers

Harmonic analysis in right ascension α

E [EeV]	events	amplitude r	phase [deg.]	$P(\geq r)$
4-8	81701	$0.005^{+0.006}_{-0.002}$	80 ± 60	0.60
> 8	32187	$0.047^{+0.008}_{-0.007}$	100 ± 10	2.6×10^{-8}

significant modulation at 5.2σ (5.6σ before penalization for energy bins explored)

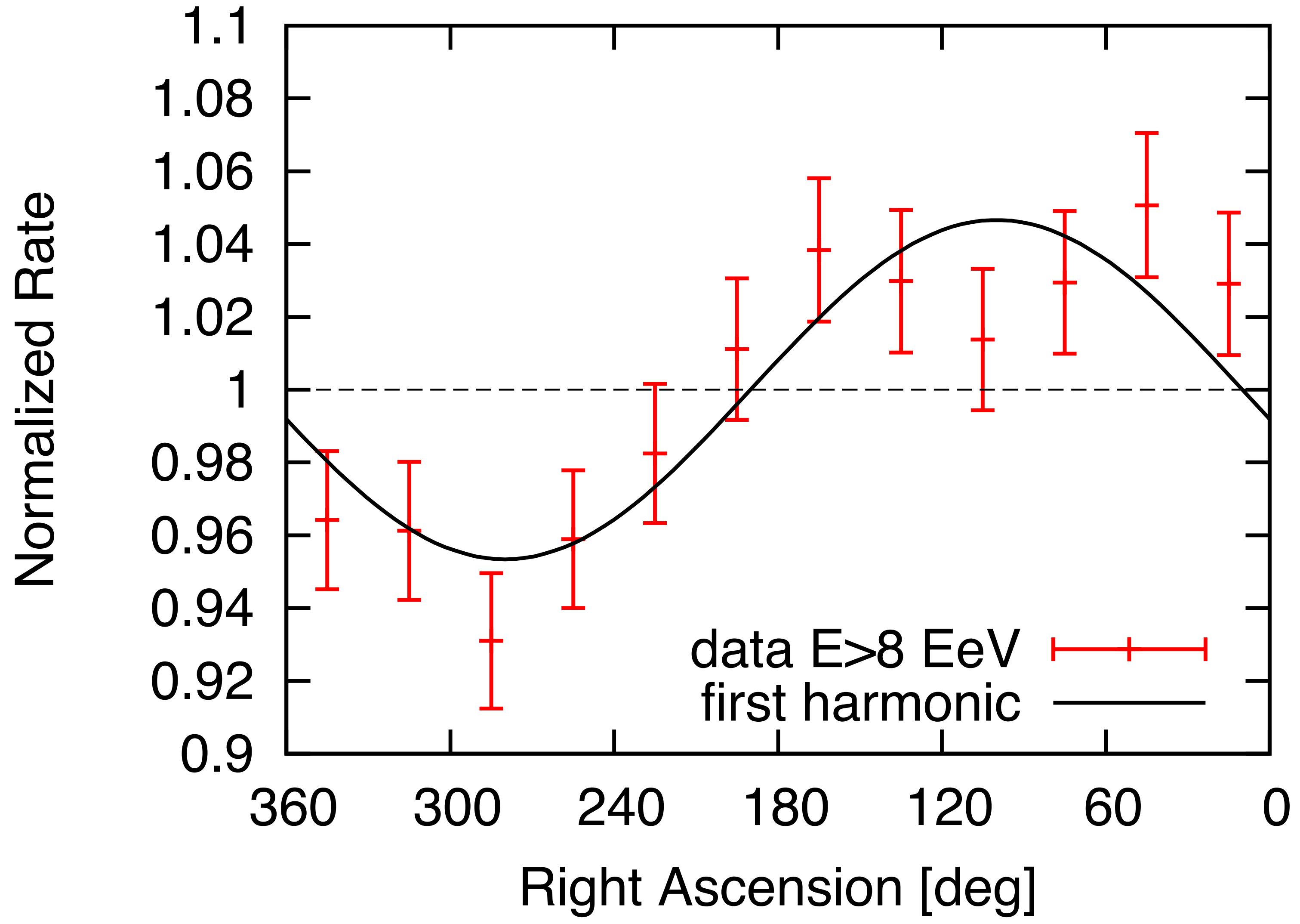

3-d dipole above 8 EeV:

$(6.5^{+1.3}_{-0.9})\%$ at $(\alpha, \delta) = (100°, -24°)$ $(l, b) = (233°, -13°)$

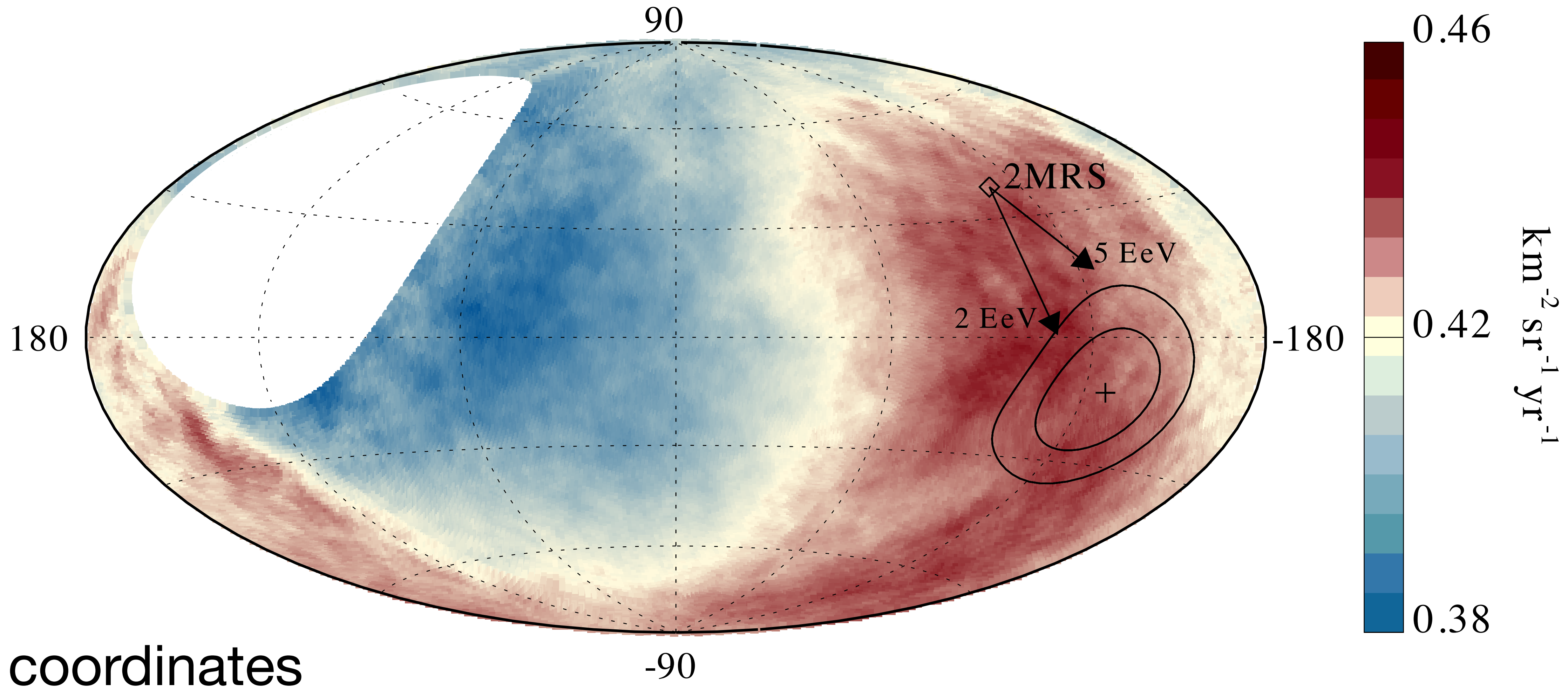

gal. coordinates

Expected if cosmic rays diffuse to Galaxy from sources distributed similar to near-by galaxies
(Harari, Mollerach PRD 2015, 2016)

Deflection of dipolar pattern due to Galactic magnetic field

Strong indication for extragalactic origin

Transition from galactic to extragalactic cosmic rays

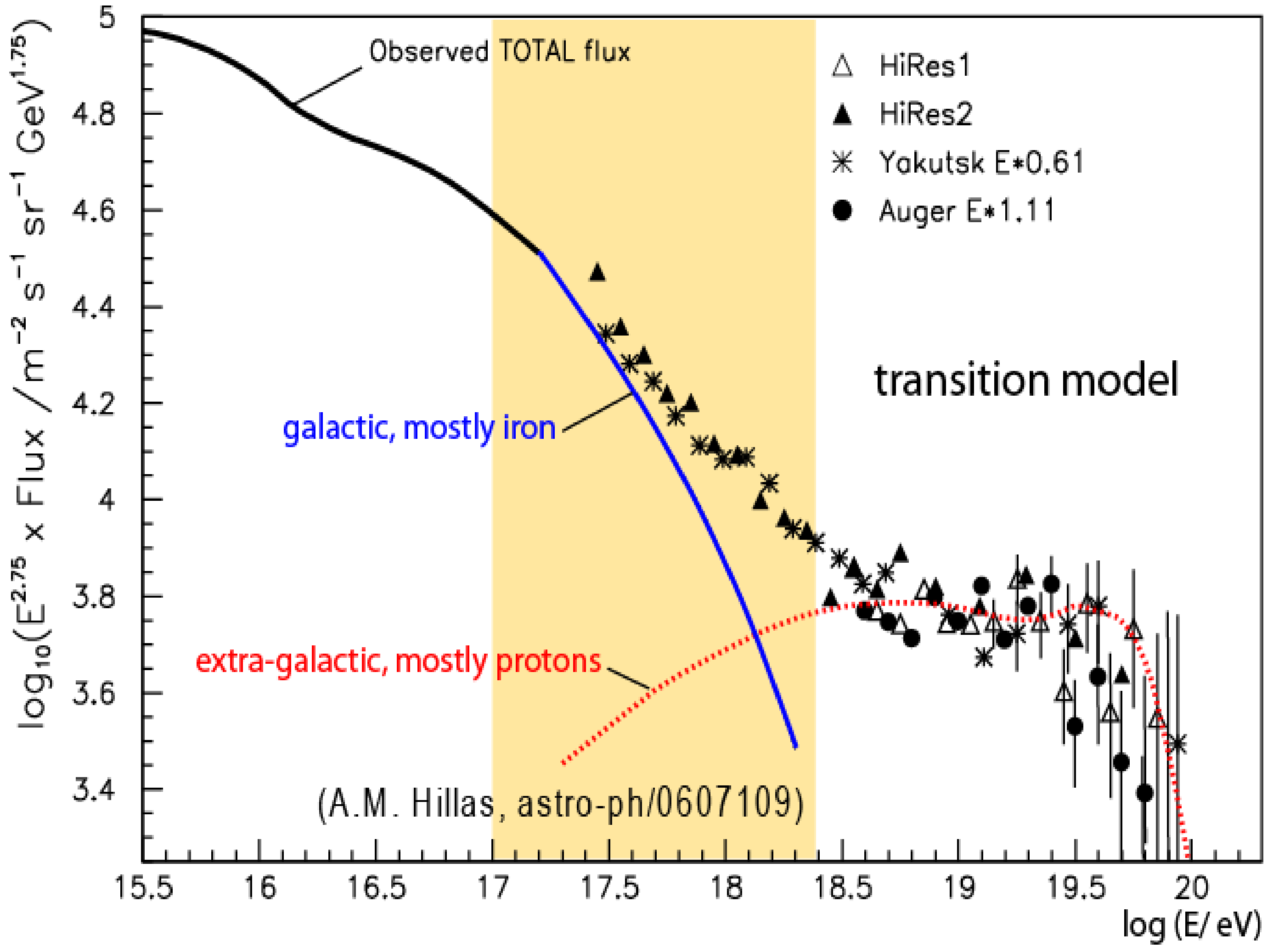

Ankle model:
Hillas, Wolfendale et al.

Simulation: Sources in galactic plane

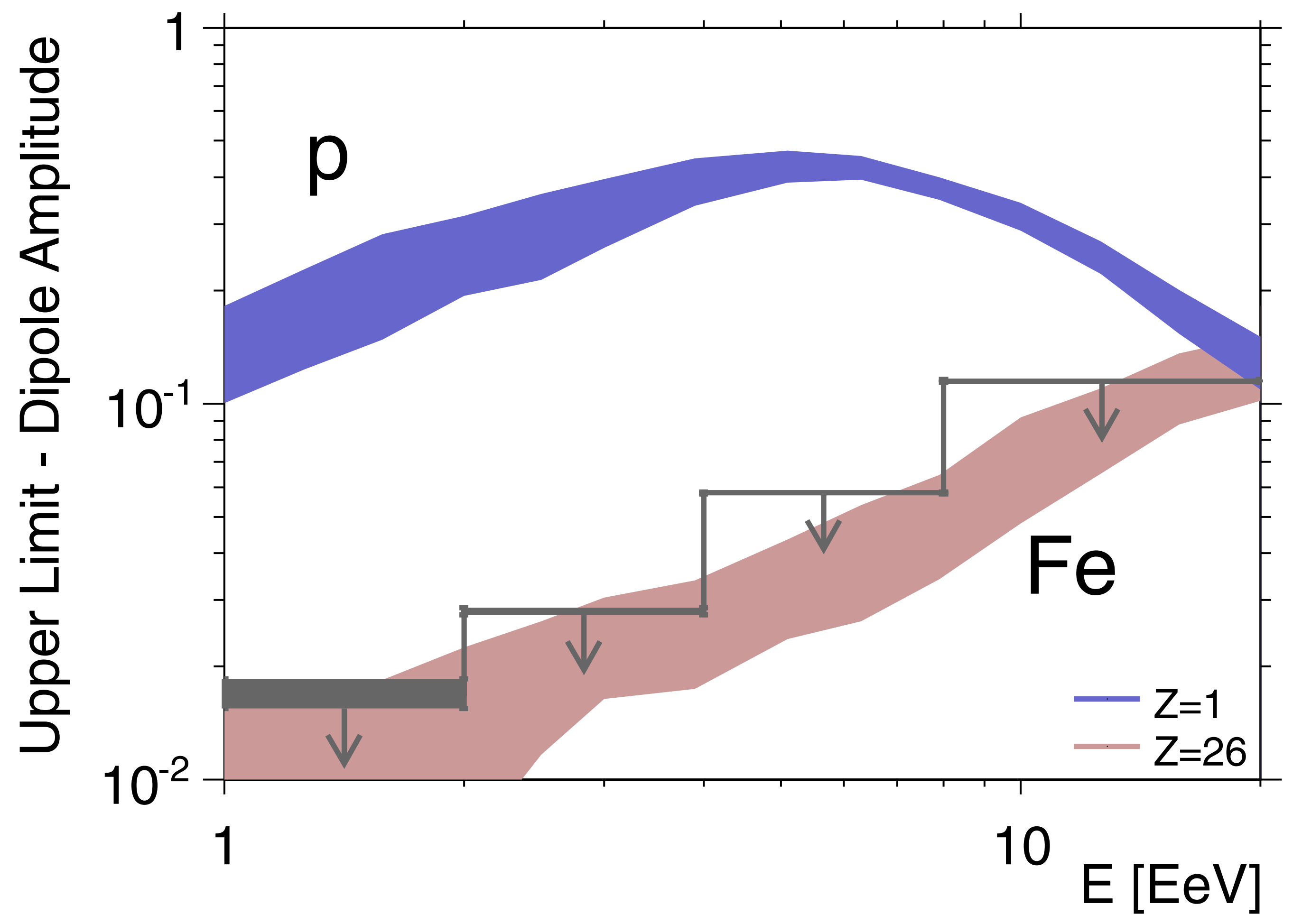

(Auger, ApJ 203, 2012, Giacinti et al. JCAP 2012, 2015)

Transition energy ~10^{18} eV

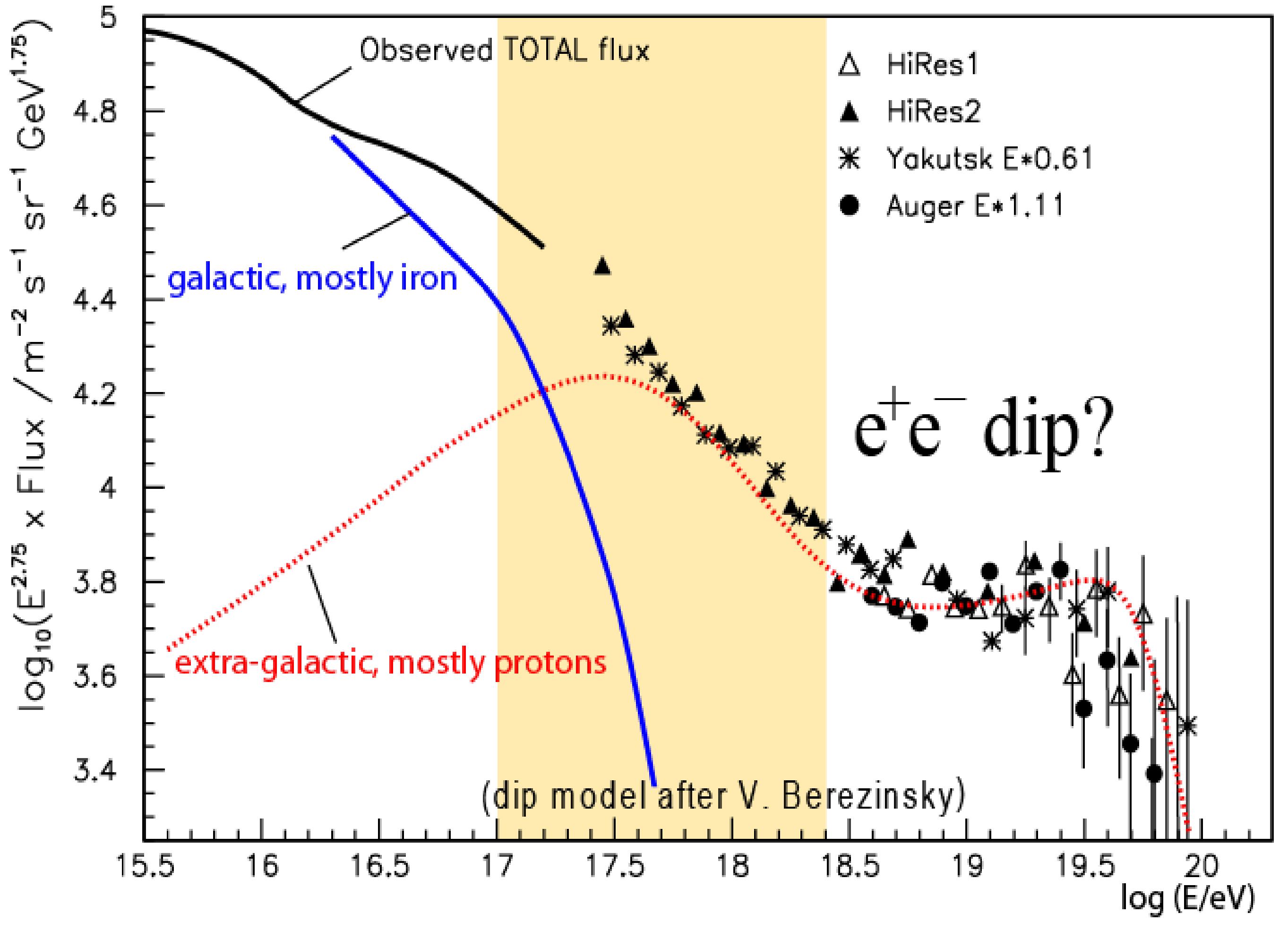

Dip model:
Berezinsky et al.

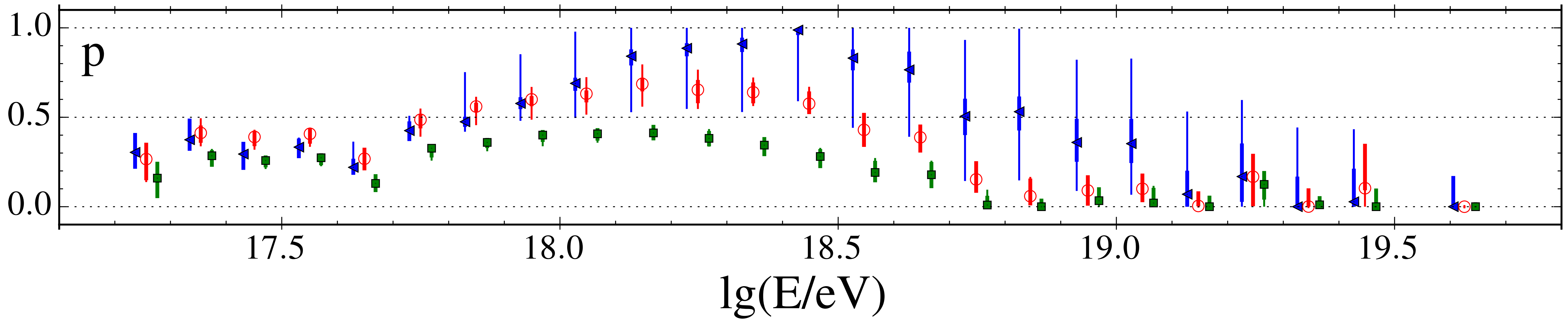

Intermediate-scale anisotropy

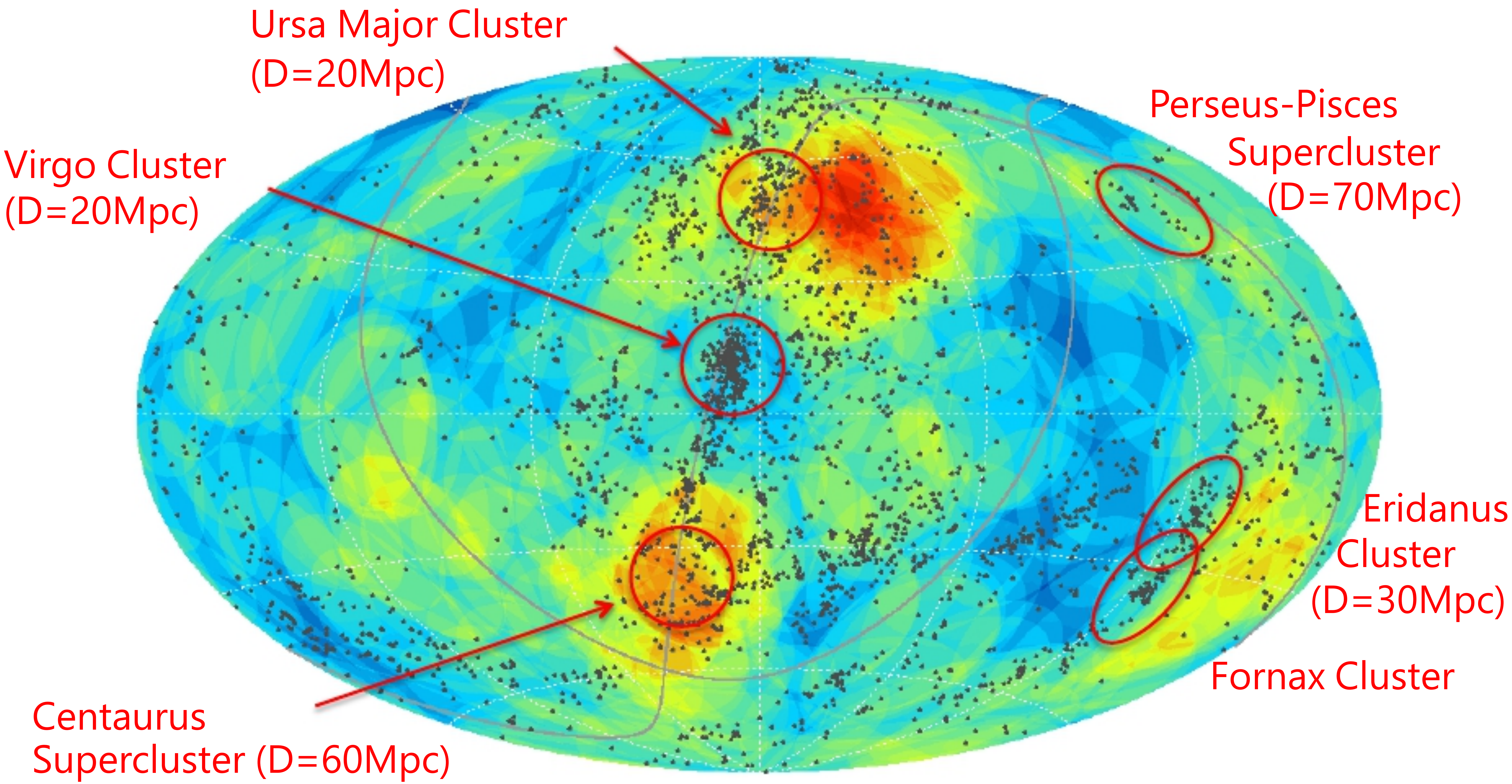

Huchra, et al, ApJ, (2012)

Dots : 2MASS catalog Heliocentric velocity <3000 km/s (D<~45MpC)

Intermediate-scale anisotropy – Hot spot (TA data)

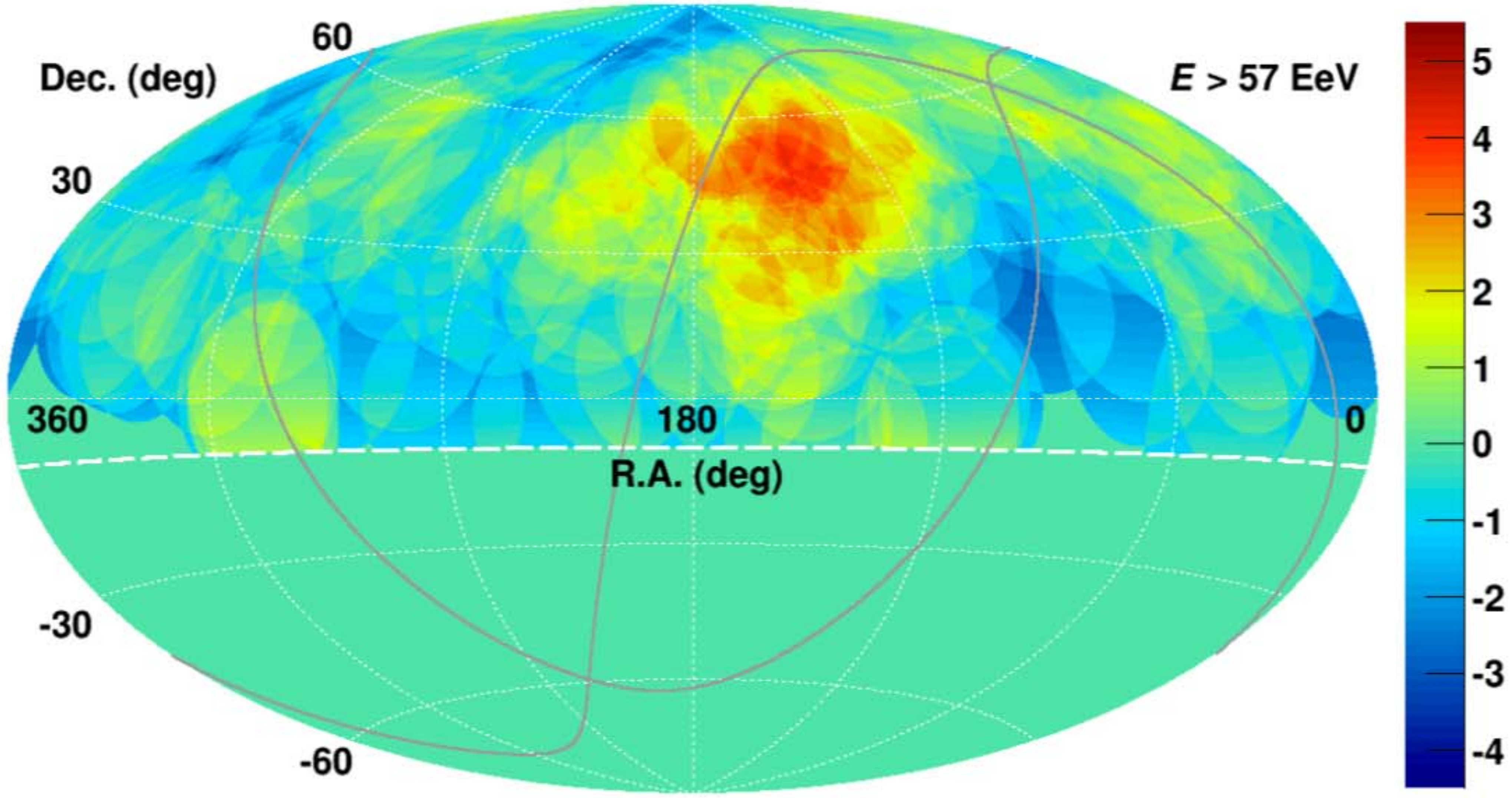

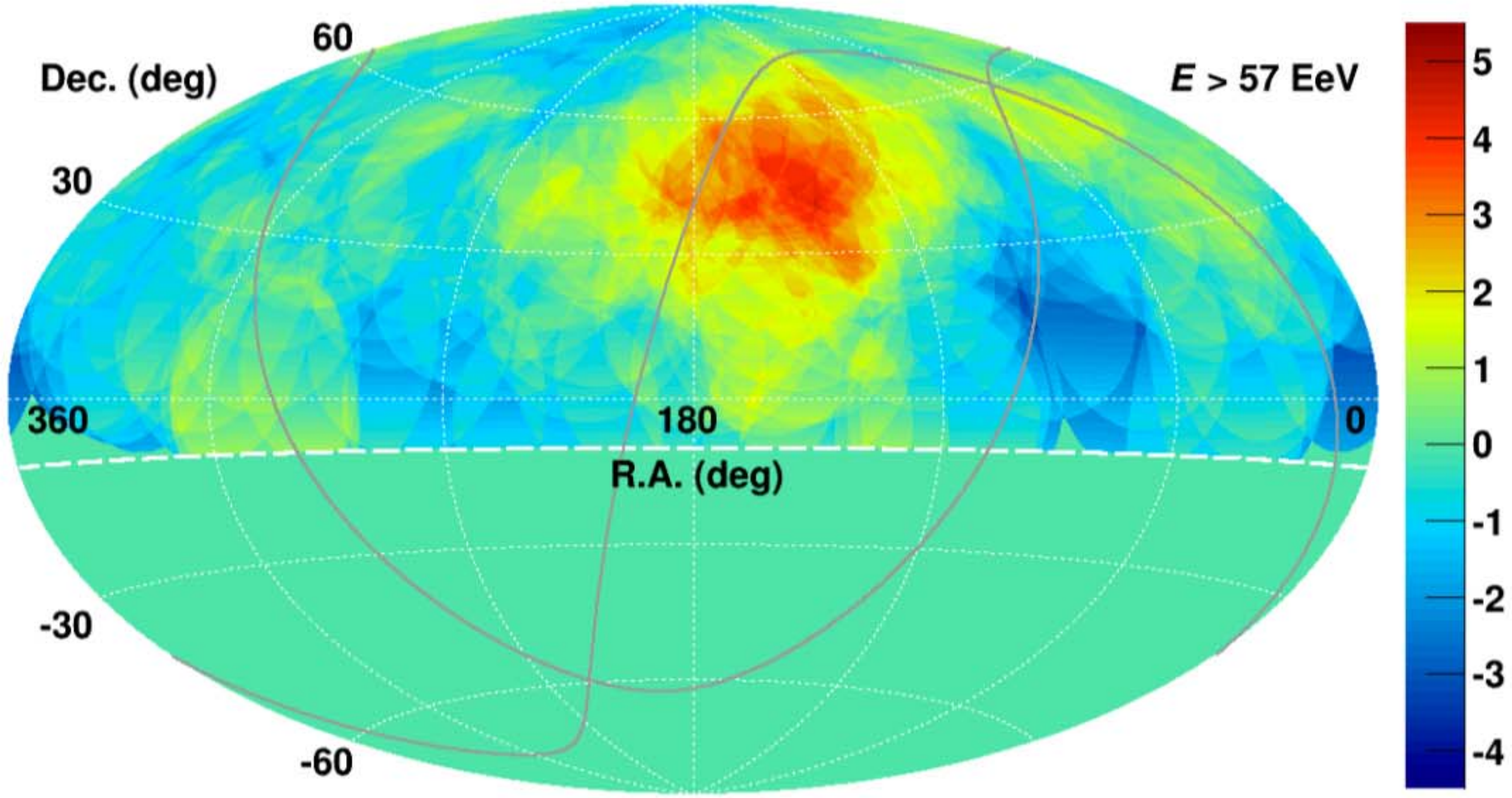

With original 20° oversampling, spot looks larger…. Thus, scan over 15°, 20°, 25°, 30°, & 35°

With 25° oversampling, significance maximum 3σ

Binsize	15		20		25		30		35	
	Local	Global	Local	Global	Local	Global	Local	Global	Local	Global
Year 5	5.12	3.14	5.43	3.55	5.16	3.19	4.82	2.73	4.33	2.05
Year 7	4.92	2.84	5.37	3.44	5.65	3.80	5.37	3.44	5.03	2.99
Year 9	4.42	2.06	4.72	2.50	5.06	2.96	5.01	2.91	4.66	2.41

(Matthews, ICRC 2017)

Intermediate-scale anisotropy – Warm spot (Auger data)

✓ Scan in parameters: E_{th} in [40; 80] EeV in steps of 1 EeV
Ψ in [1°; 30°] in steps of 0.25° up to 5°, 1° for larger angles

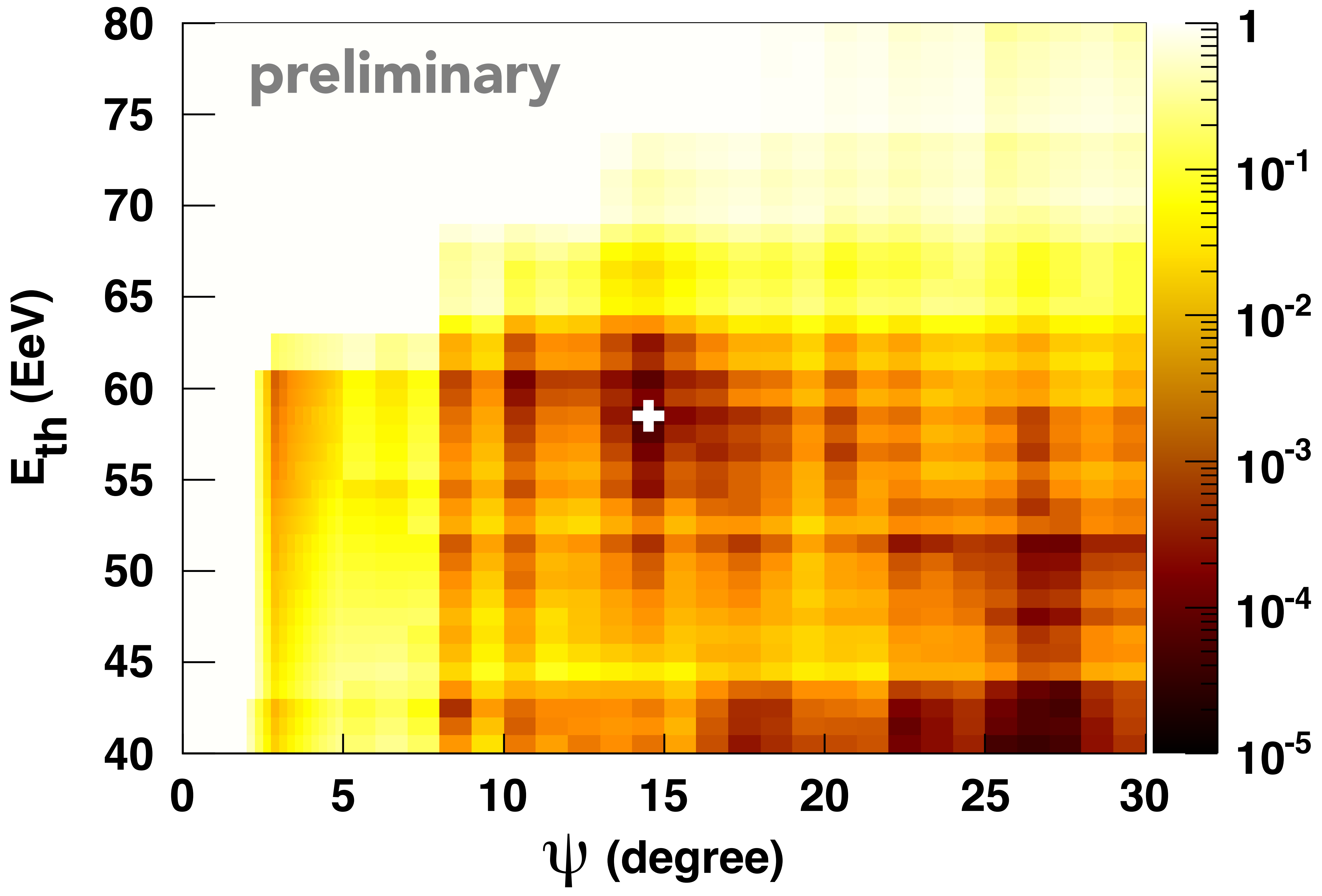

Largest excess

$E_{th} = 58$ EeV, Ψ = 15°

$n_{obs} = 19$, $n_{exp} = 6.0$

$P \sim 1.1 \times 10^{-5}$

Post-trial probability

$\sim 1.1 \times 10^{-3}$

(fraction of isotropic simulations that have a smaller probability under the same scan)

Region of secondary minima above ~40 EeV

(Giaccari ICRC 2017)

Anisotropy – Correlation with catalogs (Auger data)

Active Galactic Nuclei

- Selected from 2FHL Catalog (*Fermi*-LAT, 360 sources):
  Φ(> 50 GeV) ---> proxy for UHECR flux
- Selection of the 17 objects within 250 Mpc
- Majority blazars of BL-Lac type and radio-galaxies of FR-I type

γ-ray detected AGNs

f_{ani} = 7%, Ψ = 7°

TS = 15.2 ➡ *p-value* 5.1×10^{-4}

Post-trial probability

3×10^{-3} (~ 2.7 σ)

Star-forming or Starburst Galaxies

Use of *Fermi*-LAT search list for star-formation objects (Ackermann+ 2012)

- 63 objects within 250 Mpc, only 4 detected in gamma rays:
  correlated Φ(> 1.4 GHz) ---> proxy for UHECR flux
- Selection of brightest objects (flux completeness) with Φ(> 1.4 GHz) > 0.3 Jy
- 23 objects, size similar to the gamma-ray AGN sample

Starburst Galaxies

f_{ani} = 10%, Ψ = 13°

TS = 24.9 ➡ *p-value* 3.8×10^{-6}

Post-trial probability

4×10^{-5} (~ 3.9 σ)

Assumption UHECRs flux proportional to non thermal photon flux

(Giaccari ICRC 2017)

Anisotropy – Correlation with catalogs (Auger data)

Starburst galaxies

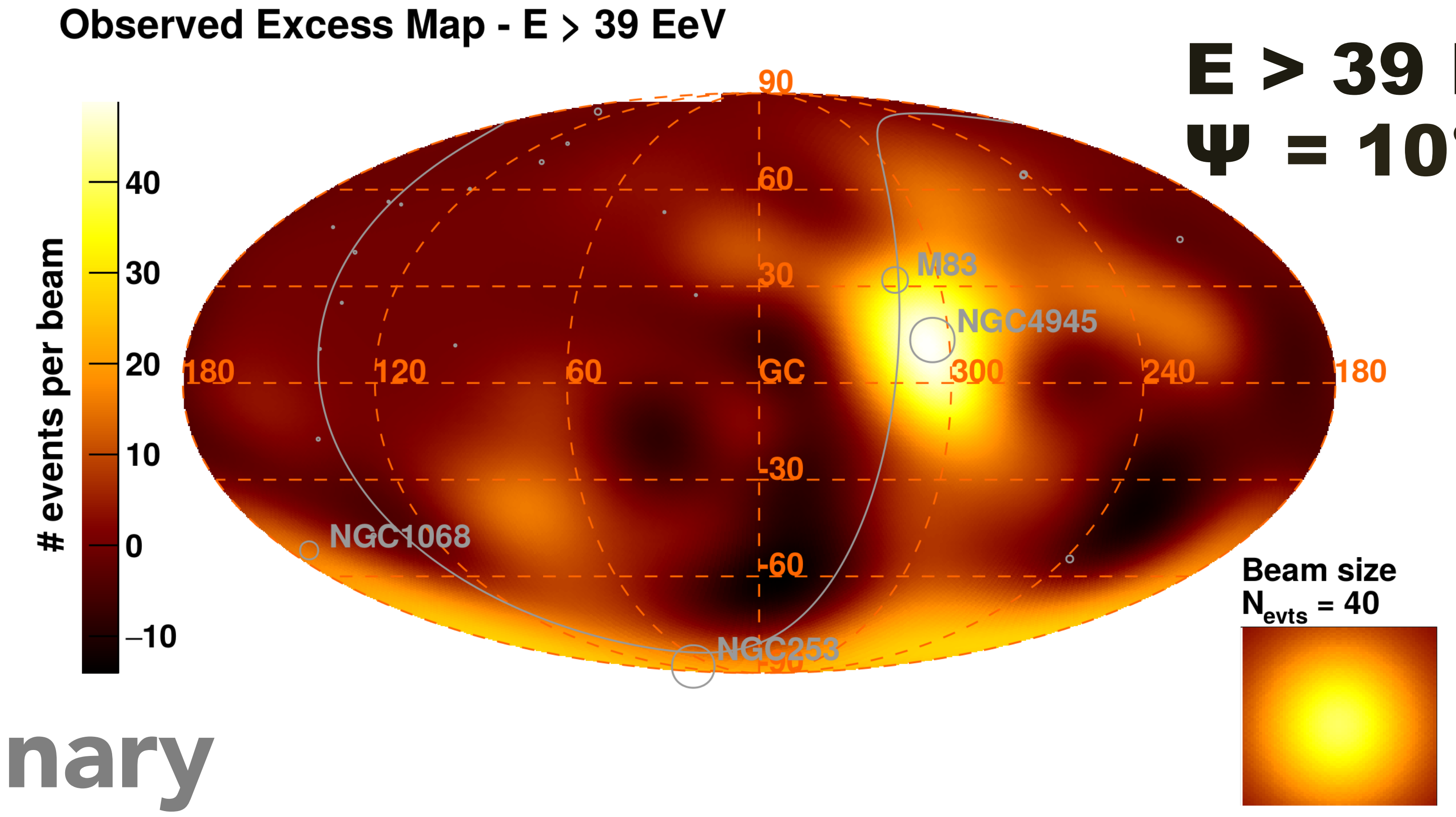

E > 39 EeV
Ψ = 10°

preliminary

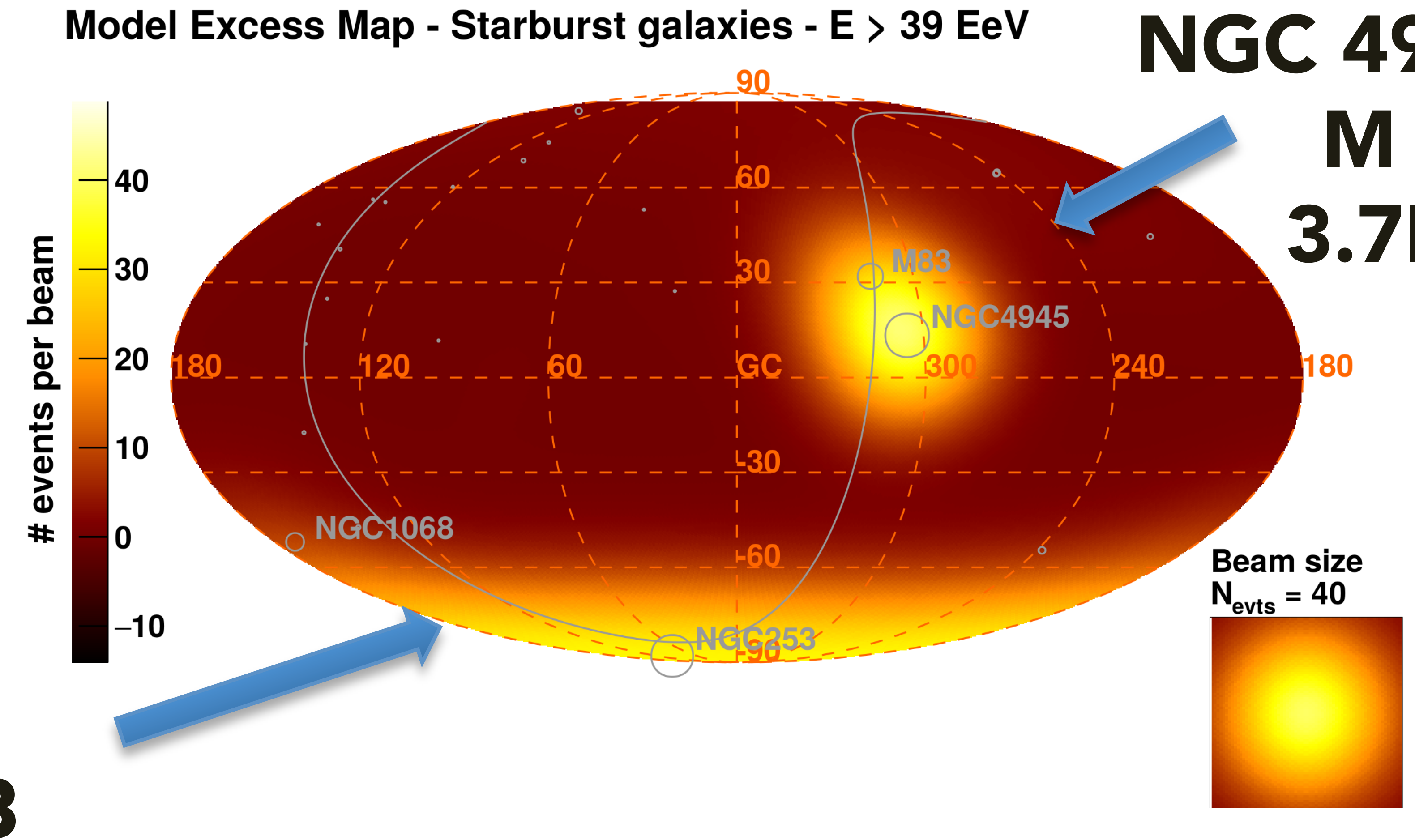

NGC 4945
M 83
3.7Mpc

NGC 253
2.5 Mpc

NGC 1068
16.7 Mpc

AGNs

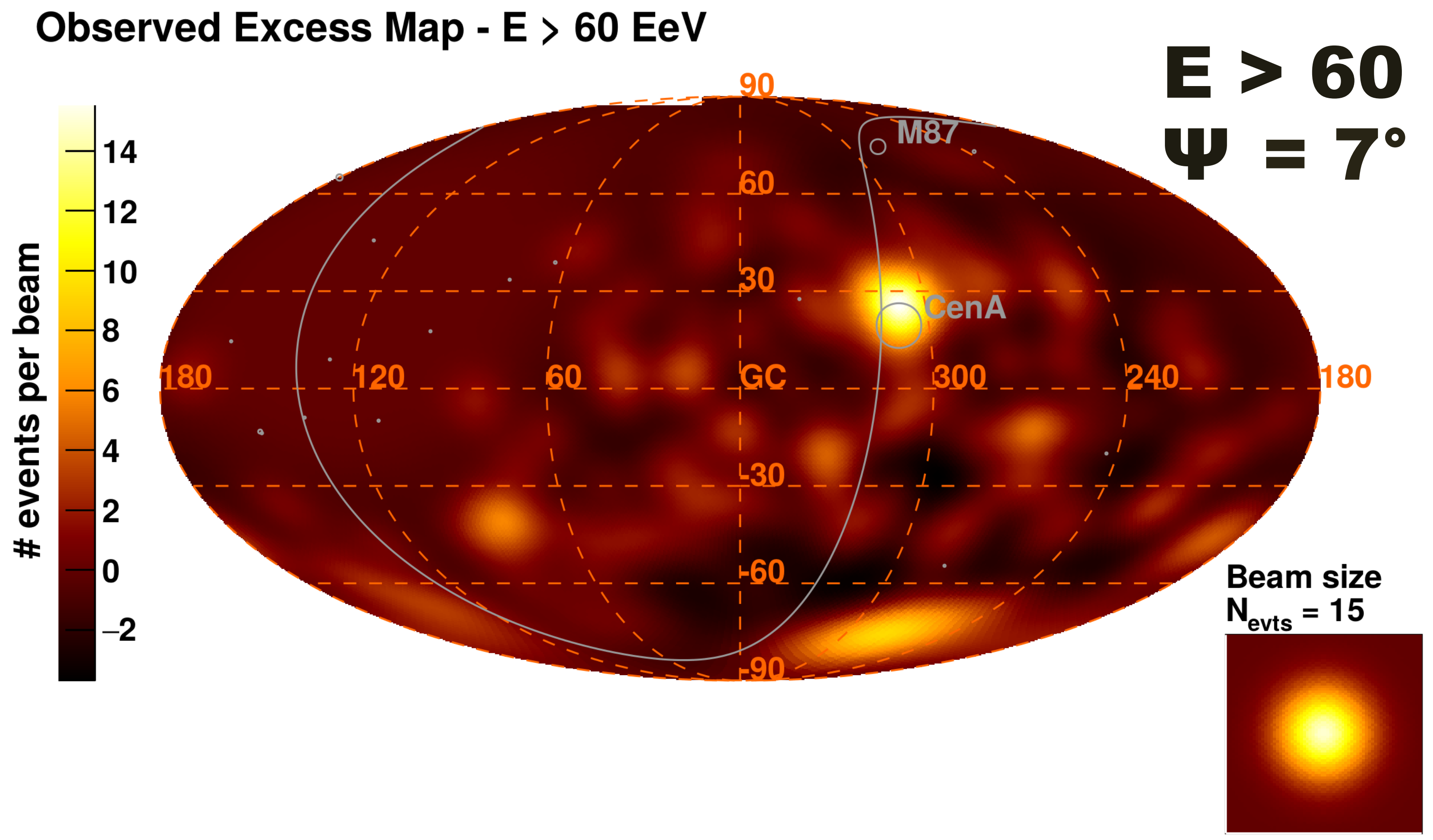

E > 60 EeV
Ψ = 7°

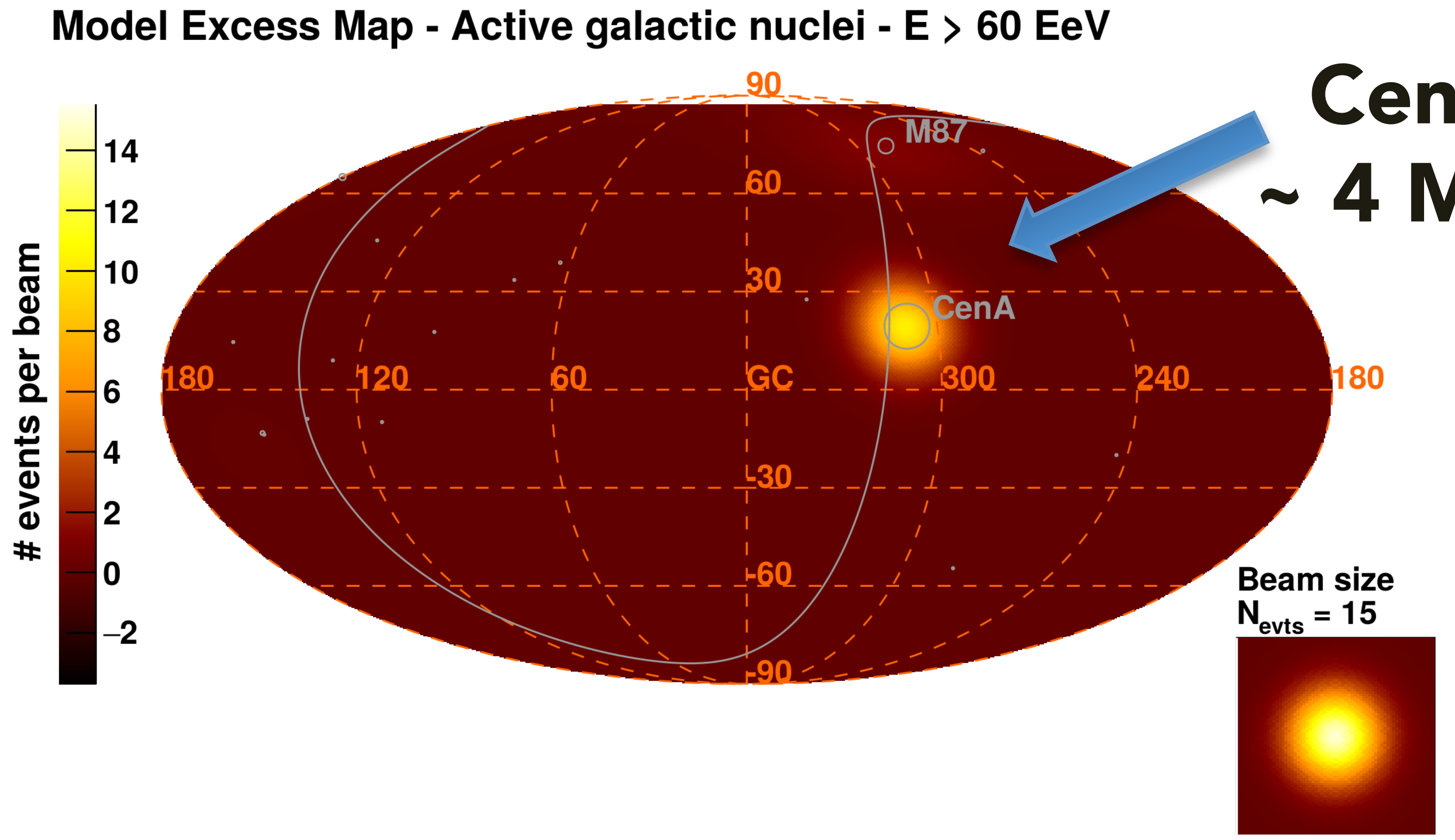

CenA
~ 4 Mpc

(Giaccari ICRC 2017)

Some general comments

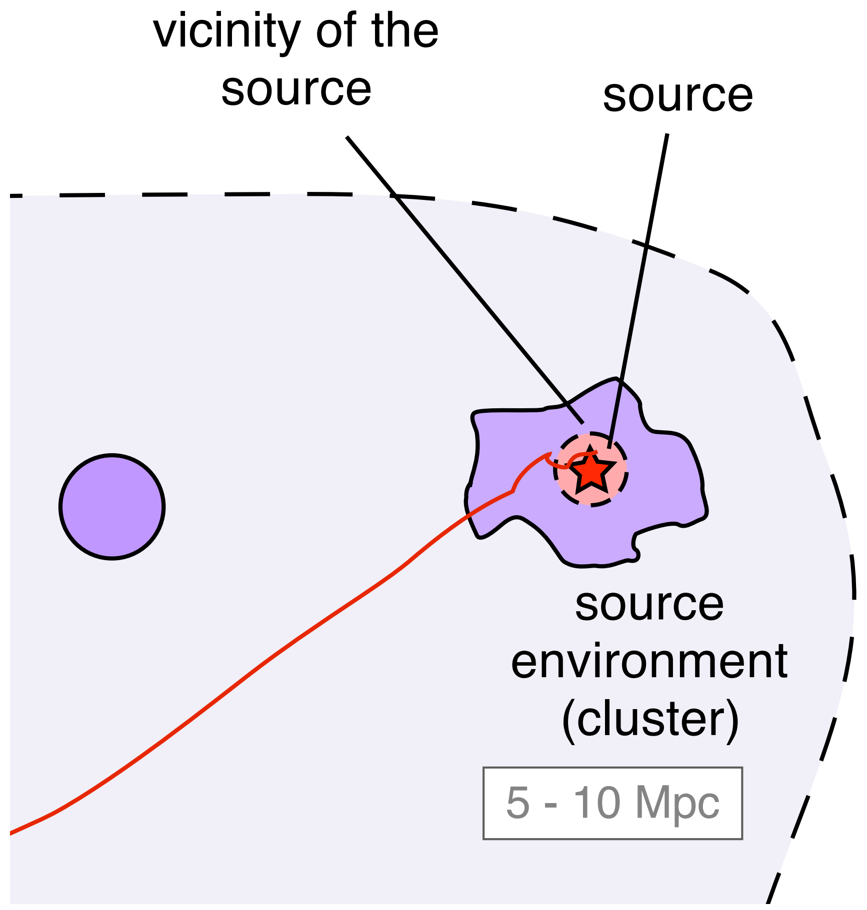

- **Complicated and unexpected picture of UHECR emerging**
  (More composition and anisotropy data needed)

- **Source models have to be more sophisticated than simple power laws**
  (environment+escape, local large-scale structure, different sources)

- **Multi-messenger data crucial for model building**

- **Further progress in modeling hadronic interactions required for reliable composition studies**

- **Auger and TA:**
  - independent analyses
  - joint working groups
  - very productive interaction

(Aloisio et al. 2014)

(Taylor et al. 2015)

(Globus et al. 2015)

(Unger et al. 2015)

(Fang & Murase 2017)

(Zhang et al. 2017)

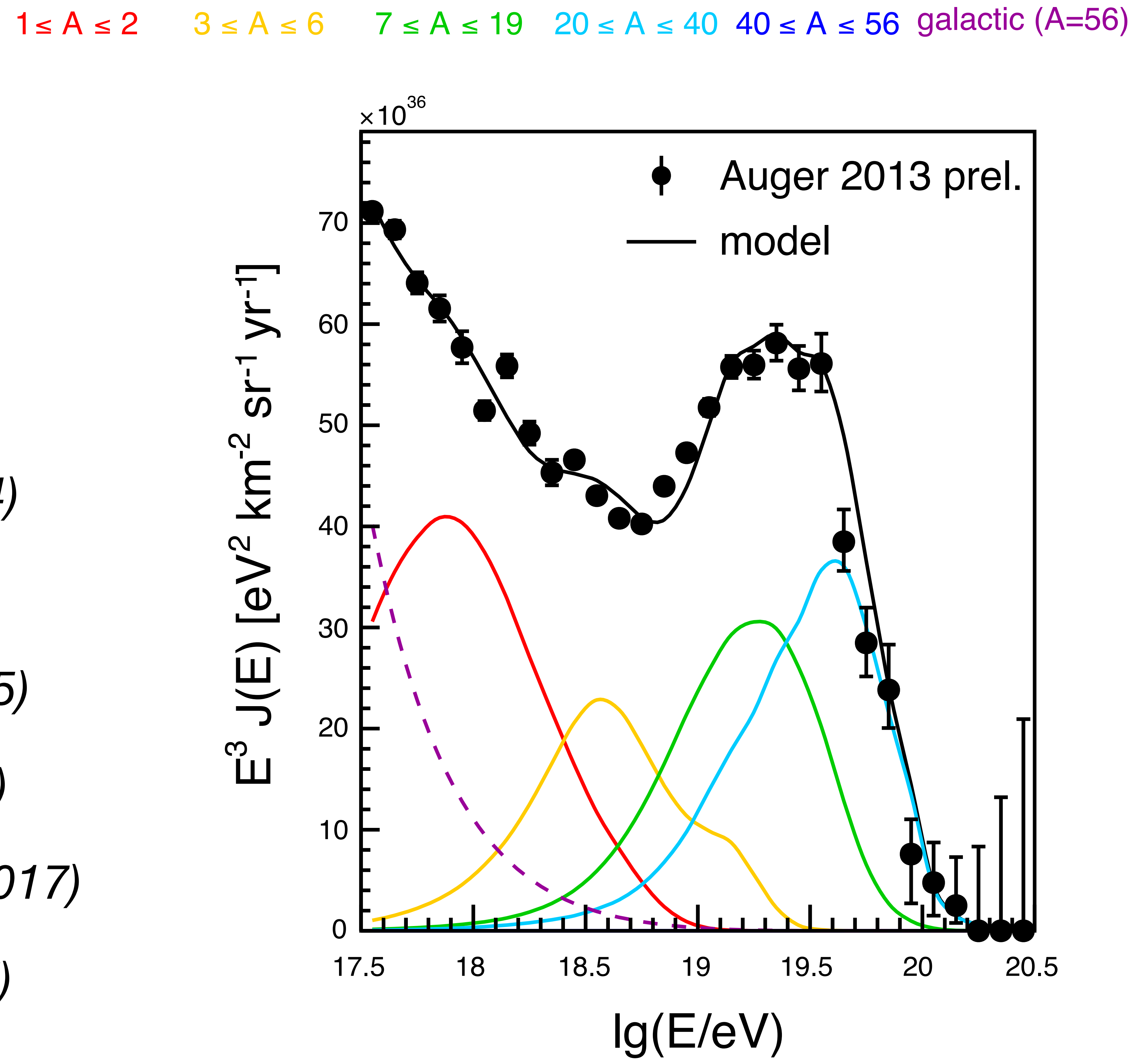

Low-luminosity (LL) and high-luminosity (HL) gamma-ray bursts

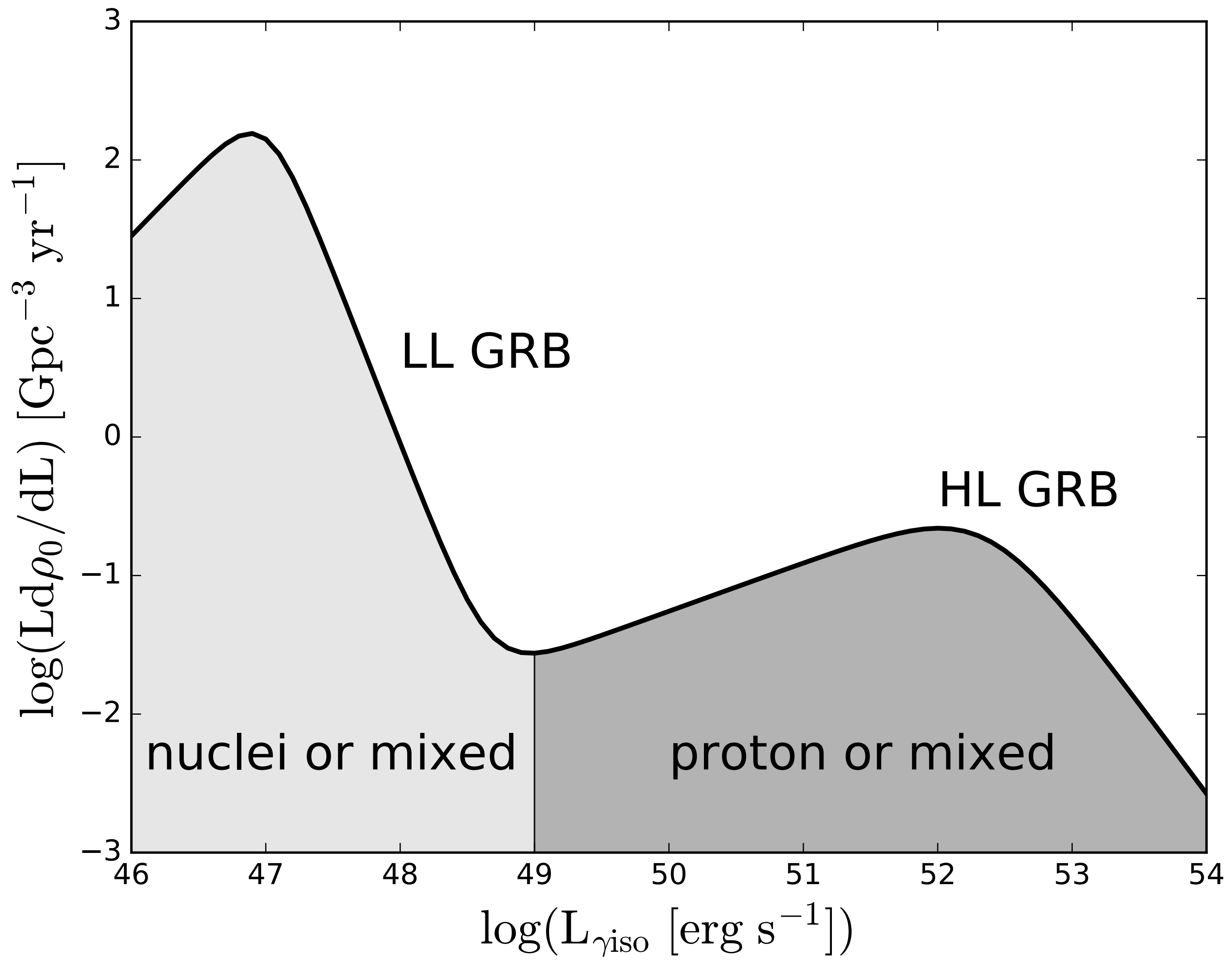

interaction time

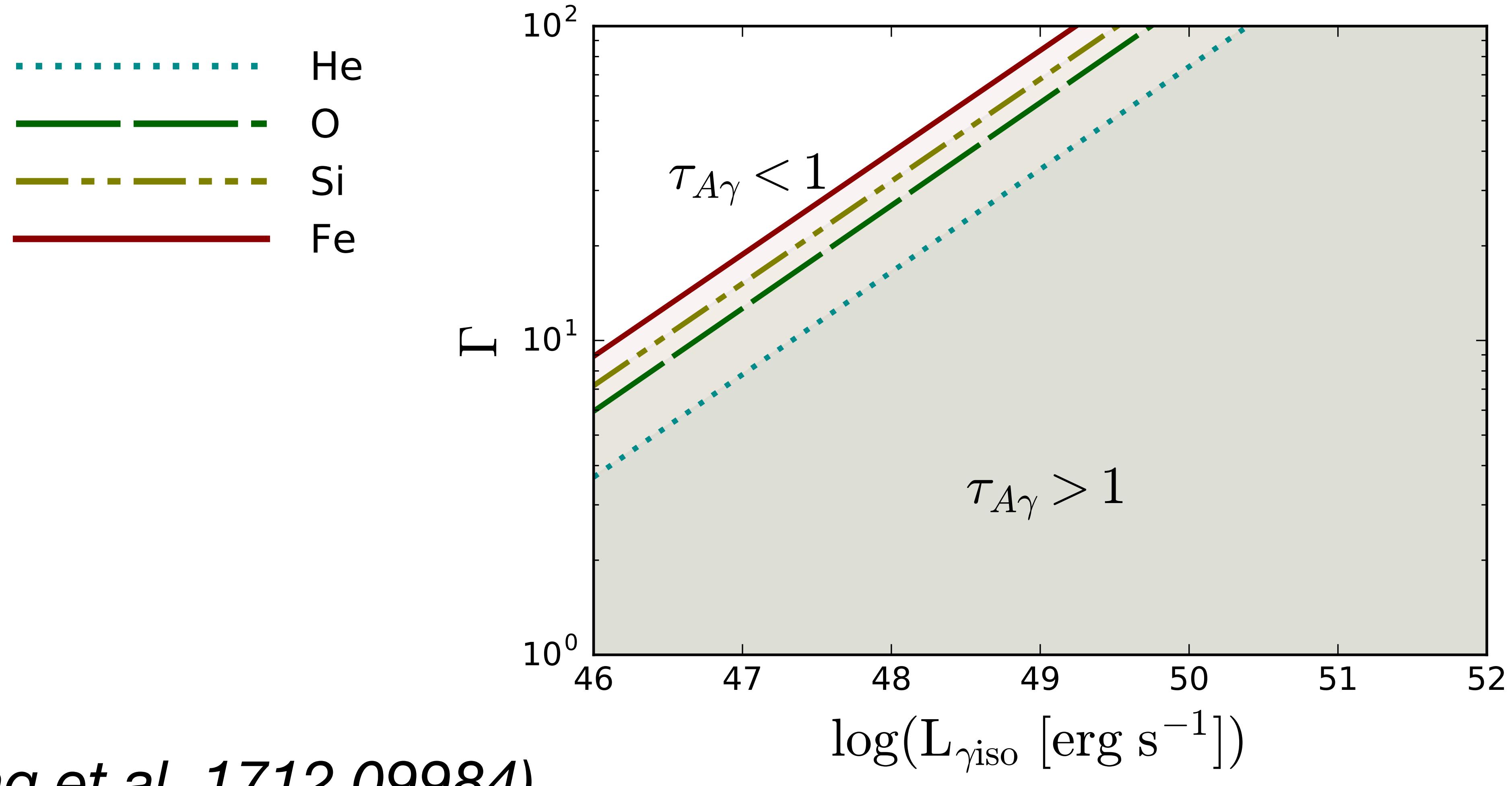

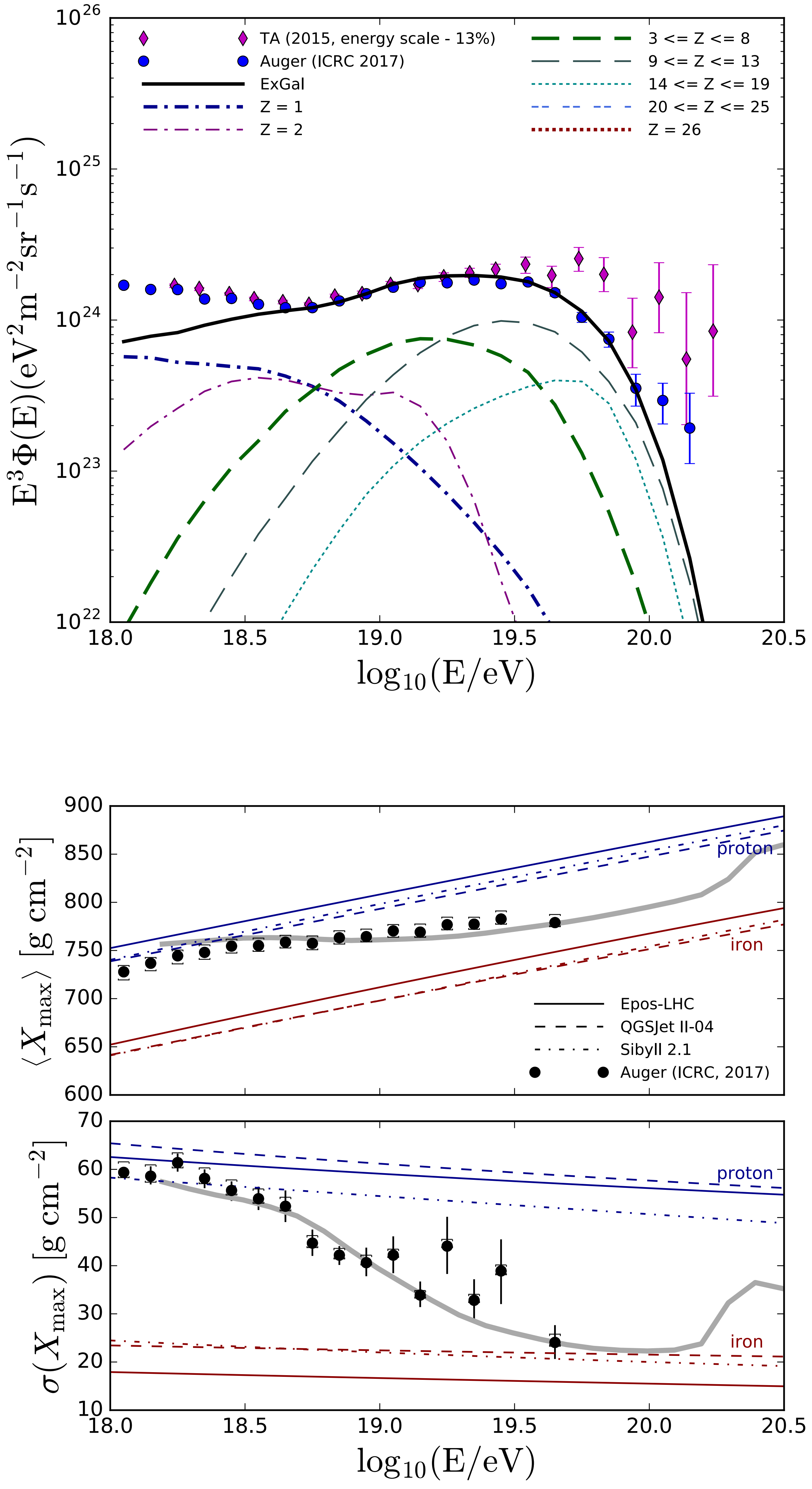

LL GRBs and Si rich progenitor

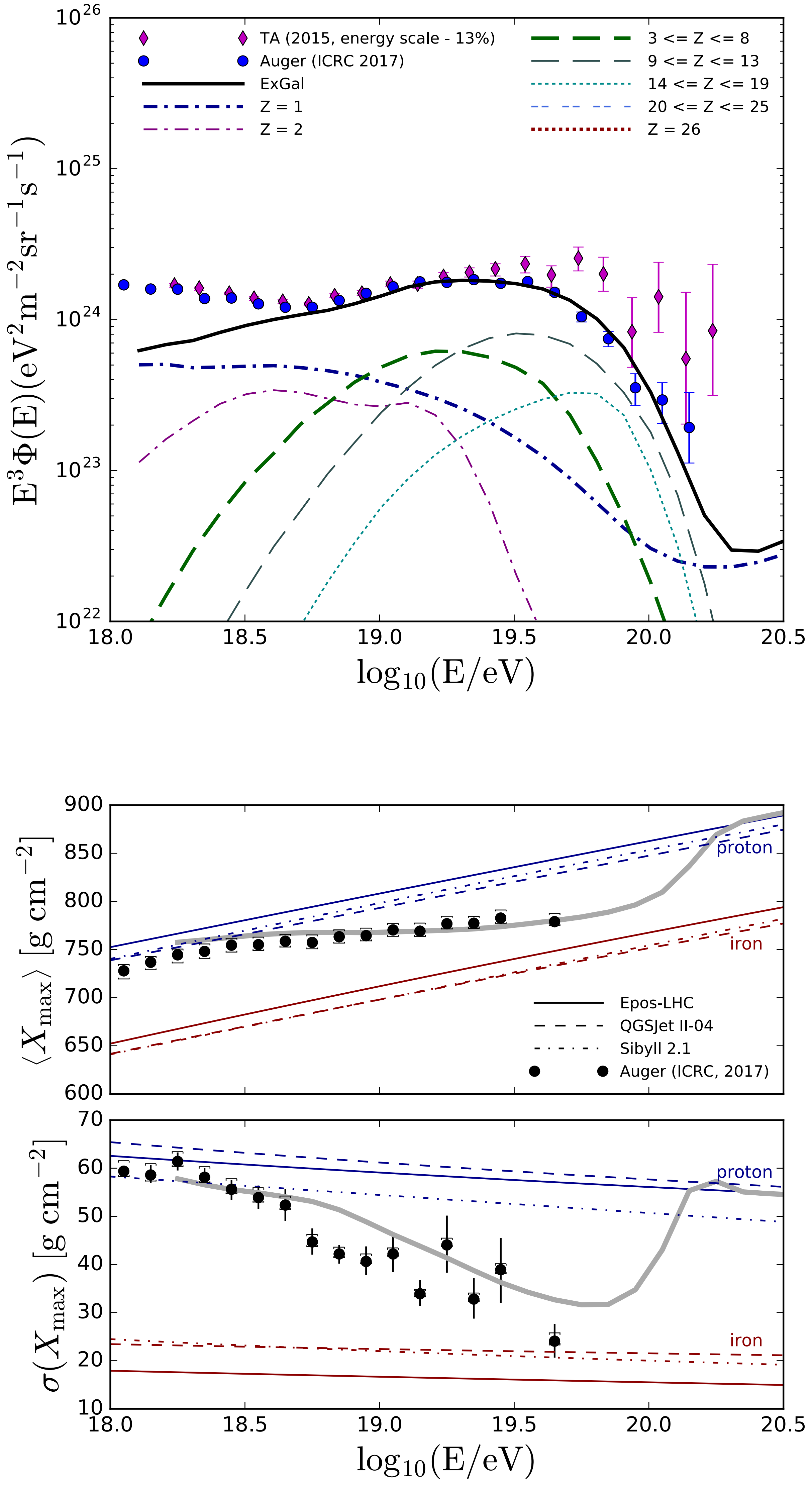

LL and HL GRBs

(Zhang et al. 1712.09984)

Neutrino and gamma-ray fluxes

Neutrinos

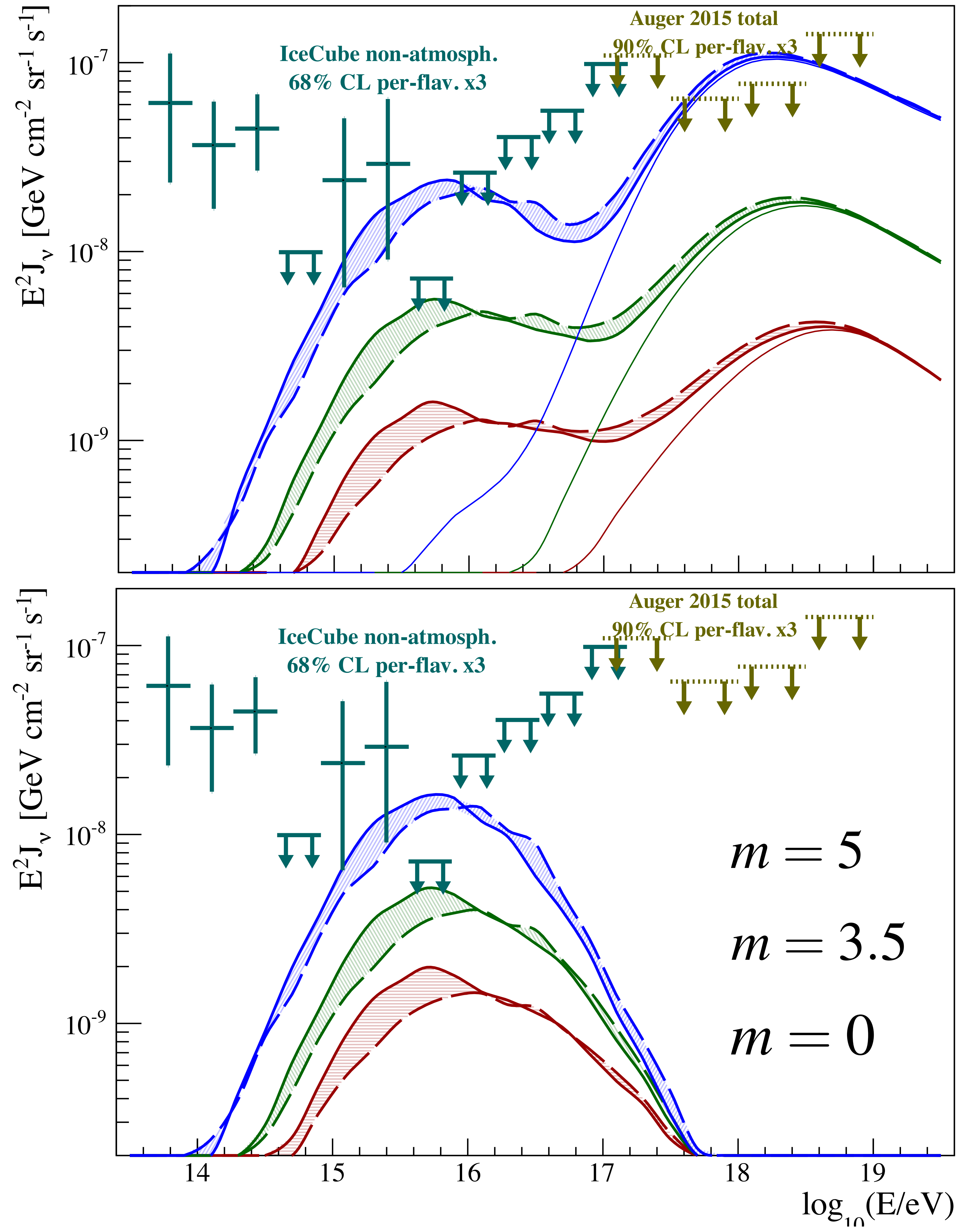

(Aloisio et al. JCAP 2015) (Ahlers, Heinze et al.)

Complementarity

Cosmic ray flux local

Neutrino flux from large distances

GZK neutrinos probe E > 10^{20} eV

Very low neutrino flux likely

Nuclei with small GZK losses?

Negative evolution of sources?

Local overdensity?

Photons

IGRB (EGB with resolved points sources removed)

n=3 to -6 evolution scenarios give rise to between **40%** and **12%** of Fermi limit

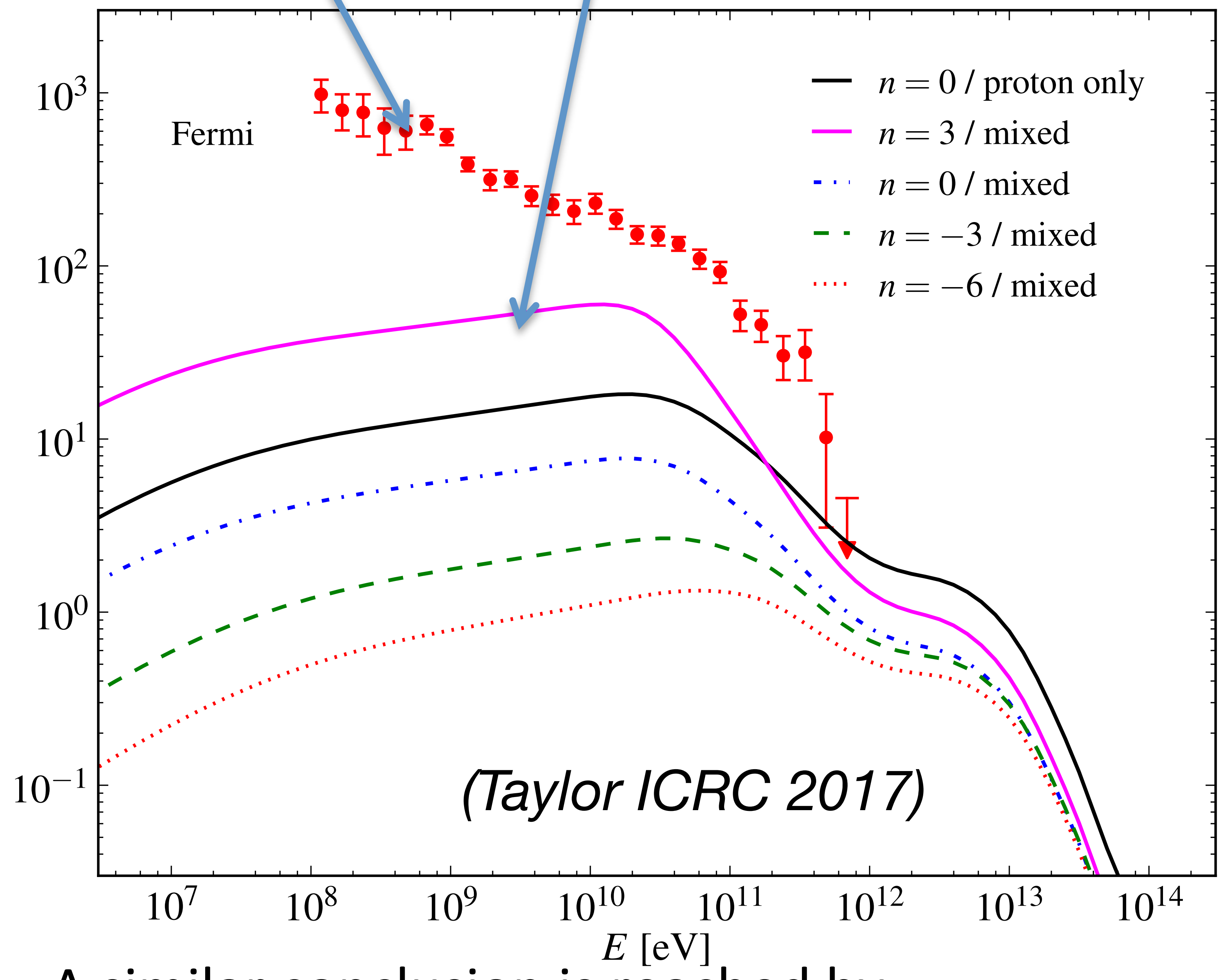

A similar conclusion is reached by **Gavish et al. (2016), 1603.04074**

Summary: non-trivial picture of cosmic rays is emerging

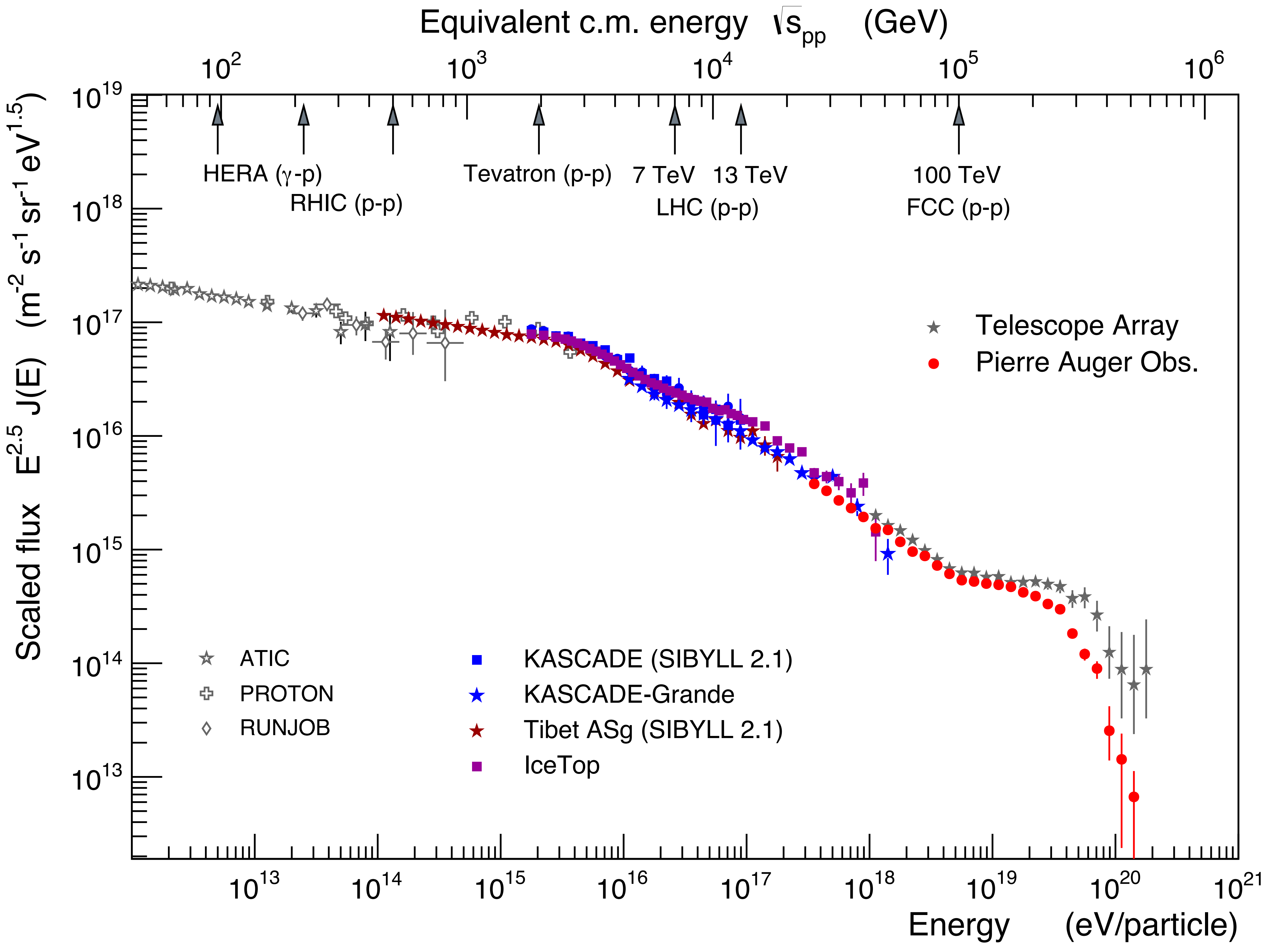

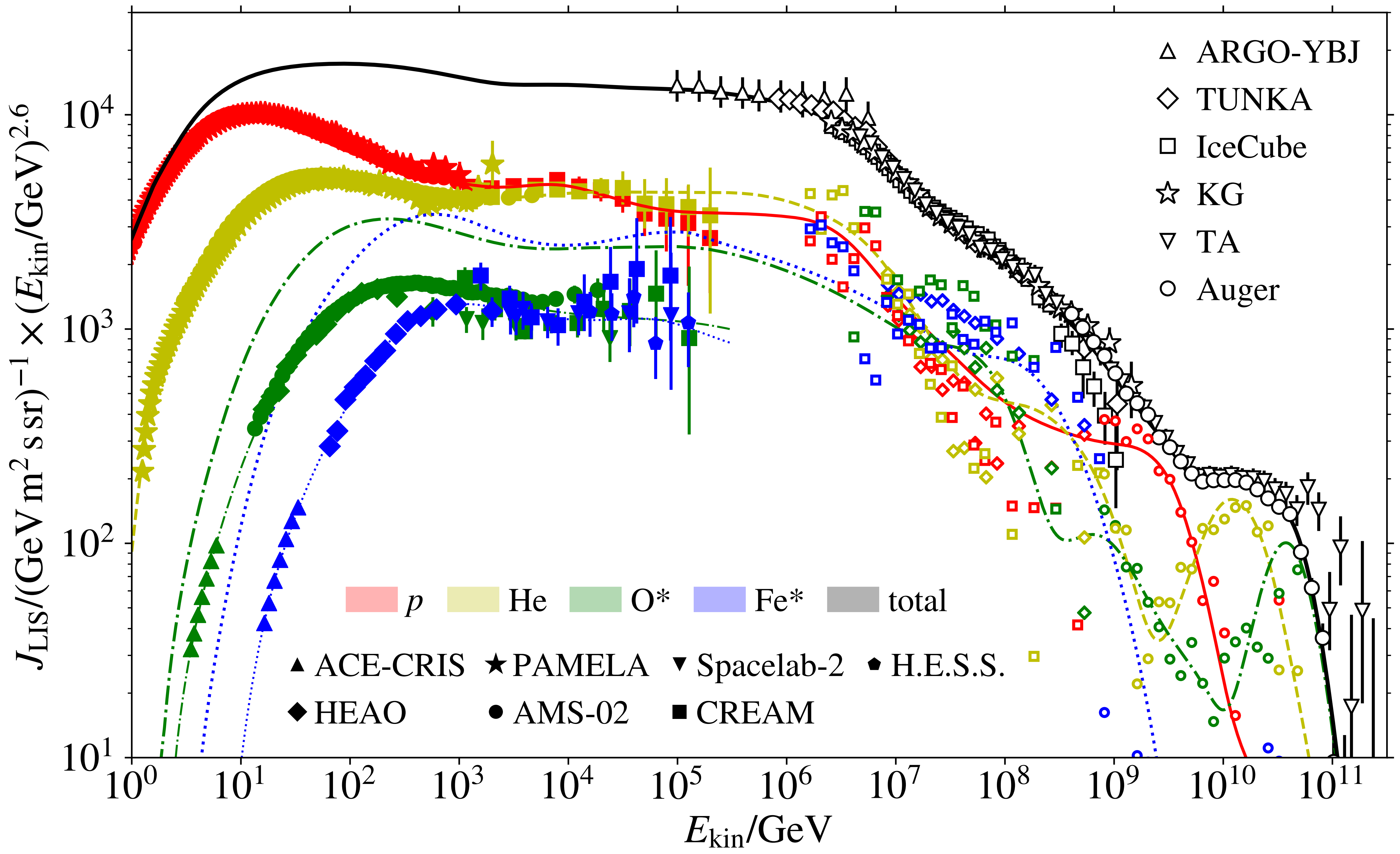

- **Many deviations from straightforward power-law model found (subject to exp. uncertainties)**
- **None of these key features satisfactorily understood**
- **Increasing number of very detailed models covering wide range of energies**
- **Multi-messenger data of fundamental importance to make progress**

Backup slides

TAx4 Project

TA SD (~3000 km^2): Quadruple area

Approved in Japan 2015

500 scintillator SDs

2.08 km spacing

3 yrs construction, first 173 SDs have arrived in Utah for final assembly, next 77 SD to be prepared at Akeno Obs. (U.Tokyo) 2017-08 and shipped to Utah

2 FD stations (12 HiRes Telescopes)

Approved US NSF 2016

Telescopes/electronics being prepared at Univ. Utah

Site construction underway at the northern station.

Get 19 TA-equiv years of SD data by 2020

Get 16.3 (current) TA years of hybrid data

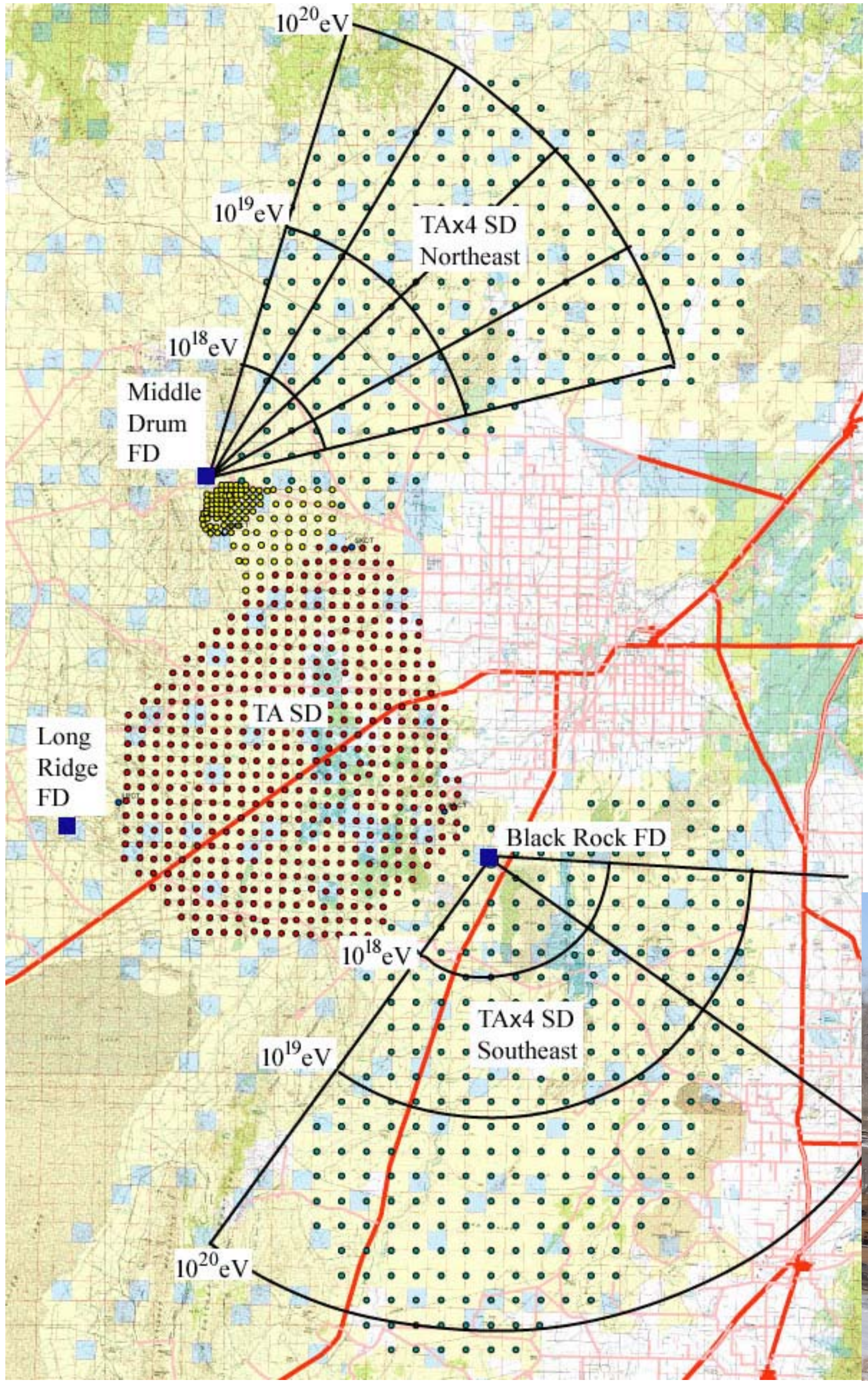

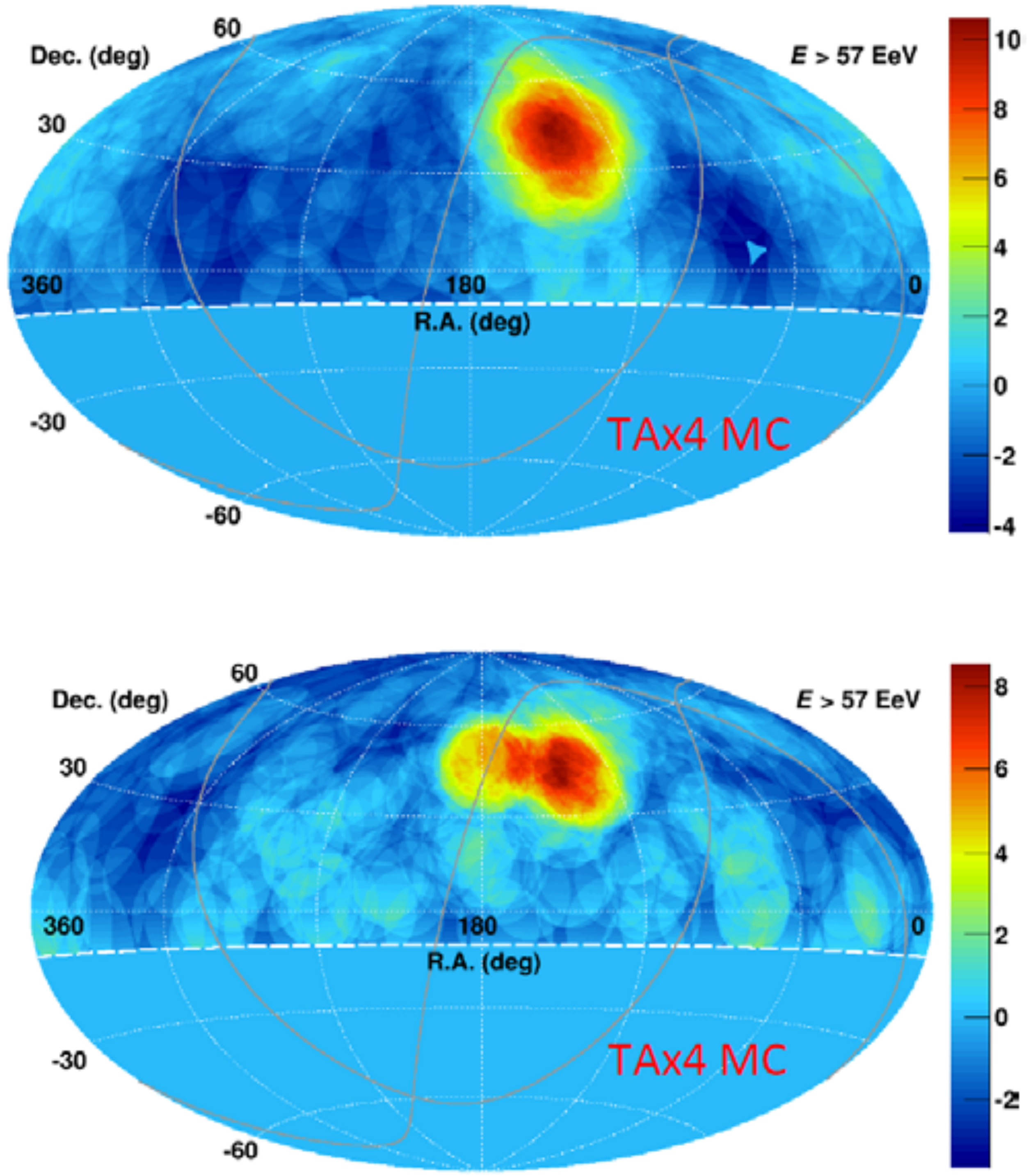

(Kido, Matthews ICRC 2017)

Upgrade of Auger Observatory: AugerPrime

100% duty cycle

Complementarity of particle response used to discriminate em. and muonic components

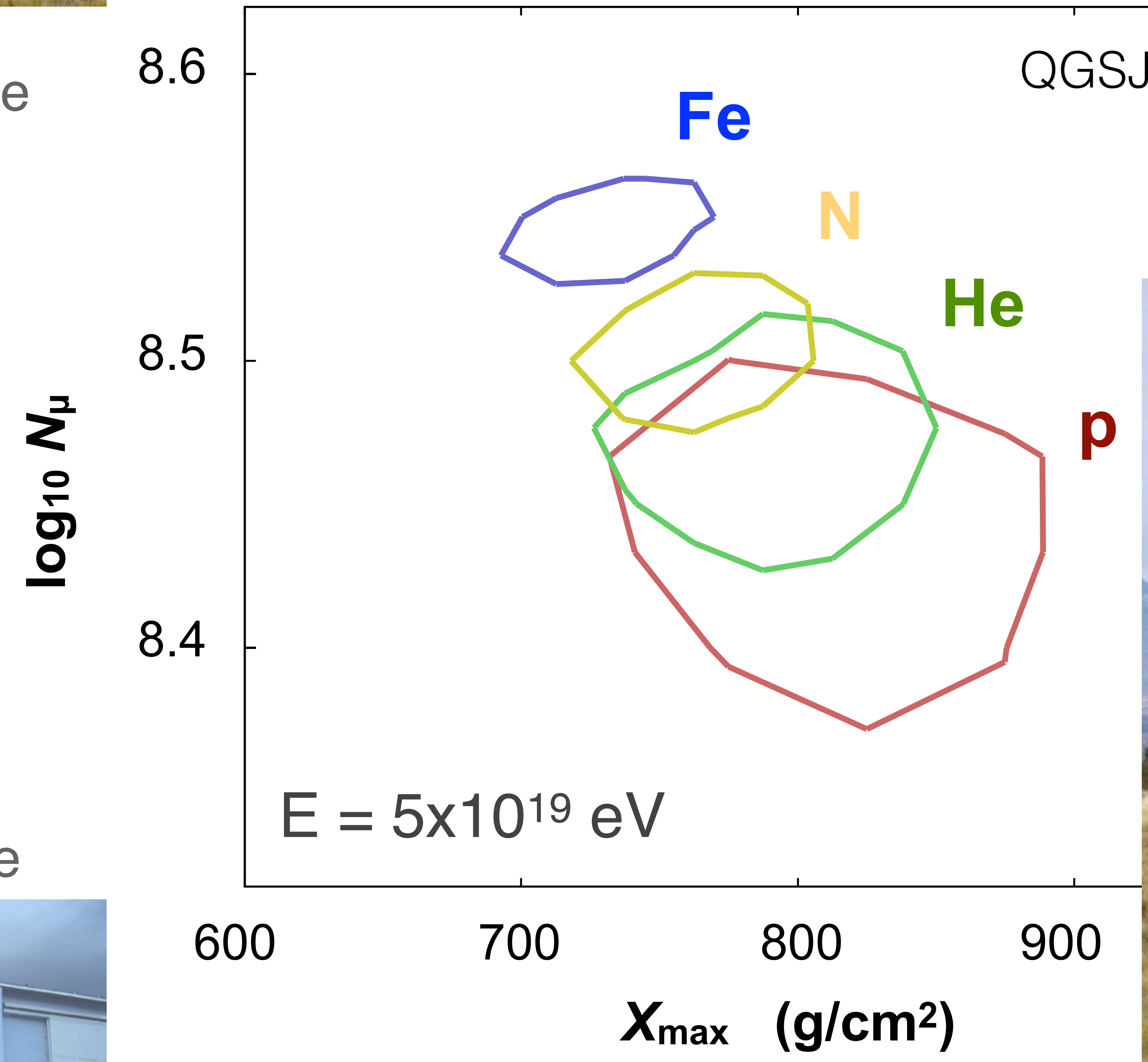

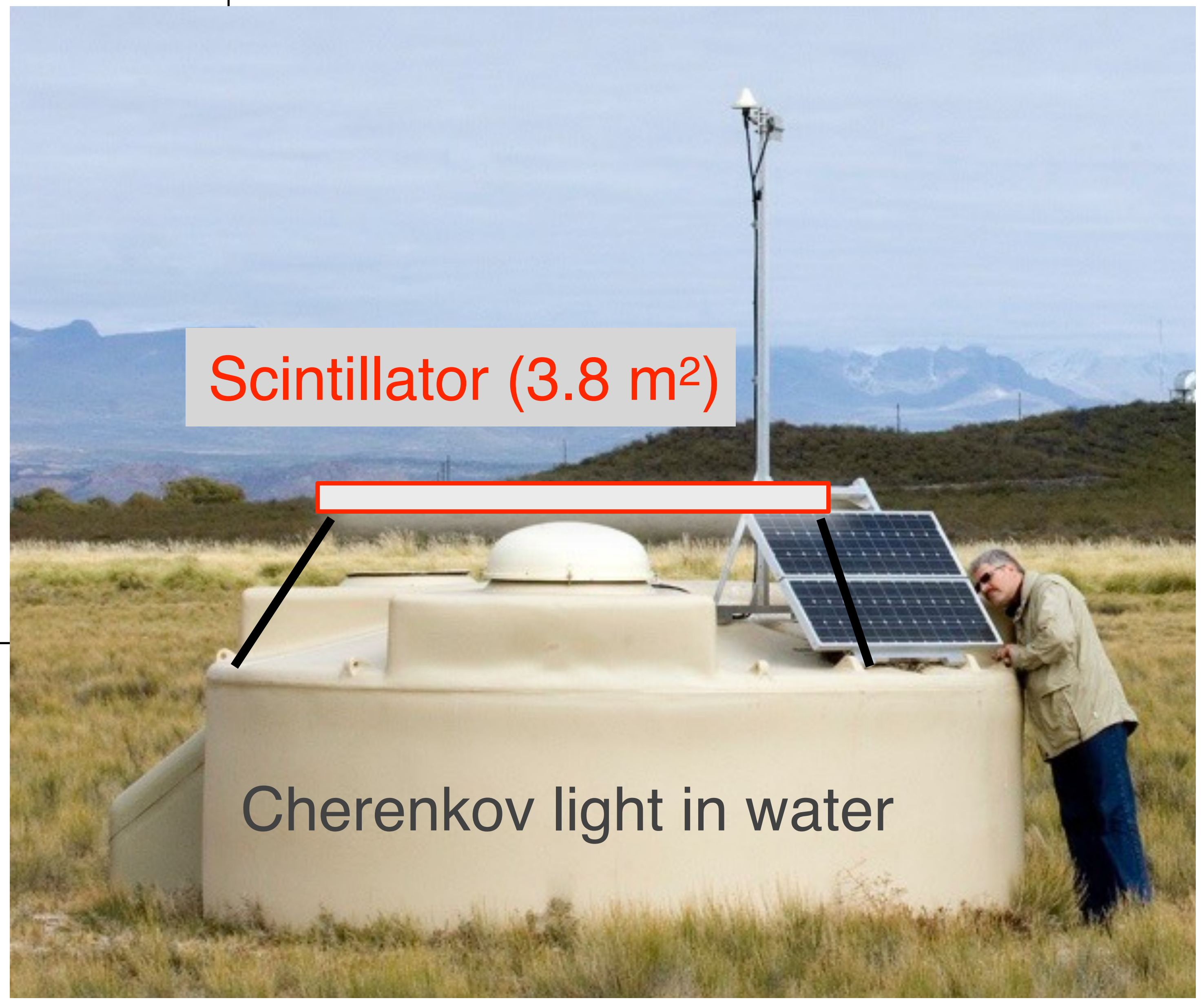

15% duty cycle

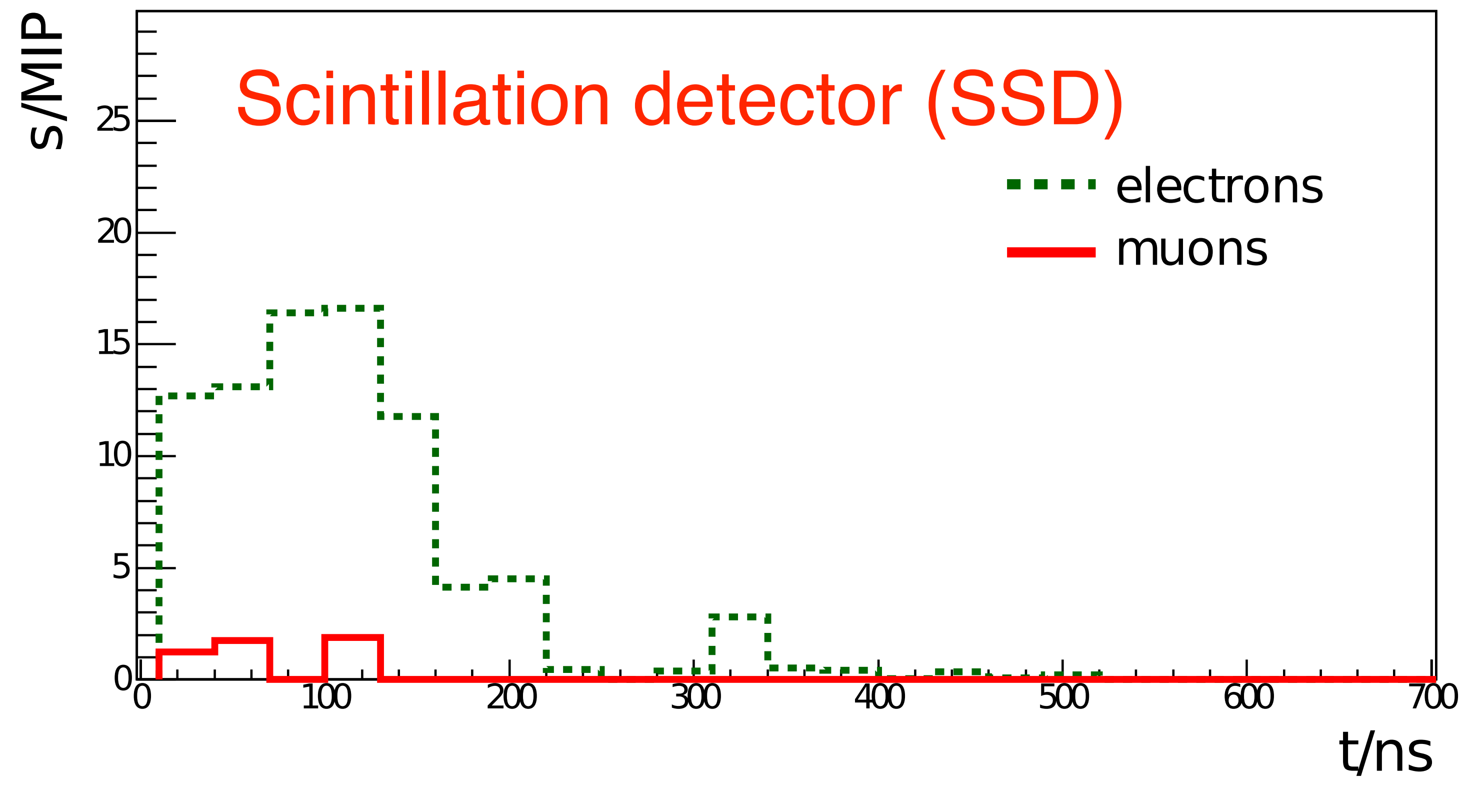

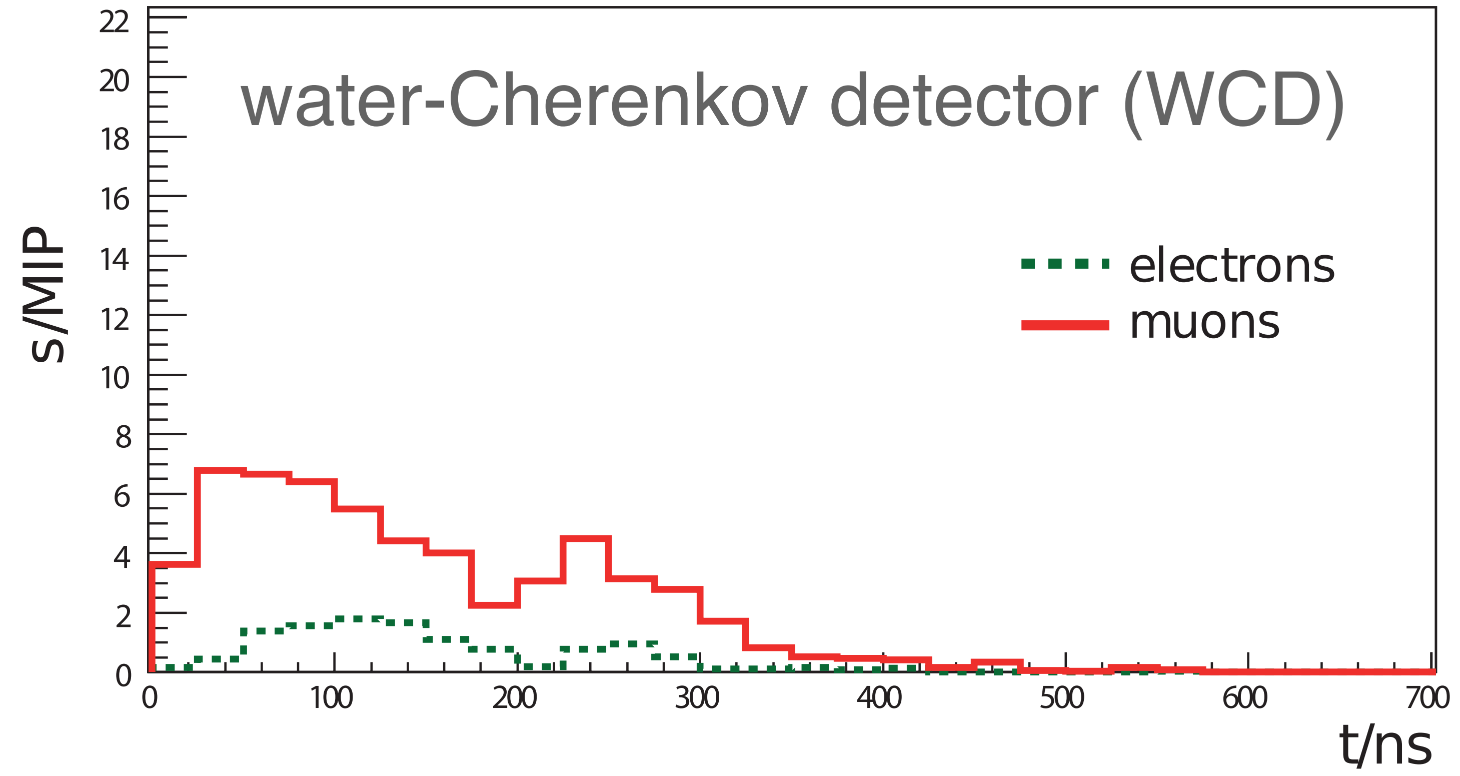

$$S_{\mu,\mathrm{WCD}} = a\,S_{\mathrm{WCD}} + b\,S_{\mathrm{SSD}}$$
$$S_{\mathrm{em,WCD}} = c\,S_{\mathrm{WCD}} + d\,S_{\mathrm{SSD}}$$

(Martello, ICRC 2017)

(AugerPrime design report 1604.03637)

Status and plans for AugerPrime

Engineering Array: 12 stations

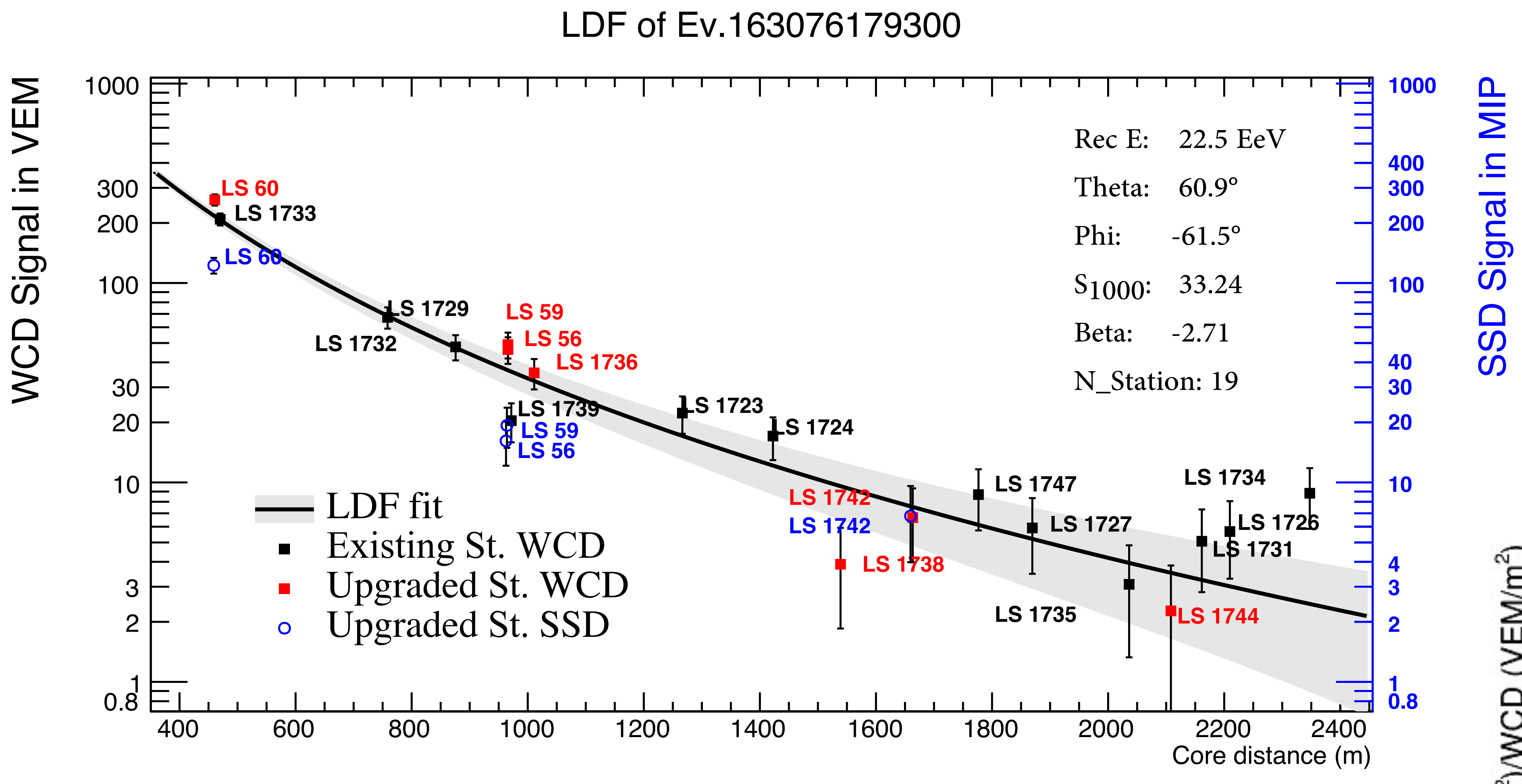

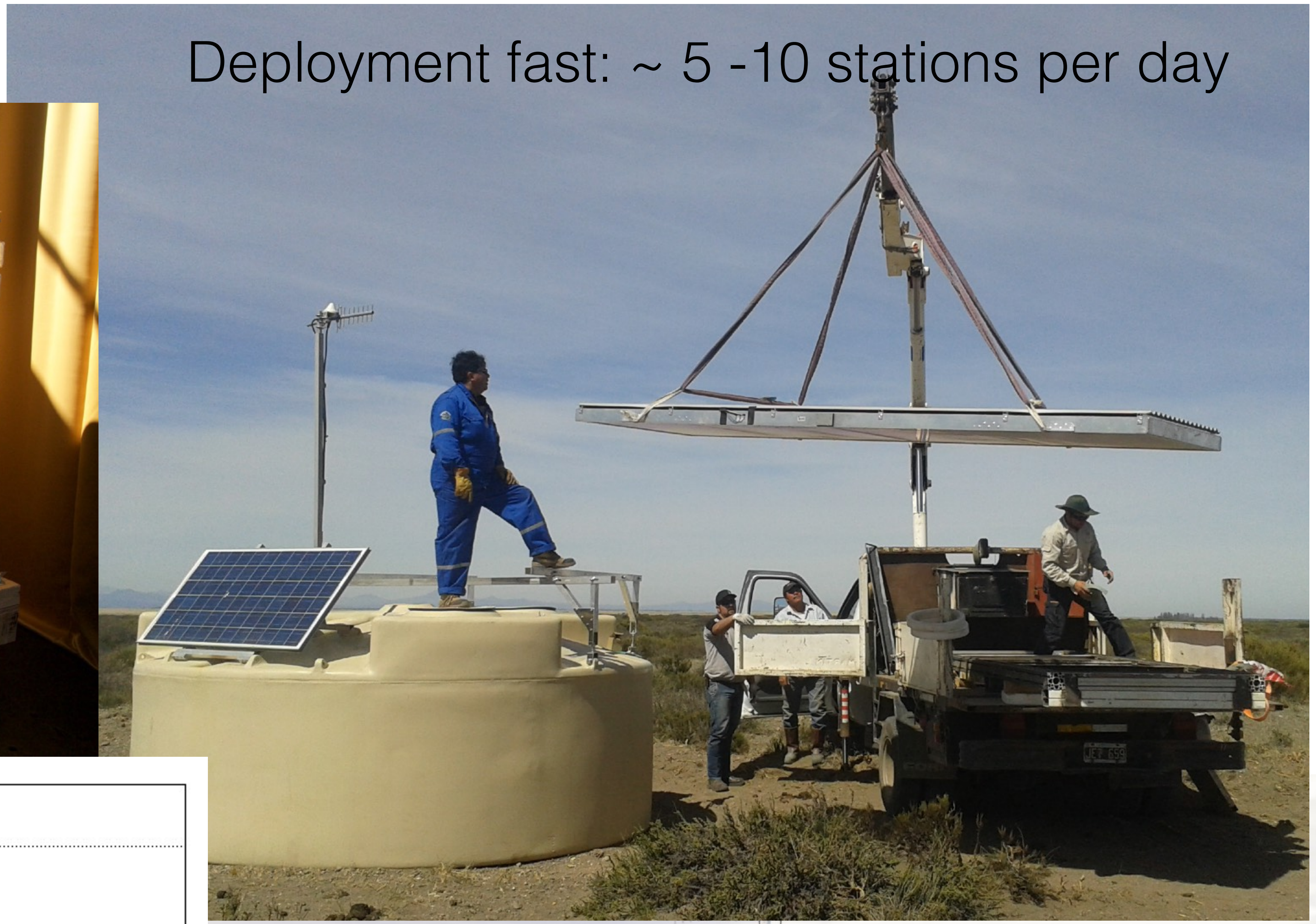

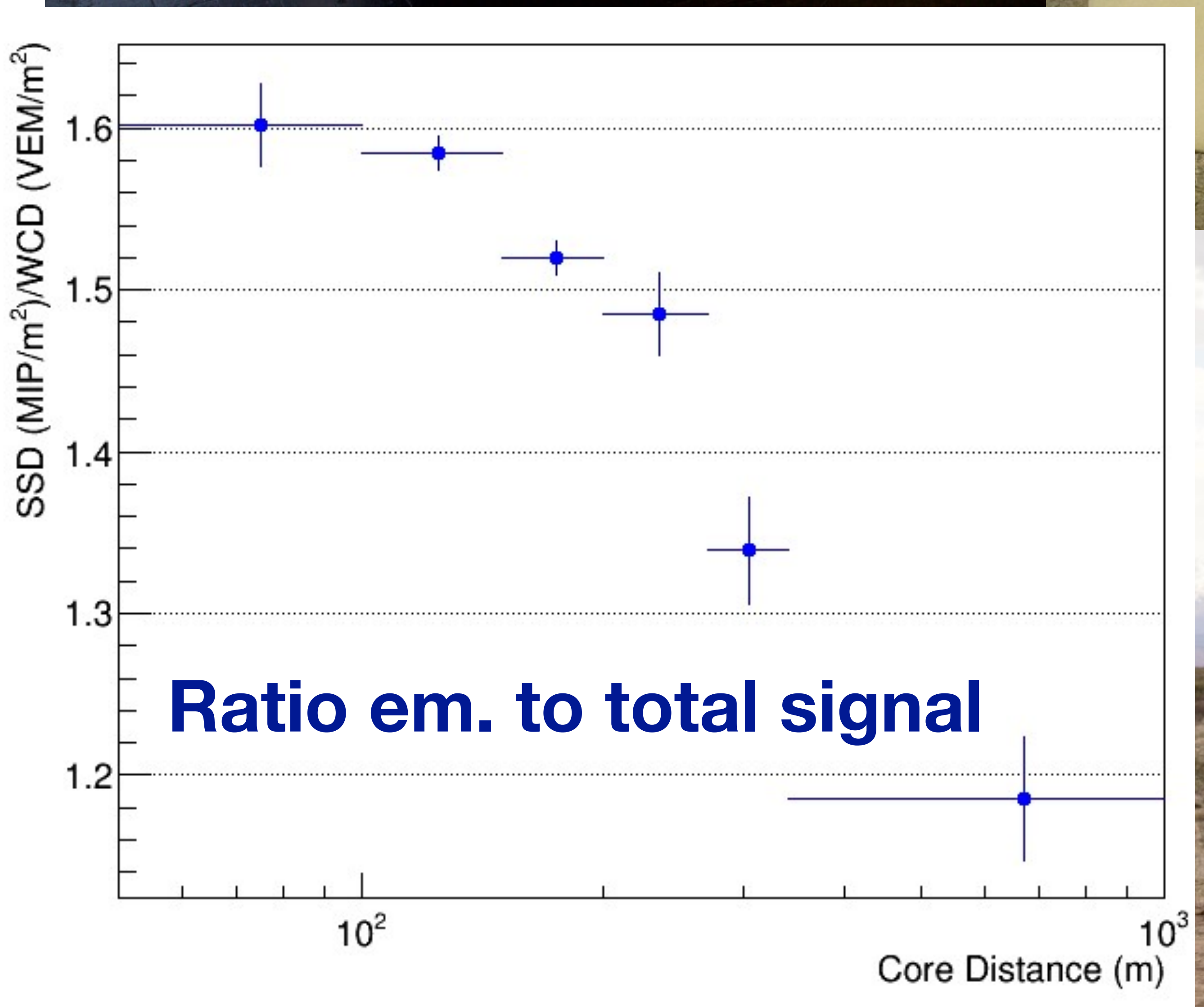

2016: engineering array

2018-19: deployment

2019-25: data taking (40,000 km^2 sr yr)

Composition measurement at 10^{20} eV

Composition selected anisotropy studies

Particle physics with air showers

Photon and neutrino limits at ultra-high energy

$$p + \gamma_{CMB} \rightarrow p + \pi^0$$
$$\searrow \gamma\gamma$$

$$p + \gamma_{CMB} \rightarrow n + \pi^+$$
$$\searrow e^+ + 3\nu$$

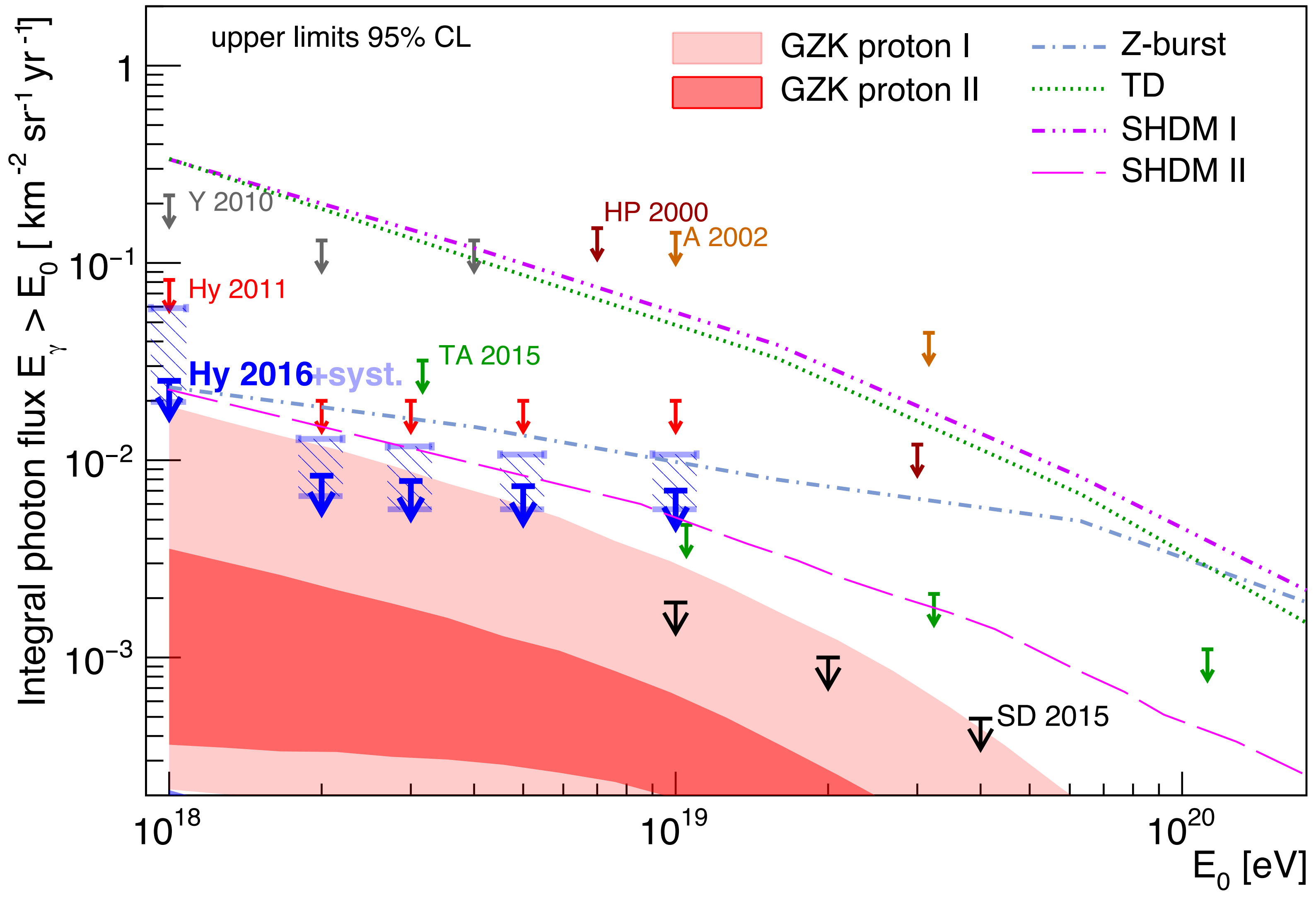

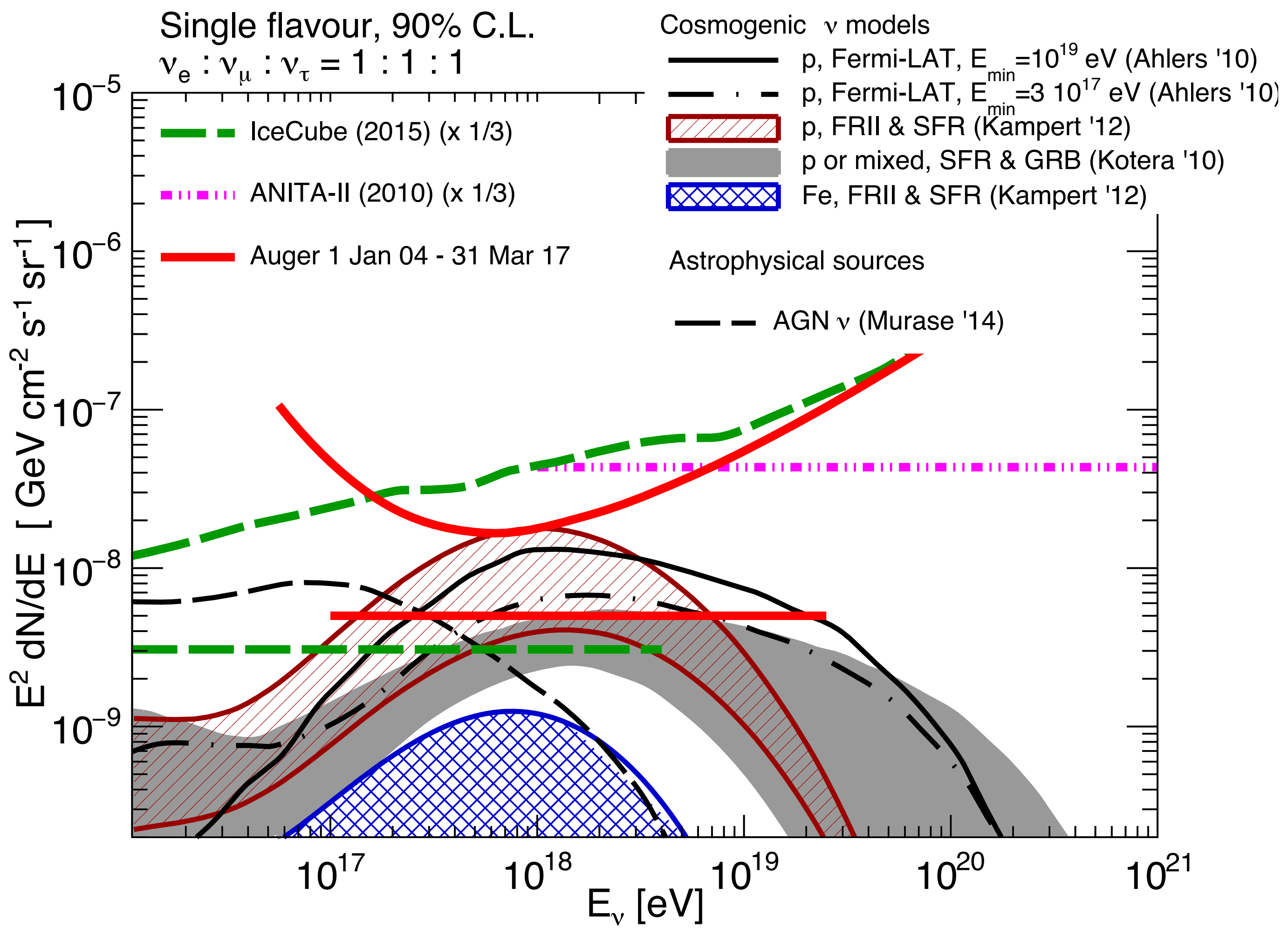

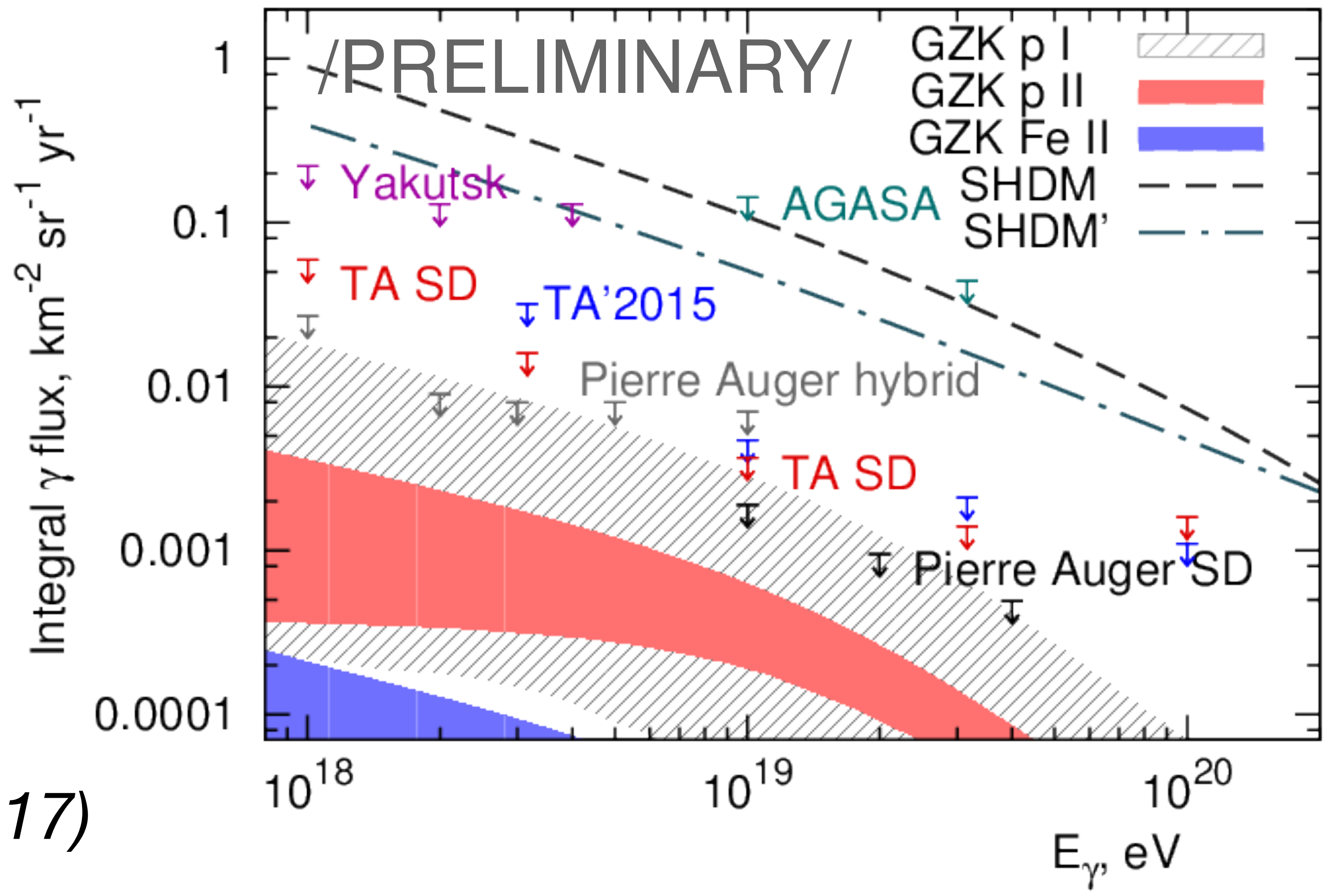

(Niechciol, Auger ICRC 2017)

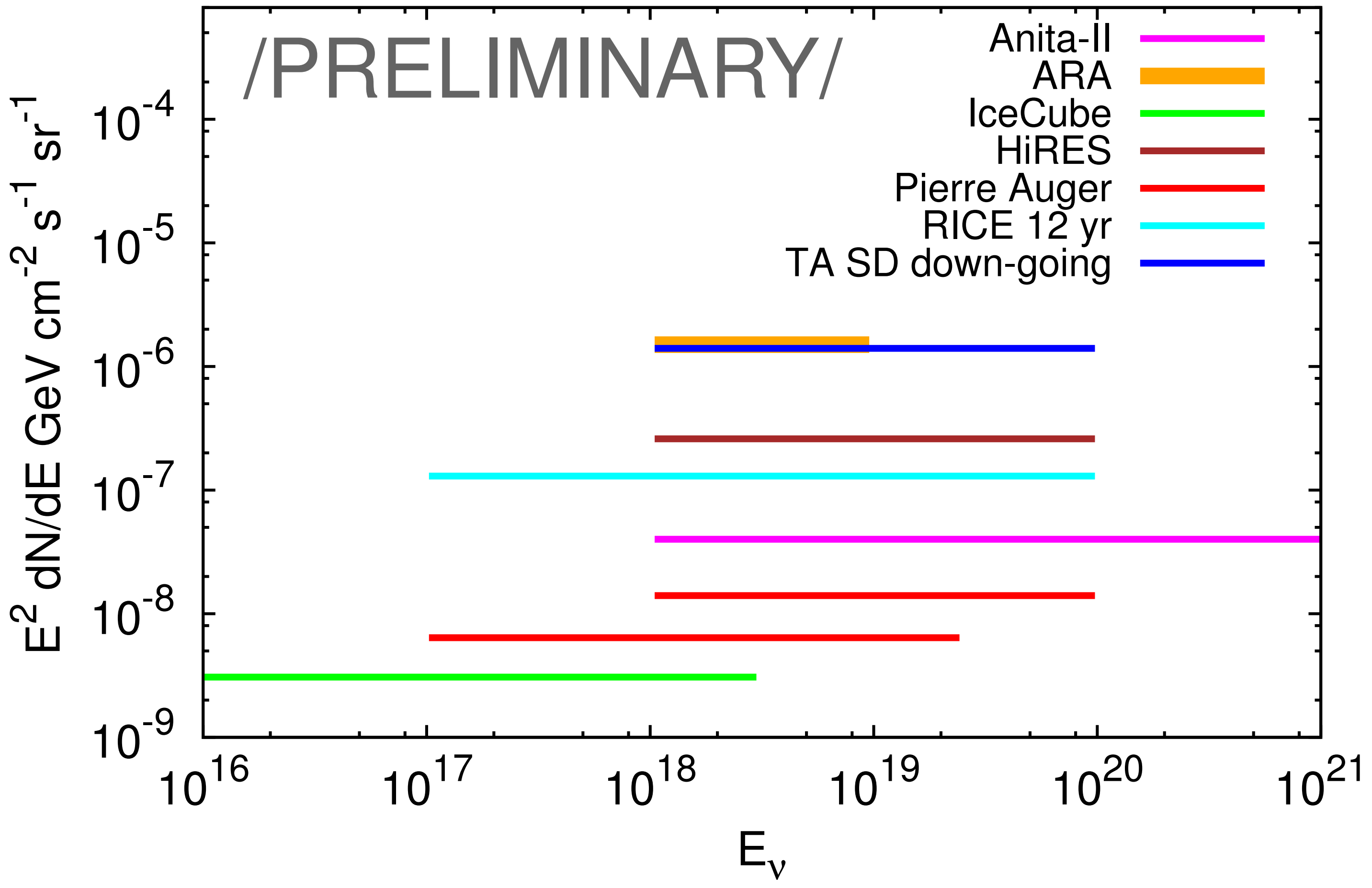

(Rubtsov, TA ICRC 2017, Zas, Auger, ICRC 2017)

Physics reach: mass sensitivity & discrimination of scenarios

Illustration with two benchmark scenarios

(note: these are not physics models)

(AugerPrime 1604.03637)

Scenario 1: maximum rigidity model

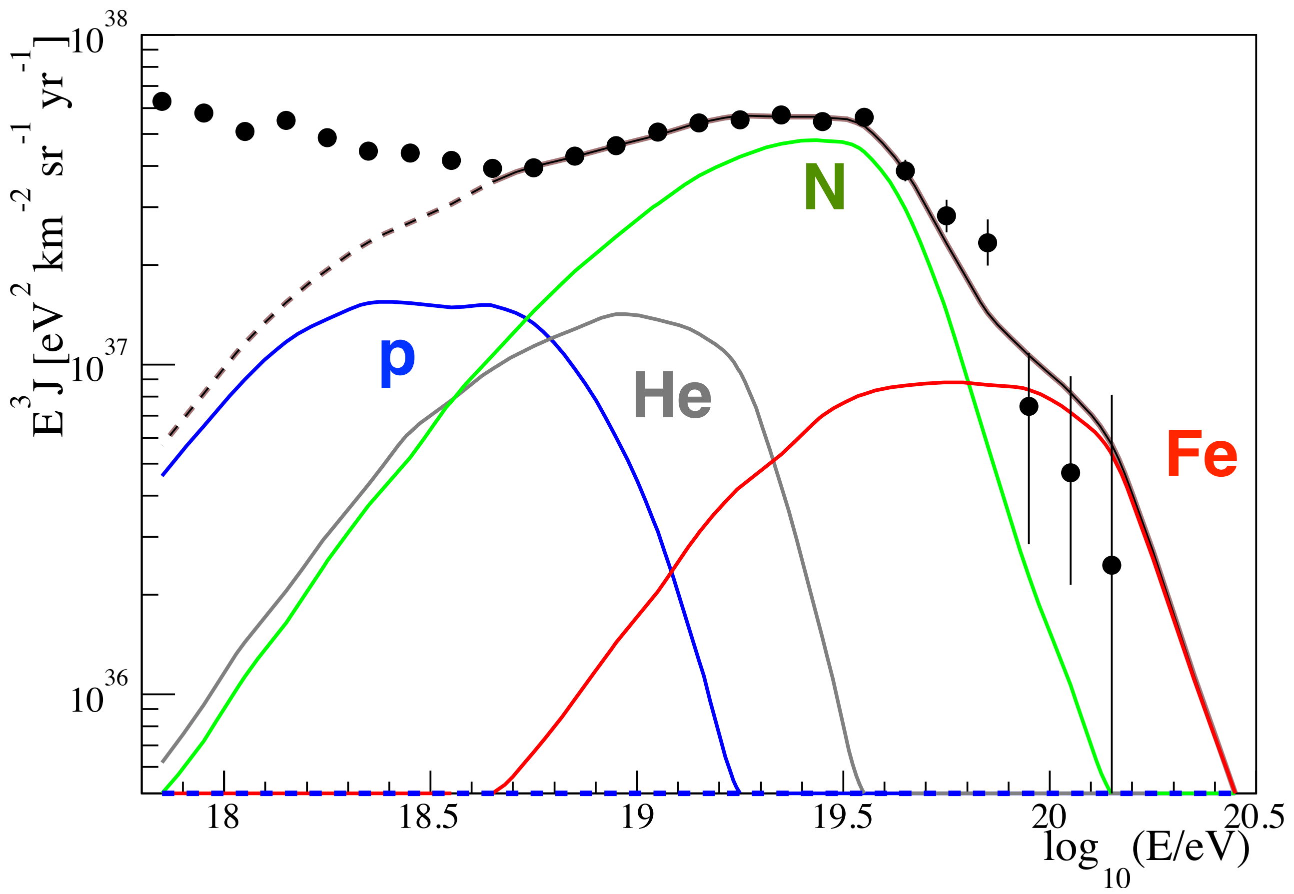

Scenario 2: photo-disintegration model

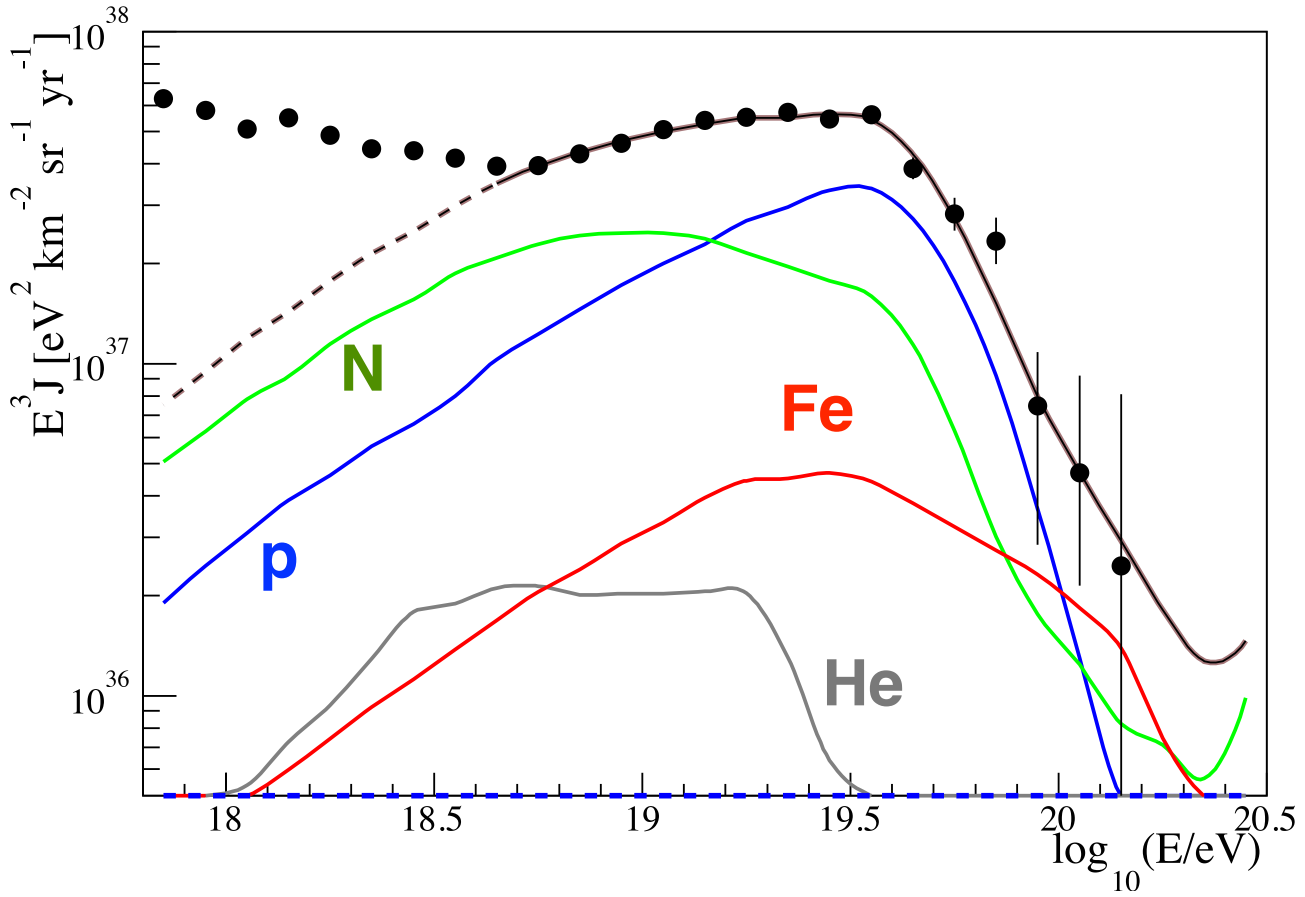

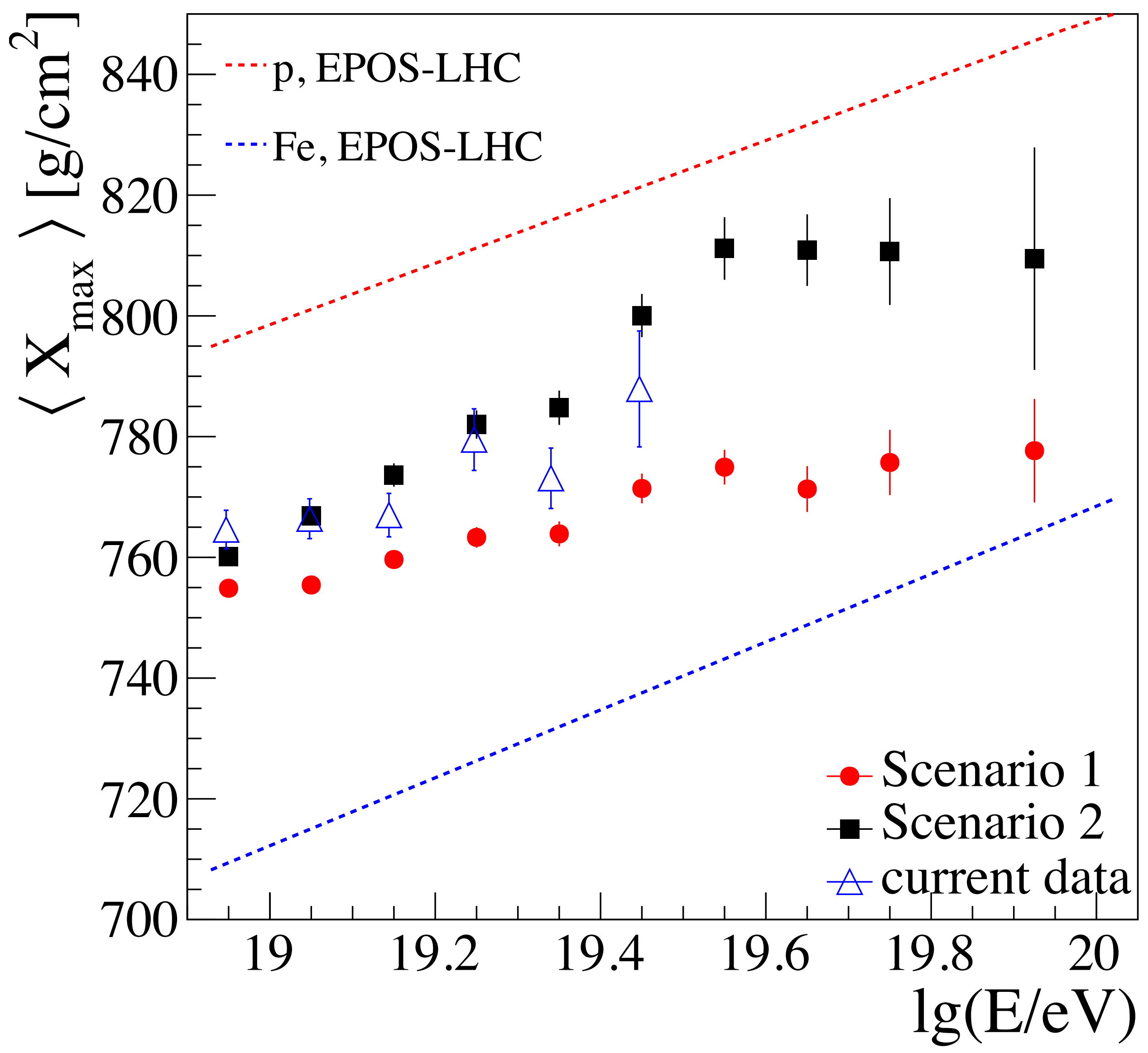

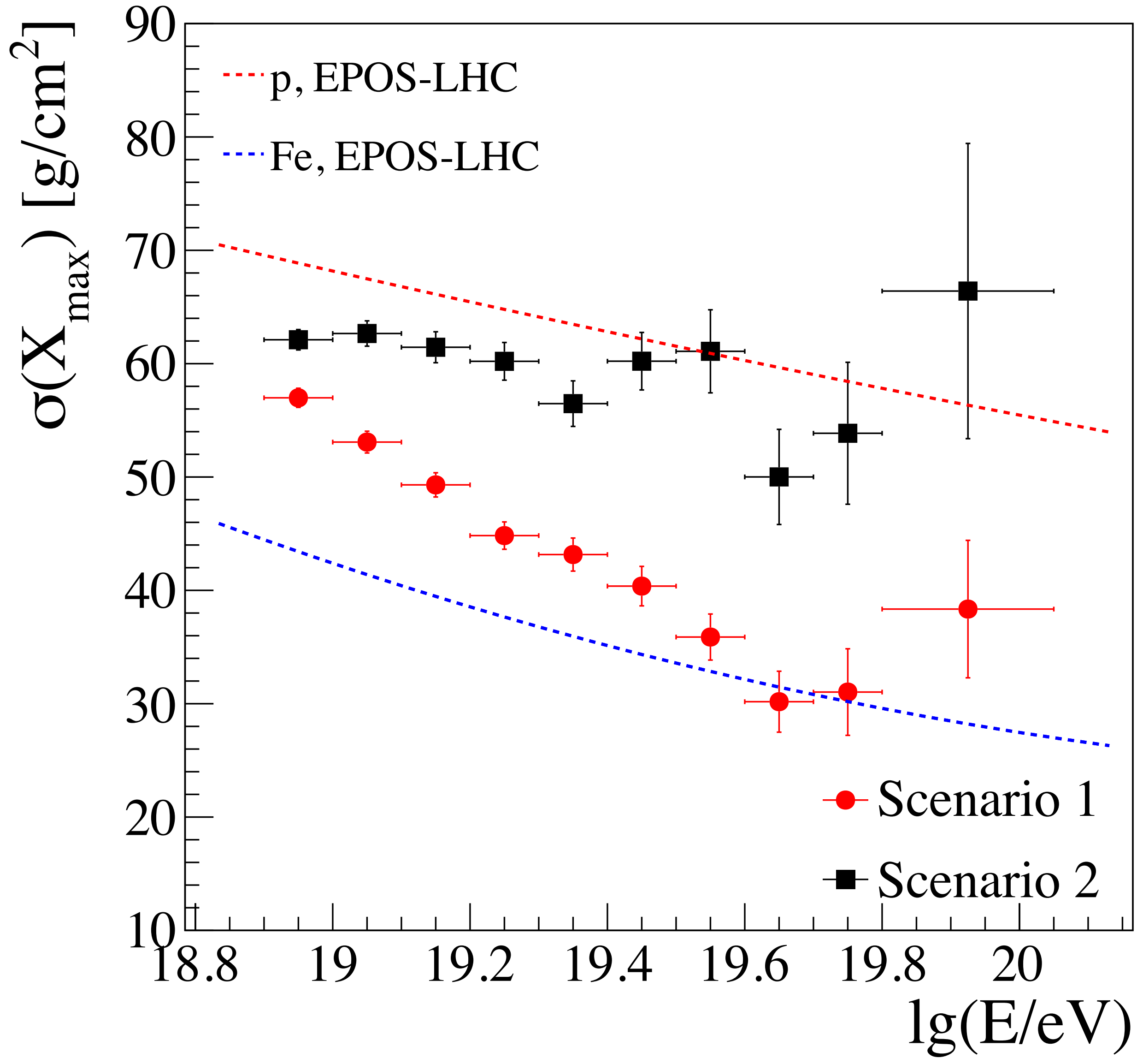

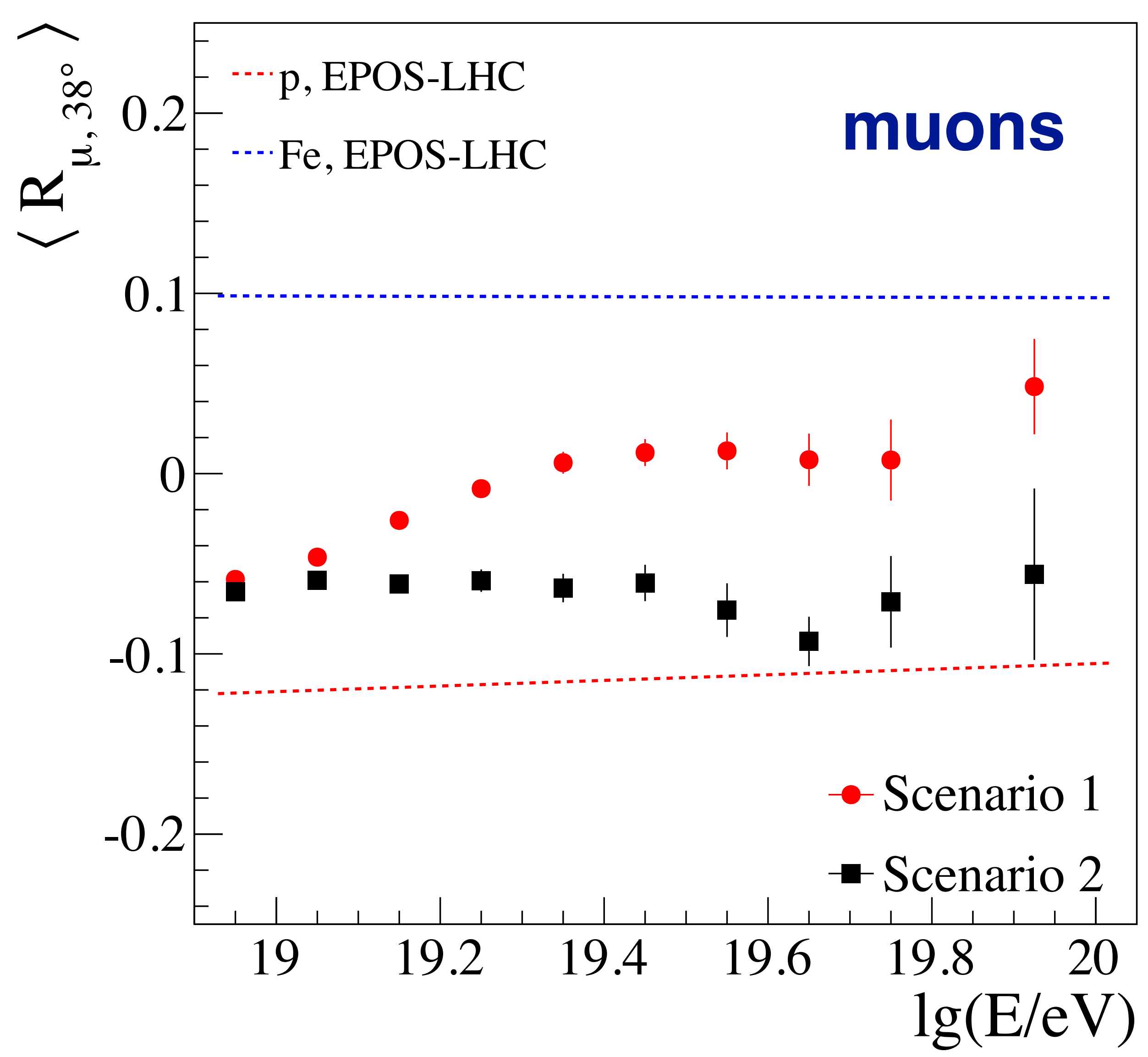

Physics reach: detection of 10% proton contribution

Reference: maximum rigidity model

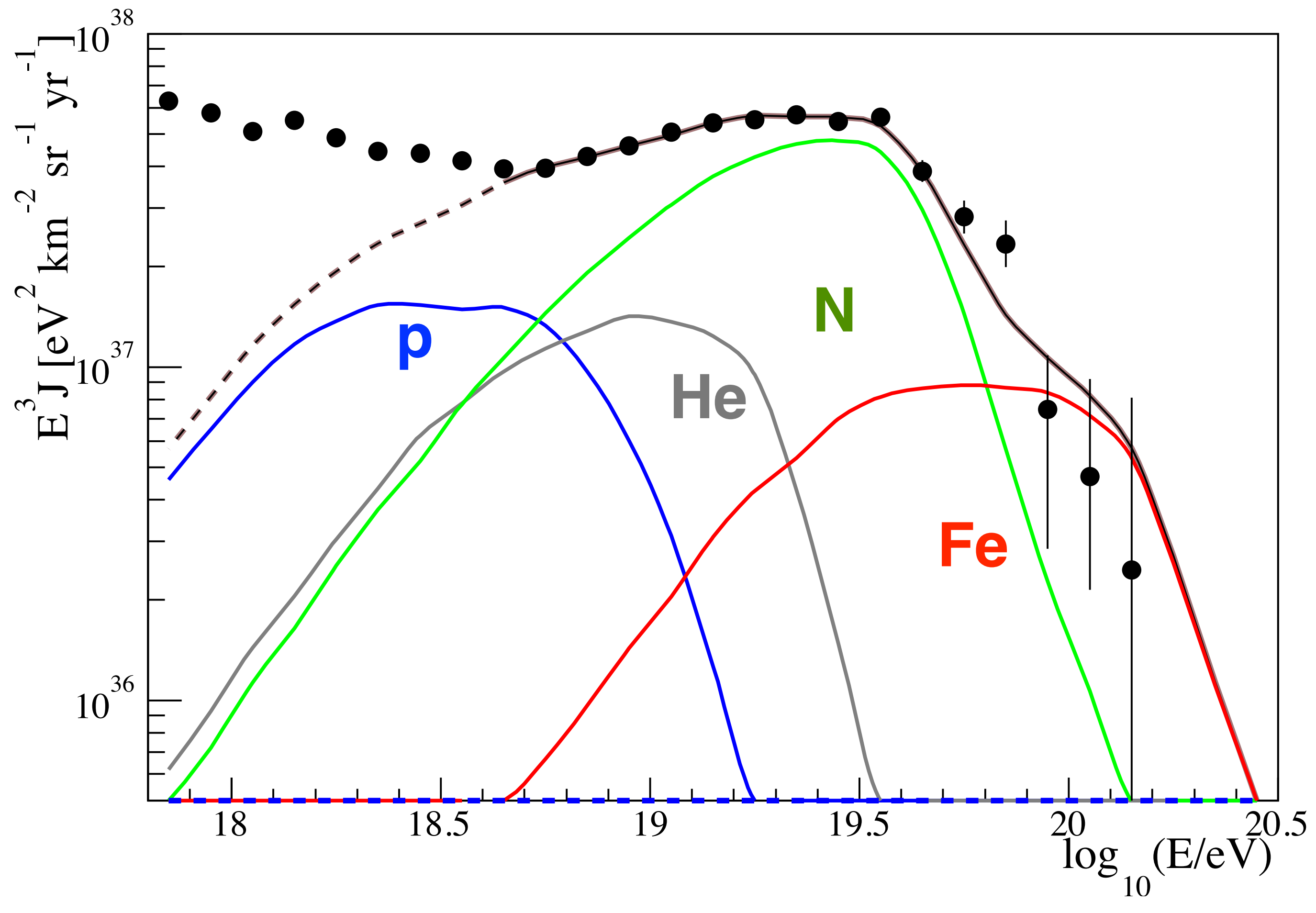

- Standard scenario 1 (no protons at high energy)
- Scenario 1 with 10% protons added

Significance of distinguishing scenarios with and without 10% protons

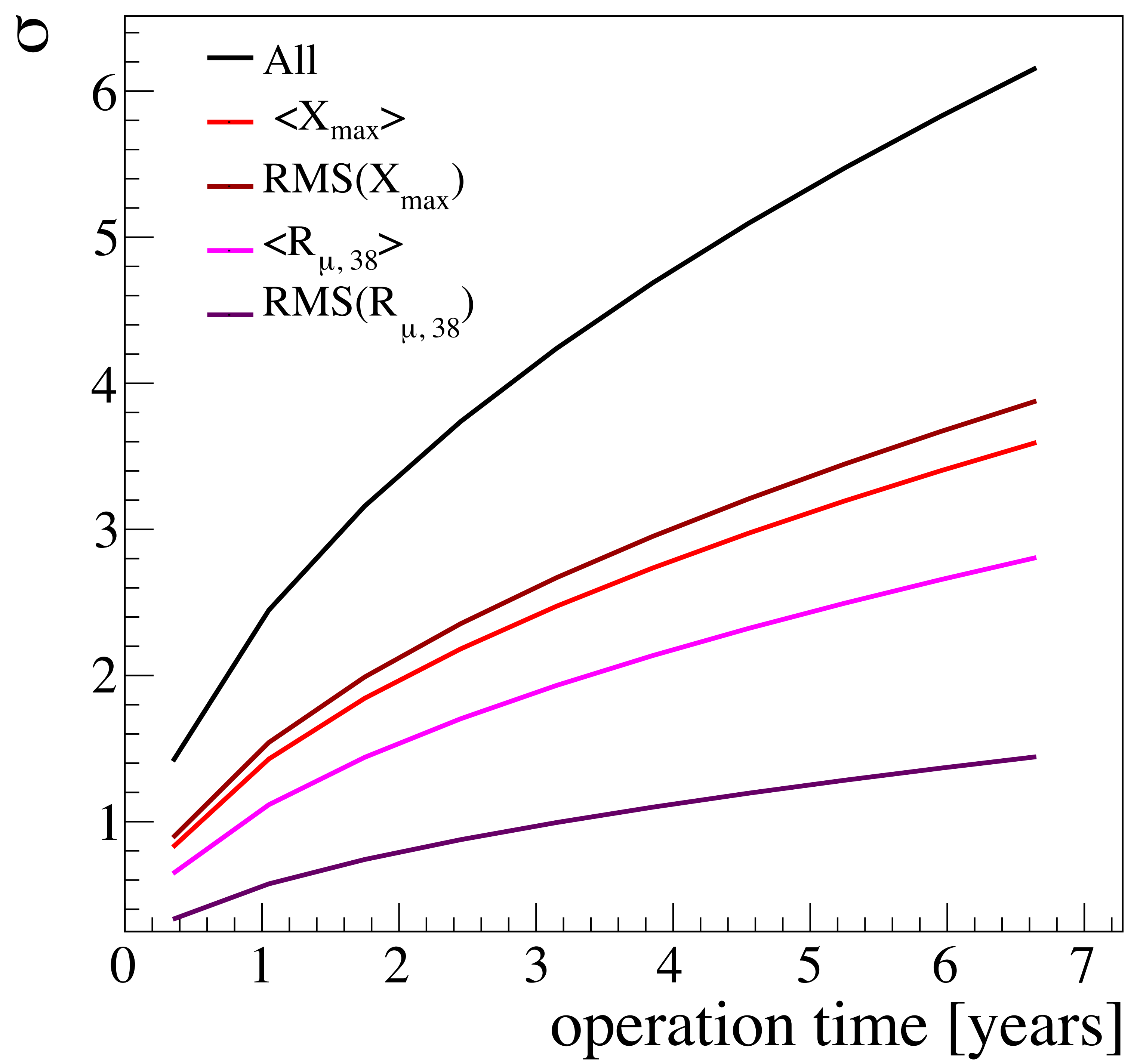

(ideal case for knowing proton predictions without uncertainty due to had. int. models)

(AugerPrime 1604.03637)

Physics reach: composition-enhanced anisotropy

Modified Auger data set
(E > 4x10^{19} eV, 454 events,
ApJ 804 (2015)15)

X_{max} assignment according to
maximum rigidity scenario

10% protons added, half of
which from within 3° of AGNs

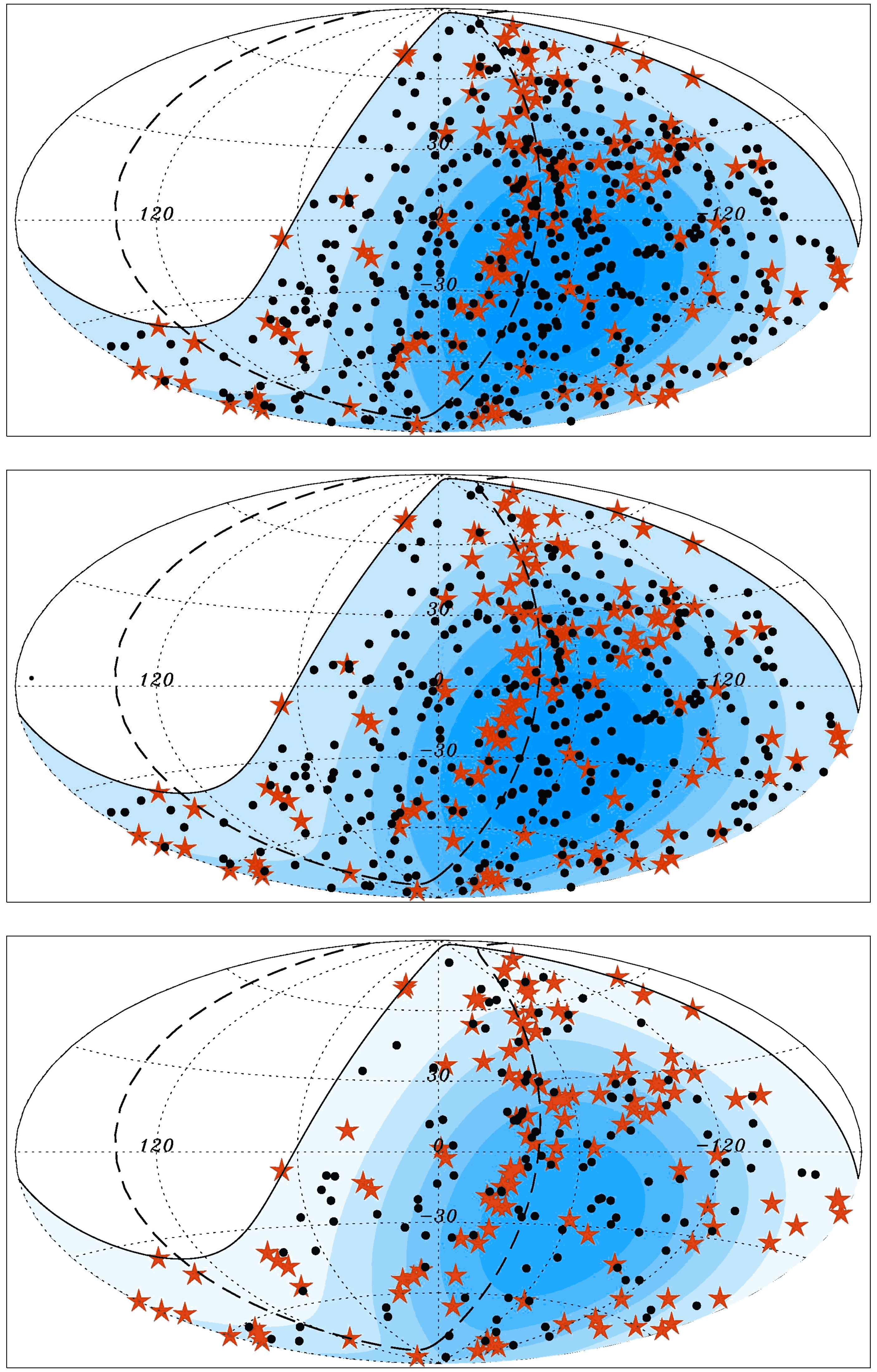

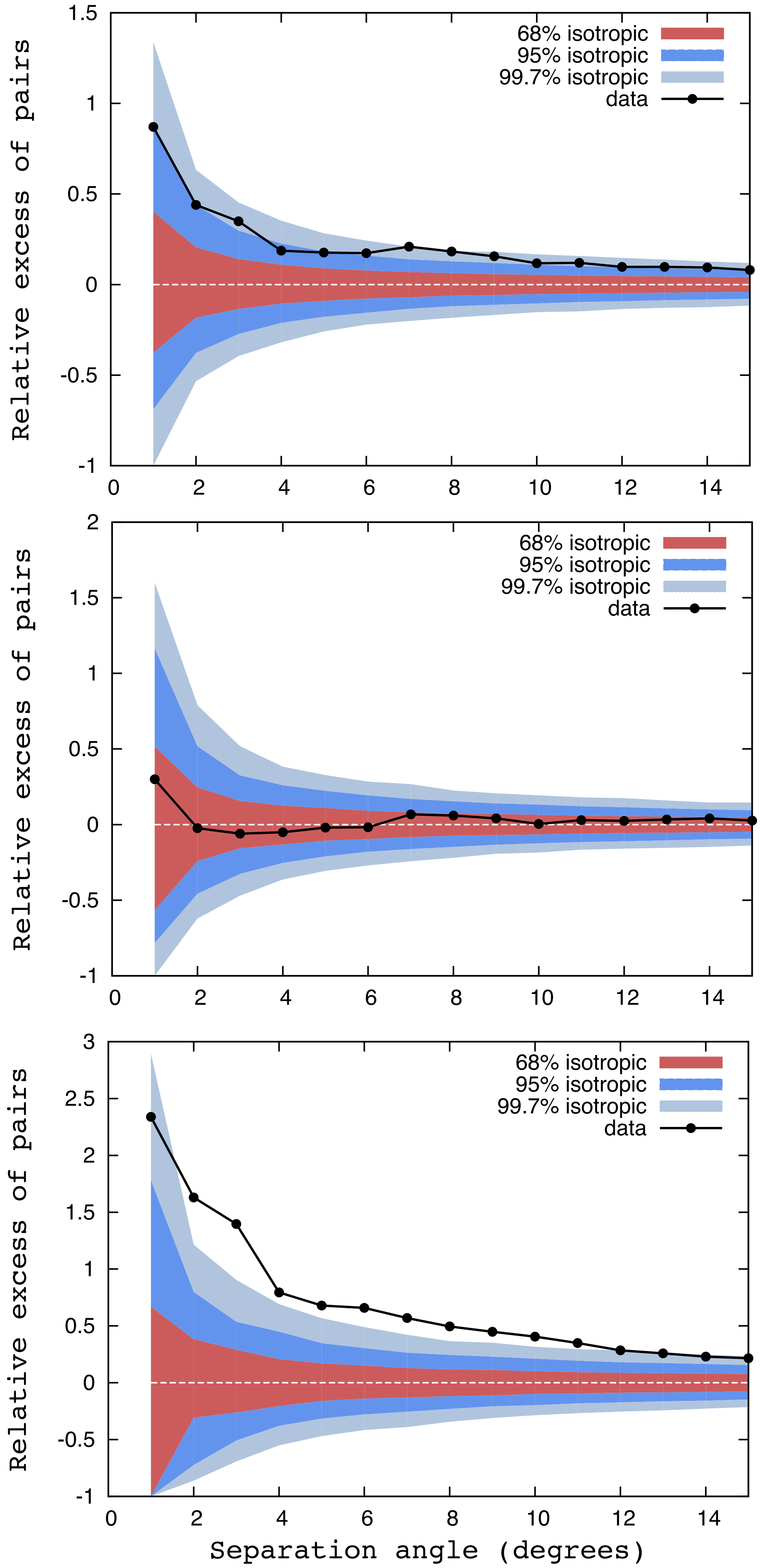

all 454 events

proton depleted data set (326)

proton enhanced data set (128)

(AugerPrime 1604.03637)

Physics reach: generic composition-enhanced anisotropy

Generic source correlation study: 75% of the protons in the data correlate with sources, sources+correlation radius cover p_{iso} of sky (folded with exposure)

Merit factor of 1.5 for discrimination light/heavy assumed

Without upgraded array

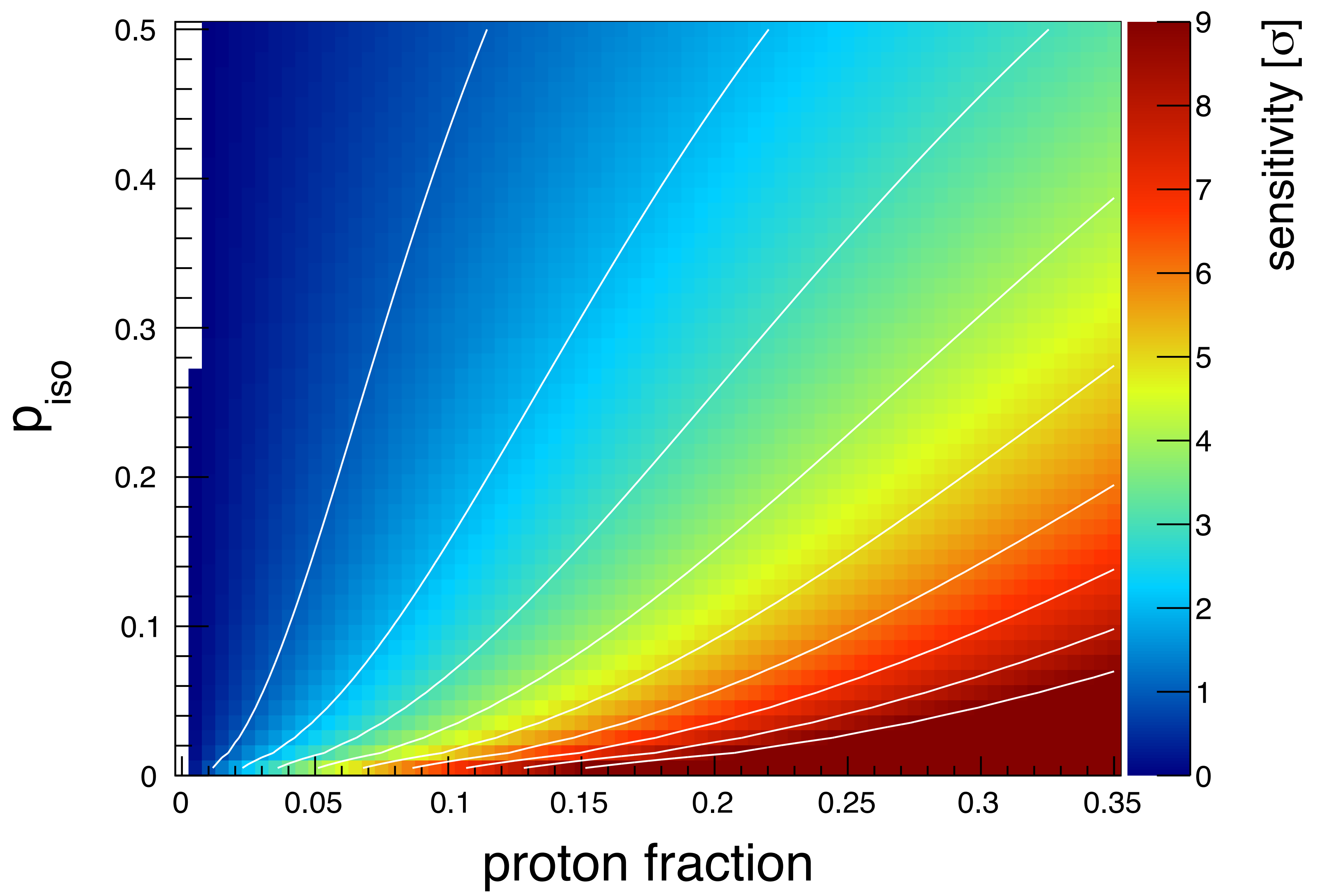

With upgraded array

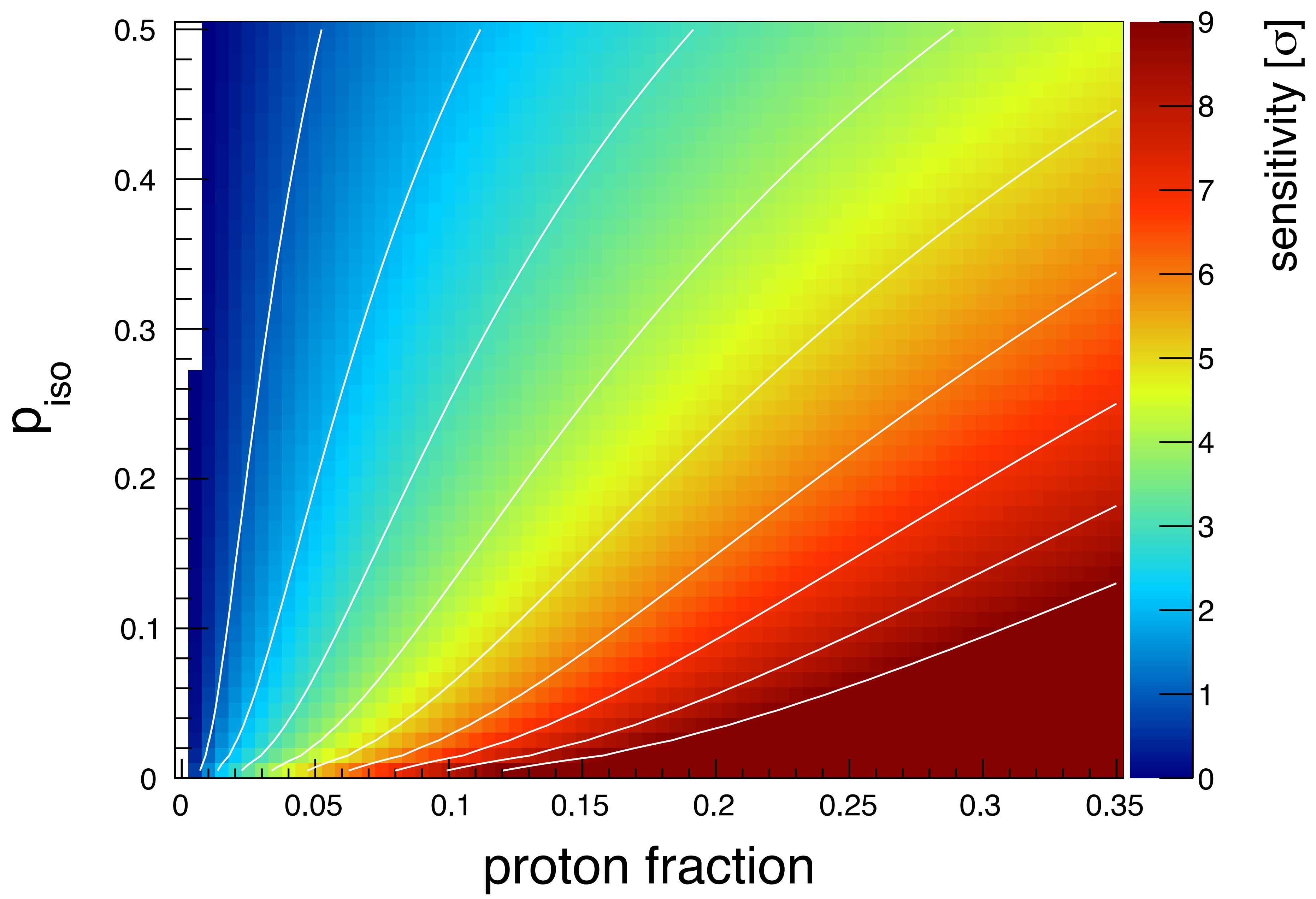

(AugerPrime 1604.03637)

Particle physics with the upgraded Auger Observatory

Results on muon number of showers still not understood, important effect missing in models?

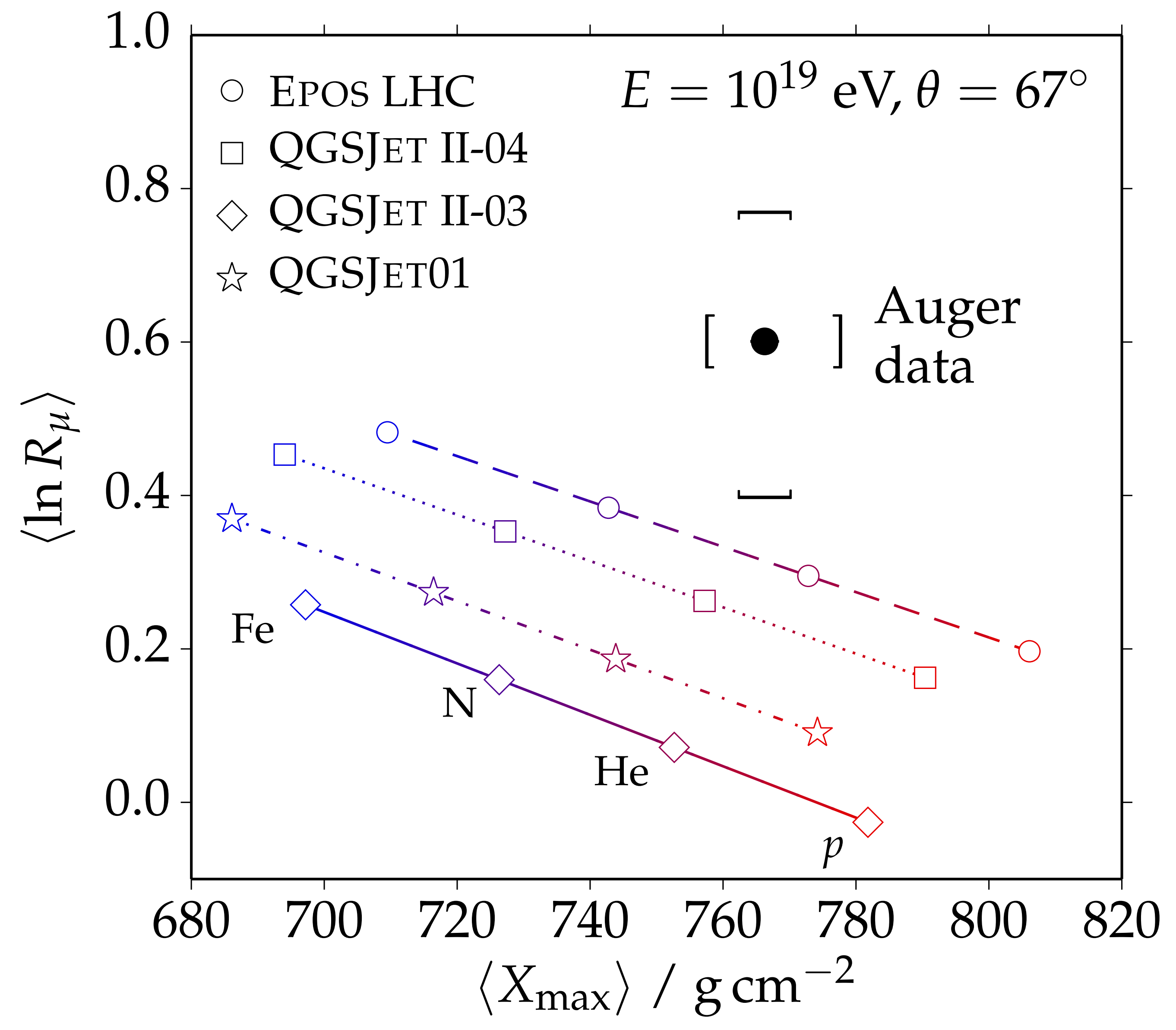

(Auger Collab. Phys. Rev. D91, 2015 & ICRC 2015)

Example of power of upgraded detectors

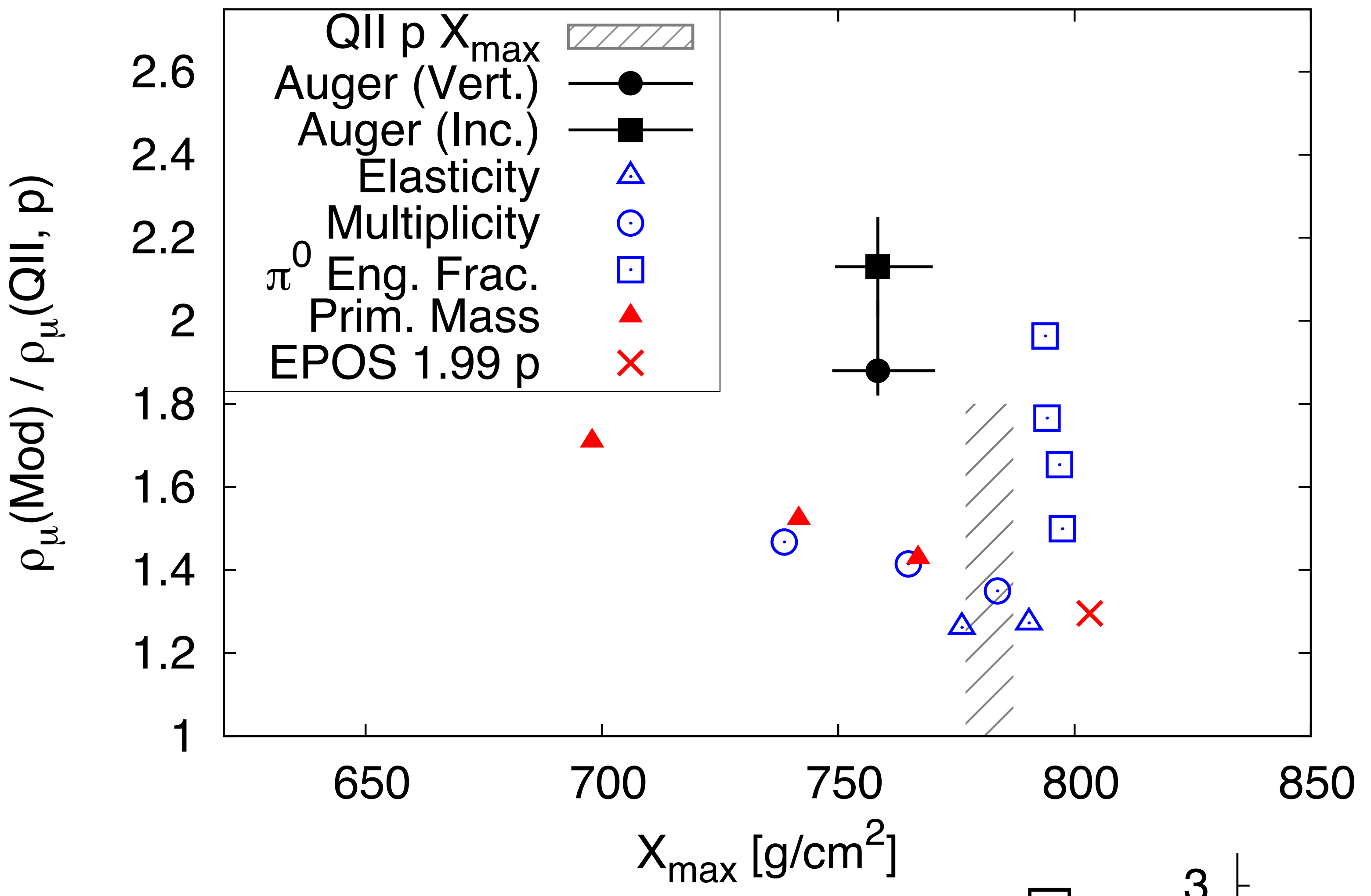

Correlations between X_{max} and muon density

(Allen & Farrar, 1307.7131)

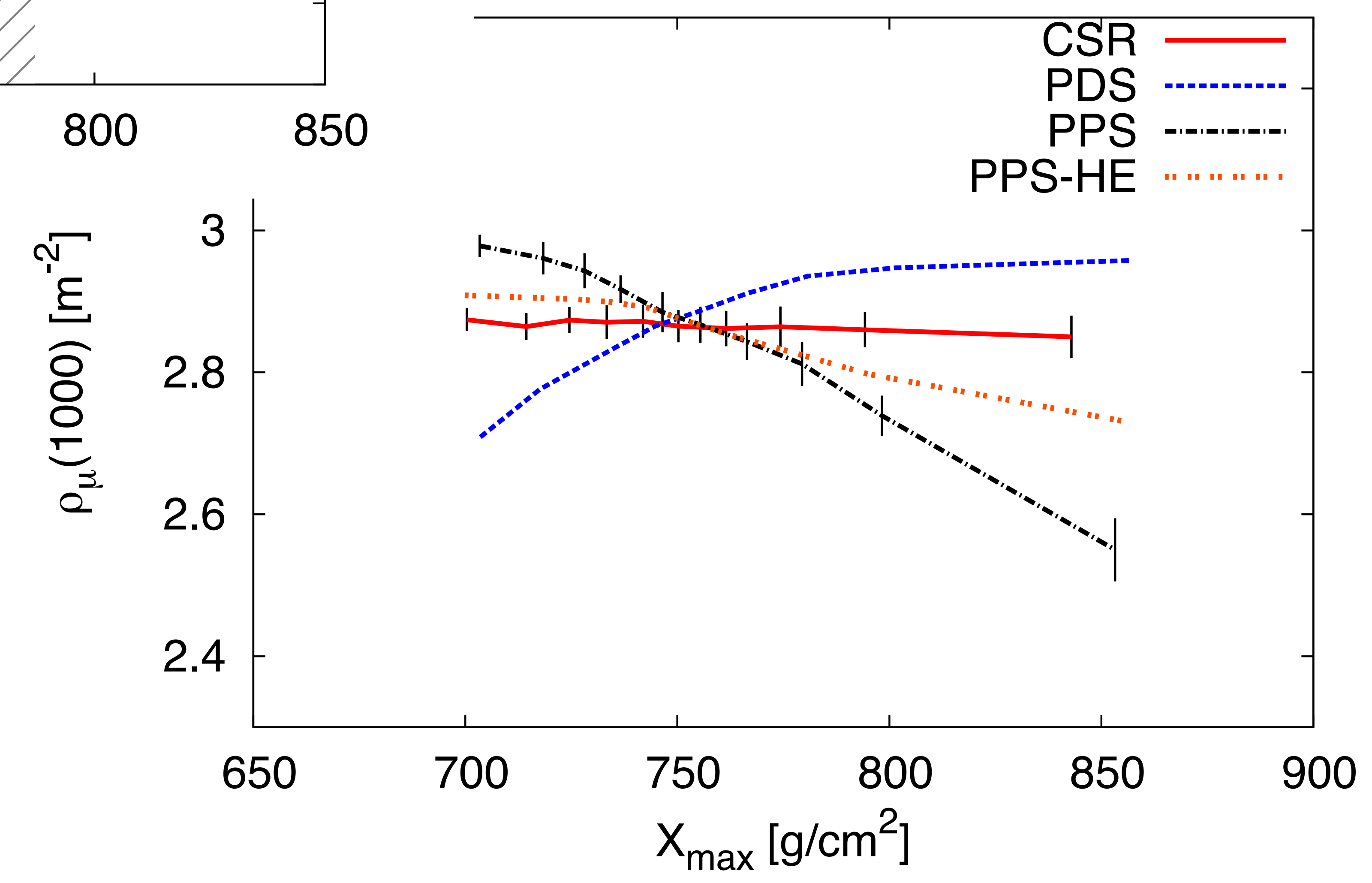

Overview of AugerPrime: items needed to make things work

1. Installation of 1700 **scintillation detectors** (3.8 m^2, 1cm thick)

2. Installation of **new electronics** (additional channels, 40 MHz -> 120 MHz, better GPS timing)

3. Installation of **small PMT** in water-Cherenkov detectors for increasing dynamic range: typical lateral distance of saturation reduced from ~500 m (E > $10^{19.5}$ eV) to 300 m

4. Cross checks of upgraded detectors with **direct muon detectors** shielded by 2.3 m of soil (AMIGA, 750 m spacing, 61 detectors of 30 m^2, 23.4 km^2)

5. **Increase of FD exposure** by ~50% (lowering HV of PMTs)

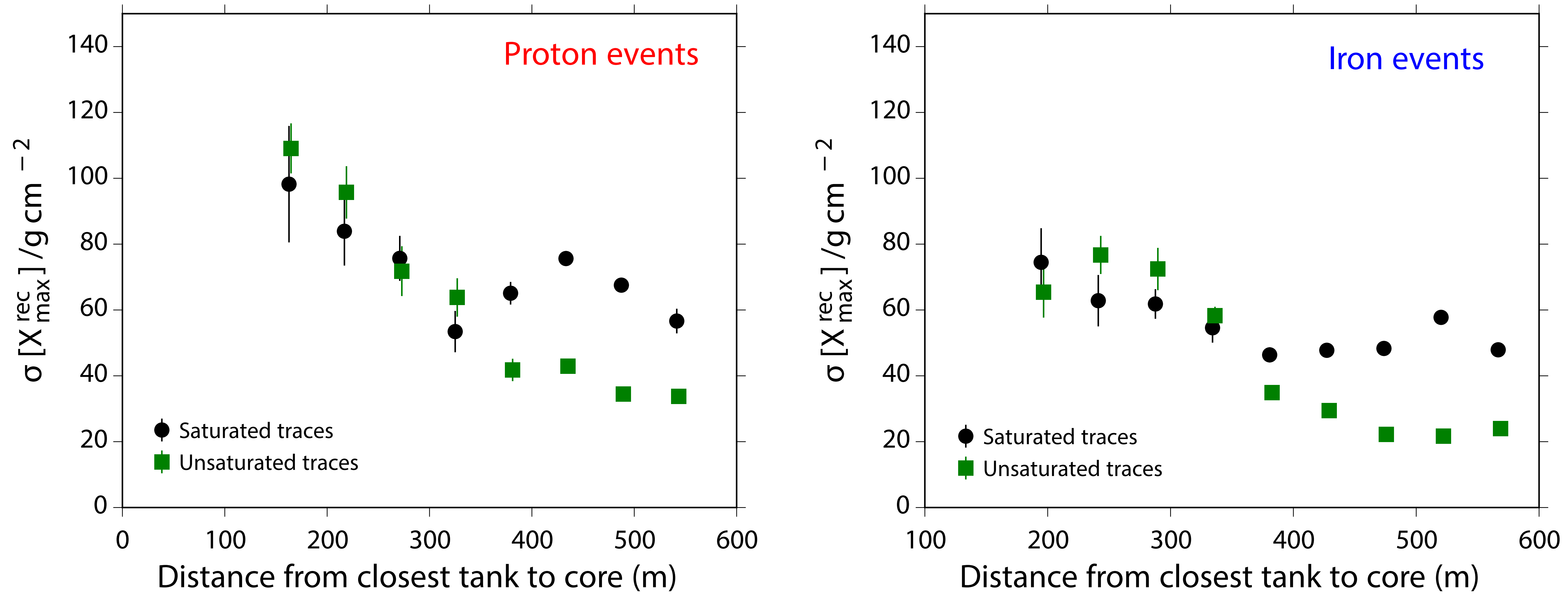

(AugerPrime 1604.03637)